TU Dortmund

Molecularly Imprinted Polymer Based Scavengers for Purifying Small and Large Active Pharmaceutical Ingredients

PhD Thesis Faculty of Chemistry TU Dortmund | Emelie Fritz

Technische Universität Dortmund
Institur für Umweltforschung der Fakultät Chemie

MOLECULARLY IMPRINTED POLYMER BASED SCAVENGERS FOR PURIFYING SMALL AND LARGE ACTIVE PHARMACEUTICAL INGREDIENTS

Promotion am

Institut für Umweltforschung der Fakultät Chemie

zur Erlangung des akademischen Grades

Doktor der Naturwissenschaften

(Dr. rer. nat.)

Prüfer:

Prof. Dr. Ralf Weberskirch

Prof. Dr. Börje Sellergren

Vorgelegt von
MSc. Emelie Fritz
geboren am 27.12.1984
133020

Die vorliegende Doktorarbeit wurde am Institut für Umweltforschung angefertigt und eingereicht an der Fakultät für Chemie der Technischen Universität Dortmund

Gutachter der Dissertation:

Prof. Dr. Ralf Weberskirch

Prof. Dr. Börje Sellergren

Tag des öffentlichen Promotionskolloquims:

Erklärung

Hiermit erkläre ich, dass ich die vorliegende Dissertation selbständig und nur mit den angegebenen Hilfsmitteln angefertigt habe. Die Arbeit wurde bisher in gleicher oder ähnlicher Form keiner anderen Prüfungskommission vorgelegt und auch nicht veröffentlicht.

Dortmund, November 2014

Emelie Fritz

To my beloved family

ACKNOWLEDGEMENTS

First and foremost my gratitude goes to Prof. Börje Sellergren for giving me the opportunity to do my PhD in his group at Institut für Umweltforschung der Fakultät Chemie, TU Dortmund and experiencing a new country. Börje has not only been a scientific mentor but also taught me to work independently and follow through with my own ideas.

I would also like to thank Prof. Dr. Ralf Weberskirch for his support as a second supervisor and his group for help with analysis.

I would like to acknowledge and express my gratitude to the European Commission under FP7-Marie Curie Action, contract PITN-GA-2008-214226 (NEMOPUR), for their financial support towards my research.

A very special thanks to Prof. Dr. Michael Spiteller who welcomed me to perform my studies in his institute and all the group members for their kindness and help throughout the years. I would especially like to express my gratitude to Marc Lamshöft and Jana Meyer for all their support with MS analysis. Cornelia Stolle and Anke Bullach for making the organization of Nebenfachpraktikum more entertaining. Another thanks goes to Sebastian Zühlke for opening up his office for me temporarly and Jürgen Jünemann for his computer support. And what would I have done without all those coffee breaks – probably would not have learnt to drink black coffee- and chats with Ulrich Schoppe.

For all my colleagues and friends in AK Sellergren, without you my PhD-time would not have been the same. From the first day I arrived you made me feel welcome and for this time with all our laughter as well as discussions, sometimes heated, I am grateful. To Ricarda, Annabell, Robert, Eric, Melanie, Mahadeo, Ali, Javier, Sudhir, Abed, Reza, Patrick, Wei, Porkodi, Wasim, Carla, and all our guest members – thank you. A special thanks to all the azubis who all contributed to this work.

I am also grateful to have the opportunity to work and travel around Europe with my colleagues in the NEMOPUR project. A special thanks to Elin Rundquist and György Székeley for good collaboration and taking care and guiding me during my secondments.

I have also had the pleasure of gaining many new and dear friends during my time in Dortmund. Ricarda, I am so grateful you decided to adopt me on my first day and all the laugther, tears, frustration we shared. You are like family. Another very dear friend that have been there through all the laughters and struggles of doing a PhD is Annabell. Not only is she a great funny-saying-inventor, she is also a wonderful friend. Andie and Steffi, Jenni and Stefan, and the rest of the "Adventure gang", thank you for all the great times. And to all the other Dortmund people.

When I heard that Elin also had an "incident" with the Dortmund map during that first NEMOPUR meeting, I knew we would become friends. I do not only appreciate the wine bottles and travel adventures we shared, but I am also infinitely grateful for her help and encouragement while writing this thesis.

My friends in Sweden are not to be forgotten, for giving me both encouragement and love dispite the distance. Thank you to my dear university friends, Frida, Hanna and Camilla. You made the university studies and all the long hours in the lab so much more fun. Hanna and Camilla my värmländska friends, thank you for helping me keep my feet on the ground no matter what. A special thank you to Frida for being a great travel-partner – who needs travel agencies when they have you – for your unwearied motivation and for giving me the honour to be Deacon's godmother. You truly are an inspiration and I am so grateful to have you as a friend. My old friends from school, Anna, Lina and Andrea, so many years have passed since we first met but I am as happy now as then to call you my friends. Thank you for always making me laugh when needed.

Last but not least, I am so grateful to my family for your love and continuous support. Mum and dad, thank you for moving and carrying large parts of Sweden up the stairs and for always believing in me. Sofie, you are the best sister one can imagine except when locking me out on the balcony, you always make me see the positive side of things and give me the motivation to keep going. I would not be who I am and where I am today without you all - you mean the world to me.

I TABLE OF CONTENTS

II LIST OF ABBREVIATIONS

4-VP	4-vinylpyridine
ABDV	2,2’-azobis(2,4-dimethylvaleronitrile)
ACE	Avoid, control, and excpel
AIBN	2,2'-azobisisobutyronitrile
API	Active Pharmaceutical Ingredient
BET	Braunauer-Emmet-Teller
BJH	Barret-Joyner-Halenda
DAD	Diode-array detector
DMAP	4-dimethylaminopyridine
DMF	Dimethylformamide
D_p	Pore diameter
DSC	Differential scanning caorimetry
DVB	Divinyl benzene
EA	Elemental analysis
EDX	Energy dispersive x-ray
EGDMA	Ethylene glycol dimethacrylate
EMA	European Medical Agency
FDA	Food and Drug Administration
GTI	Genotoxic impurity
HEMA	Hydroxyethylmethacrylate
HPLC	High pressure liquid chromatography
HTS	High-throughput system
ICH	International Conference on Harmonization
IF	Imprinting factor
k	Capacity factor
LC-MS	Liquid chromatography mass spectroscopy
LOEL	Lowest observed effect limit
MAA	Methacrylic acid
MAAM	Methacrylamide
MBA	N,N’-methylenebisacrylamide
MeCN	Acetonitrile
MeOH	Methanol

MIPs	Molecular imprinted polymers
MISPE	Molecularly imprinted solid phase extraction
MPTP	1-methyl-4-phenyl-tetrahydropyridine
NDAs	New drug applications
NIP	Non-imprinted polymer
NIPAm	N-isopropylacrylamide
NOEL	No observed effect limit
OH-	Alcohol
OSN	Organic solvent nanofiltration
PDE	Permissible daily exposure
PEG	Polyethylene glycol
PES	Polyether sulfone
PGIs	Potential genotoxic impurities
QCM	Quartz crystal microbalance
S_A	Surface area
SEM	Scanning electron microscopy
SPE	Solid phase extraction
TAA	Thioacetamide
TASO	Thioacetamide sulfoxide
TCDD	2,3,7,8-tetrachlorodibenzo-p-dioxin
TFC	Thin film composite
TGA	Thermogravimetric analysis
TiO_2	Titanium oxid
TTC	Threshold of toxicological concern
USP	U.S. Pharmacpeia
UV-light	Ultraviolet light
V_p	Pore volume
α	Separation factor

III SUMMARY

The work prestented in this thesis discusses molecularly imprinted polymer (MIP) based scavengers for the purification of active pharmaceutical ingredients (APIs). The manufacturing of APIs often involves the use of highly reactive reagents, which could remain as undesired residues in the final product. Genotoxic impurities (GTIs) represent a class of compounds of special concern, which can participate in alteration of DNA and subsequently cause cancer. Regulatory agencies have recently issued new guidelines on the control of GTIs. In general, product risk assessment can be influenced by the presence of GTIs, therefore the control and removal of GTIs are of great interest to the pharmaceutical industry.

Novel molecularly imprinted polymers have been designed and synthesized that can recognize pharmaceutical impurities such as acetamide, thioacteamide and aminopyrimidine. Thorough evaluation and characterization have demonstrated the feasibility to use MIPs as selective sorbents for purification of APIs. Rebinding tests indicate that high affinity interactions are present between the binding sites of the MIP and the target impurities, resulting in a highly efficient purification. Different MIP formats were successfully synthesized for the purpose to increase the binding capacity. The new MIPs developed offer a new and inventive purification technique for the pharmaceutical industry as an efficient and selective sorbent.

The successfully developed acetamide MIPs were tested in combination with organic solvent nanofiltration (OSN). This case study investigated the hybrid approach of MIPs and OSN for application in the pharmaceutical industry. Upon comparing the effectiveness of MIPs and OSN, it was concluded that the MIP based scavengers function better at low GTI concentrations, whilst OSN functions better at high GTI concentrations. Hence OSN can be used as a rough cleaning phase and the MIPs as a polishing phase, indicating that a hybrid approach can be beneficial for removal of impurities in the pharmaceutical industry.

Furthermore, a novel and more effective HTS screening method based on grafting of PES membranes for MIP libraries was developed in this work. It was shown that successful grafting of both membrane filter plates and loose membrane discs is supported by calculations of the grafting amount and permeability. Furthermore TGA, SEM and EDX analysis also strongly indicate that polymer is successfully grafted on the membrane surface. The rebinding tests

performed on both the grafted membranes filter plates and grafted loose membrane discs display that a difference in binding between the MIP and NIP can be observed.

MIPs intended for the use as catalysts promoting cyclisation of end-products in peptide synthesis were synthesized and investigated. The first preliminary tests showed that by using reduction and oxidation protocols for peptides, somatostatin and desmopressin could be opened and re-closed and simultaneously followed by LC-MS analysis. By studying the linear to cyclic peptide ratios obtained by LC-MS, it can be observed that the ratio of linear to cyclic peptide decreases, meaning that the cyclic form possibly increases and thus indicating that the presence of polymer promotes the cyclisation of somatostatin. Furthermore, the preliminary results suggest that the imprinted polymer promotes the cyclisation better than the corresponding NIP and the promotion also exhibits selectivity for the imprinted somatostatin since desmopressin does not display any significant change in ratio compared to the free solution control sample.

ZUSAMMENFASSUNG

Die vorliegende Doktorarbeit präsentiert die Arbeit an molekular geprägten Polymeren (MIPs) zur Aufreinigung von arzneilich wirksamen Bestandteilen (APIs).

In der Herstellung von APIs werden häufig hochreaktive Reagenzien benötigt, die als unerwünschte Überreste in dem Endprodukt verbleiben können. Genotoxische Verunreinigungen (GTIs) stellen eine Verbindungsklasse von besonderer Bedeutung dar, da sie eine Rolle bei der Veränderung von DNA spielen und, darauf basierend, Krebs hervorrufen können.

Regulierende Stellen haben letztlich neue Richtlinien zur Kontrolle von GTIs herausgegeben. Generell kann die Risikoeinstufung eines Produktes vom Vorhandensein von GTIs beeinflusst werden. Aus diesem Grund ist die Kontrolle und die Entfernung von GTIs von großem Interesse für die pharmazeutische Industrie.

Neue molekular geprägte Polymere, die pharmazeutische Verunreinigungen wie Acetamid, Thioacetamid und Aminopyrimidin erkennen können, wurden entwickelt und synthetisiert.
Durch die umfassende Untersuchung und Charakterisierung wurde die Möglichkeit, MIPs als selektive Bindungsphase für die Aufreinigung von APIs zu verwenden, gezeigt. Bindungstests weisen darauf hin, daß zwischen den Bindungsstellen des MIPs und der Ziel-Verunreinigung Wechselwirkungen mit hoher Affinität bestehen. Dies führt zu hocheffizienter Aufreinigung.
Um die Bindungskapazität zu erhöhen, wurden verschiedene MIP-Formate erfolgreich synthetisiert. Die neuentwickelten MIPs stellen in ihrer Nutzung als effiziente und selektive Bindungsphasen eine neue und innovative Aufreinigungstechnik für die pharmazeutische Industrie dar.

Die erfolgreich entwickelten Acetamid-MIPs wurden in Kombination mit lösemittelstabiler Nanofiltration (OSN) getestet. Die Fallstudie untersuchte den Hybrid-Ansatz von MIPs und OSN für die Anwendung in der pharmazeutischen Industrie.

Bei dem Vergleich der Effektivität von MIPs und OSN wurde beobachtet, daß die MIP-basierten Fänger bei niedrigen GTI Konzentrationen besser arbeiten, wohingegen OSN besser

bei hohen GTI Konzentrationen funktioniert. Ein Hybrid-Ansatz kann gewinnbringend für die Entfernung von Verunreinigungen in der pharmazeutischen Industrie sein, indem OSN als Grobreinigung und die MIPs als Feinreinigung dienen.

Darüber hinaus wurde in dieser Arbeit eine neue und effektivere HTS-Methode basierend auf der Polymerisation von PES-Membranen für MIP-Bibliotheken entwickelt. Es wurde gezeigt, daß sowohl die Polymerisation von Membran-Filterplatten als auch losen Membran-Plättchen von Berechnungen der Polymerisationsmenge und Durchlässigkeit gestützt wird. Darüber hinaus weisen die Ergebnisse von TGA, SEM und EDX-Analysen stark darauf hin, daß Polymer erfolgreich auf die Membranoberfläche aufpolymerisiert wurde. Die Bindungstests, die sowohl mit den Membran-Filterplatten als auch den losen Membranplättchen durchgeführt wurden zeigen, daß ein Unterschied zwischen MIP und NIP in der Bindung besteht.

MIPs zur Verwendung als Katalysator für die Zyklisierung von Endprodukten in der Peptidsynthese wurden synthetisiert und untersucht. Die ersten, vorläufigen Tests zeigten, daß bei der Verwendung von Reduktions- und Oxidations-Protokollen für Peptide sowohl Somatostatin als auch Desmopressin geöffnet und wiederholt geschlossen werden konnten. Dies wurde mit LC-MS Analysen verfolgt.

Die Annahme, daß durch das Polymer die Zyklisierung von Somatostatin begünstigt wird, wird gestützt von den LC-MS Ergebnissen. Das Verhältnis verschiebt sich von linearem zu zyklischem Peptid. Darüber hinaus weisen die vorläufigen Ergebnisse darauf hin, daß das geprägte Polymer die Zyklisierung besser als das NIP unterstützt. Dieses Verhalten scheint außerdem selektiv für das geprägte Somatostatin zu sein, da Desmopression im Vergleich zu der Kontrollprobe in Lösung keine signifikante Änderung in den Verhältnissen zeigt.

1. INTRODUCTION

"...98.5% purity doesn't mean very much when we are talking about biologically active contaminants that, in varying minuscule amounts, can create powerful effects..."

P. Raphals[1]

This quote effectively summarizes the significance of the work described in this thesis. Carrying this in mind the first chapter will describe the development of active pharmaceutical ingredients (APIs), as well as the components of importance used for the development of new improved purification techniques with a beneficial impact on the pharmaceutical industry.

1.1 IMPURITIES IN ACTIVE PHARMACEUTICAL INGREDIENTS

The presence of even small concentrations of impurities can disrupt the production and sales of drugs. Therefore the ability to monitor and control these impurities at very low concentrations is of great importance. Screening for impurities throughout the entire API synthesis process, and not only in the finished product, is hence necessary since impurities can be eliminated during the process itself, *e.g.* degradation, or new impurities can form by side-reactions. Generally a finished synthesized API is assessed for toxicity by first using in vitro screening and if acceptable concentrations of harmful substances are established animal testing will performed before permission for Phase 1 human trials can be given by the regulatory agencies. To obtain this permission a thorough summary for the new API, containing the actual and potential impurities with the highest likelihood to form during synthesis, purification and storage should be completed according to the ICH Guidance Q3A (R2)[2]. Depending on the level of toxicity of the impurities and the dosage of the drug the limits of the impurities present are determined. For common impurities, *e.g.* residual solvents, general limits based on toxicology data have been decided. The permissible daily exposure (PDE) is calculated using Equation 1 below.

Equation 1 PDE = (NOEL x weight adjustment) / (F1 x F2 x F3 x F4 x F5)

Where NOEL is the so called no observed effect limit, F1 is the extrapolation between species (e.g. 12 for mice to humans), F2 is the individual variation, F3 is the length of the toxicology

study, F4 is the severe toxicity factor, and F5 is the factor used only when the LOEL (lowest observed effect limit) is accessible. Residual metals also need to be kept within the existing specifications.[14]

The acronym ACE, short for Avoid, Control, and Expel beautifully sum up the methods used to control impurities. When the cause of the impurity formation is *e.g.* the use of a specific solvent, it can be avoided by changing the solvent[3]. Another way to control impurities is to spot them in the early phases of synthesis, as this offers more opportunities to expel them by taking preventive measurements in the workup process[4].

One well-known case of impurity contamination of drugs on the market is Viracept produced by Hoffmann- La Roche. In June 2007 the drug was withdrawn from the market after patient complaints of unusual smell and after analysis Roche found high concentrations of the impurity ethyl mesylate.[5] This was reason for concern as ethyl mesylates have proven to be carcinogenic, genotoxic, as well as teratogenic. Roche found the source of the impurity and managed to remove it down to the specification levels, allowing the drug to be reinstituted to the market. However, this example clearly illustrate the importance to remember that the superior method to control GTIs is to really understand the mutagenicity by evaluate actual data and not only theory.

The development of drugs comes with great responsibilities. Hence, with the potential risk of exposing patients to impurities it is of great importance to understand the toxicity of all compounds involved. Predicting the toxicity of the drug substance and related impurities can however prove difficult. This was the case with the eosinophilia myalgia syndrome caused by impurities in L-tryptophan nutritional complements, which was the example the opening quote of this thesis was referring to.[1] The impurity that is believed to have caused the syndrome is the derivative of bis-tryptophan as illustrated in Figure 1[6,7]. The thalidomide drug case is another well-known unfortunate incident caused by impurities. The drug thalidomide was given to pregnant women to treat nausea, however the (S)- enantiomer lead to adverse limb deformation in the fetus they carried. After ingestion of the drug the (R)- enantiomer is transformed into the toxic (S)- enantiomer via racemization. When synthesizing the drug meperidine isostere the impurity 1-methyl-4-phenyl-tetrahydropyridine (MPTP) was formed by accident. This impurity can cross the brain barrier after which it most likely forms the cation MPP^+, which causes permanent Parkinson like symptoms in people that used the meperidine isostere drug

recreationally[8]. During the Vietnam war the defoliant Agent Orange, a 1:1 combination of 2,4-D and 2,4,5-T, was dropped on the landscape. The main components were quickly metabolized but the impurities present, particularly 2,3,7,8-tetrachlorodibenzo-p-dioxin (TCDD), turned out to be both carcinogenic and teratogenic also in very low concentrations.[14] These examples demonstrate the importance of understanding the possible impurities present in drugs we produce. Hence improved techniques to detect and remove these impurities to stringent low levels are of great importance.

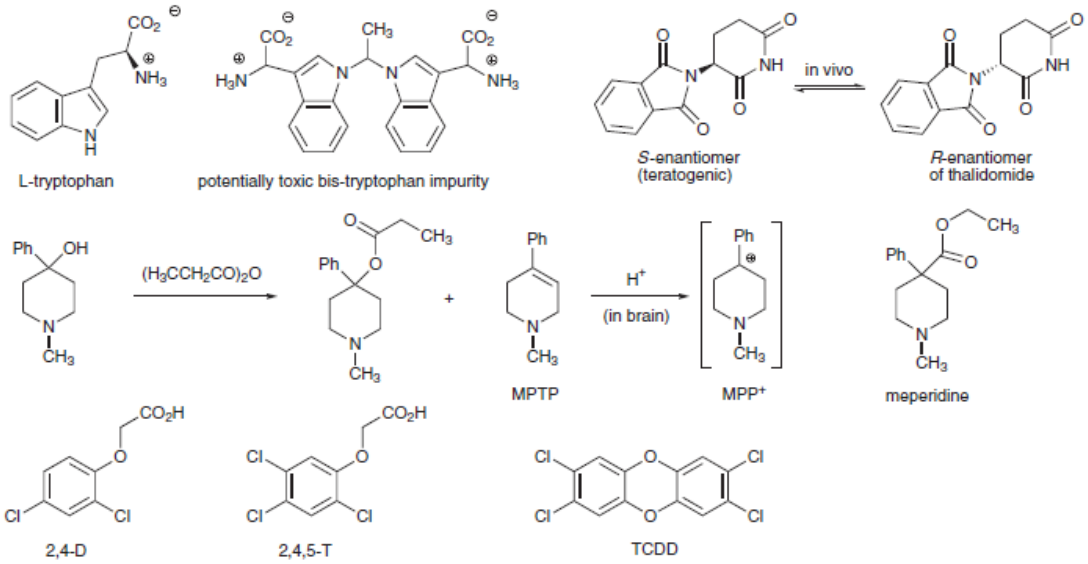

Figure 1 Illustrates a number of example of toxic impurities present in some chemicals.[14]

1.2 Purification of Active Pharmaceutical Ingredients

Various regulatory authorities are responsible for setting the purity standards for APIs that reach the market. Hence, before pharmaceutical and biotechnology companies are allowed to introduce a drug to be sold to patients they need to receive approval from these different agencies. The purity standards set relate to the potencies, identity and levels of impurities, as well as physicochemical properties. One of the main regulatory agencies is the Food and Drug Administration (FDA) which is responsible for approving new drug applications (NDAs). These NDAs have to fulfill requirements based on the testing methodology developed by the U.S. Pharmacopeia (USP), a non- profit, government organization, which the FDA is enforcing.

Drug specifications and standards for environmental impact *etc.* may however differ for the regulatory authorities in other countries *e.g.* the European Medical Agency (EMA) for the European Union. In an effort to make these guidelines globally analogous, the International Conference on Harmonization (ICH) continuously works on standardizing regulations.

In order to reach the standards set and make sure a pure API with tolerable concentrations of impurities are obtained, a variety of purification processes are used. The processes applied depend on the specific product formed with some examples including crystallization, drying for removal of volatiles, washing cycles, resolution separation, preparative column chromatography, fractional distillation, membrane processes, and application of resins and scavengers. Generally the higher the selectivity towards an impurity is, the lower the API losses are and the more efficiently the impurity is removed. In addition to the removal of impurities directly as they form, it can be beneficial to have an additional purification step after the workup to obtain a higher purity[9,10,11]. The conventional purification techniques used in API are summarized in Figure 2 together with the two new emerging techniques investigated in this thesis.

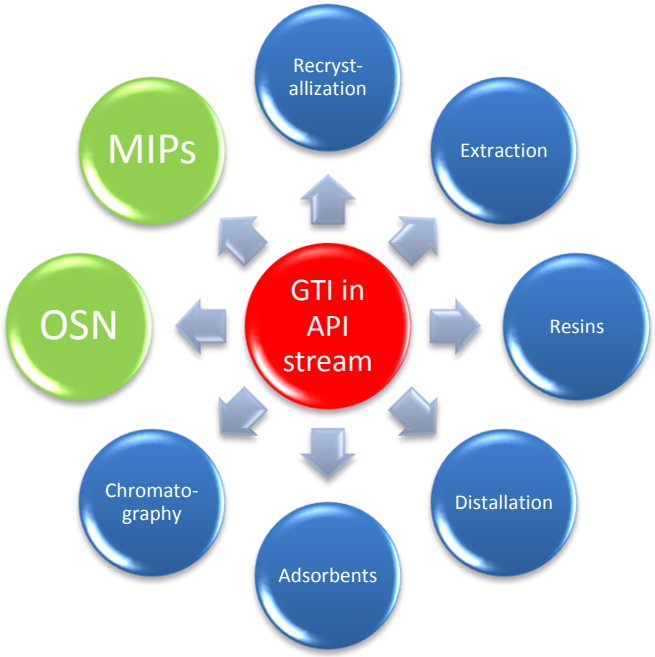

Figure 2 Examples of conventional techniques (blue) used for purification together with the techniques investigated in this thesis; MIPs and to a smaller extent OSN (green).

To make certain that the drugs that reach the markets are safe and efficient, are the most important assignments of the different regulatory agencies. Even a slight variation in the drug substance concentration can make the drug, not only unproductive, but also toxic depending on the safety margin of the API. Therefore reproducibility in all stages, from compound synthesis all the way to the production of different batches is of great importance. The aim of process development is to decrease heterogeneity by overcoming the problems the conversion of solids and liquids into homogeneous mixtures can present. Also therapeutically inactive compounds, i.e. excipients, influence the formulating process and because of the variety of different operations involved in the process, for example blending, milling, drying, compression and film coating, a broad range of material science is crucial for a successful API formulation[12]. The control of the physical characteristics; hygroscopicity, particle size and distribution, is hence highly important in order to obtain reproducibility in produced batches and can be obtained by choosing the excipients and processes with the appropriate characteristics. Formulation has a substantial impact on the total cost of bringing drugs to the market and could even cancel ongoing clinical trials or discontinuing the sales if specifications are not met[13]. In general the preferred design for small molecule APIs is solids with the ability to crystallize and re-crystallize, because they are convenient tools for both drug substance and product quality control. Furthermore, crystalline drugs generally offer a satisfactory shelf life because of their good stability compared to amorphous solids[14]. Roughly 70-90 % of the substances under development exhibit poor solubility, nevertheless they do reach the market, meaning that the window of potential active pharmaceutical ingredients broadens[15]. Crystallization is also an effective technique for impurity removal and is hence commonly used for this purpose. In order to reach the specified impurity level sometimes numerous repeating re-crystallization cycles are necessary. This opens up for process optimization and the development of new purification techniques.

1.3 GENOTOXIC IMPURITIES IN ACTIVE PHARMACEUTICAL INGREDINTS

The definition of impurities in pharmaceutical products is any substances that is not the active ingredient thus not presenting any therapeutic benefit for the patient, an impurity may or may not cause undesirable effects.[16] A sub-category of impurities present in APIs with strictly controlled allowed limits is compounds with potential genotoxic effects. One of these unwanted effects of genotoxic materials is cancer; with cancer being a leading cause of death worldwide. According to the World Health Organization the numbers of deaths from cancer are predicted to almost double from 7.6 million in 2008 to 13.1 million by 2030. Hence great efforts are made to understand and control genotoxic impurities during the development process.

Genotoxins, also called mutagens, are potentially carcinogenic by causing damage or modifications to the DNA which can lead to transcription and protein translation problems.[14,17] Over the last decade the concern about genotoxic impurities has increased significantly in the pharmaceutical industry, which is reflected in the number of hits in literature on "genotoxicity" and "genotoxic impurity".[18] The strict allowed amounts are due to the fact that genotoxins belong to a class of extraordinary toxic impurities as classified by the ICH Q3 A2. As a result genotoxic impurities must be controlled down to ppm or even ppb levels, which is difficult to analyze and control and can cause delays in the development of APIs.[19] The mechanism by which genotoxins cause damage to DNA entail an electrophilic attack on the nucleophilic parts of the DNA, more precisely the nitrogen and oxygen in pyrimidine and purine bases. Genotoxic compounds that are bidentate have the capability to react with two nucleophilic sites simultaneously and form either: (1) a bicyclic or tricyclic system from one molecule; (2) two different molecules in the same or opposite DNA strands resulting in inter- or intrastrand coupling; or (3) a DNA-protein adduct[20]. A number of functional groups considered to be so called structural alerts for genotoxicity are summarized in Figure 3.

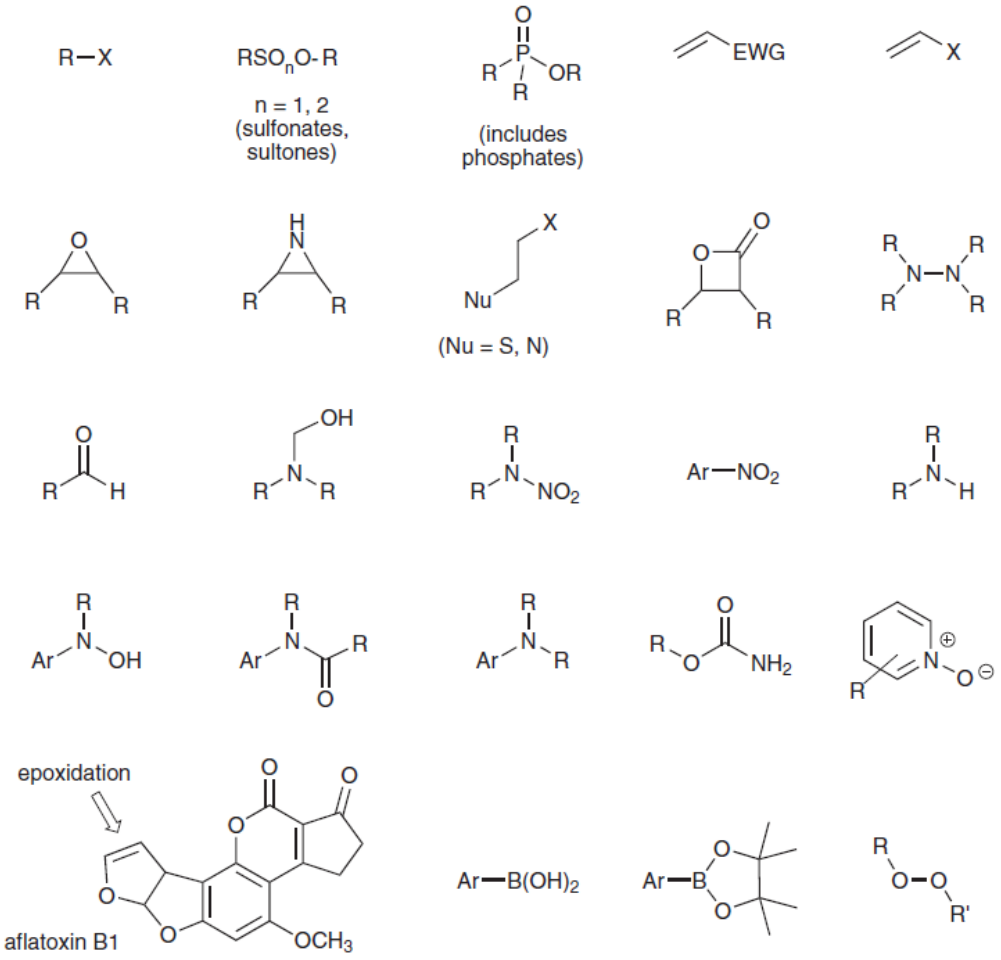

Figure 3 Structural alerts of functional groups that may be potential genotoxins. Where R= aryl, alkyl, H; EWG= electron-withdrawing group; X= leaving group, *e.g.* Br.[14]

As a result of the many possible structural variations and that the structures do not necessarily need to be related, genotoxic impurity control is very complex. Some of these structural alerts are described in more detail hereafter. Aldehydes belong to another group of compounds that are potentially genotoxic, via reaction with the deoxyguanosine residues at the N_1 and the exocyclic amine sites. Metabolic epoxidation of aromatic hydrocarbons may result in genotoxicity, one example being the particularly potent mutagen aflatoxin B_1. Aryl boronic acids and boronic esters have demonstrated mutagenicity in bacteria, at this point no animal testing data is existing. [14,21,22,23,24]

Tools, such as software programs and databases, for prediction of a compound's genotoxicity are available and approved by regulatory authorities. However, it should be noted that these software are operated by people, and the quality of the results are therefore strongly dependent

on the data inputted. To improve the prediction of a compounds genotoxicity it is standard to include (1) computational screening; (2) microbial screening, *e.g.* the Ames test; and (3) animal testing, commonly on mice and rats. The aim of this screening and testing is to establish an upper limit dosage, at which there is limited risk of causing cancer. Potential genotoxic impurities (PGIs) can be complicated to isolate, identify, and prepare at an early stage in the development, and are thus often not tested in animals. Therefore PGIs are per definition impurities with inadequate toxicological data to determine the tolerable exposure limit. If PGI formation cannot be avoided best practise state that the limit should be reduced to the lowest possible value[25]. In clinical trials PGIs are subject to the so called threshold of toxicological concern (TTC), where the standard limit is 1.5 mg day^{-1} for clinical trials exceeding 12 months (higher exposure doses are allowed for shorter clinical trials) [26]. The TTC values are based on the tolerable risk of 1 in 100.000 developing cancer by exposure at the given doses.

A number of repair mechanisms for handling foreign compounds are available in biological systems. Compounds can, for example, be removed unchanged via capture by present nucleophiles, or be metabolized. Genetic materials can also be repaired by enzymes, or affected cells can be programmed to die. Additionally, when the damage is not too widespread the organism can also survive and the modified genes will then be incorporated in the following generations. This means that PGIs can be active in vitro tests but in animal tests no activity is detected[27].

1.4 GENOTOXIC IMPURITIES OF INTEREST

In this section a number of genotoxins of interest for this thesis is described in greater detail, including mode of toxicity.

1.4.1 ACETAMIDE

Acetamide is a derivate from acetic acid and ammonia, and is a white, odorless, hygroscopic solid which is often used in electrochemistry and organic synthesis (Figure 4). Acetamide dissolves easily in water, displays amphoteric properties and hydrolizes slowly except for when an acid or base is present. In combination with acids, *e.g.* HBr, HCl, HNO_3, acetamide forms solid complexes.

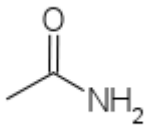

Figure 4 Schemetic structural drawing of acetamide.

Acetamide is generally produced via dehydration of ammonium acetate according to the reaction below.

$$NH_4OOCCH_3 \rightarrow H_2O + CH_3CONH_2$$

For industrial production the above method is transformed into a continuous process. Acetamide can also be synthesized via hydrolysis of acetonitrile under evaluated temperatures in acidic or basic environments.

$$CH_3CN + H_2O \rightarrow CH_3CONH_2$$

Acetamide can be used for a large variety of applications. Amongst other, suppressing acid formation in explosives, inks, lacquers and perfumes. It can also be used as a mild moisturizer or as a softener for leather, paper, plastics and textiles. Other applications are in pharmaceutical, pesticide and antioxidant synthesis.[28]

Acetamide is a recognized carcinogen to humans, hence its presence in API manufacturing is monitored and strictly controlled.[29,30,31,32] It is generally formed from as a side-product in the synthesis route rather than from degradation[33] and although it is normally only used indirectly as building blocks in API synthesis, such as the derivates 2- and N-bromoacetamide or trifluoroacetamide, acetamide itself is a potential impurity in the formed API compounds. Another potential contamination source of acetamide in APIs is the hydrolysis of acetonitrile. Acetonitrile is not only a commonly used solvent for synthesis in the pharmaceutical industry, but it can also be used directly as a reagent in the actual API synthesis[34].

Based on evaluation of the data published it is concluded that the carcinogenic effects of acetamide are most likely not caused by a genotoxic mechanism, but can be assigned to inhibition of gap-junction intercellular communications (GJICs).[29,35] Gap junctions are proteins responsible for the exchange of small molecules and ions between the plasma membrane channels and neighboring cells. This communication between cells is crucial for the control of cell differentiation, growth and death, and the subsequent maintenance of homeostasis[36].

1.4.2 THIOACETAMIDE

Thioacetamide (TAA) is a compound containing a thio-sulfur group and has been used for a variety of different purposes, including as an organic solvent, fungicide, stabilizer of motor oil and as an accelerator in the vulcanization of rubber (Figure 5).[37] In 1948 Fitzhugh and Nelson were the first to report TAA as a hepatotoxic agent after investigating its toxic effects after contamination of orange juice, originating from its use as a fungicide in orange groves.[38] It has been found that single doses, ranging between 1-2 mmol/kg, of TAA in animal models can generate centrolobular, middle part of an organ, necrosis followed by regenerative response.[37,38] When the toxin is administrated chronically hepatocellular carcinoma is induced and recent in vivo studies in rodents demonstrated very selective liver damages such as cirrhosis, fibrosis and hepatic necrosis and apoptosis.[39,40,41]

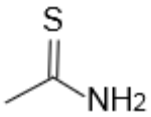

Figure 5 Structure of thioacetamide.

The toxicity of TAA is initiated by metabolic activity via a mixed-function oxidase system[42,43]. Two oxidations are the first steps in the metabolism of TAA (Figure 6), forming the reactive metabolites thioacetamide sulfoxide (TASO) and thioacetamide-*S*,*S*dioxide by *S*-oxidation. These metabolites eventually modify amine-lipids and proteins with following function impairment and cytotoxicity. Together with reactive oxygen species (ROS) these intermediates form free radicals responsible for liver damages. Studies have shown that rodents developed cell death by apoptosis and necrosis concurrently when given TAA[44]. The mechanism behind the liver damages caused by TAA has been thoroughly investigated. The results show that the formed reactive metabolites cannot only bind covalently to cellular macromolecules but also stimulate oxidative stress[42]. It has been observed that lipid peroxidation, gluthion depletion and reduction of thiol groups follow ROS formation after thioacetamide exposure[42,43]. Another effect observed is that intracellular storages of calcium has been mobilized, both this and ROS have been shown to activate a number of processes responsible for cell damage and proliferation[45]. In the cells mitochondria are well-known as the suppliers of energy; however, they also work as hubs where important signals carrying information for initiation of cell death come together. Thus mitochondria compose a target for the toxic effects of TAA. The subsequent elevated formation of ROS species and interference of calcium homeostasis have the possibility to enhance the permeability of the inner membrane of the mitochondria, as well as disrupt the membranes and inhibit mitochondrial respiration[41,46].

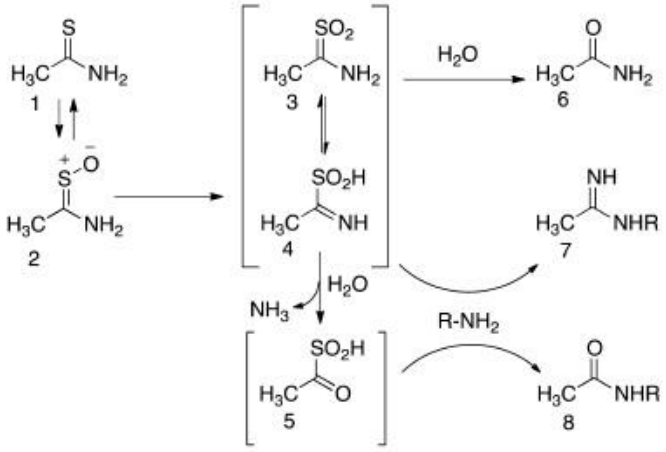

Figure 6 Describes the metabolism of TAA in rat hepatocytes. The first step (1) is a reversible S-oxidation to TASO (2). More oxidation follows creating the highly reactive species TASO2 (3 and 4). TASO2 can directly imidoylate amine groups on cellular proteins or PE phospholipids (7). Other possible fates are the formation of acetamide (6) or the reactive derivative acetyl sulfinic acid (5) after reaction with water. (5) reacts with protein amine groups to form amide derivatives (8).[41]

1.4.3 AMINOPYRIDINES AND RELATED COMPOUNDS

Some commonly used starting materials and catalysts in API synthesis are aminopyridine derivatives. The derivative 4-dimethylaminopyridine (DMAP) is for example used as the catalyst for synthesis of glucocorticoids, acylations, amino-group protection, esterifications, and sylilations[47,48,49,50,51,52]. DMAP is regarded as a potentially genotoxic impurity because it contains alerting genotoxic structures[53]. Other closely related compounds are aminopyrimidines and because of their structural similarity they are also considered as compounds of concern. Aminopyrimidines have for examples been used as nucleic acid base mimics, a base for anticancer drugs *e.g.* as inhibitors of a subfamily of receptor protein kinases, and in medicinal chemistry as an aniline replacements [54,55,56]. One biologically active pyrimidine containing compound is Wy-14,643 (4-chloro-6-(2,3-xylidino)-2-pyrimidinylthioacetic acid), which has been reported as a non-genotoxic carcinogenic. Non-genotoxic carcinogens stimulate tumor formation via mechanisms other than direct DNA interactions, for example by interfering with signal transduction mechanisms and gene expression regulating cell growth and death.[57,58]

Although most aminopyrimidines do not exhibit direct toxic effects its corresponding derivatives can show signs of toxicity. However, the mechanism of the oxidative metabolism of 2-aminopyrimidine derivatives is not well-known except for sulfadiazine, a sulfamide with high liver toxicity.[59]

1.5 MOLECULARLY IMPRINTED POLYMERS - FUNDAMENTALS OF IMPRINTING

Molecular interaction in nature, for example hydrogen bonding, ion pairing, and hydrophobic interactions, are essential for the function of a variety of systems that we all depend upon. Two examples illustrating such interactions are enzymes and antibodies with their remarkable capacity to distinguish and bind specific substrates with high accuracy. Self-organization and self-assembly are distinct chemical and physical interactions which form the basis of the characteristics displayed by enzymes and antibodies. This realization has lead to an increased interest in nanostructured materials and their possible application in mimicking biological materials. By studying the design and synthesis of complex biological molecular structures and configurations a new generation of separation, sensing, catalysis, and diagnostic materials can potentially be identified. The common theme linking these systems is molecular recognition with a high degree of affinity and selectivity for a specific molecule. Based on this a number of methods exploiting template mediated and self-assembly synthesis have been generated. [60,61,62] An example of such a material is Molecularly Imprinted Polymers (MIPs), which are known for their robustness and antibody resembling capability to specifically bind and discriminate different molecules.[63] The technique molecular imprinting developed while striving to mimic nature's remarkable capacity to distinguish and bind specific substrate with high accuracy with man-made synthetic materials.[64] It is an interdisciplinary technique linking together elements from a number of disciplines in chemistry e.g. polymer, organic, analytical, physical and biochemistry.[65] Today one can choose from a number of formats when synthesizing MIPs.[60,62,66,67,68]

The majority of imprinting is prepared by the synthesis of a polymer network around a template of interest (Figure 7) spanning from small molecules, biological macromolecules or microorganism, to crystal particles and even individual ions[63]. During the imprinting various interactions including covalent, electrostatic, hyrdrophobic, van der Waals bonds and metal

coordination form between the functional monomers and the template. In the presence of a cross-linker such interactions hold the template in place during the polymerization process. As a result the formed highly cross-linked polymer material contains binding sites complementary in shape, size and functional groups for binding of the template after template removal. The functionality of MIPs is hence based on acting like a template memory with selective and strong binding capacity of the template or related structures; mimicking antibodies. MIPs exhibit some additional advantageous characteristics to naturally occurring recognition systems, such as high tolerance for mechanical stress, high pressures, high temperatures, wide pH ranges, a variety of solvents and strong radiation. Furthermore, the relatively simple synthesis process in combination with the possibility to store the MIPs under harsh conditions and their capability to repeatedly bind templates, have resulted in an significant interest of these materials and their possible applications.

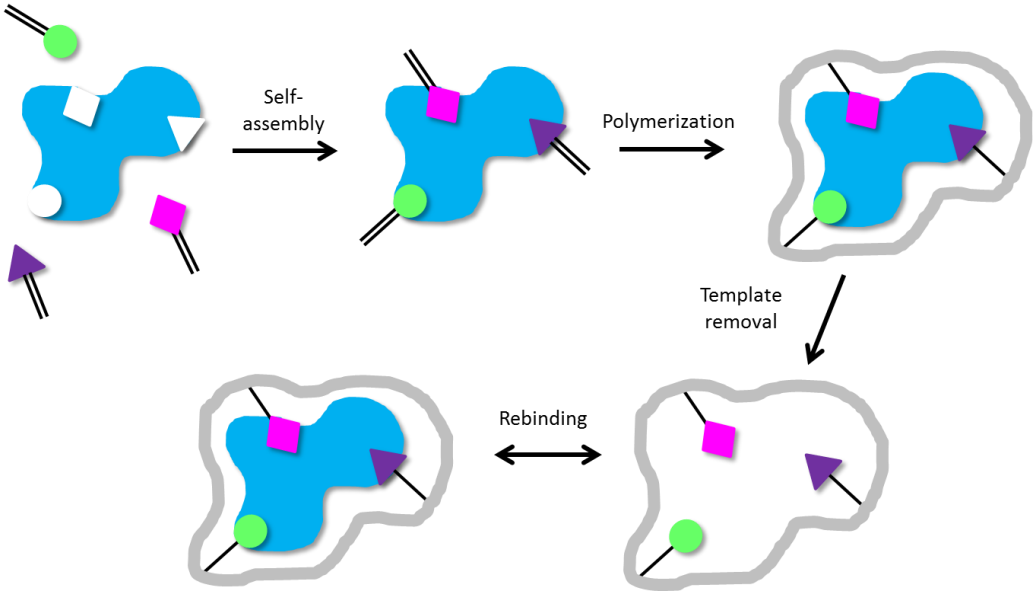

Figure 7 Schematic drawing of MIP concept.

A large variety of MIP applications has already been demonstrated in solid phase extraction, affinity separation, biosensors, immunoassays and controlled drug release systems.[60,69] Literature has also been published demonstrating possible applications of MIPs as a separation media in the pharmaceutical industry and in bio- and pharmaceutical analysis[70,71]. However, the use of MIPs for removal of genotoxins from APIs is a novel application area and the first publications on the topic have only recently been published indicating a current and growing interest[10,72,73,74].

The simplicity of the required materials, equipment and processes all contribute to the growing interest in MIPs and the molecular imprinting technique. Additionally, in most published papers MIPs are produced using free radical polymerization indicating that they can easily be produced with readily available equipment in most laboratories. This facile production method has led to a broad application range for MIPs, nevertheless the challenge remains to overcome the shortcoming that no general imprinting protocol exist and a comprehensive procedure is still necessary to target a wide range of molecules.

Depending on the chemistry and morphology design for the desired MIP, the imprinting process can be divided into three steps, binding site design, scaffold design, and morphology design (Figure 8). The first step of imprinting is to consider the template of interest and create a binding site with functional groups corresponding to the template molecule. By studying the functional and structural characteristics of the imprinting target, and simultaneously having the operating conditions of the MIP in mind, possible polymerization mixtures are chosen. The interaction between template and functional monomer can be either covalent or non-covalent. This is then reflected in the type of binding occurring in the resulting binding site in the polymer matrix. One approach taking advantage of both covalent and non-covalent imprinting is the so called hybrid approach. However, for this approach the actual recognition interactions are still non-covalent. [75] An additional significant imprinting technique of interest for research groups is metal ion imprinting and metals can also be used for creating coordination sites for templates.[76,77] Non-covalent imprinting remains the most generally used technique, where the template of choice is mixed in a pre-polymerization mixture of one or more functional monomers and then polymerized after addition of a surplus of cross-linker. [78,79] After removal of the template by extraction the resulting polymers are generally employed in separation processes, for example as stationary phases in chromatography.

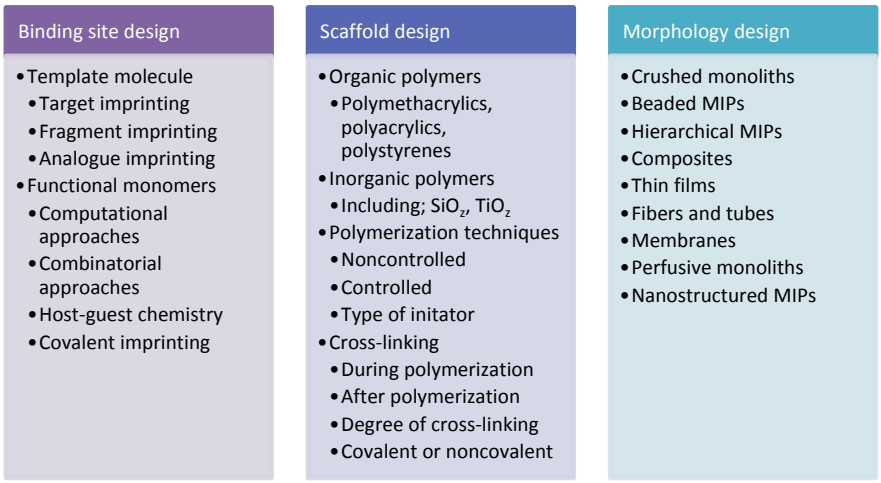

Figure 8 Overview of the steps involved in MIP design. Adapted from reference 63.

The structure of the polymer network influences the formed binding sites and hence determines the capability of the MIP to bind the imprinted molecule. The majority of MIPs reported are synthesized using free radical polymerization, where the template and functional monomer complex are mixed with an excess of a cross-linker and a solvent named porogen.[80] This kinetically controlled polymerization fixates the polymer chains in an asymmetrical glass-like structure by the cross-linker. In turn the solvent does not only serve as monomer and template solubilizer, but it is also involved in the important phase separation process to create pores in the polymer network. The formation of such pores is further necessary to enable transport, template removal and binding to the binding sites generated. A number of factors including the solvent, which affects the pore size, and surface area, which affects the amount of cross-linker, determine the resulting highly heterogeneous amorphous structures of MIPs which are illustrated in Figure 9.

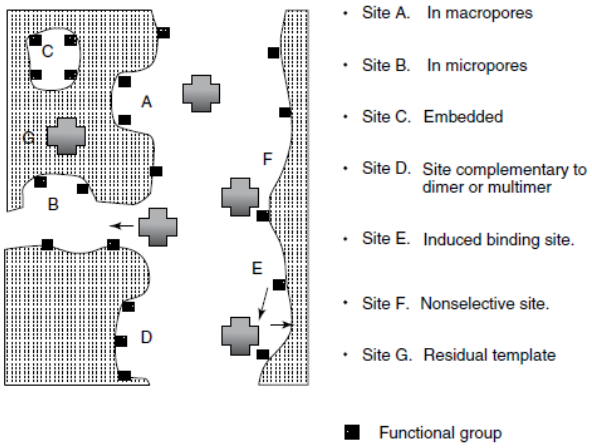

Figure 9 Schematic drawing showing possible binding sites present in a MIP.[63]

The heterogenic amorphous MIP structure exhibits some drawbacks such as template bleeding, slow mass-transfer and non-specific binding, and other MIP formats are therefore being investigated in an attempt to improve the overall performance. Suggested formats include, but are not limited to, beads, nanoparticles, membranes, films, fibers, and tubes.[81,82,83] This shows the complex mixture of different chemical and materials sciences involved in the MIP synthesis. The most important factors influencing the final MIP will be discussed in more detail in the sections below.

1.5.1. FREE RADICAL POLYMERIZATION

For large industrial scale free radical polymerization offers a straightforward technique for preparation of polymers. Because this technique displays a high flexibility in purity of the reagent and experimental conditions, the majority of vinyl polymers are for example synthesized via free radical polymerization.[84] Furthermore, free radical polymerization is compatible with a large variety of functional monomers and has a high tolerance towards additional chemicals, such as an imprinting template, making it an attractive technique for MIP formation. Not surprisingly this is reflected in the number of reported MIPs adopting free radical polymerization as the main mechanism for formation.[60]

Free radical polymerization can be divided into either a homogenous or heterogeneous reaction. A homogeneous polymerization is a so called one-phase reaction, which is independent of the number of compounds in the polymerization mixture. A well-known example of homogeneous polymerization is for example bulk. Conversely, a polymerization with more than one phase is termed a heterogeneous reaction, with important examples including emulsion- and suspension polymerizations. The three main steps involved in the chain reaction of free radical polymerization are shown in Figure 10 and will be explained in further detail in section 1.5.1.1 - 3.[85]

I	→	2R*	**Initiation**
R* + M	→	M1*	
M1* + M	→	M2*	**Propagation**
Mn* + M	→	Mn+1*	
			Termination
Mn* + MZ*	→	Mn-MZ	combination
Mn* + MZ*	→	MnH + $MZ^{=}$	disproportionation

Figure 10 Simple schematics of the main steps responsible for the chain reaction in free radical polymerization.

1.5.1.1. INITIATION

The generation of free radicals by an initiator starts the polymerization. An initiator is a compound that decays after exposure to either thermal or UV irradiation. The formed free radical then attacks the double bond of the monomer present, thus forming a free radical on the monomer *i.e.* intermediate radical. The rate of this initiator decay (υ_i) is described by;

Equation 2 $\upsilon_i = d[RM^*]/d_t = 2k_d f [I]$

Where [I] is the concentration of initiator, [RM*] the propagation species concentration with respect to time, k_d the rate or decay constant, *f* the efficiency of the initiator to propagate chains, and the 2 represents the two radicals formed per initiator compound.

1.5.1.2 PROPAGATION

The reaction of a free radical and a monomer forms a chain carrier. By addition of new monomers propagation rapidly occur causing mainly linear polymer chains to be formed. The propagation reaction can be described by the following equation.

Equation 3 $RM_n^* + M \rightarrow RM_{n+1}^*$

Where RM_n^* is the chain carrier, M free monomer and RM_{n+1}^* the formed chain carrier with an additional monomer.

The rate of propagation can be described as;

Equation 4 $\upsilon_p = k_p [M][M^*]$

Where v_p is the rate of propagation, k_p the propagation constant, [M] is the free monomer concentration, and [M*] is the concentration of free monomer radicals. The concentration of growing reactive chains is described by [M*]. By observing the decrease of monomer concentration the progress of the reaction can hence be tracked.

1.5.1.3 TERMINATION

Until the free radicals react to form covalent bonds, the propagation process runs continuously. This can normally be observed when the concentration of free radicals is high or in the case when chain transfer agents are present. The two types of termination processes include the

formation of a macro-chain by the recombination of two macro-radicals, and the disproportionation that results in a double bond and a C-H bond terminates the chain. When considering these two processes a number of possible termination reactions can take place during the polymerization including:

a) The combination of two active chain-ends
b) An active chain terminus and an initiator radical can react
c) The radical can be transferred from one molecule to another, such as initiator, monomer, solvent or template
d) Termination by reaction of an active compound with impurities present, *e.g.* free oxygen or inhibitors

The termination rate (υ_t) can be described as:

Equation 5 $\upsilon_t = 2k_t[M^*][M^*]$

Where k_t is the termination rate constant and [M*] the concentration of free monomer radicals.

When equilibrium between the production and the utilization of free radicals occur a so called steady-state has been reached which can be described as:

Equation 6 $2k_t [M^*]^2 = 2k_d f [I]$

Where k_t is the termination rate constant, [M*] the concentration of free monomer radicals, k_d the rate or decay constant, f the efficiency of the initiator to propagate chains, [I] is the initiator concentration, and the 2 represents the two radicals formed per initiator compound.

When combining Equation 6 with Equation 4 the polymerization rate (υp) can be described as:

Equation 7 $\upsilon p = kp\,[M](f\,kd\,[I]/kt)1/2$

1.5.2 IMPRINTING CONCEPTS

Multiple concept on how to establish the specific binding functionality in the cavities in the polymers have been developed. Depending on the pre-arrangement of the monomers, and the template in the pre-polymerization mixture, the imprinting is categorized as covalent, non-covalent or semi-covalent.

1.5.2.1 COVALENT IMPRINTING

Covalent imprinting was first reported in the early 1970s by Wulff *et al.*.[86] As the name suggests during covalent imprinting the template is bound covalently to the functional monomer before polymerization (Figure 11). After the formation of the polymer the covalent bonds are cleaved to release the template. This forms binding sites that are able to rebind the template via the same covalent bonds that were initially used in the imprinting step. The main advantage of covalent imprinting is that every polymerizable template results in one imprinted binding site containing functional monomers arranged in the best possible geometrical arrangement. In theory covalently imprinted polymers should therefore offer binding sites with high binding capacity and strong affinity. Furthermore, the highly stable complexes formed in the binding sites make it possible to use polar solvents without damaging the formed structure. However, the downside to the stability is the inherent slow template binding and subsequent release[87]. In spite of the advantageous attribute of covalent imprinting some disadvantages are present. One of the more serious limitations being the restricted number of chemical functional groups that can easily form the required reversible covalent bonds, with examples of suitable groups including disulfides[88], ketals[89], imines[90] and boronate esters[91]. Needless to say the number of accessible template with fitting functional groups is yet another limitation to the covalent imprinting approach. The process of removing and rebinding the template, *i.e.* creating and breaking the covalent bonds, should be quick under general process conditions, thus further limiting the application of covalent imprinting.[63] Finally important to note is that though examples of covalent imprinting can be found in literature[92,93], it has not become the first method of choice.

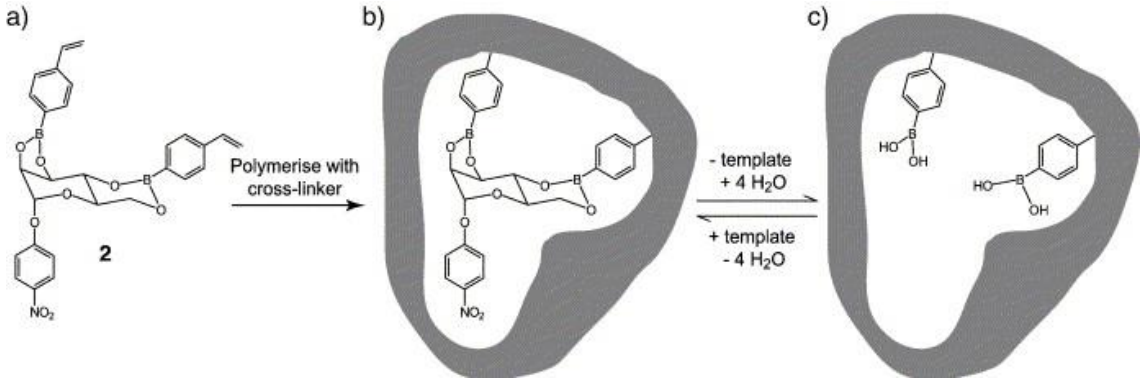

Figure 11 Imprinted 4-nitrophenyl-α-D-mannopyranoside-2,3:4,6-di-*O*-(4-vinylphenylboronate) MIP (**2**). (a) the covalent template monomer, is synthesized via condensation of 4-vinylbenzeneboronic acid with 4-nitrophenyl-α-D-mannopyranoside. (b) After copolymerization with cross-linker (divinylbenzene or ethyleneglycol dimethacrylate) the polymer is formed. (c) The template is removed by hydrolysis of the boronate ester groups and addition of 4 equivalents of water to reveal the imprinted binding site.[93]

1.5.2.2 NON-COVALENT IMPRINTING

The non-covalent technique was first introduced in the early 80s by Mosbach *et al* (1981).[94,95] In the non-covalent imprinting interactions such as hydrogen bonds, electrostatic interactions and coordination-bond formation are used as the fundamental basis, and the stability of these interactions determines the imprinting success. Because hydrogen bonds depend on both distance and direction between the template and the functional monomer, thus creating highly defined binding sites, they tend to be the primary choice of use[87]. It is fairly straight-forward to imprint lipophilic, low-molecular weight templates that contain basic or acidic functionalities when using non-covalent imprinting[60]. Because of its simplicity non-covalent imprinting has further become the preferred method of choice for synthesis of MIPs currently reported in the literature.

During non-covalent imprinting a self-assembled complex is formed between the template and the functional monomer when these are dissolved in an appropriately selected solvent. After addition of an excess of cross-linker the mixture is then polymerized resulting in an insoluble porous polymer material, containing binding sites according to the pre-formed self-assembled complex. After polymerization the template can be removed easily by using a relative mild solvent for extraction and the formed binding site is able to rebind the imprinted template, or analogues, via the same non-covalent interactions.

A variety of commodity monomers able to form non-covalent interactions can be used as functional monomers, and systems based on acrylic and methacrylic monomers, such as methacrylic acid and ethyleneglycol dimethacrylate as cross-linker, have repeatedly been demonstrated as suitable systems for MIPs. As a result numerous reports on different templates containing hydrogen bond- or proton-accepting functionalities that are imprinted with methacrylic acid have been reported in literature with one example included in Figure 12.[96]

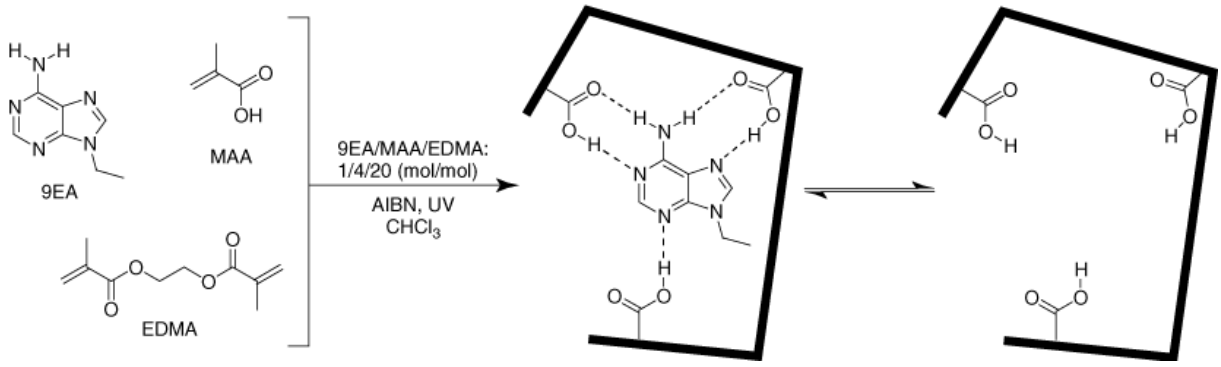

Figure 12 Non-covalent imprinting of 9-ethyladenine (9EA) with functional monomer MAA and cross-linker EDMA.[63]

The widespread usage of methacrylic acid as a functional monomer in non-covalent imprinting can be explained by the fact that it can easily form corresponding interactions, such as hydrogen bonds or hydrogen-bonded ion pairs, with the template. Furthermore, for many single systems specific binding constants are formed between methacrylic acid and the template, with values of the constant ranging from single figures up to several hundred for weak hydrogen bonds, cyclic hydrogen bonds or hydrogen interactions formed in non-polar aprotic solvents respectively.[63] In the self-assembly phase between the functional monomer and the template, methacrylic acid acts as either an hydrogen bonding donor or acceptor, hence creating ionic interactions to amines and hydrogen bonds to amides, carboxyls and carbamates. Sellergen *et al.*(1993)[97] were the first to report successful enantiomeric separations using this approach and by using enantiomeric derivates of amino acids and a number of highly selective chiral stationary phases were demonstrated.[95,97,98]

Non-covalent imprinting has been thoroughly studied using L-phenyl alanine as imprinting template in a model system. Phenomena such as band broadening by chromatography, the influence of the solvent on the ion exchange retention, protonation state effect on imprinting and photo- versus thermal polymerization, have been studied in detail and have provided a

better fundamental understanding of the non-covalent imprinting approach.[79,97,99,100,101,102] Additionally, the association constants between specific templates and methacrylic acid can easily be determined by NMR spectroscopic and chromatographic studies of the self-assembled complex in the pre-polymerization mixture. In order to improve the capacity of MIPs synthesized via non-covalent imprinting aspects of supra-molecular chemistry is considered, and has resulted in novel functional monomers that are designed to form stronger interactions with a specific template than the commodity acrylic monomers.

Despite the versatility of non-covalent imprinting, the technique displays some drawbacks like highly heterogeneous binding site distribution, low binding capacities and also, rather frequently, poor target specificity when using polar solvents like for example water. This can be explained by the fact that the interaction between templates and functional monomers are relatively weak. Subsequently one has to add an excess of functional monomer in respect to the amount of template and use low polar solvents that the maximum number of binding complexes are formed in relation to the template.[60] This leads to materials with binding sites that are not clearly defined and with an inhomogeneous distribution, because a large quantity of the functional monomer is randomly distributed in the polymer thus creating non-specific binding sites. Optimized reaction conditions that present favorable and stable pre-polymerization complexes, are therefore required to enable successful non-covalent imprinting.

1.5.2.3 SEMI-COVALENT IMPRINTING

A third imprinting approach is the semi-covalent approach which is a hybrid between covalent and non-covalent imprinting. The semi-covalent approach demonstrates similarities to covalent imprinting in the first step of imprinting, where the functional monomer is covalently bound to the template. However, the binding step displays non-covalent binding properties that are activated after the template is removed following the polymerization. The semi-covalent method can thus be considered as a mixture of both covalent and non-covalent imprinting as indicated by the name.

Semi-covalent imprinting can be divided into two types where in the first the template is connected directly to the monomer, and in the second a spacer group connects the template and monomer[62]. The first report on semi-covalent imprinting using the first approach was published

in the early 1990s by Sellergren and Andersson.[103] In this work a structural analogue of p-aminophenylalanine was imprinted and two polymerizable groups were attached to the monomer via ester bonds. Following the template removal carboxylic acid groups were then exposed in the binding site, and rebinding of the target analyte occurred via a mixture of hydrogen bonds and electrostatic interactions.[103] The second kind of semi-covalent imprinting is also known as the sacrificial spacer approach and was first established by Whitcombe *et al.* (1995)[104], who used a spacer group in the imprinting process to circumvent crowding in the binding site and promotes unrestricted rebinding of the analyte.[104] Another example of semi-covalent imprinting using a sacrificial spacer group for imprinting of cholesterol is illustrated in Figure 13.

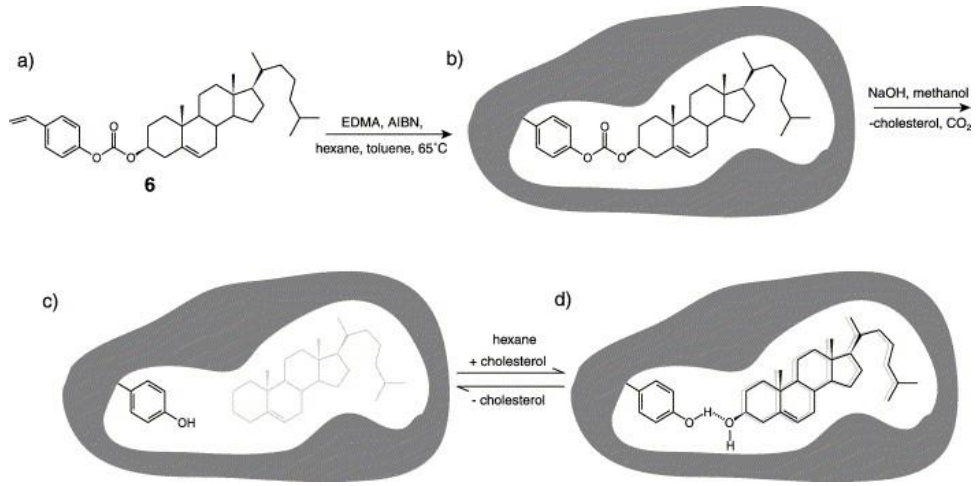

Figure 13 Imprinting of cholesterol by the sacrificial spacer (semi-covalent) method. (a) is the template monomer, cholesteryl (4-vinyl)phenyl carbonate and (b) the formed polymer. (c) template is removed by alkaline hydrolysis and (d) template rebound in the binding site. [93]

Finally, MIPs can also be prepared by additional combined techniques, including metal-ion mediated imprinting[62]. Recent advancement of such techniques has been reported by Takeuchi *et al*. (2009)[88], where covalent imprinting was initially used for the polymerization, after which the template is removed and the free functional groups in the binding sites are modified post polymerization. Analysis of the materials showed that only the post modified polymers containing the cofactor bind the target analyte to a high degree – just like enzymes are dependent on cofactors for catalytic activity.[88]

1.5.3 TEMPLATES - FROM SMALL MOLECULES TO BIOMOLECULES

The molecularly imprinting technique offers the possibility to imprint molecules ranging from small size, like acetamide, to large biomolecules, such as peptides and proteins. Furthermore, the template used for imprinting dictates the entire polymerization process; from the choice of functional monomer to the solvent system used. Hence, it is of immense importance to gather knowledge of the characteristics of the template or analyte intended for imprinting and rebinding prior to designing the imprinting process.

Synthesized MIPs that can bind not only the imprinted templates but also other target analytes or structurally similar analytes, are fundamental in the continuous development of new MIPs. One of the advantages of such MIPs is that in addition to the compound intended for rebinding in the imprinting process, other target analogues can also be used as a template for the imprinting step. Depending on the nature of the end-use template, an analogue can be a better option for imprinting for example if the template is toxic and/or very costly, can possibly cause interference or reactivity problems, or if it promotes extreme template bleeding. A suitable analogue for imprinting should fulfill a series of criteria including:

- Be accessible in large quantities to a reasonably low cost
- Be soluble in the pre-polymerization mixture
- Exhibit good cross-reactivity in the resulting binding sites

Due to these specific criteria it is easy to realize that the choice and/or the design of templates is a complicated assignment, which may include numerous repetitions and synthesis of different possible template candidates that exhibit appropriate properties. However, depending on the specificity intended for the MIP, where high specific binding of a single molecule and exclusion of templates similar in structure are necessary, it might not be possible to use analogue replacement.

One favorable approach for template design may be to synthesize libraries based on the specific functionalities of the targets. A simpler target with some, or all, functionalities may then be used for complex natural compounds that contain a limited number of functional groups. Nemoto *et al*. (2007)[105] used this method to synthesis domoic acid, a fish poison, imprinted

polymers by employing commercial available di- and triacids such as triacid pentane-1,3,5-tricarboxylic acid as templates (Figure 14)[105].

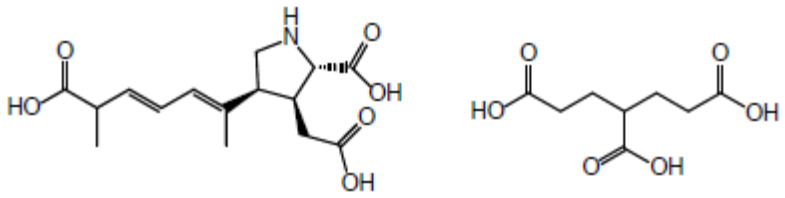

Figure 14 Left: Structure of the fish posion domoic acid; Right: Structure of the template used for imprinting, pentane-1,3,5-tricarboxylic acid

However, if the desired targets are too complex, exhibit poor solubility, are not commercially available or difficult to synthesis in large quantities the established imprinting methods are not effective. This is especially true for biomolecules, such as proteins, nucleic acids and polysaccharides. In order to imprint these compounds an aqueous environment might be necessary to dissolve and/or stabilize the target so that it is close to its natively preferred configuration. The obvious disadvantage of using an aqueous medium is that stable electrostatic interactions, the foundations of molecular imprinting, can be interrupted by water's polar influence and predisposition to hydrogen bonding. In addition, these compounds are hard to encounter in large enough quantities to enable the imprinting process. One approach to circumvent this is to use fragments corresponding to sub-structures of the target as templates for imprinting[106,107,108]. However, the obvious risk of using only parts of the target, or similar compounds, is the potential formation of less specific binding sites rather than binding sites with considerable affinity for the large biomolecule target. The first reports demonstrating this approach was the imprinting of peptides[106] and vitamins[107]. This so called epitope imprinting has further been combined with surface imprinting approaches to develop MIPs demonstrating cross-reactivity with peptides[109] and proteins[108] by using just short peptide sequences *i.e.* epitopes.

1.5.4 FUNCTIONAL MONOMERS

One of the most widely used monomers in MIP formation is methacrylic acid (MAA). Although MAA is an incredibly resourceful functional monomer in forming fine imprints, a number of other commercially available monomers may be used to form optimal interactions with different functional groups, *e.g.* monomers with amine groups for acidic functionalities on the template. Vinyl pyridine (VP) and meth acrylamide (MAAM) are examples of other commonly used functional monomers in non-covalent imprinting (Figure 15). In order to find the most favorable functional monomer for the template of choice, theoretical predictions based on structural observations of the intermolecular interactions can be used. A number of different techniques can be used to gain information of the self-assembled complexes formed in the pre-polymerization solution, *e.g* data modeling NMR, UV-vis, or IR [79,110,111,112]. However, trial and error is still commonly used and has proven to be effective in the design of MIPs with noteworthy imprinting effect, especially in combination with high-throughput techniques.[63,91]

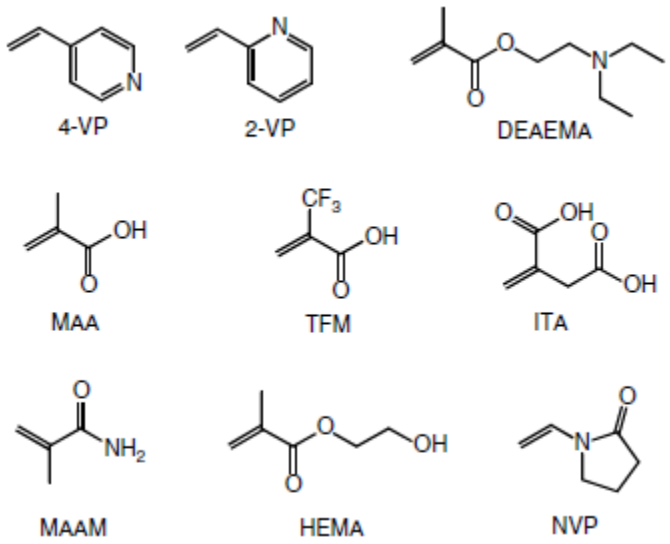

Figure 15 Examples of commercially available functional monomers used in non-covalent imprinting.[63]

As mentioned earlier non-covalent imprinting comes with some limitations, including the heterogeneous binding site distribution, poor binding capacities and reduced performance in polar solutions. One contributing factor to the limitations observed is that the commodity monomers used for imprinting do not always provide an optimal fit for the templates. The development of new functional monomers for use is hence of great interest for the imprinting community. One approach to improve the recognition properties of MIPs could be to mimic

techniques used in nature, in the sense that recognition is achieved by a number of different functional monomers, and not only by one single functional monomer. In Figure 16 an example of a MIP synthesized using a mixture of functional monomers is illustrated. Despite the theoretical simplicity of this approach, it is associated with some drawbacks due to the fact that the fundamentals of non-covalent imprinting are the self-assembly principle. When adding more than one monomer to the pre-polymerization mixture the number of possible interactions also increases. Therefore the self-assembly equilibria present in the pre-polymerization solution do not only consist of template- monomer complexations, but also direct monomer-monomer interactions.[63]

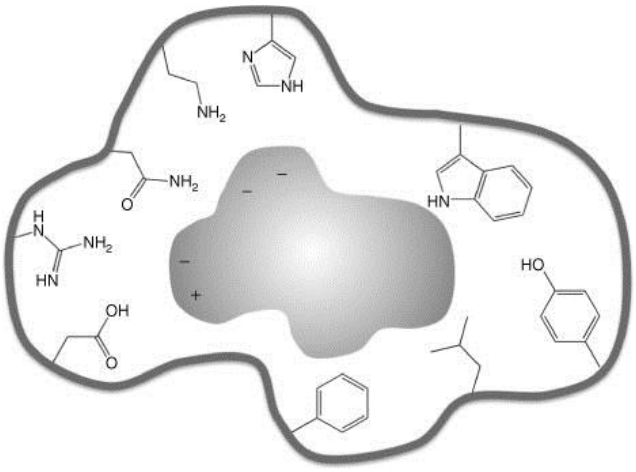

Figure 16 A schematic drawing of an amino acid analogue monomer imprinted MIP.[63]

Even if a limited number of commodity monomers have been used for most of the successfully synthesized MIPs, a stoichiometric non-covalent imprinting could offer improved MIPs with either higher selectivity or better binding capacity. This can be obtained by using host-guest or supramolecular chemistries inspired by Nature.[66] MIPs synthesized with stoichiometric non-covalent imprinting exhibit relatively clear-cut binding sites with the functional groups mainly placed within them. Takeuchi *et al*. (1995) were one of the first to report MIPs synthesized using this technique, using a designed bis(acrylamido)pyridine monomer to imprint a barbital (Figure 17)[113]. For this MIP the designed monomer has an hydrogen bonding donor-acceptor-donor element that corresponds well to the acceptor-donor-acceptor element in the template.

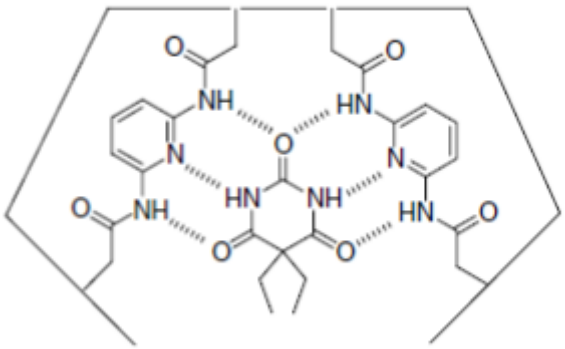

Figure 17 Imprinted barbital and the proposed formed binding sites.[63]

1.5.5 CROSS-LINKER SYSTEMS

Another critical part in the imprinting process is the type and amount of cross-linker used, as this can have a variety of effects on the performance on the synthesized MIP. Cross-linkers are responsible for the three-dimensional structure of the MIP by "freezing" the self-assembled complex formed in the pre-polymerization mixture. Hence, a high level of cross-linking produces rigid binding sites, as well as satisfactory porosity, in the polymer and thus influence the selectivity of the resulting MIP.[60] Depending on the ratio of cross-linker to monomer different polymer morphologies can be obtained, ranging from gel-like polymers to stable macro-porous materials when using low and high amount of cross-linker respectively. MIPs also obtain their characteristic mechanical stability from the cross-linker systems, making them insoluble in organic solvents, which is a prerequisite for many applications.

In addition to the template the solvent system also influences the choice of cross-linker, with organic solvent and aqueous solutions requiring different cross-linkers. Examples of cross-linkers for imprinting in aqueous solutions are acrylamide, N,N'-methylenebisacrylamide (MBA), N-isopropylacrylamide (NIPAm) (Figure 18), whereas ethylene glycol dimethacrylate (EGDMA) and divinyl benzene (DVB) are commonly used cross-linkers for imprinting in organic solvent (Figure 19).

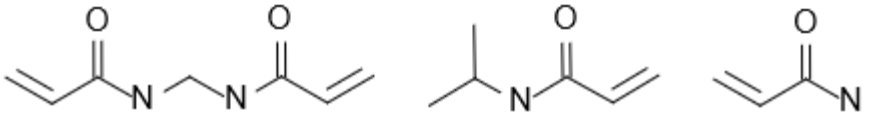

Figure 18 Structure of some cross-linkers commonly used for imprinting in aqueous solutions. From left to right; N,N'-methylenebisacrylamide, NIPAm,acrylamide

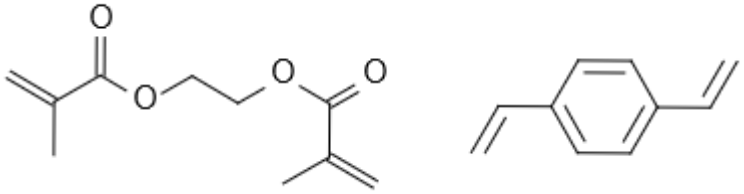

Figure 19 Structures of EDMA and DVB commonly used cross-linkers in organic solvents.

A number of factors influence the choice of (co-)monomer – cross-linker systems. Firstly, one has to consider the reactivity of the double-bonds in the monomers, which for homogeneous polymerization to occur should be related. Secondly, depending on the polarity of the pre-polymerization complex a suitable co-monomer – cross-linker system has to be selected. For a rather weak pre-polymerization complex a less polar environment is required compared to when a stronger complex is used. For non-covalent imprinting in organic solvents the most frequently used monomer systems include:

- Hydroxyethylmethacrylate (HEMA)/EGDMA
- Methacrylic acid (MAA)/EGDMA
- Styrene/DVB

The HEMA/EGDMA system exhibit polar characteristics and is therefore a suitable choice for pre-polymerization complexes with strong affinity between template and monomer. However, because of the OH-group present in HEMA, polymers synthesized with this system have a tendency to swell in contact with aqueous solutions. A less polar alternative is the MAA/EGDMA system. Since EGDMA is a di-ester of MAA and ethylene glycol the double bond reactivity of EGDMA and MAA is comparable. This in addition to the mechanical and thermal stability of the MAA/EGDMA complex, has made it the most frequently used monomer

system to date. Additionally, MAA/EGDMA also shows further advantages in offering an overall good wettability and fast mass transfer. For template/functional monomer complexes with weaker interaction characteristics, the styrene/DVB cross-linker system is more appropriate because of its less polar characteristics compared to MAA/EGDMA. Thus, the crosslinker system does not interfere with the self-assembly of the template and functional monomer.

1.5.6 INITIATORS

The polymerization technique is selected according to the characteristics of the chemicals used. In theory this means a variety of techniques can be used, but free radical polymerization as previously discussed, is by far the most frequently used method. Initiation of free radical polymerizations can be done by a large variety of initiators. The class of azo-initiators, which cleave bonds homolytically, is frequently used in molecularly imprinting with two of the more common examples of azo-initiators shown in Figure 20. There are two ways in which decomposition can occur, either by thermal or photochemical initiation, depending on the initiator used in the synthesis.

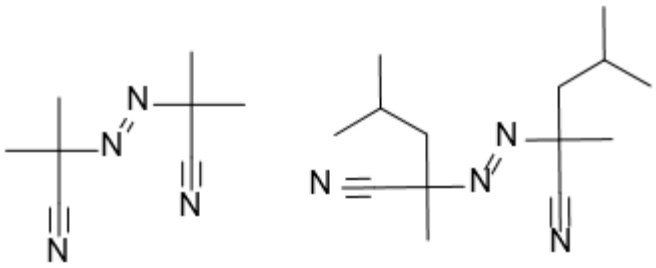

Figure 20 The two frequently used azo-initiators AIBN (Azobisisobutyronitrile) and ABDV (Azobisdimethylvaleronitrile). Decomposition temperature AIBN: 60 °C, ABDV: 45 °C) or photochemically.

1.5.7 SOLVENTS

The terms solvents and porogens are both used during discussions about molecular imprinting, but one should differentiate between the two. The purpose of a solvent is to solubilize all the

reactants in the polymerization mixture, as well as to disperse the produced reaction heat. The solvents used should also promote a homogeneous cross-linking in the polymer. It is more complicated to choose the optimal solvent in precipitation polymerizations compared to bulk polymerization, as in the first step the solvent should exhibit good solubilization for the reagents but the synthesized polymer should be insoluble to promote precipitation.

A porogen on the other hand, is a solvent that promotes pore formation in the polymer matrix during the polymerization. In molecular imprinting pore formation is a crucial part of the synthesis, because pores are necessary to enable the template to access the cavities. Even if the porogen used for synthesis influences the pore size, the formed polymer matrix generally has a broad pore size distribution, and the pore size of MIPs may vary from micro- to meso- to macro-sized pores. To better understand the influence on the final MIPs various commonly used solvents in molecular imprinting have been carefully studied. Table 1 summarizes the properties of a number of solvents.

Table 1 A summary of the properties of a number of solvents.

	Disperion	**Polar**	**Hydrogen bonding**	**Hydrogen bonding capacity**
	δ D	**δ P**	**δ H**	
MeCN	15.3	18.0	6.1	Poor
Benzene	18.4	0	2.0	Poor
$CHCl_3$	17.8	3.1	5.7	Poor
CH_2Cl_2	18.2	6.3	6.1	Poor
Cyclo-hexane	16.8	0	0.2	Poor
Ethy acetate	15.8	5.3	7.2	Poor
DMF	17.4	13.7	11.3	Moderate
H_2O	15.5	16.0	42.4	Strong
HOAc	14.5	8.0	13.5	Strong
Isopropanol	15.8	6.1	16.4	Strong
MeOH	15.1	12.3	29.3	Strong
THF	16.8	5.7	8.0	Moderate
Toluene	18.0	1.4	2.0	Poor

One very important aspect to consider when choosing a solvent for imprinting, is that it should not interfere with the self-assembled complex in the pre-polymerization mixture. With the complex in mind the solvent should be chosen by, not only considering solubility properties but also the properties summarized in Table 1. When studying the H-bond and polar terms and the H-bond capacity of the solvents listed it is evident why imprinting in *e.g.* water or MeOH is generally avoided. Although MeCN and DMF exhibit high polar terms compared to water and MeOH their H-bond capacity is less pronounced. It is hence of great importance to know what type of interactions are present in the selected system. Electrostatic interactions may be disrupted by polar solvents, whereas solvent with a high dielectric constant could have an influence on the forces between a positively and a negatively charged compound. Conversely, hydrogen bonds are susceptible to protic solvents and even though it is acknowledged that the structure of the MIP is significantly influenced by the porogen used, its effect on the actually imprinting step is more disputed.

1.6 Different Formats and Formation of Molecularly Imprinted Polymers

MIPs exhibit a number of advantages over biological receptors, including their good mechanical and chemical stability, low preparation cost and broad possible operating conditions. However, as mentioned earlier MIPs also display some limitations *e.g.* heterogeneous binding site distribution, poor selectivity, binding capacity and accessibility of binding sites, and further improvements are highly desirable.[102] Overcoming current MIP limitations provides an interesting possibility for developing new applications, and the development of new formats and synthesis techniques aimed at improving the homogeneity of the binding sites, the binding capacity, the mass transfer and the accessibility, is constantly ongoing in the MIP community. There are a variety of different types of MIPs that can be synthesized depending on the intended end purpose. Commonly used formats include monolithic bulk polymers, polymeric membranes or polymeric beads.

1.6.1 PARTICLES

Monolithic MIPs are synthesized via free radical bulk polymerization. When using a high cross-linking level solid polymer materials are formed displaying good mechanical and thermal stability. Bulk polymerization is an uncomplicated technique where all the components are mixed and polymerized in one pot. During synthesis the template, functional monomer, co-monomer (if used) and cross-linker are dissolved in the chosen solvent, and with either thermal or photochemical initiation the polymerization is started. After polymerization and incubation the resulting material is isolated from the polymerization tube. The formed polymer is crushed and sieved into the desired particle size and the template and unreacted compounds are removed by soxhlet-extraction. The common particle size for chromatographic applications is between 26 and 36 µm, whereas a larger particles (36-63 µm) are used for solid-phase extraction (SPE).

Because of its simplicity, bulk polymerization is an attractive method for preparing MIPs but as mentioned before it also exhibit some limitations. Apart from the heterogenous binding sites formed because of the nature of the polymerization, the work-up of the monolith polymer also contributes to limitations of the method. When crushing the monolith into the desired particle size, irregularly shaped and sized particles are formed (Figure 21). This may cause problems when using the MIPs in a number of end-applications, for example through the creation of back-pressure in HPLC column when the particles are used as stationary phases or the generation of light-scatter in optical applications. Another crucial weakness of bulk polymerization is that a large part of the polymer is lost during the crushing and sieving process. Additionally, the heterogeneously distributed binding sites, make complete template removal very challenging. This is due to the highly cross-linked polymer matrix that partly or completely captures the template, leading to template bleeding hence causing false positives in the analysis or to an irreversible blocking of the binding sites respectively.

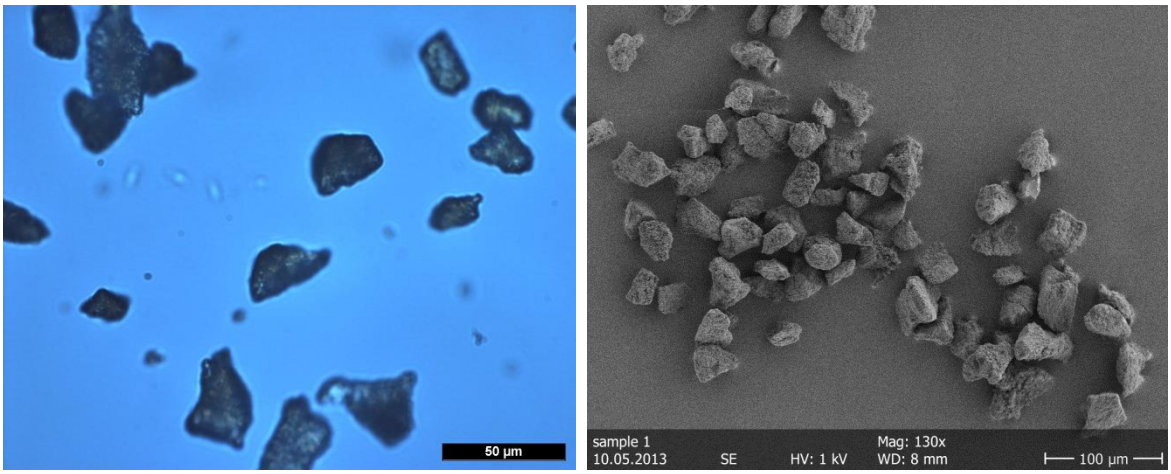

Figure 21 Microscopy (left) and scanning electron microscopy (SEM) (right) pictures of acetamide imprinted bulk polymers.

To overcome the limitation of bulk MIPs there is growing interest in developing MIPs with spherical shapes and narrow size distrubutions. Taking inspiration from conventional polymer chemistry, suspension and emulsion polymerization techniques have hence been tried for MIP production.[81,114] Another early approach tested for synthesizing uniform and spherical particles is to use a silica mold and graft a layer of MIP on the surface. This technique has further been developed and for more current application it is more common that the initiator or the template is immobilized on the surface of porous silica, and the polymerization is taking place in the pores. Following the polymerization the silica mold is removed by etching, leaving mirrored porous polymer beads as illustrated in Figure 22.[109,115,116,117]

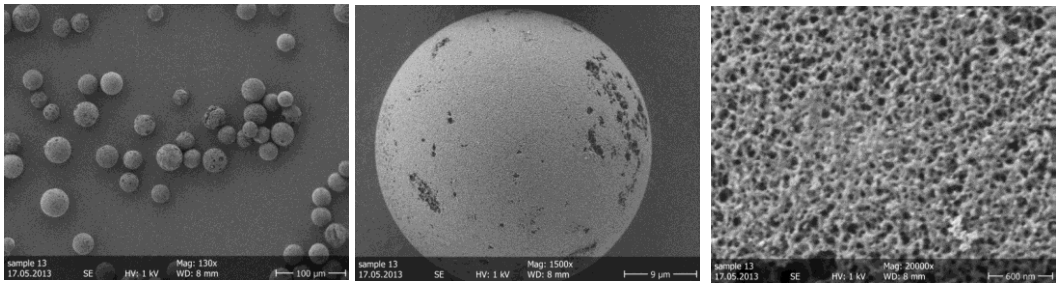

Figure 22 SEM pictures of acetamide imprinted porous silica particles after etching of the silica.

In the attempt to develop spherical MIPs other techniques have also emerged, such as mini-emulsion where polymer beads are synthesized by a two-phase polymerization and inverse micro-emulsion technique that Shea *et. al*. (2010) used to synthesize nanoparticles imprinted with a hydrophilic peptide.[63,118] Precipitation polymerization is one technique which has proven

useful for molecular imprinting and the synthesis of spherical particles, and because of its simplicity become a commonly used technique. This technique can also be used to prepare nanoparticles, submicron particles, micro-gels as well as particles within the micron range. However, to circumvent agglomeration a high dilution is necessary, resulting in a potentially lower yield of the process.[119,120,121,122]

1.6.2 IMPRINTED POLYMERIC MEMBRANES

By customizing the characteristics of membranes a number of possible applications are anticipated in *e.g.* industrial separations and purifications. Depending on the mode of transportation the imprinted membranes can be divided into different categorizes namely adsorption and active transport (Figure 23). The mechanism of transport can be either retention of template transport by adsorption, or active transport where the template more easily travel trough the membrane compared to other compounds. The first technique used to synthesize molecularly imprinted anisotropic microporous membranes, was a combination of a phase inversion technique in combination with the imprinting procedure in one step. By using this method membranes with affinity for templates ranging from small molecules to proteins have been produced. However, in an attempt to overcome robustness limitations often observed in one-pot synthesized membranes, composite membranes have gradually gained importance and are becoming the more common alternative for manufacture of imprinted membranes. Rather than one-step synthesis the imprinting step for composite membranes is separated from the phase inversion, or the synthesis method used for membrane formation. Most commonly the imprinting is carried out by either grafting the MIP onto the membrane surface or by incorporating pre-synthesized particles into the membrane.[63,123]

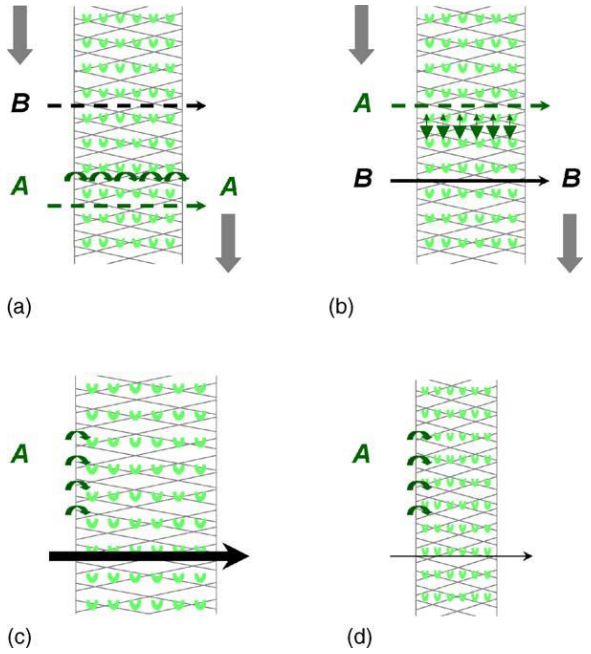

Figure 23 Summary of separation mechanisms for molecularly imprinted membranes: (a) a concentration gradient drives the transport of A , whereas the nonspecific transport of B is hindered, (b) MIP binding sites at the surface bind A and hinder the transport through the membrane, while the transport of B is driven by diffusion, (c) increase of the membrane permeability, caused by *e.g.* increased membrane swelling, (d) decrease of the membrane permeability, for example, caused by *e.g.* decreased membrane swelling as a result of A binding to MIP sites.[123]

1.7 APPLICATIONS

One area where MIPs have proven to make an impact is in SPE and trace analysis. Molecularly imprinted solid phase extraction (MISPE) offers a reproducible and effective solution opportunity to improve sample extraction techniques, capable of enriching as well as cleaning up samples for analysis, a step that often prolong the sample preparation procedure.[124] A variety of examples of MISPE applications have been published to date,[125,126,127,128] and the range of successful application demonstrate that MISPEs can in fact compete with, and in some cases even outdo, the performance of some generic techniques such as enrichment based on metal mediated chelation, Lewis acidic metal oxides (*e.g.* TiO_2), and strong cation-exchange chromatography. The successful applications of MIPs in MISPEs can clearly be observed in the large number of published papers coming up to almost 200 publications during 2010[63]. Examples include the analysis of the tobacco-specific biomarker NNAL in urine samples and the selective enrichment of sulfopeptides in a strong pH-dependent manner.[125,128] The factors contributing to the success of MISPEs are the clear-cut procedure in how affinity for specific

compounds or group of compounds can be synthesized, as well as the relative inexpensive production and the robustness of the materials.

Another area in constant need of improved and economically viable affinity-based separations is large-scale processes in many chemical industries. Some examples include water purification from toxic organic pollutants and purification of raw material or unwanted compounds, such as flavors, in food processing. This is especially true for API purification in the pharmaceutical and biopharmaceutical industries, where delays caused by purification problems may lead to increased production costs and, more importantly, longer time for the drug to reach the market.[63] MIPs could also possibly be a tool for second generation development of a drug production process optimization.

Reports on successful examples of MIP applications in a variety of industries have already been published to date. One such example addressed the challenge faced by governmental water purification of removing trace amounts of endocrine disrupters from water. These chemicals affect the hormonal, *i.e.* endocrine, system in mammals and can create adverse developmental, immune, neurological and reproductive effects.[129,130] In an effort to use MIPs for removing trace amounts of endocrine disruptors that slip through the current purification system, MIPs targeting chemicals mimicking the natural female hormone 17-β-estradiol have also been synthesized and evaluated. Mattiasson with colleagues (2007) demonstrated that effective purification of wastewater down to trace levels of 17-β-estradiol was possible with the help of MIPs.[129] Another application where MIPs have proven useful is the removal of riboflavin, vitamin B2, from beverages.[131] A general occurring problem in the beverages industry is chemical processes that influence the quality of the product. Flavor in for example beer, milk and wine can be compromised by photo-oxidizing reactions driven by riboflavin, and these products are hence normally placed in light-protected containers. For the removal of riboflavin a very selective purification process is needed so that no other substances are removed unintentionally. Riboflavin template water-compatible MIPs was synthesized and demonstrated to effectively remove roughly 90% of the riboflavin present in beer.[131,132] Cobalt imprinted MIPs with excellent selectivity for iron-containing ions could possibly be applied in reactors in nuclear power plants to improve the decontamination processes. Metal oxides are formed when structural materials in *e.g.* water cooling systems, come in contact with coolant agents, causing these oxides to entrap the radioactive ions. MIPs could offer a competitive alternative to current

techniques which often require time-consuming and expensive cleaning procedures for removal of radioactive ions.[91]

Due to the high binding selectivity MIPs could potentially be used as chemical sensors and assays. As a result a large number of publications on MIP-based sensors have been published over recent years for intended use in areas including electrochemical, mass-sensitive, optical and surface Plasmon resonance analysis[133,134,135,136,137]. The examples mentioned combine different MIP materials, ranging from meth- acrylates, styrene based, polyurethanes to inorganic sol-gel materials, with quartz crystal microbalance (QCM). QCM devises combined with MIPs were first developed by Dickert et al. (2000) with the application for observing engine oil degradation and the polyaromatic hydrocarbon concentration in water.[138] Other examples of sensor applications are MIPs with fluorescence characteristics. This can be achieved by either imprinting of a molecule that is fluorescent or by using a fluorescent component, *e.g.* a functional momoner, in the MIP itself.[139,140,141] Furthermore, MIPs could potentially replace expensive antibodies in immunoassays by offering advantages like improved stability, as well as functionality in both aqueous and organic media. However, the inherited disadvantages, like the necessity for template molecules for MIP production and the cross-reactivity often correlated with MIPs, limit the applications to date.[142,143] Although a large number of successful MIP-based sensors have been published to date, further studies investigating the binding mechanisms between the MIP and the analyte, as well as the selectivity and evaluation of roughness, should be conducted. Furthermore, in order to achieve real implementations in industry of MIP-sensors, the gap between fundamental research and application needs to be eliminated, such as scale-up and reproducibility. With this in mind, pharmaceutical industry with its strict quality controls conditions and high purity requirements could benefit from MIP-based sensors to detect trace amounts of unwanted compounds.[144]

MIPs applied in therapeutic applications have also been investigated, for example for drug delivery using hydro-gels and in a more recent approach where the MIP itself acts as an API capable to inhibit the enzyme trypsin.[122,121,145,146] As demonstrated in this section the possible applications for MIPs range over a large number of possible applications. However, work presented in this thesis focuses primarily on MIP applications in the pharmaceutical industry.

1.7.1 MIPS AS CATALYSTS

MIPs share some similarities with enzymes in the sense that they are capable of binding specific molecules. This in turn could present the opportunity to use MIPs in organic synthesis and in catalysis. Because of the flexibility in the design of MIPs and their robustness, industrial process applications in synthesis and catalysis are further appealing. One part of this work will hence focus on examining the possibility to use MIPs as catalysis for peptide synthesis in the pharmaceutical industry.

Development of innovative catalysis with improved performance in the chemical industry is of high interest, as the quality of catalysts influences the advancement of both research and production synthetic work. Synthesized catalytic materials may exhibit a high catalytic activity combined with substrate, reaction, and stereoselectivity equivalent to that of enzymes. In addition, synthetic catalysts can be superior in availability, stability, and in the number of different reactions catalyzed. The development of synthetic catalysts has shown great progress in recent years and a large variety of compositions have been used to synthesize new catalytic materials, such as crown ethers, cyclodextrins, or large ring systems. Synthetic polymer materials offer an exciting opportunity to prepare new synthetic catalysts because they generally exhibit high chemical, heat, and solvent resistance, and are because of their widespread use in industrial applications suitable for scale-up processing. Compared to other host materials polymers are inherently more complex systems because of their three-dimensional structure. However, the same characteristics also give them a clear advantage as some of the distinctive capabilities of enzymes are directly linked to their polymeric nature. A successful synthetic catalyst should exhibit well-defined cavities according to the substrate or transition state structure, with stereochemically directed functional groups. Additionally, the interactions binding the template can be rather complicated and it should therefore be possible to incorporate a mixture of binding types such as, electrostatic, hydrogen bonding or hydrophobic interactions, in the cavities. MIPs fit these criteria and are therefore an interesting option for producing synthetic catalyst materials.[63,66]

The first applications of MIPs as a synthetic catalysts in chemical synthesis were the so called micro-reactors[147,148,149]. Micro-reactors function as catalysts in the sense that they provide orientation for selective reaction, *e.g.* enantiomeric product excess. In order to achieve this, the

MIP is imprinted with the reaction product and when the precursor is inserted in the formed cavity the formation of the imprinted structure is favored over other possible reaction products. Successful examples of stereoselective cyclo-addition reactions were performed using MIPs to form cyclopropanedicarboxylic and cyclobutanedicarboxylic acids [147,148]. Other examples using MIP micro-reactors have been published with chiral cavities for asymmetric synthesis, and the first enantioselective synthesis of an amino acid, L-DOPA[149,149]. Another interesting approach for using MIPs as catalysts is called anti-idiotypic, which has been used in assisting drug-screening. Yu *et al.* (2002) demonstrated this approach by imprinting a proteinase kallikrein inhibitor, and using the synthesized MIPs as reactors for the production of new enzyme inhibitors.[150]

MIPs applied as catalysts can be divided into two main types. One is the imprinting of low-molecular-weight templates, which exhibit good catalytic activity when used in solutions. The templates can be the reaction template or, if information is available, a transition-state analogue, and the end product. These MIPs can in some ways be considered to be synthetic metalloenzymes.[63] Examples of application of such MIP-based catalysts include catalysis of hydrogenation reactions and Suzuki coupling reactions[151,152]. The second main type of MIP-based catalysts is bio-inspired and aim to mimic enzymes. The goal for such catalysts is to produce a MIP with a binding cavity having enzymatic features which promotes stabilization of the transition state and stereoselectivity. A number of attempts have been published with MIPs mimicking the actions of for example chymotrypsin and more recently carboxypeptidase A, with the latter showing equivalent and even better catalysis compared to the corresponding enzyme[153,154,155]. However, although MIPs have been demonstrated to exhibit comparable catalytic activities to enzymes, further improvements are needed before MIPs will be superior to enzymes in respect of reaction variety, increased reaction rates, stereochemical selectivity, and yield.[63,66]

1.8 High-throughput Synthesis and Screening Techniques

In order to produce customized MIPs for specific targets a rapid polymer development and optimization is required. The normally used bulk polymerization procedure is rather time-consuming and is hence not effective for screening of possible polymer compositions when

short time-lines are required. Improved performance of MIPs can be accomplished by combined screening techniques, using scale-down mini-MIPs based on the monolithic bulk approach[156,157]. Mini-MIPs enables an opportunity to do a thorough and methodical screening of possible polymer compositions within a reasonable time-frame.[91,158] To facilitate the analysis the smaller material quantities, MIPs are normally synthesized and tested for imprinting effect by equilibrium batch re-binding in multi-well plates. The only difference between the mini-MIPs compared to the normal bulk polymerization material is the amount synthesized, which offers the opportunity to partially automate the polymerization process. Plate technology, in particular plate readers and pipetting robots, is useful for high-throughput synthesis and screening of mini-MIPs (Figure 24). However, one shortcoming shared with the monolithic approach is template removal where the extensive washing process considerably slows down the optimization of the MIP composition.[159]

Explorasep™ is a commercially available screening method based on the cross-reactivity exhibited by MIPs, *i.e.* structures other than the imprinted template also show affinity. Explorasep™ are based on 96-well plates with MIP libraries consisting of different functional monomers, *e.g.* acidic, basic or neutral compounds. Re-binding tests can quickly provide results on suitable affinity materials for different compounds.[160]

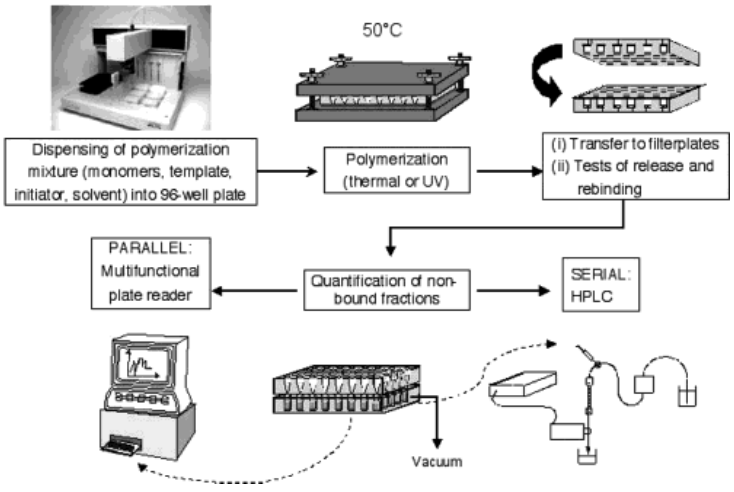

Figure 24 Example of a high-throughput synthesis and screening setup for MIPs.[158]

1.9 ORGANIC SOLVENT NANOFILTRATION

Another upcoming technique showing promising performance for separation and purification purposes in the pharmaceutical and fine chemical industries is organic solvent nanofiltration (OSN). The removal of genotoxic impurities and the development of sustainable, green processes are hence areas of great interest in these industries.[161,162] Strict regulations for genotoxins in APIs and general high costs for down-stream separation processes further calls for new innovative techniques to solve these challenges, with OSN and MIPs potentially suitable techniques for use.[163,164,165,166]

Nanofiltration has already been successfully applied in a range of aqueous application including water softening and waste-water treatment. However, polymeric membranes developed for aqueous applications can display some disadvantages when exposed to organic solvents and some chemical compounds, in degradation and chemical instability, aging, and plasticization.[167] A new generation of polymeric OSN membranes has been developed specifically for use in organic solvents and they demonstrate improved chemical stability as well as pH resistance.[168] Depending on the separation requirements the molecular weight cut-off of the membranes can be modified accordingly by altering the ratio of the solvents used in the membrane synthesis.[169] Furthermore, separations using OSN membranes can be performed at room temperature, allowing OSN to be used in separations with thermally sensitive compounds.[170] A number of examples where OSN membranes have been tested for use can be found in literature, including examples in API purification, catalyst recycling, peptide and oligonucleotide synthesis, and solvent recovery.[9,171,172,173]

Similar to MIPs, membrane separations is an interdisciplinary field, involving materials science, chemical synthesis and characterization, and process engineering. The separation range for currently commercially available OSN membranes range between 100-2000 g mol^{-1}, However, to date the mechanism of how the separation in fact works is not entirely understood. The association between the size of the compound and the related rejection is rather strong, resulting in better rejection of larger compounds than smaller ones[174]. However, other factors such as the charge of the compound and interactions occurring between the compound, the solvent and the membrane have also been proven to influence the performance of the membranes.[175,176,177] Membrane performance is generally described with regards to two main

factors the membrane selectivity and the flow. In membrane terms the flow is measured in flux, or permeation rate, where the flux is defined as the volume of solvent passing through the membrane per unit area and unit time (L m^{-2} h^{-1}), and the permeability is defined as the flux including the dependency on operating pressure (L m^{-2} h^{-1} bar)$^{-1}$). The membrane selectivity is defined as the rejection, which is expressed as a percentage, of a compound that is unable to pass the membrane. More specifically the rejection is determined as $((C_f - C_p)/C_p)*100)$, where C_f is the concentration of compound in the feed and C_p being the concentration of compound in the sample which passed the membrane also known as permeate. Another well-recognized term used for expressing a given membrane's separation performance is the molecular weight cut-off (MWCO). The MWCO value can be determined from rejection of compounds with increasing molecular weights plotted versus rejection in a so called MWCO-curve.

OSN membrane filtration can be performed as either dead-end or cross-flow operation (Figure 25). In dead-end filtration, pressure pushes the feed over the membrane perpendicular to the surface, and in cross-flow the solvent is passed in a loop enabling the feed to be added in a flow pattern that is parallel to the membrane surface. However, the permeate still passes through the membrane in a perpendicular fashion. This enables better stirring and minimizes the build-up of a concentration gradient on the surface and means that the operation is less prone to fouling.

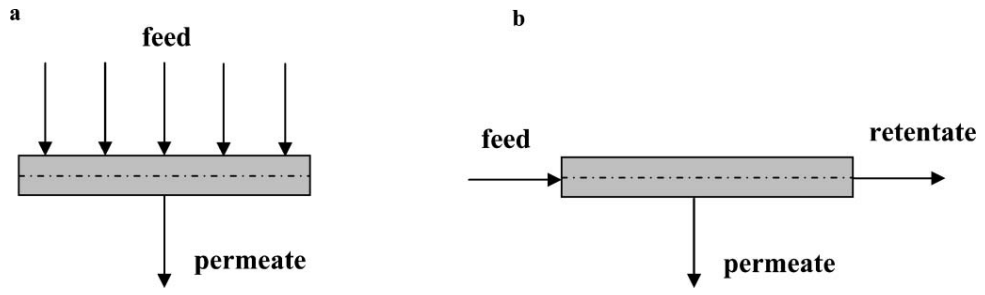

Figure 25 Schematic drawings of dead-end (a) and cross-flow (b) filtration.[170]

Fouling is phenomena often seen in aqueous membrane filtration and is described as the decrease in performance of the membrane because of the accumulation of suspended or dissolved compounds on the surface, and in the pores of the membrane.[178] One process potentially contributing to fouling is concentration polarization, which is the gathering of retained compounds as a layer at the interface between the membrane and the feed solution. This leads to a higher concentration of the compound at the surface compared to the rest of the

feed solution which in turn can have a negative effect on both the flux and the rejection performance.[170]

For membrane preparation a number of different characteristics are taken into consideration for the choice of materials, chemical and thermal stability, commercial availability and price, and film forming properties. Consistent purity to enable FDA approval is further important factors for applications in the food and pharmaceutical industries. One of the most flexible, cost efficient and reproducible methods for preparation of polymeric asymmetric membranes is phase inversion. Asymmetric membranes consist of a porous layer with a skin-layer on top. The permeability and selectivity are influence by the thin skin-layer depending on the composition, thus affecting the overall performance. Thin film composite (TFC) membranes represent another central class of polymeric membranes. In TFCs an ultra-thin layer functions as a separation barrier on top of a porous support, the ultra-thin layer can have the same or different chemical composition or structure. Structural differences between asymmetric membranes and TFCs are illustrated in Figure 26. For the synthesis of the separating ultra-thin layer of TFC membranes dip-coating or interfacial polymerization is used, whereas the support-layer is synthesized via conventional phase inversion. The inherent layered design of TFC membranes offers the possibility to vary the chemistry and performance, as the two layers can potentially be optimized independently to obtain optimal membrane performance.[170,179]

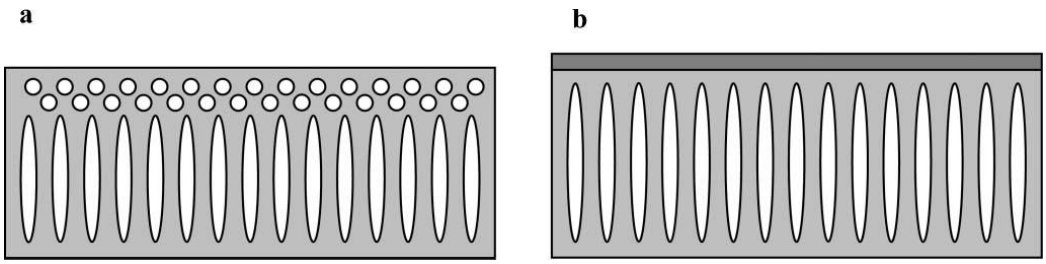

Figure 26 Schematic drawing of the main polymeric membrane types in OSN, (a) integrally skinned asymmetric membrane, (b) thin film composite (TFC) membrane.[170]

1.10 THERAPEUTIC PEPTIDES IN THE PHARMACEUTICAL INDUSTRY

The field of peptide therapeutics has gained increasing interest in the last years from the development expansion in the late 1990s, with a number of successful peptide therapeutics, including glucagon-like peptide 1 receptor (GLP-1R) agonists, having reached the market. [180]

Peptide therapeutics are generally administered intravenously, but can also be either injected, inhaled, or orally delivered. In the early clinical development phases, metabolic disease and oncology are the main peptide therapeutic applications, whereas in the later clinical development phases infectious disease replaces metabolic disease. Peptide therapeutics come in a number of different formats such as linked to small molecules, biopolymers, carbohydrates, lipids, polyethylene glycol (PEG) or proteins. Additionally, peptide therapeutics can exhibit different modes of action including cell-targeting or cell-penetrating. Because of the general short half-lives of peptides in the body, sometimes just minutes, the therapeutic applications of peptide therapeutics are limited. However, by attaching the peptides to molecules such as PEG or immunoglobulin the half-life can be considerably prolonged to days or even weeks.

The development of intracellular targeted peptides is currently limited due to the cellular membrane hindering many drugs and peptides to cross over the membrane. Peptides that are specially designed to penetrate the cell membrane and target intracellular processes are hence of great interest to the pharmaceutical industry. The peptides that have overcome this hindrance are in general cationic or amphipathic molecules, for example peptides integrating sequences called cell-penetrating peptides. The progress in this area is reflected in the number of peptides integrating other compounds entering Phase I studies in recent years.[180]

As mentioned earlier peptide therapeutics can act on a wide range of targets. Analysis of the peptide therapeutics pipeline shows that roughly 10% of the targets are bacterial, fungal or viral organisms. The mode of action of the therapeutic peptides vary from ion channels, intracellular targets, non-enzymatic transmembrane proteins, non-transducing receptors, pumps and transporters, and receptor enzymes with each group compromising less than 10% of the development compounds. The by far most common targets are cell surface molecules, especially the G-protein-coupled receptors taking up 39% of the peptides in the clinical pipeline. This observation can be explained by the fact that the easy access position and wide range of functions associated with the G-protein-coupled receptors, thus making them attractive drug targets.[180,181]

Because of the powerful potential drug applications, peptide therapeutics also exhibit great commercial value as seen in the increase in global sales between 2009 and 2011[180]. The development of new peptide therapeutics further offers a considerable commercial value for the

pharmaceutical industry in a variety of applications in markets such as diabetes and oncology drugs.

New peptides with innovative structures and mode of actions, for example peptide-drug conjugates and controlled peptides, are also developed as the next generation of peptide therapeutics. Such developments could possible expand the number of targets and applications for peptide therapeutics in the future. One interesting design is to freeze the peptides in specific conformations, leading to high-affinity compounds that are stable, less subjected to degradation and with improved pharmacological characteristics. By controlling the structure of the peptides the cell membrane permeation can also be improved, enabling intracellular processes to be successfully targeted. Although the potential of structurally designed peptides have been recognized, the lack of fundamental understanding of cell permeability processes makes it difficult to develop these peptides.[180,182]

1.10.1 SOMATOSTATIN AND SOMATOSTATIN ANALOGUES

Somatostatin is a cyclic tetradecapeptide with the sequence H-Ala-ly-Cys-Lys-Asn-Phe-Phe-Trp-Lys-Thr-Phe-Thr-Ser-Cys-OH (Figure 27). There are two forms of somatostatin produced by tissue-specific protelytic cleavage of a widespread pro-hormone precursor present in mammals. One is somatostatin-14 and the second somatostatin-28, containing 14 and 28 aminos acids respectively. The bioactivity of somatostatin is limited by its fast proteolytic degradation in the blood, where the half-life in plasma is approximately 1 minute.[183] The broad spectrum of biological activity of somatostatin can be divided into four processes at a cellular level, including neurotransmission, grandular secretion, smooth muscle contractility, and cell proliferation.[187] Hence, the synthesis of somatostatin analogues exhibiting increased half-life is of great importance for drug applications. Somatostatin is generally synthesized using solid phase techniques for peptides, however, the yields are somewhat limited and the product contains relatively large amounts of impurities. This is not uncommon when using solid phase technique, and in the case of somatostatin synthesis dimerization is also observed.[184]

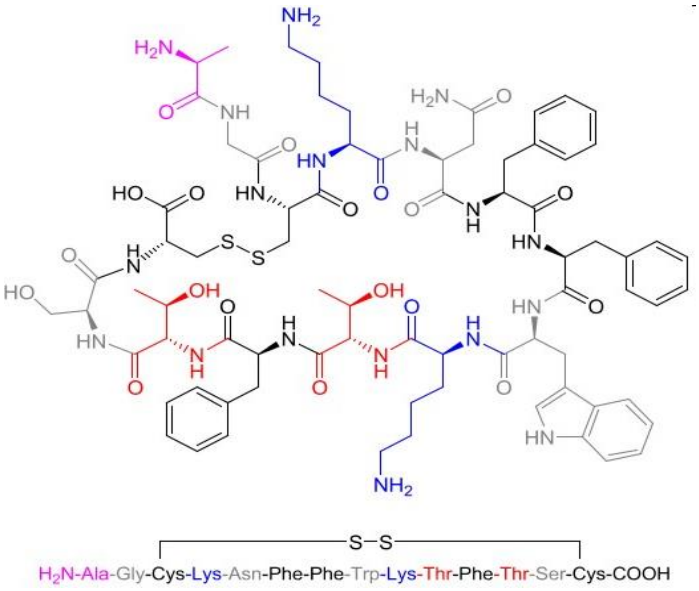

Figure 27 Structure of somatostatin.

Depending on the chemical type of the active ingredient or the mode of action for treatment of a specific condition, an API can be categorized in one or more drug classes. Somatostatin is a hormone which is synthesized by the hypothalamus, pancreas and gastrointestinal tract and was first discovered as in inhibitor of growth hormone release, but is now recognized to be involved in a number of gastrointestinal processes. The gastrointestinal processes are mediated via high-affinity membrane receptors present in different density in the tissue. A schematic drawing of the mode of action for Somatostatin is illustrated in Figure 28. For example somatostatin acts by inhibiting the growth hormone release from the anterior pituitary, and insulin and glucagon from the pancreas. Furthermore, somatostatin decreases the release of most gastrointestinal hormones as well as lowering the gastric acid and pancreatic secretion. Somatostatin has also been used to lower bleeding from esophageal varcies using its capability to decrease abdominal blood flow. Somatostatin is also present in a number of locations in the nervous system and displays neural control over a large number of physiological functions. With this broad spectrum of effects in mind it is not unexpected that somatostatin has been the focus of many pharmaceutical research studies. Additionally, analogues of somatostatin have also been used for treatment of vasoactive and intestinal peptide secreting tumors, carcinoid tumors, gucagonomas tumors in the pancreas, and various pituitary adenomas, non-cancerous tumors in the pituitary gland. Somatostatin analogues have also been proven effective for treatment of conditions where growth hormone is over-secreted.[185,186,187] Somatostatin analogues are also leading the way in demonstrating the growing potential for the development of peptides for rare diseases including the unique somatostatin receptor agonist pasireotide, which is the first FDA

approved drug for Cushing's syndrome (currently in Phase III for acromegaly, a syndrome cause by excess production of growth hormone).[180]

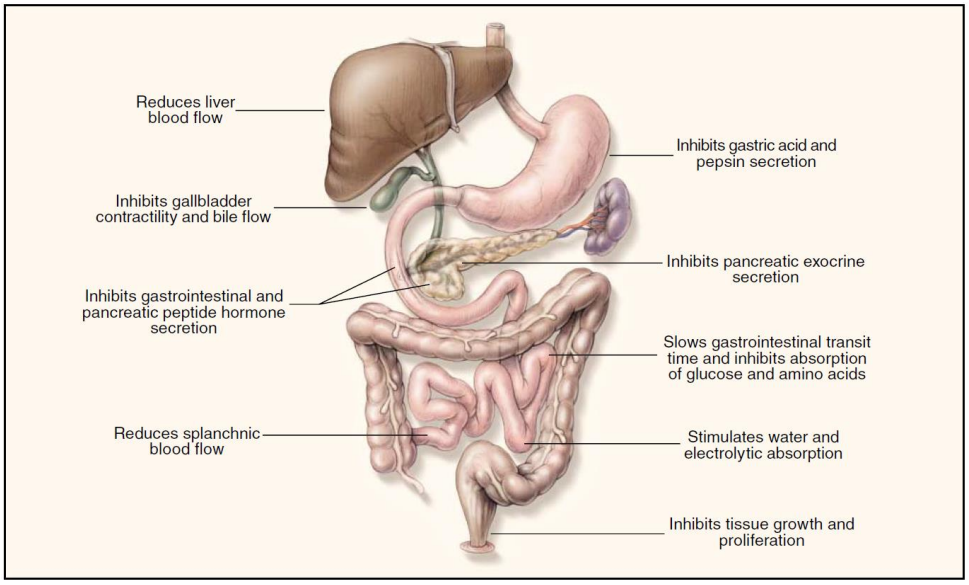

Figure 28 Gastrointestinal actions of somatostatin. [188]

1.11 CHARACTERIZATION TECHNIQUES

There are a number of different polymerization techniques that can be used to make MIPs. These polymerization techniques also offer a possibility to accumulate useful information about the properties of the materials according to the different modes of preparation. This is especially important as the chemical and morphological traits of MIPs are challenging to characterize in detail because the imprinting takes place at molecular level. Some of the main characterization techniques used for MIP characterization are discussed in details in the sub-sections below.

1.11.1 HIGH PERFORMANCE LIQUID CHROMATOGRAPHY AND MASS SPECTROMERTY

High performance liquid chromatography (HPLC) is an analytical separation technique that provides an efficient peak-resolution in a relatively short amount of time. The general setup of an HPLC consists of a continuous or discontinuous pump, a sample injector, a column filled with stationary phase, and a detector. The pump pushes the mobile phase against high pressure

creating a constant flow of the mobile phase, transporting the injected sample over the column where it is separated. The detector transforms the measured characteristics, commonly mass or volume based concentration, into an electronic signal. A commonly used concentration-based detector is the diode-array detector (DAD) where the measured absorption signal is converted by a diode array. The difference between a DAD- and a normal spectrometer-detector is that the entire UV/VIS spectrum is scanned rather than just one single wavelength, thus different wavelengths are measured in parallel. This provides the possibility to demonstrate the results acquired in a three-dimensional chromatogram presenting information about the sample's absorption, retention time, and wavelength. By alternating the polarity of the stationary and mobile phases separation of the analyte can be achieved. There are two common stationary phases used for HPLC analysis called normal- and reversed- phased. Normal-phase consists of a polar stationary phase in combination with a non-polar mobile phase, whereas reverse phased is a non-polar stationary phase combined with a polar mobile phase.

In the MIP field HPLCs are used for evaluating the performance of the imprinting. However, the performance of MIPs are not evaluated by using HPLC in the conventional way to separate components in a mixture but rather by using the MIP as the stationary phase to investigate binding capacity. During testing empty HPLC columns are slurry-packed with the MIP materials and then applied as the stationary phase in the analysis. A void-marker that is not retained on the column, *e.g.* acetone, is initially injected to determine the dead volume. The imprinted template, or a structurally related compound, are then injected and the retention times for the void-marker and the template are compared. In case of a well-functioning imprinting the template compound will be retained longer in the column than other control compounds, because the specific binding will outperform the non-specific binding resulting in longer retention times[87]. HPLC analysis is limited in that extensive peak broadening and tailing are commonly observed features when analyzing MIPs, due to the heterogeneous distribution of binding sites[189]. Additionally, to make sure that the retention observed is a result of the imprinting effect, the same analysis is implemented using a control NIP. Based on the information attained from HPLC important characteristics of the MIP can be calculated, including the capacity factor k, imprinting factor IF, and separation factor α as defined in Equation 8,Equation 9,and Equation 10 below.

The capacity factor is calculated according to Equation 8 below.

Equation 8 $k = (t_R - t_0)/t_0$

Where t_R is the retention time of the template and t_0 the retention time of the void marker. When the capacity factor for both MIP and NIP is calculated, k_{MIP} and k_{NIP} respectively, the imprinting factor of the MIP can be defined according to Equation 9.

Equation 9 $IF = k_{MIP}/k_{NIP}$

The separation factor can be calculated from the capacity factors from two different compounds k_1 and k_2, when a mixture of compounds is injected on the MIP packed column and the two resulting peaks show sufficient resolution (Equation 10).

Equation 10 $\alpha = k_2/k_1$

The resolution and retention times are strongly affected by the mobile phase used for HPLC analysis. This is because the stationary phase is less flexible than the mobile phase, therefore the selection of mobile phase is essential for a satisfactory analysis. Generally organic solvents are considered to be the most suitable for low to moderately polar templates, however, the retention times may be improved by using aqueous solution. The drawback when using aqueous mobile phases is that the retention time of polar templates decreases.[60]

1.11.2 Scanning Electron Microscopy

A scanning electron microscope (SEM) forms an image by scanning a probe (a focused electron beam) across a sample. By interacting with a thin surface layer, a couple of micrometers maximum, a signal is detected from low energy secondary electrons emitted from the sample surface. From this procedure compositional and topographic information about the sample can be obtained. The main components of a SEM are normally gathered in one unit formed of the electron optical column with an electron gun and three condenser lenses, which forms the electron beam, and the general source for display and electron beam scanning. A raster, placed above the sample, scans the electron beam. The SEM has higher resolution and a larger depth

of field in comparison to reflected light optical microscopy. The specimen chamber, where the sample is mounted, is large enabling samples of a large size to be analyzed and furthermore the sample preparation is uncomplicated, as long as the sample can handle high vacuum and drying. Because of their non-conductivity most polymer samples need conducting coatings, or low accelerating voltages, in order to avoid them from getting charged by the beam. The qualitative interpretation of the resulting SEM pictures is straightforward as they produce a picture of the sample in the same direction as the electron beam. The interaction with the beam, the detector and signal processing used, all have an influence on the formed SEM pictures.

A number of phenomena arise when a sample is hit with the electron beam, namely; secondary electrons are emitted, emission of backscattered electrons, absorption of electrons, X-ray formation, and occasional photon emission. The mentioned events are all correlated and to some degree affected by the sample's topography, atomic number and chemical characteristics. However, topography is the largest influence on the formed backscattered, secondary and absorbed electrons, therefore these are the main phenomena used for studying the surface of a sample. Beam electrons that are elastically scattered by the nuclei and leave the surface are called backscattered electrons. These backscattered electrons hold a large amount of energy and can therefore origin from depths more than 1µm. Because the electrons leave the surface over a broad area, a good resolution can be achieved depending on the beam voltage and the characteristics of the sample. Interaction of the primary electron beam with the sample further generates secondary electrons. These are emitted from the top layer, a few nanometers, of the sample and are therefore released with low energy. The electronic circuit scanning the electron beam over the sample is hence the factor that determines the magnification and resolution of the SEM pictures. The maximum magnification achieved using SEMs is ×300 000 and the diameter of the electron beam hitting the sample gives the theoretical resolution. The practical resolution on the other hand is influenced by a number of other factors, including the sample preparation and a variety of instrumental settings, and realistically a resolution of 1 nm can be achieved under the correct circumstances.[190,191]

1.11.3 Energy Dispersive X-ray analysis

By studying x-rays emitted from SEM analysis information about the elemental composition of the sample can be obtained. This technique is called energy dispersive x-ray (EDX) analysis.

X-ray photons are created when a high energy electron beam hits a sample. Analytical details about the sample can then be gained from the subsequent x-ray energy spectrum, where the photons are recorded as sharp peaks. When the sample is hit by the high energy electron beam an inner shell electron is removed from its position, and when these excited electrons return to their ground state x-rays are released from the atoms. The produced x-rays can be divided into the two types called characteristic and continuum x-rays. The characteristics x-rays have, as the name implies, well identified energies corresponding to the atoms in the sample. Conversely, the continuum x-rays display a broad spectra of energies and represent the background in the x-ray energy spectra. The continuum x-rays are formed when the incoming high energy electrons are disrupted by scattering from the nucleus, resulting in x-rays with valuable information.

The EDX spectrometer gathers the emitted x-rays and produces an energy spectrum. Each x-ray that hits the detector creates an electron pair hole, which subsequently produces a current pulse. The number of electron pairs created is further proportional to the energy of the detected x-ray photon. After amplification of the pulses and separation according to size by a multichannel analyzer, an energy spectrum is formed. One drawback with this technique is that some of the element peaks may overlap thus causing indistinct results.[191]

1.11.4 THERMOGRAVIMETRIC ANALYSIS

Thermogravimetric analysis (TGA) is a technique that measures the weight loss of a sample as a function of temperature or time. TGA hence enables transitions, or degradation processes, in the polymers to be followed by the mass change. TGA can also be useful for determining the amount of residual silica present in composite materials. During analysis the sample is burned in a furnace under either an inert or an oxidizing environment. The heat transfer of the sample is depending on the speed of the flowing gas, and the change of mass in the sample during the analysis is measured by an electromagnetical or photoelectrical compensating scale. Based on the compensation signal the mass of the sample depending on temperature or time can be decided. By simultaneously recording the change in mass, temperatures, and heat mass transfer of the sample, information about the sample's vaporization and melting behavior, *i.e.* mass loss or no mass loss respectively, can also be determined. The mass change for polymers can be

demonstrated as either one-phase or as several phases. The mass loss (m_L) is then calculated according to Equation 11.

Equation 11 $m_L = ((m_s - m_f)/m_s) \times 100\ [\%]$

Where m_S is the starting mass and m_f the final mass.[192]

1.11.5 Differential Scanning Calorimetry Analysis

A differential scanning calorimeter (DSC) analyses the heat flow (dH/dt) of a sample pan relative to a reference pan. The DSC instrument registers endothermic and exothermic changes in the sample which in turn provide information into the glass transition temperature, crystallization, melting and decomposition of polymers. The analysis can give quantitative and qualitative information about the physical and chemical changes in the polymer (Figure 29).

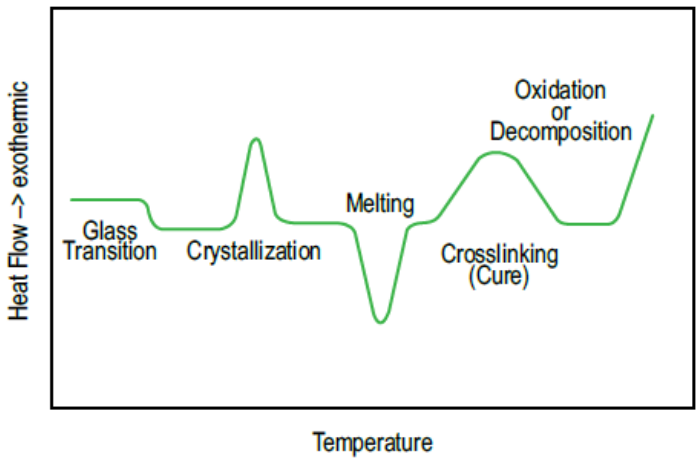

Figure 29 Typical thermogram with the main transitions observed in DSC.

1.11.5.1 Thermoporometry using DSC

DSC can also be used to measure the porosity of materials in a swollen state; so called thermoporometry.[193,194] Using thermoporometry the pore diameter of porous polymer materials can be calculated. A small specific amount of sample is weighed into the sample pan and after a specific volume of acetonitrile is added, the melting point of acetonitrile is followed and studied. In order to calculate the pore diameter[193] from the resulting DSC curves the change in temperature (ΔT) is calculated using Equation 12 and Equation 13:

Equation 12 $\Delta T = T - T_0$

Where in this case T_0 is the melting point of the used pure acetonitrile (-46 ± 0.3 ^{0}C), obtained from linear regression. By substituting the calculated ΔT value in Equation 13.

Equation 13 $Rp(Å) = (-309/\Delta T) + 13$

The constant 13 correspond to the non-freezable solvent, forming a layer at the surface of the internal pores with a thickness of 13 Å.

In addition to the pore diameter, pore volume is an essential parameter for characterization of porous polymer materials. Thermoporometry can also be used to calculate the total pore volume, *e.g.* the cm^3 pore per gram porous solid[194]. The pore volume can be calculated according to Equation 14 below:

Equation 14 $$\boldsymbol{Vp} = \frac{\boldsymbol{\Delta Hpore\ Cliq}}{\boldsymbol{\Delta Htot\ Csolid\ \rho liq}}$$

Where C_{liq} represents a known mass of liquid, ρ_{liq} is the density of the solvent, which is added to specific amount of porous solid C_{solid}. The DSC melt endotherms determine ΔH_{pore}, the pore melt peak area, and ΔH_{tot}, the combined pore and excess melt peak areas.

The ratio between the two ΔH-values is related to the amount of liquid enclosed in the pores. A number of assumptions are made for Equation 14, including a temperature independent heat fusion ΔH and liquid density, and satisfactory peak separation of the pore and excess melt peaks for separate integration. Furthermore, assumptions that the entire volume of liquid freezes and melts during the initial quench cooling and heat steps, respectively, are made and thus the amount forming the thin liquid layer at the pore surfaces is negligible.

When the pore diameter and volume are known the surface area of the sample can be determined using the Wheeler equation as detailed in Equation 15.[195]

Equation 15 Surface area (SA) = 4000 x V_p/D_p

Where V_p is the pore volume and D_p the pore diameter.

1.11.6 NITROGEN ADSORPTION

By measuring the adsorption of an inert gas, typically nitrogen, on the surface of a solid material physical gas adsorption can provide information about the morphology of a material. Depending on whether the material is porous or not, the gas is adsorbed on the surface of the pores or the outer surface. The most common method used for analyzing nitrogen adsorption is the Braunauer-Emmet-Teller (BET) method. From the resulting physisorption isotherms one can gain characterization parameters relating to the specific surface area (S_A), pore volume (V_p) and pore diameter (D_p)[196].

It is practical to divide pores according to their apparent sizes. The IUPAC classification[197] states that porous materials can be divided into the three following groups:

1) Macropores which have pores with diameters larger than 500 Å
2) Micropores which has diameters smaller than 20 Å
3) Mesopores which are used for pores with a diameter between 20 – 500 Å

By plotting isotherms based on the adsorption data obtained one can gain information of the surface area and porosity of the material. These plots are obtained by measuring the quantity of nitrogen adsorbed on a surface over a wide range of relative pressures at constant temperature. By measuring the amount of nitrogen eradicated from the sample as the relative pressure is decreased. The resulting isotherms are divided into five types as shown in Figure 30.

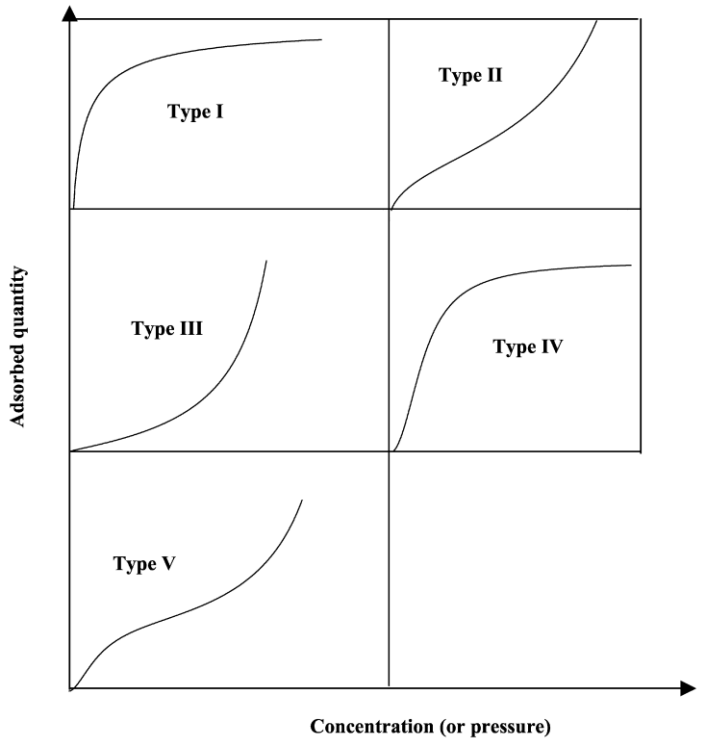

Figure 30 Adsorption isotherm types I to V, classification according to Brunauer, Emett, and Teller.[198]

The isotherm type applicable for composite MIPs and thin-walled beads is Type IV. This type is correlated with mesoporosity and generally displays hysteresis loops between the adsorption and desorption isotherms. The hysteresis loop and the steep slope at higher relative pressures are attributed to capillary condensation occurring in mesopores. Monolayer-multilayer adsorption is responsible for the initial part of the isotherm and by using the BET method the surface area of the material can be calculated.[199,200] Only a certain part of the isotherm, relative pressure (p/p_0) between 0.05 – 0.30, is taken into account for the linearity entailed for the BET plot.

The total pore volume is obtained from the assumption that the pores are filled with liquid adsorbate at a relative pressure close to unity, and by measuring the amount of gas adsorbed calculations can be made. For mesoporous materials the isotherms form a plateau at a high relative pressure ratio of $p/p_0 > 0.95$, as an indication of complete filling of the mesopores with the adsorbate liquid. By using the normal liquid density calculation (Equation 16), the amount of adsorbed nitrogen is converted into the corresponding volume and subsequently the specific pore volume can be determined.[201]

Equation 16 $V_{liq} = (P_a\ V_{ads}\ V_m)/(RT)$

Where P_a and T are ambient pressure and temperature and V_m is the molar volume of liquid nitrogen (34.7 cm^3/mol).

Given that pores which would not adsorb nitrogen below a relative pressure of 1 have a negligible contribution on the overall pore volume and surface area of the material, an estimation of the average pore size can be obtained from the pore volume. Assuming cylindrical pore geometry Equation 17 can be used to determine the average pore radius (r_p);

Equation 17 $r_p=(2*V_{liq})/S$

Where V_{liq} is derived from Equation 1 and S is the BET surface area.

The pore size distribution is defined by the distribution of pore volume relative to the pore size. It is commonly acknowledged that the desorption, rather than the adsorption, isotherm is more fitting for the evaluation of the pore size distribution for a sample. The desorption isotherm is closer to the real thermodynamic stability because it displays a lower relative pressure, therefore resulting in a lower free energy. The Barrett, Joyner and Halenda (BJH) method is a common way to calculate pore size distribution from the resulting isotherms.[202] The BJH method works under the assumption that the initial relative pressure $(P/P_0)_1$ is close to unity, and all pores are filled with liquid. At the surface of the largest pores a layer of nitrogen with a thickness of t_1 is physically absorbed. As P/P_0 decreases the nitrogen is evaporating from the inner capillary with a radius r_K. The correlation between the pore volume V_{p1} and the inner capillary volume V_K is given by Equation 18:

Equation 18 $V_{p1} = (V_{K1}\ r^2_{p1})/r^2_{K1}$

When the relative pressure is lowered from $(P/P_0)_1$ to $(P/P_0)_2$ a volume V_1 will desorb from the pore surface. This represents not only the volume in the pores decreasing but also a subsequent reduction in thickness of the adsorbed layer by an amount Δt_1. As the relative pressure decreases the average change in the thickness is $\Delta t_1/2$. The pore volume of the largest pore can therefore be expressed as detailed in Equation 19:

Equation 19 $V_{p1} = V_1 (r_{p1}/(r_{K1} + \Delta t_1/2)^2$

Where V_{p1} is the pore volume, r_{p1} the pore radius, r_{K1} the capillary radius, and Δt_1 the difference in thickness.

This process is repeated when the relative pressure is repeatedly decreased. The BJH method offers a way of computing the cumulatively summed up pore areas for every step in the desorption process.

1.11.7 ELEMENTAL ANALYSIS

One technique commonly used to obtain insight into a material's qualitative and quantitative elemental composition is elemental analysis (EA). EA is based on the combustion of a dry sample in an environment containing an excess of oxygen. From the resulting combustion products the composition can then be determined based on calculations. EA is a useful technique for determination of polymerization completion, as well as chemical composition of MIPs. By comparing the EA results and the theoretic calculated polymer composition from the components in the polymerization mixture, assuming a quantitative yield of polymerization to obtained values from EA, the degree of inclusion of the monomers can be determined. A high yield of monomers included in the final polymer is indicated by an agreement of the theoretical and measured values.[203] Unfortunately the sensitivity of the EA technique is not good enough to determine the residual template remaining in the MIP.[87]

The theoretical molecular mass of the repeat unit can also be calculated from the molar ratio of the compounds, including monomer, co-monomer, cross-linker, and their specific molecular weight as detailed in Equation 20 .

Equation 20 $\boldsymbol{M\ (repeat\ unit) = \sum_i ai * Mi}$

Where *a* is the relative amount and M is the molecular mass of the compound *i*.

When all the sources have been considered the mass-percentage of a specific element in the MIP can be calculated as detailed in Equation 21.

Equation 21 $$\%\,(\boldsymbol{element}) = \frac{\sum \boldsymbol{Ni} * \boldsymbol{ai} * \boldsymbol{M}(\boldsymbol{element})}{\boldsymbol{M}(\boldsymbol{repeat\ unit})}$$

Where *Ni* is the number of atoms in the compound and *a* is the relative amount and M is the molecular mass of the compound *i*.

2 OBJECTIVE

Impurities in APIs can cause undesired and even toxic effects in humans, therefore the control and selective removal of these compounds are crucial. Thus in order to ensure that the APIs that reach the market are safe regulatory authorities issues guidelines limiting the allowed amount of trace impurities in APIs. Especially genotoxic impurities have gained increasing attention over the last decade by both regulatory agencies and the pharmaceutical industry.

With the increasing concern of control and removal of genotoxic impurities in combination with the recent regulation and guidelines presented by regulatory agencies in the US and Europe, require control of potential genotoxins in drug substances to be limited to levels of ppm. In order to comply with the strict regulations pharmaceutical companies have employed a range of approaches including re-design of processes to avoid generation of genotoxins, alteration of process parameters to reduce impurities to acceptable levels, increased process understanding to prove that genotoxin cannot be formed or is effectively removed and toxicity studies to demonstrate that genotoxins are not harmful at the low levels envisaged. If genotoxins are formed despite the introduced controls the drug substance may still be viable for use after removal of the harmful material. However, as extremely low contamination levels are required, efficient impurity removal and high accuracy low level analysis is crucial. Hence with new guidelines the need for new innovative, selective and efficient purification techniques increases, and provides an opportunity for emerging technologies to fill this need.

Two emerging separation techniques, indicating promising performance in lab-scale studies, are MIPs and OSN. MIPs can be designed to selectively bind to specific impurities hence enabling specific removal of a selected genotoxin. OSN separates solutes primarily based on steric factors and as many genotoxins are small (commonly 50-150Da) compared to drug substances (commonly 250-1000Da) a large separation potential is often present. Thus, these techniques could possibly be beneficial for API purification.

This work was part of a large European project NEMOPUR, New Molecular Purification Technology for Pharmaceutical Production, with the aim to develop new generation of technologies and processes for more selevtive, sustainable and energy efficient separation for the pharmaceutical industry. In the project collaboration partners from academia, small to

medium enterprises as well as large pharmaceutical companies representing the end-users, were working together. The project was designed to take advantage of the academic research expertise in combination with the industrial experience in developing new purification techniques that will meet the need of the pharmaceutical industry, focusing on MIPs and OSN.

For the work presented in this thesis the implementation of MIPs for different applications in the pharmaceutical industry was studied in detail. Within the framework of the project two impurities were chosen for concept testing, acetamide a small genotoxiv impurtiy and somatostatin a cyclic peptide. This thesis is further divided into three parts with the first section studying the synthesis and characterization of new MIP based scavengers for the removal of genotoxic impurities, the second part detailing the development of a new high-through-put screening method by grafting of MIPs onto polymeric membranes, and the last part investigating the synthesis, optimization and use of MIPs as catalysts for the synthesis of a cyclic peptide (Somatostatin).

MIPs have previously demonstrated good imprinting of small compounds, therefore removal of acetamide down to stringent levels might be a suitable application. However, for implementation in pharmaceutical industry the MIPs have to demonstrate high selectivity and loading capacity in order to limit any API loss in the removal process, thus new MIPs demonstrating those characteristics will be developed. Furthermore, the objective is to demonstrate that the newly developed MIP based scavengers can be applied over a broad range of compounds and API solutions, so in addition to acetamide other impurities with relevance to the pharmaceutical industry will be investigated.

One bottleneck with MIP synthesis is the screening process to obtain high selectivity. For implementation of MIP based scavangers in pharmaceutical industry the tedious monomer screening process for composition optimization should be made more efficient in order to meet tight timelines. Hence, a new more time-efficient HTS screening method based on grafting MIPs on membrane surface will be developed.

Cyclic peptides display some advantages over linear peptides, including stability because of their resistance to proteases and efficient crossing of cell membranes. Thus, they are of great interest to the pharmaceutical industriey. Although peptide macrocycles are found in many natural products, current synthetic methods are inefficient, resulting in low yields, and are in

many cases not economically sustainable. Developeing a robust, large-scale manufacturing process might be challenging depending on the peptide synthesized, where a number of protecting groups, coupling and oxidation chemistries is needed. Many cyclic peptides are first synthesized as linear and then consequently folded stepwise to get the right configuration. For minimization of API peptides loss during synthesis and purification further work in process development is needed.[204] Thus, new peptide imprinted MIPs will be developed for process optimization of cyclic peptide synthesis, where the MIP based scavengers act as catalysts promoting cyclisation of the peptide.

3. RESULTS AND DISCUSSION

3.1 ACETAMIDE IMPRINTED POLYMERS

For removal of acetamide from API-solutions imprinted polymers were prepared. In order to synthesize polymers with a high capacity for pharmaceutical applications different formats were compared.

The first generation of polymers prepared was in the bulk format. This is the most commonly used format synthesizing molecularly imprinted polymers and can easily be used for chromatographic testing of recognition and selectivity properties of the polymer. For the work presented common commercially available monomers and cross-linkers for facilitating future scale-up processes were used.

The evaluation of the bulk polymers included employing them as a stationary phase in HPLC analysis, batch rebinding test followed by LC-MS analysis and solid phase extraction experiments evaluated by LC-MS.

In order to increase the loading capacity other formats where prepared and evaluated. For a material with increased porosity, polymers prepared via precipitation polymerization were synthesized and thoroughly characterized. Subsequent testing with batch rebinding experiments followed by LC-MS analysis was performed. Furthermore pore-filling of a solid silica support, which after etching procedure provided uniformly shaped porous particles was investigated. Also this material was characterized and tested with batch rebinding test followed by LC-MS analysis.

3.1.1 MONOLITHIC POLYMERS VIA BULK-POLYMERIZATION

Free radical solution polymerization initiated by UV-light was employed for the bulk polymer synthesis.

3.1.1.1 COMPOSITION OF THE BULK POLYMERS

To meet the criteria set in the project for new effective and cost efficient purification techniques for the pharmaceutical industry, common commercially available monomers and cross-linkers were chosen.

A well-described procedure for synthesizing imprinted polymers is based on a pair of these monomers and cross-linker, namely methacrylic acid (MAA) and ethylene glycol dimethacrylate (EGDMA) respectively.[205,206,207,208] The polymerization is initiated by either heat or UV-light. The monomers used for the bulk polymers presented in this work, MAA and methacrylamide (MAAM), have also proved to exceptionally complement the hydrogen bond donor-acceptor motif in acetamide, which offers the possible binding sites formation of binary hydrogen bonds between the monomer and acetamide as shown in Figure 31. [209,210,211,212,213]

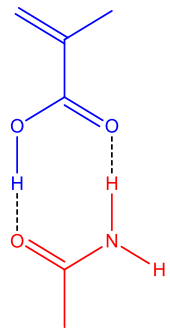

Figure 31 Host-guest interactions between the functional monomer MAA and the template acetamide.

The porogens were selected considering the solubility of acetamide as well as the polarity of the porogen in its role as a solvent. Toluene was selected for its low polarity index 2.4 in order to facilitate the host-guest interactions but because of some limitations in solubility of acetamide, acetonitrile (polarity index 5.8) was also selected (Table 1).

3.1.1.2 PREPARATION AND TESTING

In total four MIPs with corresponding NIPs were synthesized by UV-initiated polymerization at 15 °C for 24 hours, followed by curing at 60 °C for 48 hours. (see Table 2 for compositions). The template was extracted with soxhlet apparatus and the amount of extracted acetamide was

quantified with LC/MS. In total 83% of the template was extracted, which is in accordance with previously published literature for bulk polymerizations.[214]

Table 2 Composition of the acetamide bulk polymers.

	Monomers	Stoichiometry	Porogen
PA1	T/MAA/EDGMA	1/4/20	MeCN
PAN1	MAA/EDGMA		
PA2	T/MAAM/EDGMA		
PAN2	MAAM/EDGMA		
PA3	T/MAA/EDGMA	1/4/20	Toluene
PAN3	MAA/EDGMA		
PA4	T/MAAM/EDGMA		
PAN4	MAAM/EDGMA		

In the first step the polymers were evaluated with HPLC analysis. After slurry-packing the polymers in columns the retention of acetamide by the MIPs compared to the control polymers (NIPs) was tested. Further analysis was performed to determine the selectivity towards acetamide over other amides. The amides selected for the selectivity test were; formamide, acrylamide, benzamide, methacrylamide and N-tert-butylacrylamide (Figure 32).

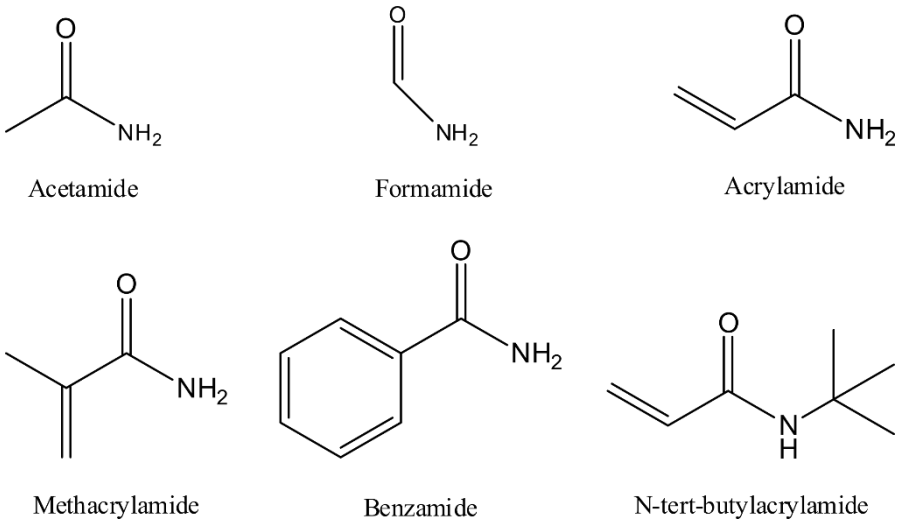

Figure 32 The template acetamide and the amides used for the selectivity test.

The obtained HPLC chromatograms and retention factors are shown in Figure 33 and Figure 34 respectively. The polymers PA1 and PA3 containing methacrylic acid as the functional monomer, demonstrated a higher retention time of the template acetamide compared to the corresponding NIPs, as displayed in Figure 33 and from the calculated k-values.

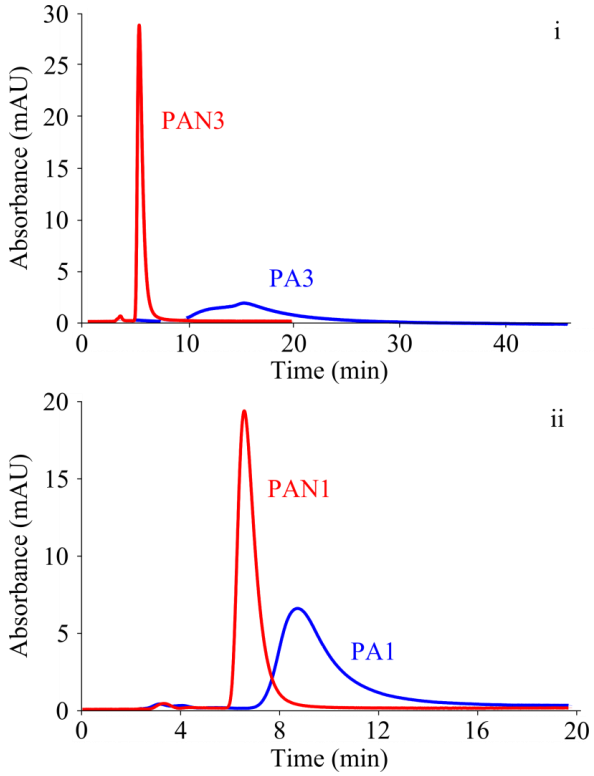

Figure 33 HPLC chromatogram for the polymers PA3 and PAN3 (i) and PA1 and PAN1 (ii). (red curve NIP, blue curve MIP). 10 µL 10 mM acetamide solution was injected on the column, monitoring the absorbance at 220 nm with a flow rate of 0.5 mL min^{-1} using MeCN as mobile phase.

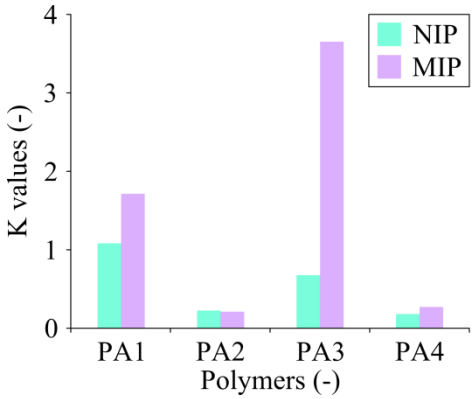

Figure 34 k'-values for the acetamide selective polymers calculated from the obtained retention times from the HPLC chromatograms.

To evaluate the selectivity performance of the synthesized MIPs other amides were injected onto the column and their retention times were analyzed with HPLC. The resulting chromatograms are shown in Figure 35 and Figure 36. Formamide was only tested on PA3 and the obtained HPLC chromatograms are shown in Figure 37. From the obtained retention times the k-values were calculated for each of the tested amides, the results are displayed in Figure 38 and Figure 39.

Upon evaluation of the chromatograms and k-values it can be concluded that the imprinting step of the two polymers PA1 and PA3 was successful. From the results it is evident that PA1 and PA3 contain imprinted binding sites complementary to the target genotoxin acetamide. The lack of imprinting in polymers PA2 and PA4 containing the amide functional monomer can be explained by the prevalence of carboxylic acids to form interactions with amides compared to the weak tendency amide- amide interactions. This is evident when comparing the dimerization constant of amides and carboxylic acids, where amides display a significant lower constant.[215]

Although both PA1 and PA3 display imprinting effects, PA3 demonstrates superior performance compared to PA1. The better retention of acetamide compared to the other amides tested and the characteristic broad and strongly tailing peaks are results of the better imprinting of PA3. The broad and strongly tailing peaks are due to the overloading of the low abundance high affinity binding sites in the polymer.[216]

The better imprinting results for PA3 compared to PA1 may best be explained by the use of the low polar solvent toluene. Because of the low polarity no competing forces are present that can disrupt the formation of the complex between template and functional monomer. Based on the results obtained polymer PA3 was considered to be the most suitable polymer and was further evaluated for its capability to scavenge acetamide from a model API and acetamide mixture.

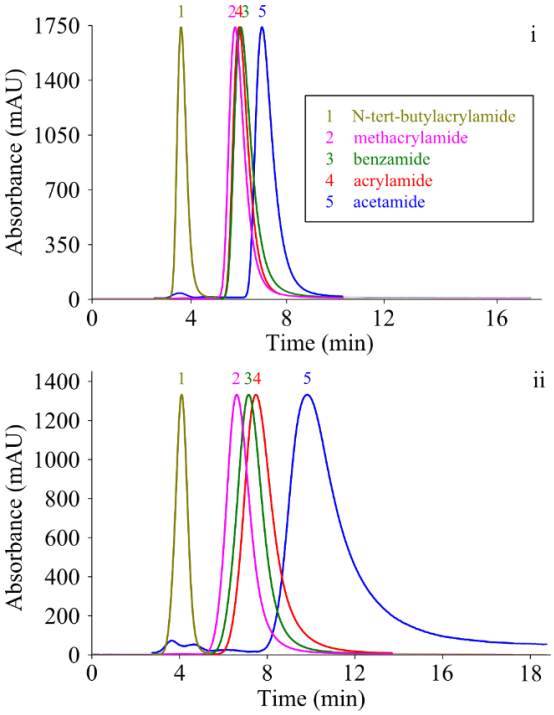

Figure 35 HPLC chromatograms for selectivity test 1 for PAN1 (i) and PA1 (ii). 10 µL of 10 mM solutions was injected on the column, monitoring the absorbance at 220 nm with a flow rate of 0.5 mL min^{-1} using MeCN as mobile phase.[11]

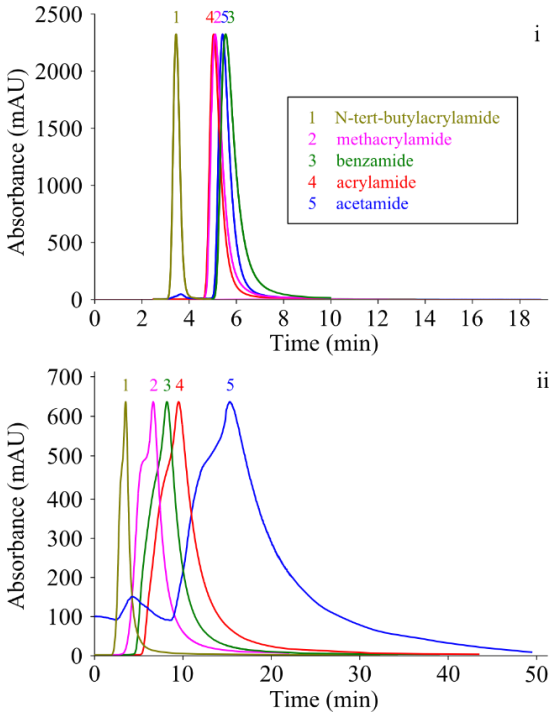

Figure 36 HPLC chromatograms for selectivity test for PAN3 (i) and PA3 (ii). 10 µL of 10 mM solutions was injected on the column, monitoring the absorbance at 220 nm with a flow rate of 0.5 mL min^{-1} using MeCN as mobile phase.[11]

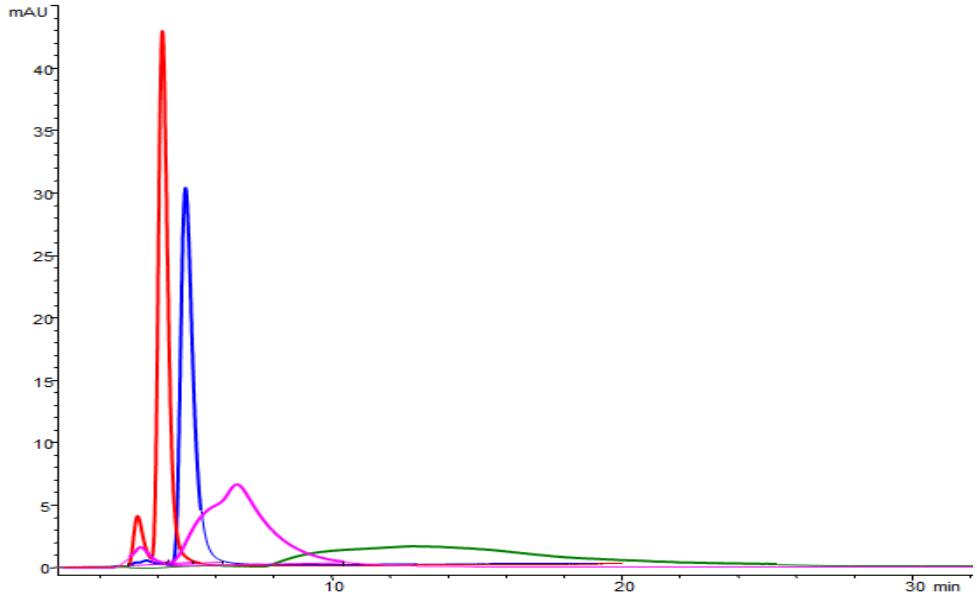

Figure 37 HPLC chromatograms for selectivity test of formamide; where the blue is acetamide and red is formamide on PAN3. The green is acetamide and pink is formamide on PA3. 10 µL of 10 mM solutions was injected on the column, monitoring the absorbance at 220 nm with a flow rate of 0.5 $mLmin^{-1}$ using ACN as mobile phase.

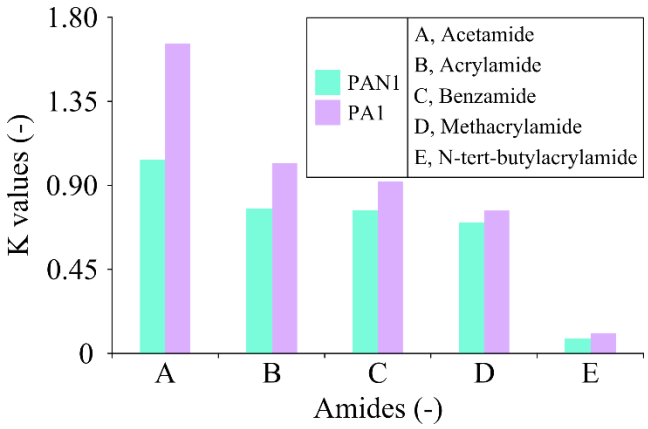

Figure 38 k'-values from the selectivity tests for PA1 calculated from the obtained retention times from the HPLC chromatograms.

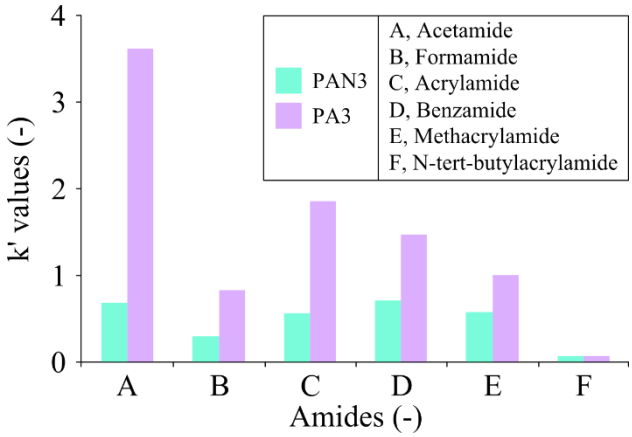

Figure 39 k'-values from the selectivity tests for PA3 calculated from the obtained retention times from the HPLC chromatograms.

3.1.1.3. TEST MODELS FOR ACETAMIDE REMOVAL

Taking into account the aim of this thesis, to examine the possibility to use MIPs as scavangers for purification in the pharmaceutical industry, the best candidate has to be tested in mixtures in order to mimic the real process conditions. The PA3 polymer was therefore tested in two different mixtures made to simulate possible API solutions. Both solid phase extraction (SPE) and competitive batch rebinding were used.

The first removal test performed employed a spiked solution with acetamide and the API Etodolac as the model system. The SPE cartridges packed with the polymers were loaded with a specific amount of the mixture and the collected fractions were analyzed on HPLC. From the HPLC results the recovery of acetamide and Etodolac was calculated, and the results are displayed in Figure 40. Comparison of the recovery amounts for the MIP and NIP shows that in the loading step PA3 binds all the acetamide whereas PAN3 elutes 23 %. In the subsequent washing step more acetamide is eluted from PAN3 while the loaded acetamide on PA3 is retained on the polymer. In addition to acetamide retention, it is also important to evaluate is the API recovery, because for potential application in the pharmaceutical industry of MIPs the API losses should not exceed predefined levels. Evaluation of the API recovery shows that more than 99 % is recovered in the elution and first washing step. The first removal tests indicate that the PA3 polymer successfully removes acetamide from the spiked mixture while eluting in principal all API.

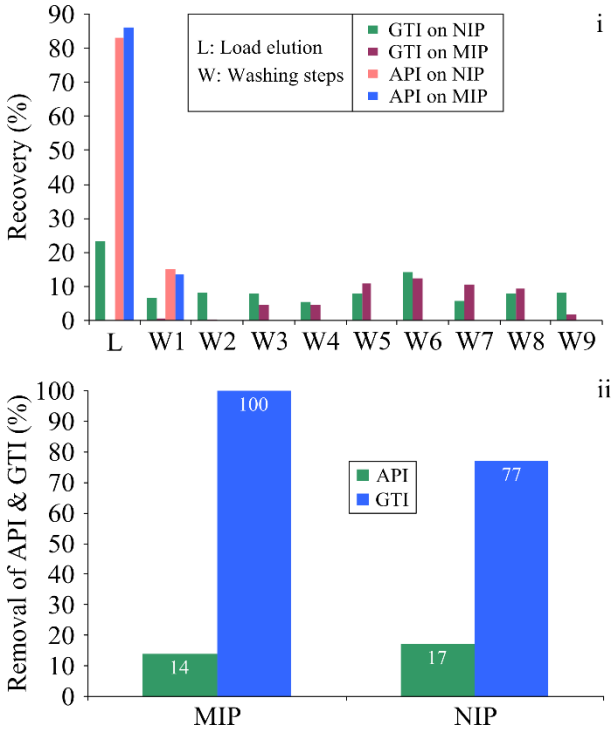

Figure 40 Recovery diagrams (in percentage) for each fraction (i) and the removal in percentage of API and acetamide in the loading step (ii). 0.5 mL of a solution of Etodolac (5 g L-1) and acetamide (250 ppm) in MeCN was loaded on 25 mg of PA3 and PAN3, followed with 1 mL washes of MeCN.

The binding capacity of the MIPs is another important feature providing an indication of the success of the imprinting. Equilibrium batch rebinding tests are used to study the template rebinding properties of the MIP respectively NIP in acetonitrile and ethyl acetate. The amount of polymer is kept constant while the template concentration is varied. By quantifying the equilibrium free concentration (C_{free}) of solute using LC-MS the amount bound template (q) is calculated and binding curves of the template acetamide are obtained when q is plotted against C_{free}. Based on the HPLC and removal tests acetonitrile is the obvious choice of solvent for the first rebinding test using the acetamide imprinted bulk polymers. Roughly 50 mg of polymer is weighed in HPLC-vials and 1 mL of rebinding solution is added to each vial. After 24 h equilibration and sedimentation of the polymer a sample is taken for quantification of the amount of bound acetamide using LC-MS. The obtained results are displayed in the plot in Figure 41. The rebinding tests show that the MIP in general binds more acetamide than the corresponding NIP, thus suggesting selective binding properties of the MIP. However, the difference in binding capacities are not as distinguished as expected, and in the end of the equilibration the MIP and NIP bind roughly the same amount of acetamide. The q-values for both the MIP and NIP reach a plateau, indicating that the binding capacity of the MIP and NIP has been reached with a value of approximately 1 and 0.8 mg/g respectively.

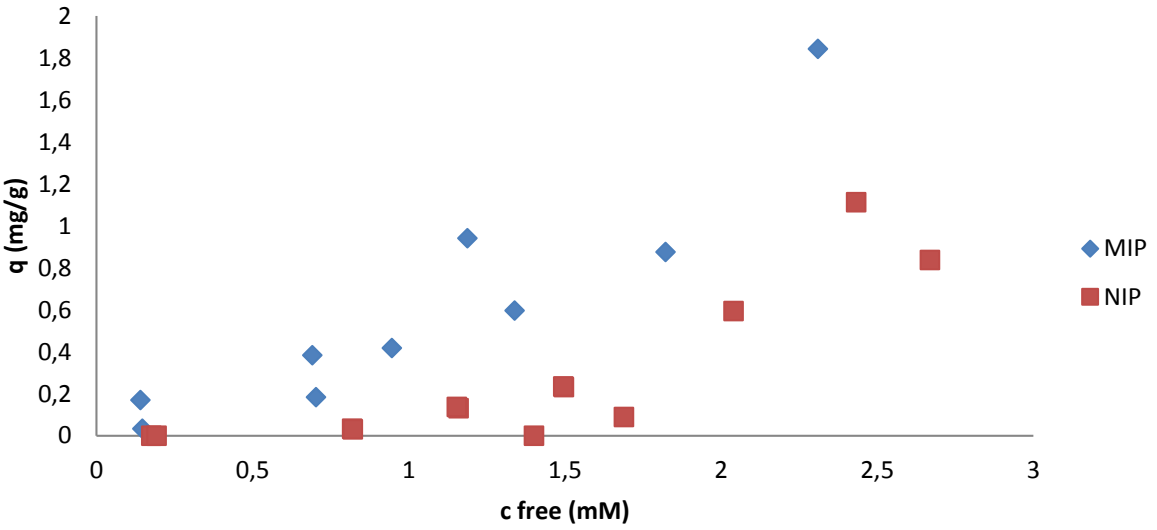

Figure 41 Rebinding curves of acetamide comparing binding properties of bulk MIP and NIP in acetonitrile.

Following the tests in acetonitrile, rebinding tests in the less polar solvent ethyl acetate was performed (dielectric constant 6 versus 37 for ethylacetate and acetonitrile respectively). The resulting isotherm binding plot from the batch rebinding tests is displayed in Figure 42. The significant difference in the amount acetamide bound between the MIP and NIP strongly indicates that selective binding sites are present in the MIP. Furthermore, the binding capacity is higher compared to the rebinding test performed in acetonitrile (1.6 and 0.9 mg/g for MIP and NIP respectively).

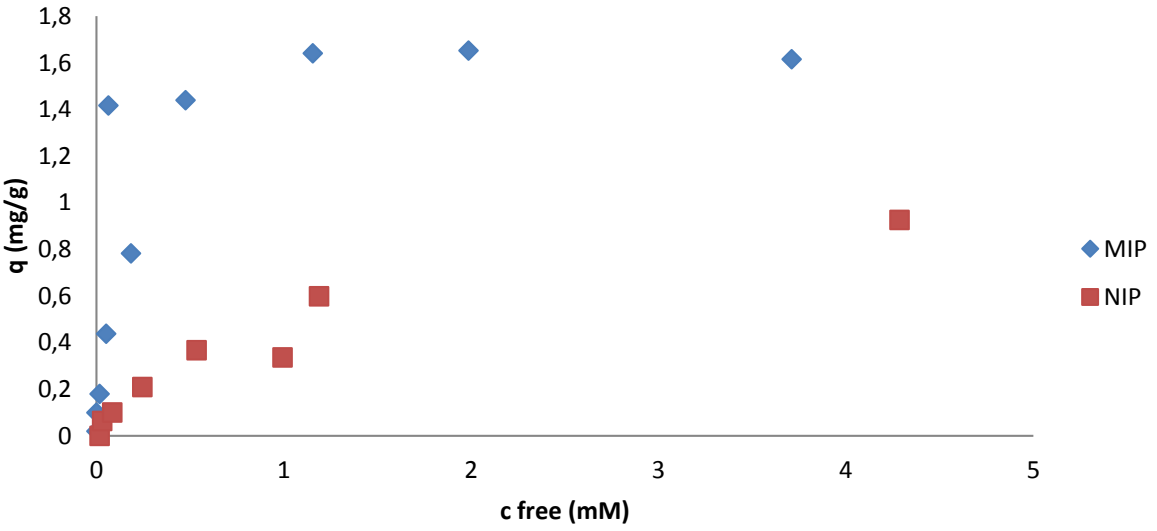

Figure 42 Rebinding curves of acetamide comparing binding properties of bulk MIP and NIP in ethyl acetate.

Following the equilibration competitive batch rebinding, the time dependence of acetamide binding and cross-reactivity of the API and acetamide were investigated for further evaluation. These tests were performed at GSK in collaboration with Elin Rundquist.

10mg of polymer is weighed in HPLC-vials and 1mL of a solution with a concentration of 40 µg/mL acetamide and 6 µg/mL API in acetonitrile was added. The different samples are let to equilibrate for five different times before analysis; 0.5 h, 1 h, 2 h, 12 h, and 24 h. The experiment was performed in five separate vials and samples were taken from each for analysis after the polymer was sedimented. In total three setups were tested; acetamide, API, and a mixture of acetamide and API. The results for the rebinding of acetamide are displayed in Figure 43.

Initially a difference in binding between the MIP and NIP is observed but over time the difference between the two decreases until it is not longer apparent. At the first test point (0.5 h) the MIP binds almost four times the amount of NIP, this is followed by a dip in binding at 1 h where both the MIP and NIP bound essentially no amount of acteamide. After 2 h a maximum is observed where the amount of bound acetamide has increased from 4 µg to close to 7 µg for the MIP and the NIP from ca 1 µg to just over 5 µg. At the 12 h measuring point no difference between the MIP and NIP can be seen and after 24 h of equilibration time no acetamide is bound to the polymers. This behavior indicates that the polymers are overloaded with acetamide. The observed behavior can best be explained by the initial higher binding of the template on the MIP due to specific binding. With increased equilibration time the impact of non-specific binding increases and no difference between MIP and NIP can be observed.

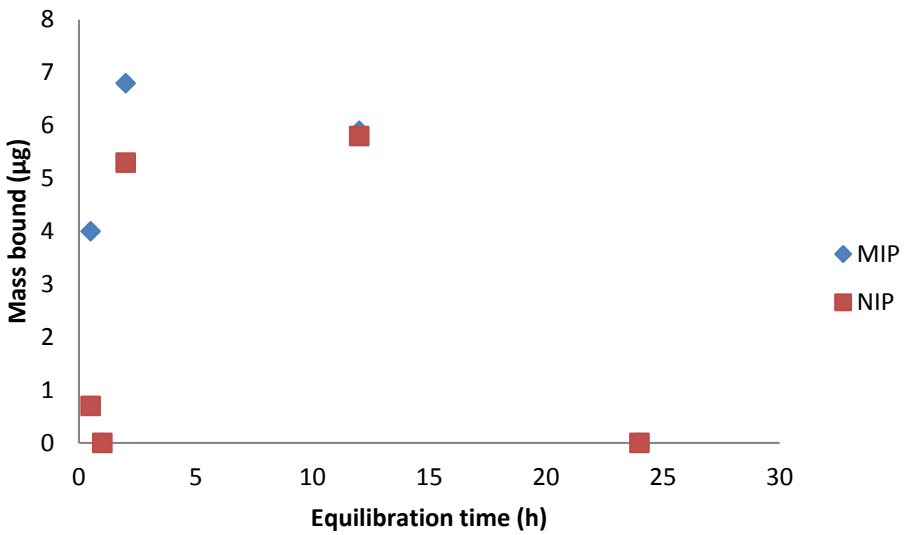

Figure 43 Diagram showing the results for the time-dependence rebinding test of acetamide in acetonitrile.

Although the MIP is imprinted with acetamide with the aim to selectively bind acetamide over other compounds, other compounds may possibly also interact with the functional monomers or the back-bone polymer and bind to the MIP. This is known as cross-selectivity. Therefore rebinding tests using only the API were also performed in order to investigate the binding behavior of the API on the MIP.

Sampling was performed according to the times used in the previous experiment. 1 mL of a solution with a concentration of 6.1 µg/mL API in acetonitrile was applied. The resulting diagram is shown in Figure 44. The same behavior as for acetamide is observed, at the first sampling points (0.5 h and 1 h) the MIP binds a larger amount of API than the NIP but over time (from 2 h to the last point at 24 h) the difference is decreased until both MIP and NIP bind the same amount.

Due to the fact that the amount of loaded API is significantly smaller than the amount of acetamide used in the previous rebinding test, it can be assumed that the observed binding results for the API cannot be explained by overloading but more likely that no significant cross-reactivity takes place. The polymer does not preferably bind the API which indicates that the imprinting step was successful.

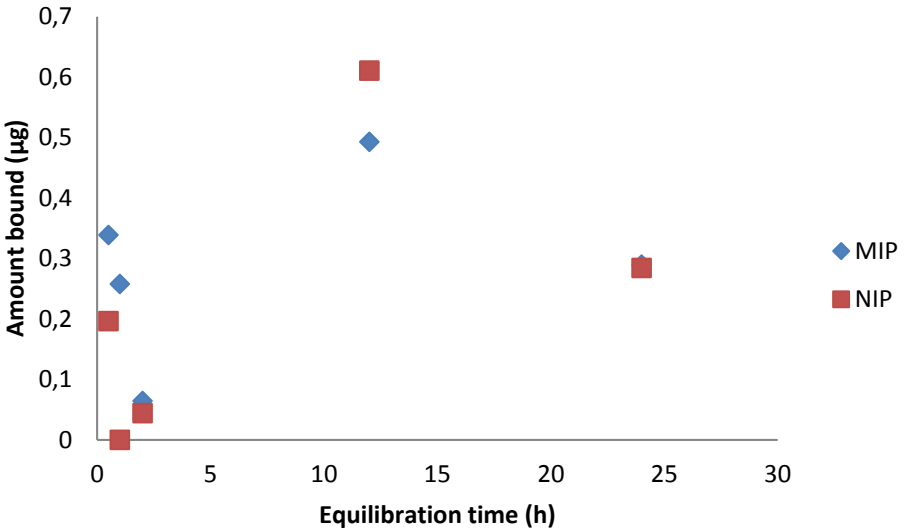

Figure 44 Diagram displaying the rebinding results of the API on the acetamide imprinted polymers.

Based on these promising results the material was tested in a competitive batch rebinding test. In this test an acetonitrile solution with a mixture of acetamide and API is added to the polymers. The same concentrations as in the two previous rebinding tests are used, 40 and 6 µg/mL acetamide and API respectively, and the incubation times are kept the same. The results are shown in the diagram below (Figure 45). The results for the competitive rebinding test display similar trends as for the acetamide and API when tested separately. Initially the MIP bound a larger amount of acetamide than the NIP, after the dip at the 1 h point the bound acetamide is increased and after 12 hours the bound acetamide decreases once again. At the last data point (24 h) the amount of bound acetamide on the MIP or NIP is close to zero, further indicating that the polymers are overloaded. No significant amount of API is bound during the competitive rebinding test, hence indicating that the API does not bind selectively to the polymer.

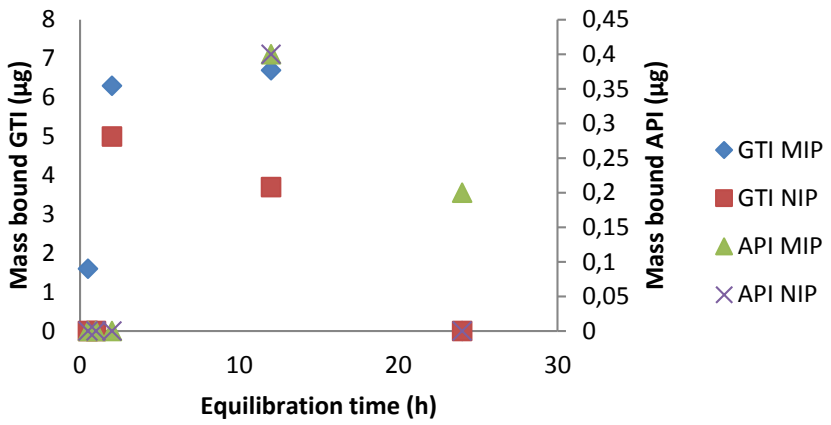

Figure 45 Result from the competitive rebinding test using a solution containing acetamide and the API.

Because of its structural similarity to acetamide, the nitrogen atom is substituted with a sulfur atom, thioacetamide is used for cross-reactivity tests of the acetamide imprinted polymers. SPE columns packed with 100 mg of acetamide imprinted polymer are used. These columns are also used for the acetamide removal tests (see section 3.2). The polymers are loaded with 80 µg of thioacetamide in acetonitrile and washed with pure acetonitrile. The obtained results are shown in (Figure 46). No thioacetamide is retained on the polymers; in the loading and wash fractions 99,6 % and 97,6 % (in total) is eluted for the MIP and NIP respectively. The 2 % difference between the MIP and NIP can be explained by dilution errors because the first two fractions were diluted 10 times for analysis. Hence no difference in binding of the MIP and NIP is observed, indicating that the acetamide MIPs specifically bind acetamide over other compounds – even structurally similar compounds.

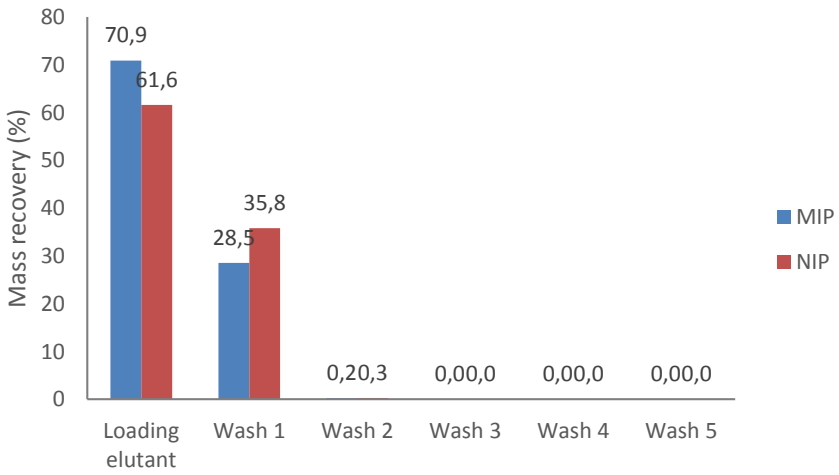

Figure 46 Diagram displaying the mass recovery from the removal test of thioacetamide on acetamide imprinted polymers.

3.1.2 SUPER-POROUS MIPS

One of the disadvantages with bulk MIPs is the relatively low binding capacity and slow mass transfer of the template. In an attempt to improve the binding capacity, a second generation of acetamide imprinted polymers are prepared. So called super-porous monolitich MIPs have previously been synthesized for capillary electrochromatography. In this technique iso-octane is used in varying ratios as a poor solvent for the synthesized polymer chains to decrease the polymer density and increase the porosity. However, with increasing porosity of the MIPs they also become more fragile.[217,218,219] Three different polymers with varying iso-octane amounts in respect to the amount of the porogen were prepared for identification of the best composition (Table 3).

The recipe for these polymers is based on the one of the bulk acetamide imprinted polymers because the monomers used displayed good imprinting (Section 3.1.1). In addition to toluene iso-octane is added in different ratios as a solvent, where toluene acts as the good solvent and iso-octane as the poor solvent. The imprinting and binding capacities of the polymers are evaluated with batch rebinding tests. For facile comparison with the bulk MIP results the rebinding tests are performed in the same solvents as used for the bulk polymers, namely acetonitrile and ethyl acetate.

Table 3 Displays the composition of the iso-octane precipitation prepared MIPs.

	Template	Monomer	Cross-linker	Initiator	Porogen (3/4 tot monomer)	
	Acetamide	MAA	EGDMA	ABDV	Tol	Iso-octane
	(mmol)	(mmol)	(mmol)	(% w/w)	(%)	(%)
MIP 25:75	1	4	20	1	25	75
NIP 25:75	-	4	20	1	25	75
MIP 50:50	1	4	20	1	50	50
NIP 50:50	-	4	20	1	50	50
MIP 75:25	1	4	20	1	75	25
NIP 75:25	-	4	20	1	75	25

The resulting rebinding test curves in acetonitrile are shown in Figure 47, Figure 48 and Figure 49. In accordance to the observations for the bulk MIP rebinding tests in acetonitrile there is no

significant difference in the binding between the iso-octane precipitated MIPs and NIPs. However, the second polymer with 50 % iso-octane and 50 % toluene displays some specific binding of acetamide by the MIP, on the other hand the binding capacity is not improved compared to the bulk polymers. A better specific binding is also observed for the third iso-octane polymer with 75 % iso-octane and 25 % toluene, but the obtained binding capacity is lower than for the 50:50 polymer.

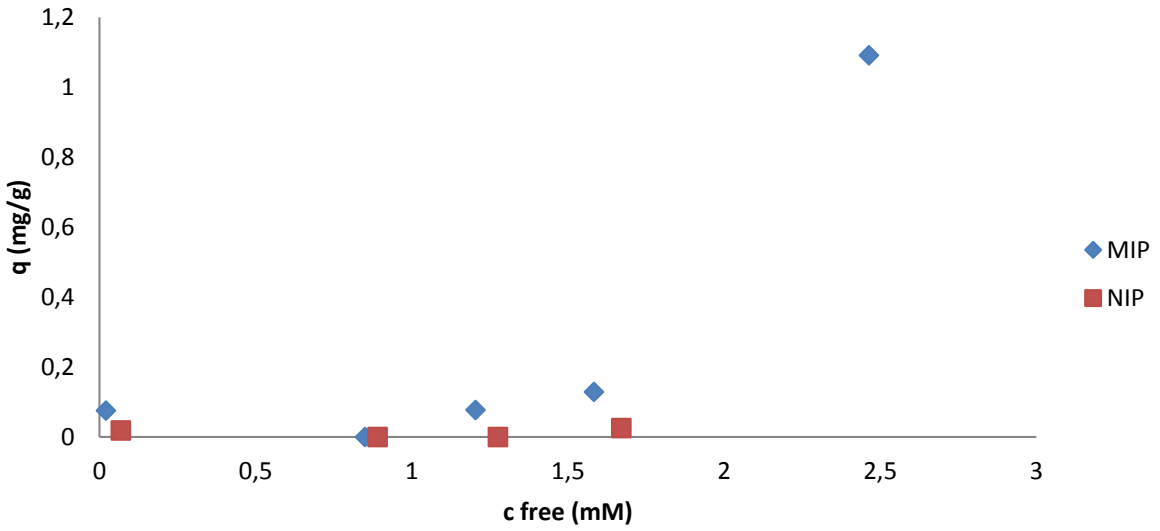

Figure 47 Isotherm binding curves for iso-octane polymer 25:75 in acetonitrile.

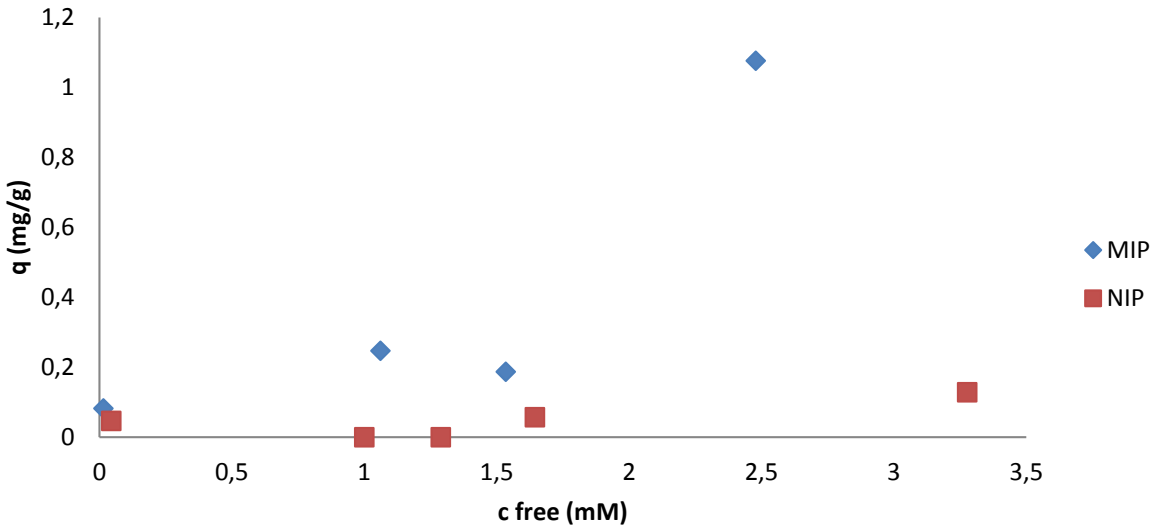

Figure 48 Isotherm binding curves for iso-octane polymer 50:50 in acetonitrile.

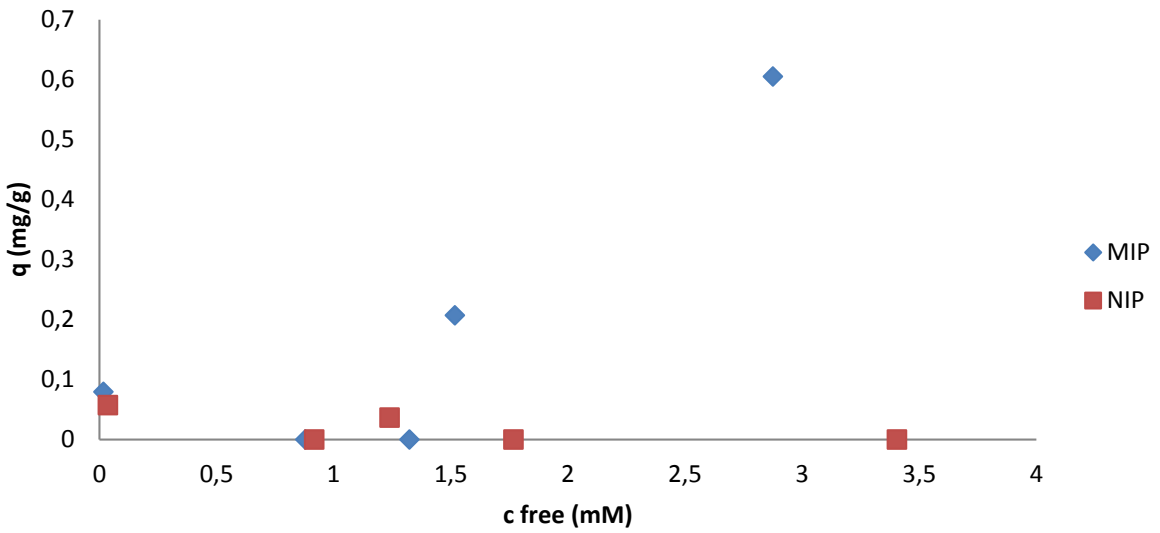

Figure 49 Isotherm binding curves for iso-octane polymer 75:25 in acetonitrile.

The rebinding tests in acetonitrile were followed by ethyl acetate rebinding tests (Figure 50,Figure **51**,Figure **52**). All three iso-octane polymers demonstrate higher binding capacity in ethyl acetate compared to in acetonitrile. However, the binding capacity overall is not improved as expected. The 25:75 and 75:25 polymers both have binding capacities around 1.2 mg/g which is lower than 1.6 mg/g obtained for the bulk polymer in ethyl acetate. For the 50:50 polymer the observed binding capacity reaches 1.6 mg/g which is comparable to the bulk polymer.

The purpose of the synthesis of the iso-polymer was the improvement of the binding capacity in respect to the bulk polymer. Based on the performed experiments it can be concluded that the binding capacity is not improved. Nevertheless, the iso-polymers show a slightly stronger selectivity compared to the bulk polymers.

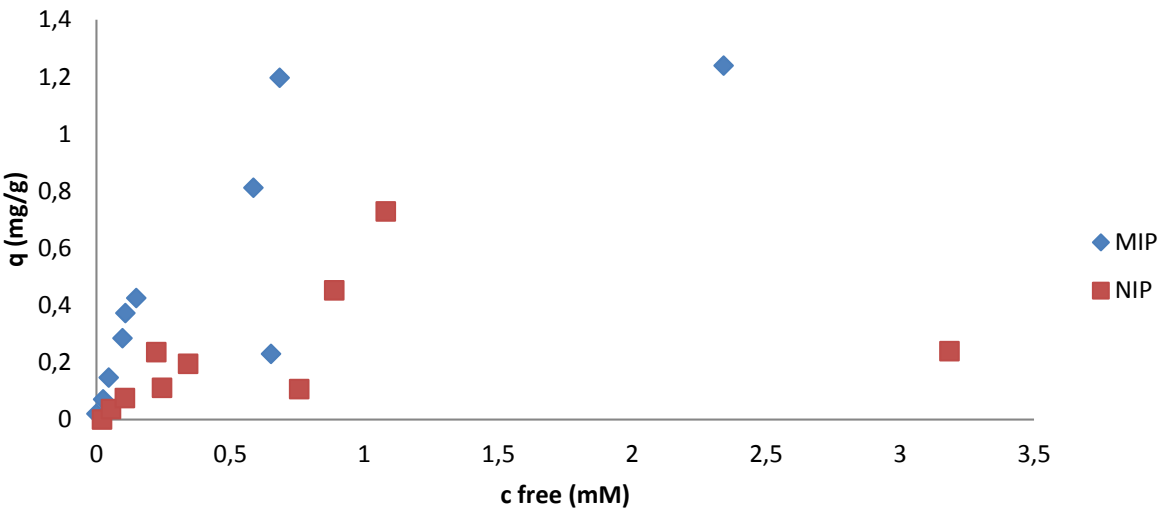

Figure 50 Displays the isotherm binding curves for iso-octane polymer 25:75 in ethyl acetate.

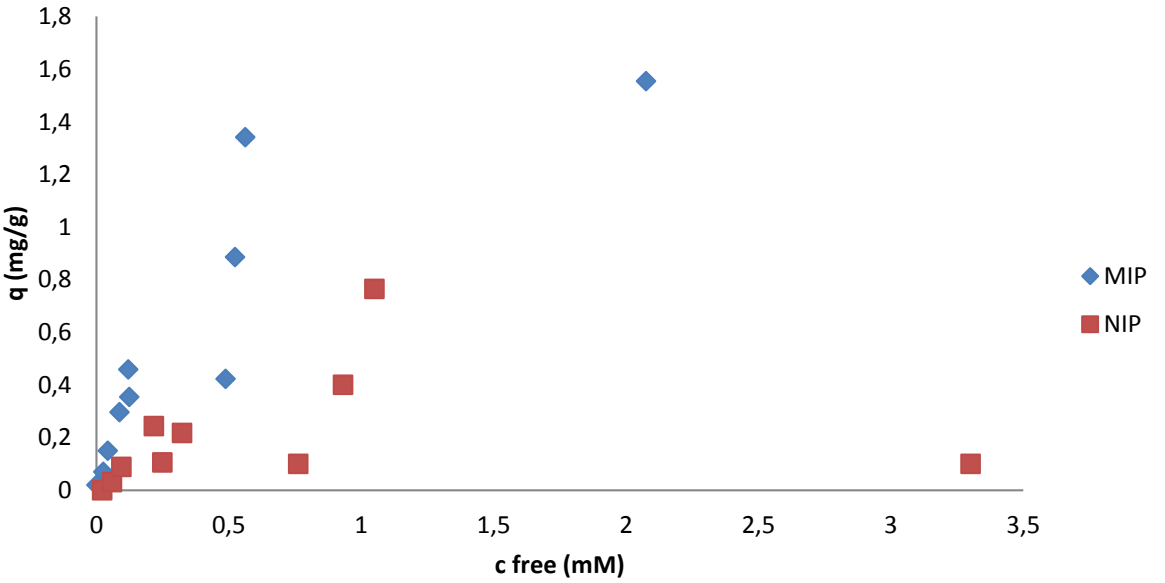

Figure 51 Shows the resulting binding curves for iso-octane polymer 50:50 in ethyl acetate.

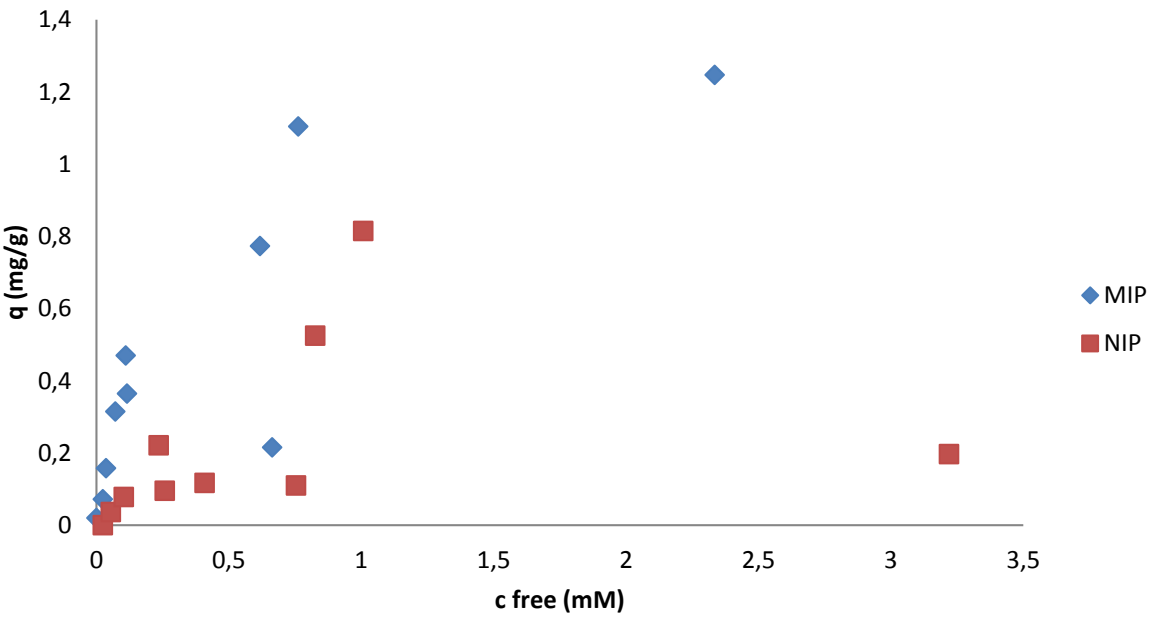

Figure 52 Ethyl acetate rebinding curves for iso-octane polymer 75:25.

3.1.3 Pore-filling of Composite Materials

A third synthesis approach was investigated since the loading capacity of the precipitation polymers did not improve as expected compared to the bulk polymers. In the third generation of acetamide imprinted polymers prepared, the pores of spherical composite materials are filled with the pre-polymerization mixture and after polymerization the silica is etched leaving a spherical polymeric replica. With the resulting defined pore system the hypothesis is that these polymers should have a better mass transfer and binding capacity of acetamide.

In total three different sets of pore-filled polymers were synthesized with varying amounts of porogen. Because of the promising results obtained upon testing the bulk polymers the PA3 composition is the basis for the synthesis.

Although the purpose of a porogen in bulk polymers is to introduce pores, in this technique the amount of the porogen toluene is decreased and even removed completely. In the pore-filling approach the silica itself functions as a mould for pores, and after removal of the silica by etching, pores are formed in the polymer. By using an excess amount of solvent in the pre-polymerization mixture in pore-filling, the risk is that the polymers become less rigid and thus possibly collapse. The composition of the three pore-filled polymers is summarized in Table 4.

Table 4 Summarizes the composition of the pore-filling polymers. The percent of toluene represents the percent of porogen used based on the bulk acetamide polymer recipe.

	Template Acetamide (mmol)	Monomer MAA (mmol)	Cross-linker EGDMA (mmol)	Initiator ABDV (% w/w)	Porogen (3/4 tot monomer) Tol (% of bulk recipe)
MIP I	1	4	20	1	50
NIP I	-	4	20	1	50
MIP II	1	4	20	1	10
NIP II	-	4	20	1	10
MIP III	1	4	20	1	-
NIP III	-	4	20	1	-

Like for the two other formats, the imprinting and binding capacity of the synthesized polymer I, II, and II are evaluated with batch rebinding tests in both acetonitrile and ethyl acetate. The resulting acetonitrile rebinding plots are shown in Figure 53, Figure 54 and Figure 55. Pore-filling I polymer has roughly the same binding capacity as the bulk polymer under the same conditions, but compared to the iso-octane polymers the binding capacity is increased with approximately 60 %. It should also be noted that the binding curve has not reached a proper plateau, which is an indication of possible increase of the binding capacity. On the other hand the specific binding of acetamide is relatively weak, with MIP I binds around 1.6 mg/g and NIP I around 1.2 mg/g.

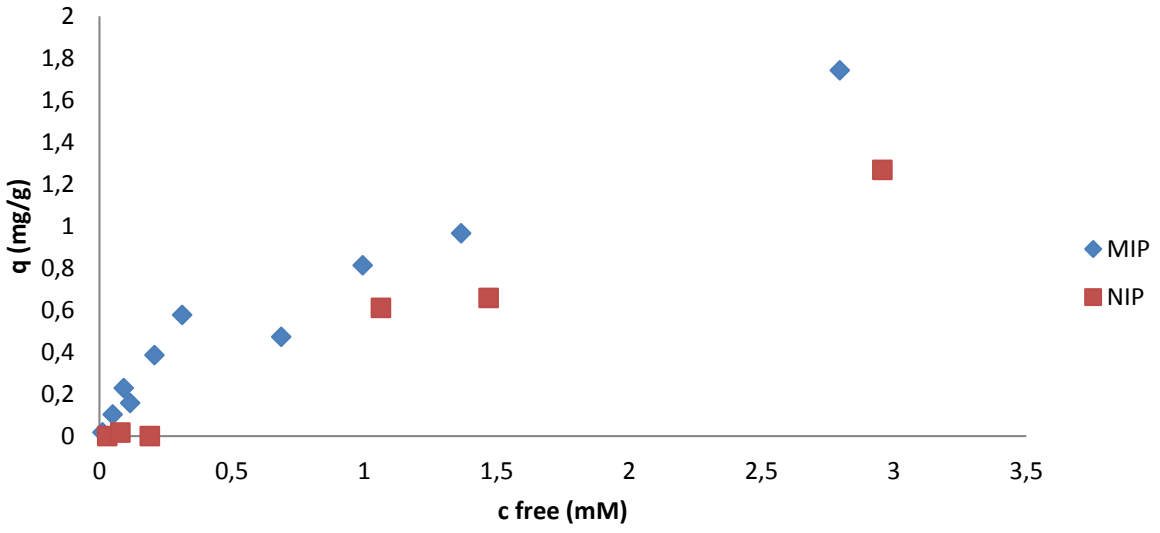

Figure 53 Pore-filling I isotherm plots of acetamide rebinding tests in acetonitrile.

The rebinding tests of pore-filling II in acetonitrile show a significant increase in binding capacity with a value of approximately 2.5 mg/g, an increase of around 55 % compared to the value obtained for the bulk polymer. Once again the plot indicates that the maximum value has not been reached, hence an increase in binding capacity may be possible. The difference between the MIP and NIP is also more significant approximately 2.5 mg/g for the MIP and 1.4 mg/g for the NIP, indicating the presence of defined binding sites in the MIP.

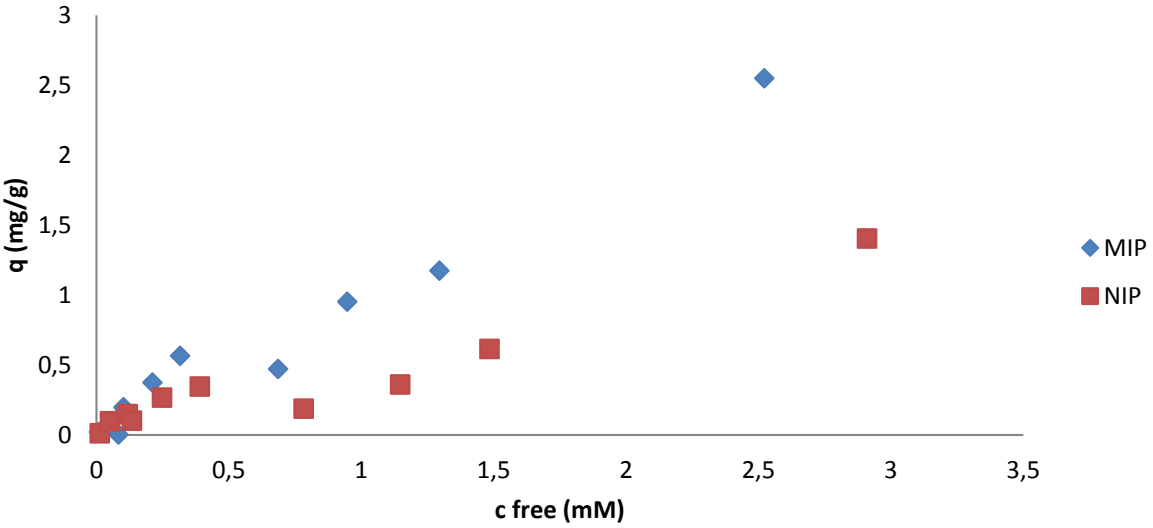

Figure 54 Displays the plot of acetamide rebinding test in acetonitrile with pore-filling II polymer.

An improvement in rebinding capacity in comparison to the bulk polymer is also displayed by the rebinding results for the pore-filling III the last polymer. Although it is slightly lower than the binding capacity for pore-filling II, it is approximately 25 % higher than for the bulk polymer. Furthermore the MIP III shows specific binding of acetamide compared to the NIP III (2.1 mg/g and 0.8 mg/g respectively).

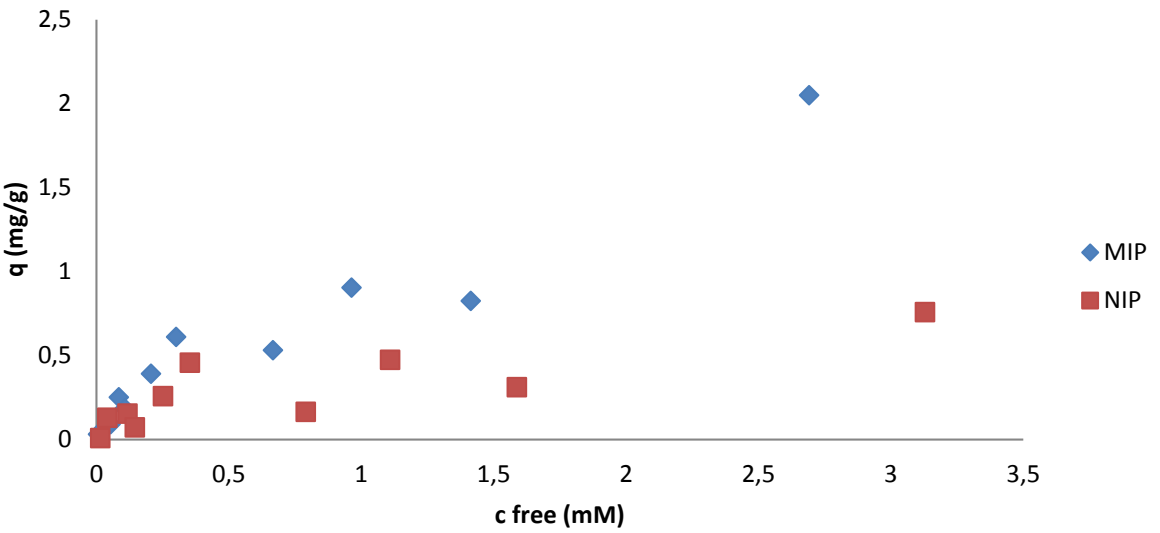

Figure 55 Show the rebinding results in acetonitrile for the pore-filling III polymer.

Following the rebinding tests in acetonitrile, tests in ethyl acetate are also performed and the results are summarized in Figure 56, Figure 57 and Figure 58. For all three polymers the resulting plots in ethyl acetate show similar binding capacity to the rebinding tests in acetonitrile and additionally the same trends for the acetamide selectivity are observed.

To summarize all the rebinding tests performed with the pore-filling polymers, it is apparent that the binding capacity is successfully increased in comparison to the bulk polymer with this approach. Between the three pore-filling polymers pore-filling I is the least successful polymer with the binding capacity more or less equal to the bulk, however the acetamide binding specificity is slightly decreased in comparison to the bulk polymer. Both pore-filling II and III display increased binding capacity, pore-filling II significantly so with an increase of around 55 % compared to the bulk. On the other hand with the high binding capacity it is observed that the specific acetamide binding of pore-filling II is sacrificed to some extent. Because the NIPs bind 56 % and 35 % of what the MIPs do for pore-filling II and III respectively.

The influence of the amount of solvent was also investigated by synthesizing three different polymers with varying amounts of solvents in pre-polymerization. With the silica forming pores the risk of using solvents that promote further pore formation is that the polymers become fragile and collapse. Thus 50 % of the solvent used for conventional bulk polymerization was the maximum used for the pore-filling. Although polymer III with no solvent present in the pre-polymerization mixture demonstrates an improved binding capacity compared to the bulk

polymers, the rebinding results indicate that a small amount of solvent in the pre-polymerization mixture promotes both the binding capacity and the specific binding.

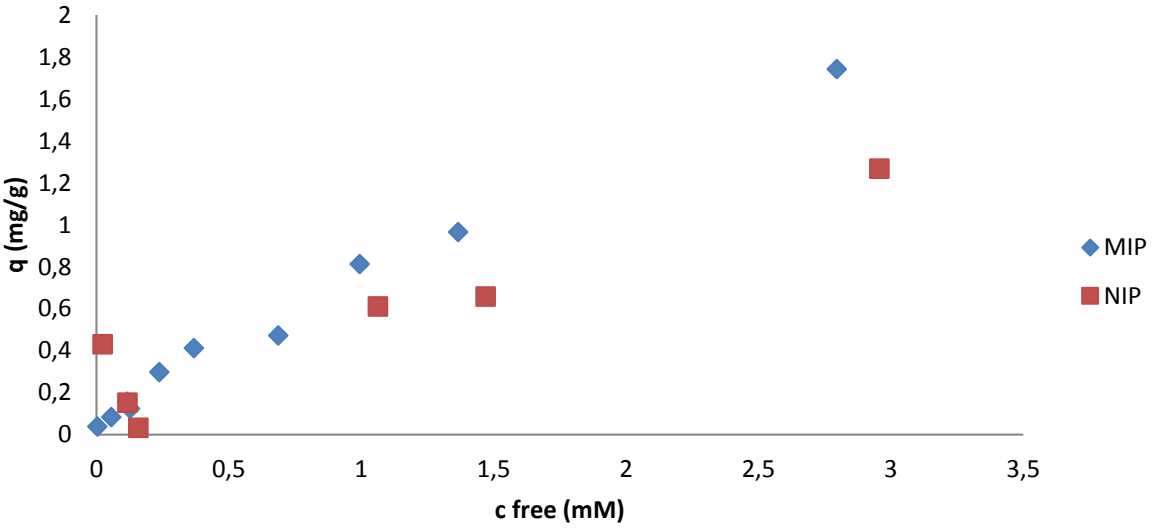

Figure 56 Porefilling I isotherm plots for acetamide rebinding tests in ethyl acetate.

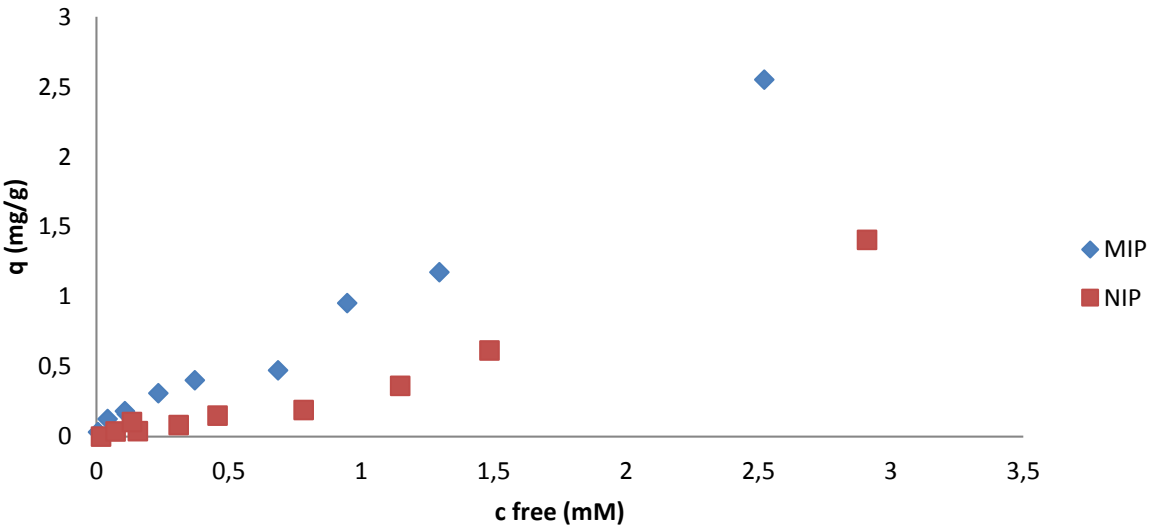

Figure 57 Shows the plot of the rebinding test results in ethyl acetate for the pore-filling II polymers.

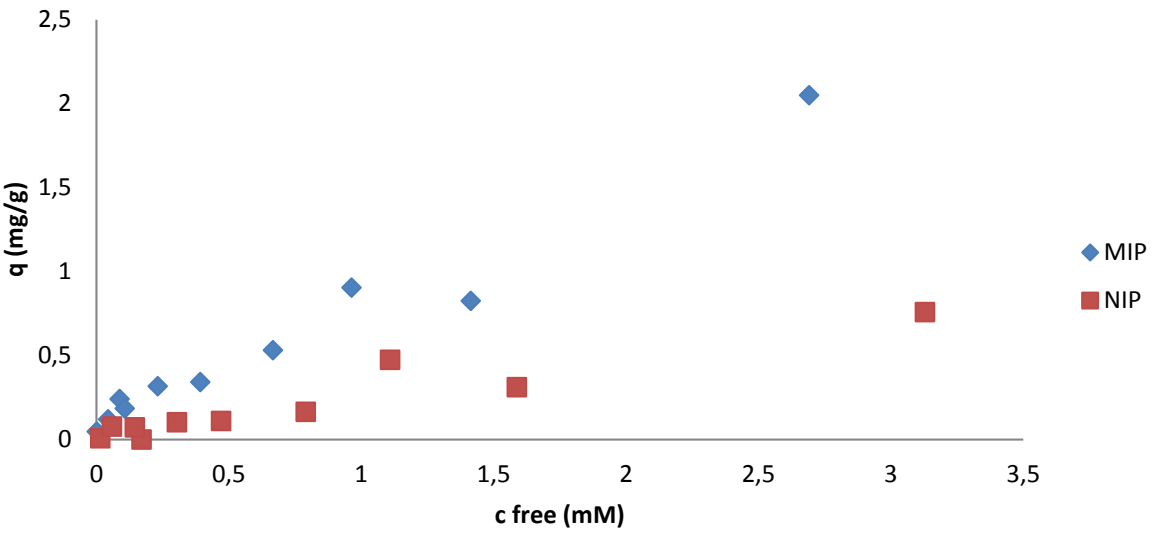

Figure 58 Displays the rebinding results for pore-filling III in ethyl acetate.

3.2. CHARACTERIZATION OF THE MIP FORMATS

In order to gain further information about the different polymer formats synthesized and in an attempt to explain the results from the experiments, the polymers were thoroughly characterized by a number of techniques.

3.2.1. MICROSCOPY

Microscopy is used for characterization of the particle shape and size distribution range. In Figure 59 microscopy pictures, typical for bulk polymers, of the acetamide imprinted PA3 and PAN3 are displayed. The irregular shaped particles have a size distribution range of around 25-50 µm as expected from the crushing and sieving procedure.

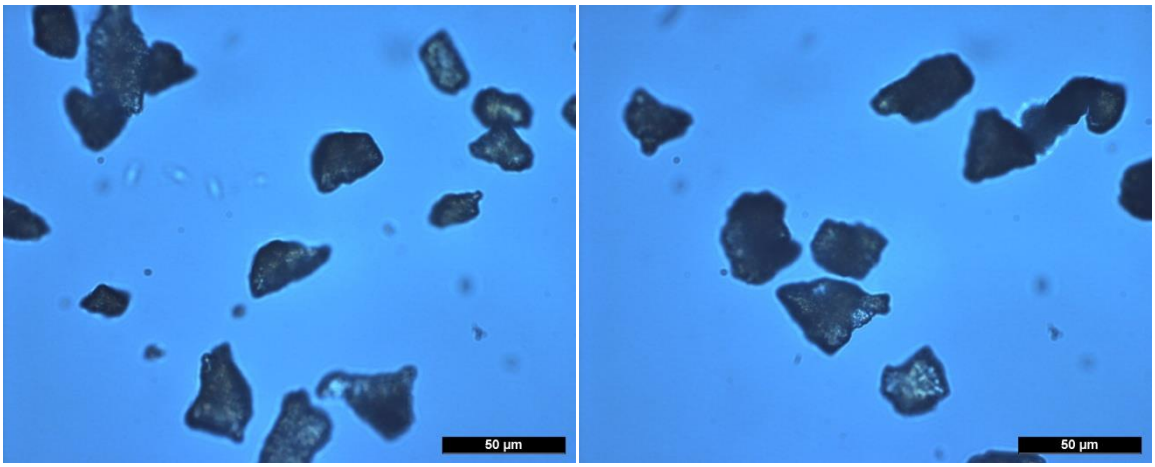

Figure 59 Microscopy pictures of the bulk polymer (left) PA3 and (right) PAN3 after crushing and sieving.

Also the iso-octane polymers were crushed and sieved to the particle size range of 25-50 µm during the work-up procedure. The resulting microscopy pictures (Figure 60) show that the majority of the particles are within the 25-50 µm range, however smaller particles are also observed. During the wet-sieving procedure particles smaller than 25 µm should be filtered out, but in this case, even after extensive washing and sieving, some remained. The difficulty to remove the smaller particles may be explained by their fragility. When doing the work-up it was observed that the iso-octane polymers are softer than the bulk polymers, so much that no pistil was needed for crushing. This behavior can be explained by the shape of the polymers, as can be seen in the microscopy pictures the larger particles are built up by agglomerated smaller almost spherical particles. Hence, making them less rigid than the bulk polymers and thus possibly more inclined to break and form smaller particles under physical stress. The iso-polymers are synthesized via precipitation polymerization meaning that the polymer particles formed will precipitate when they reach a certain size and are no longer soluble in the solvent. Therefore, smaller particles are formed in comparison to bulk polymers where the synthesis of the polymer is not limited by solubility.

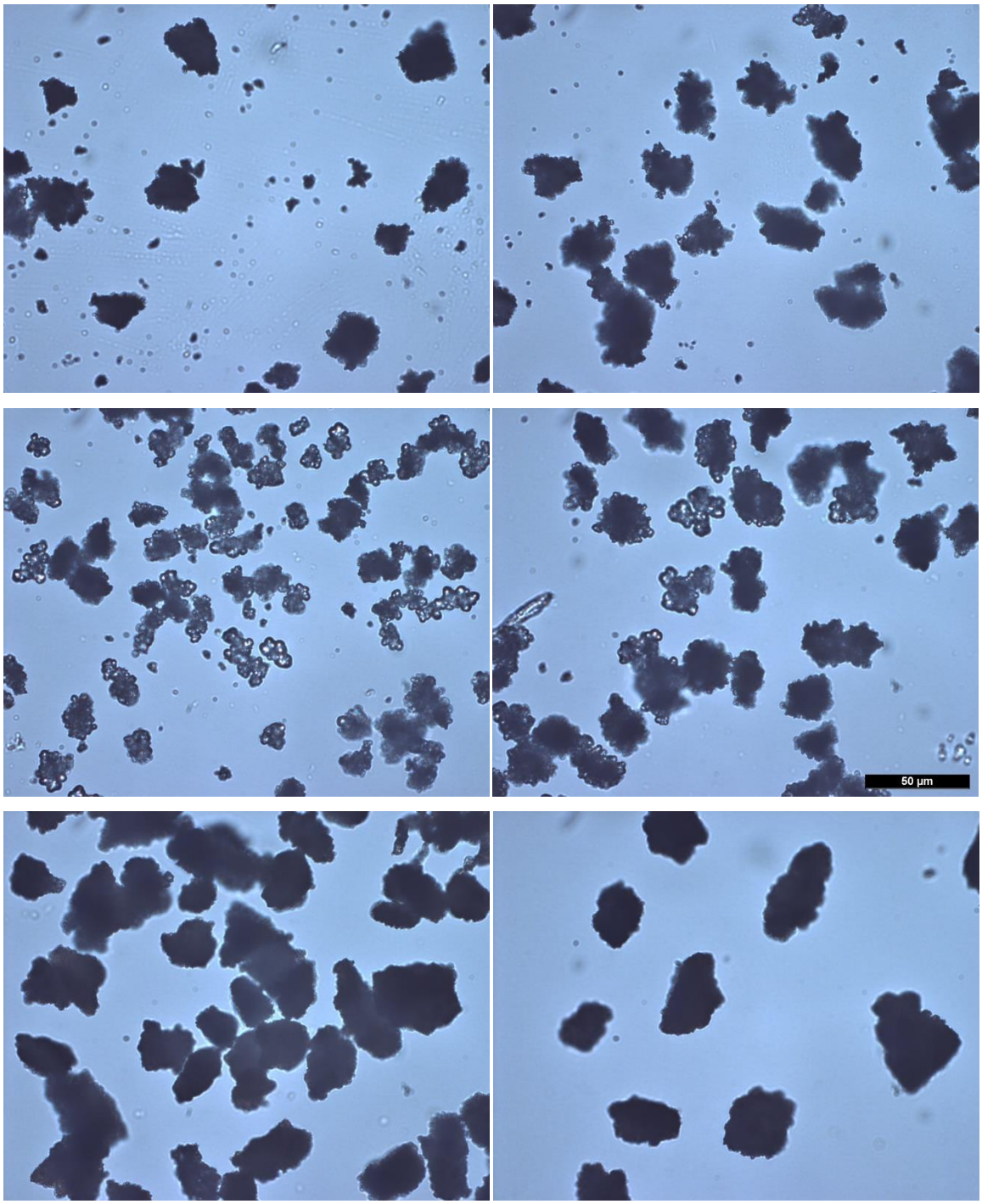

Figure 60 Microscopy pictures of the iso-octane polymers. Top left down: MIP 25:75, NIP 25:75, MIP 50:50, NIP 50:50, MIP 75:25, NIP 75:25.

The last polymer format synthesized is the pore-filled composite material. In this approach spherical porous silica is filled with pre-polymerization solution and after polymerization the silica is removed by etching, leaving polymer replicas. Microscopy pictures (Figure 61) do not only give an indication of the particle size range but also whether the silica particles are filled properly with pre-polymerization solution. The silica particles filled with polymerization

mixture, in the middle, have a solid darker grey shade to them compared to the non-filled silica particles, indicating that the pores of the silica have been filled. After etching (right picture) it is observed that the formed polymer mirror images of the silica exhibit the same size range as the silica composites. In addition, the polymer particles after etching tend to keep the darker grey coloring indicating that the etching process to remove the silica is successful. In order to confirm that the particles shown on the right hand side consist of polymeric material thermal gravimetric analysis before and after etching is performed.

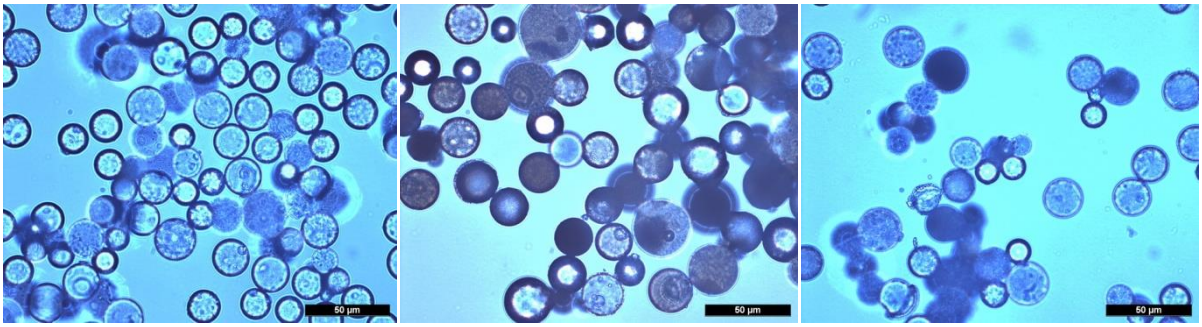

Figure 61 Displays pore-filling composite microscopy pictures: (left) bare silica (middle) silica with polymer and (right) polymer replica of the etched silica.

3.2.2. THERMAL GRAVIMETRIC ANALYSIS

Thermal gravimetric analysis is used to characterize the decomposition behavior and thermal stability of the different acetamide imprinted polymers prepared. By studying the obtained decomposition patterns one can obtain information of the chemical composition and the polymerization process of the polymer. Weight losses occurring at temperatures lower than 150 ^{0}C are generally attributed to loss of water and decomposition of unreacted monomer, cross-linker and monomer-template complex.[220,221,222]

The TGA curves (Figure 62) for the bulk polymers show that there is no significant difference in the decomposition patterns of PA3 and PAN3. Two decomposition steps are observed for both polymers, with exothermic peaks around 300 ^{0}C and 420 ^{0}C. Decomposition starts around 230 ^{0}C which means they are rigid up to this temperature, and beyond that they start to disintegrate.

(A)

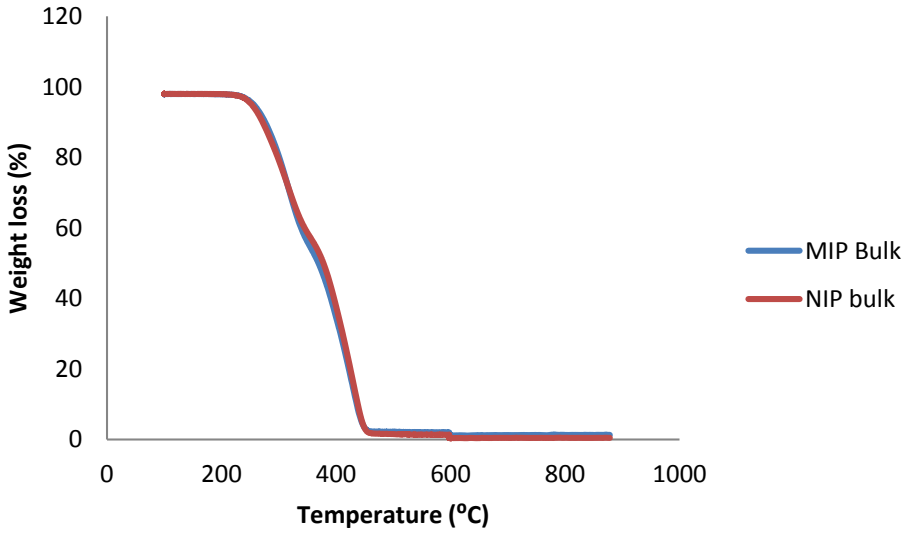

(B)

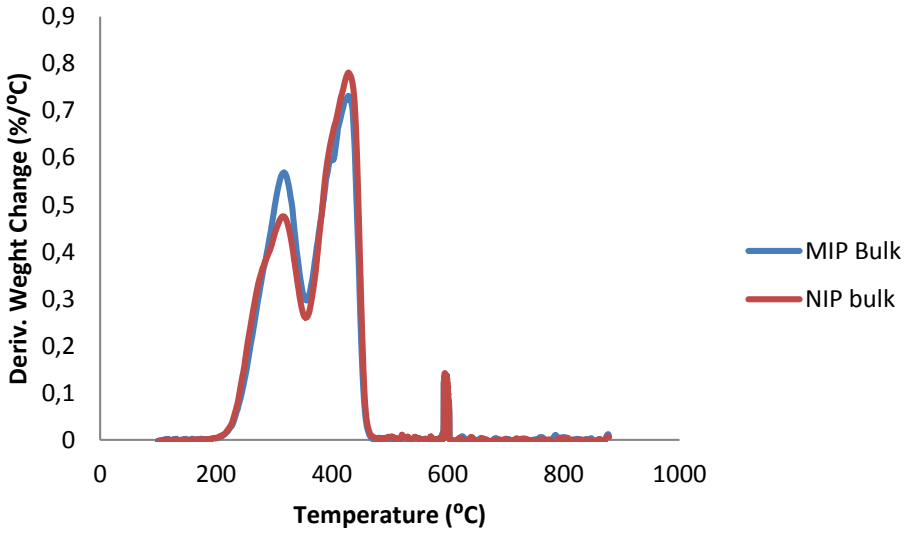

Figure 62 TGA curves of bulk polymers PA and PAN3. (A) The weight change in % as function of temperature (◦C), and (B) the derivative of the weight change as function of temperature (◦C).

In comparison to the bulk polymers the decomposition patterns of the iso-polymers indicate three-step decomposition rather than a two-step (Figure 63). In addition to the exothermic peaks around 300 ^{0}C and 420 ^{0}C, a third one is observed around 250 ^{0}C. The observation of the iso-polymers starting to degrade earlier than the bulk polymer indicates that shorter polymer chains are present. Due to the fact that above 150 ^{0}C excess water, unreacted monomer, cross-linker and monomer-template complex should be degraded, the peak at around 250 ^{0}C is most likely polymer. As previously mentioned, the iso-polymers are synthesized via precipitation polymerization meaning that the polymer particles formed will precipitate when they reach a

certain size and thus no longer are soluble in the solvent. The third peak at around 250 ^{0}C occurs as a result of the decomposition of lower molecularly weight polymer chains, which are not observed in the bulk polymers where the polymer chains can grow larger.

(A)

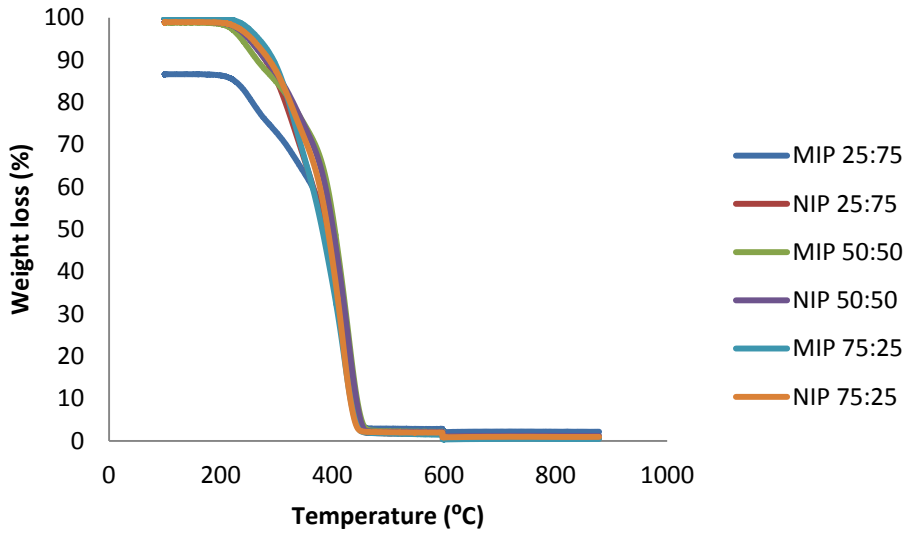

(B)

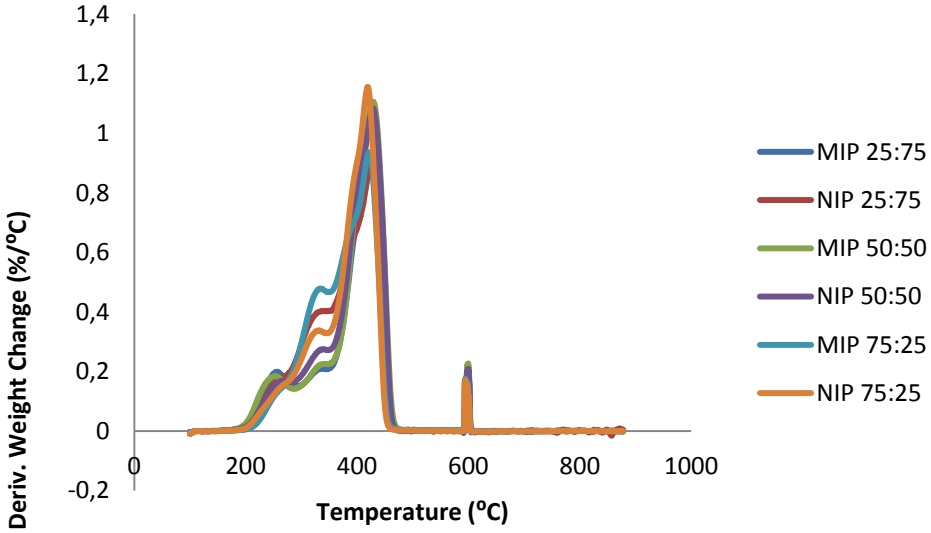

Figure 63 TGA curves of iso-polymers MIP 25:75, 50:50, 75:25 and NIP 25:75, 50:50, 75:25. (A) The weight change in % as function of temperature (°C), and (B) the derivative of the weight change as function of temperature (°C).

In addition to gaining information about the decomposition behavior and thermal stability, TGA analysis is used to follow the progress of the pore-filling procedure for study of the pore-filling and removal of the silica by etching. The TGA curves before etching (Figure 64) are analyzed

after polymerization in order to observe the ratio of polymer to silica formed. Decomposition of the three polymers is not all following the same pattern and after complete combustion all but MIP I and NIP I display a total weight loss of approximately 40 %. For the MIP I and NIP I the total weight loss is smaller with around 30 %, this is in accordance with the amount of solvent used in the pre-polymerization preparation (Table 4 in section 3.1.3). Since the same amount of pre-polymerization mixture is used to fill the pores for all three polymers, a smaller solvent to monomer and cross-linker ratio means that a larger quantity of polymer is formed. The amount of solvent decreases from 50 % to 10 % and the last polymer not containing any solvent, polymer I, II and III respectively. It appears that at some level decreasing the solvent does not influence the amount of polymer formed, because both polymer II and III display the same total weight loss. However, the decomposition patterns of polymer II and III exhibit some differences. The onset temperature where polymer II starts to degrade is roughly the same as for polymer I and III but the slopes differentiate. In diagram B (Figure 64) it is observed that polymer II has a two-step degradation compared to a three-step for polymer I and III. As discussed earlier the first peak in the three-step degradation occurs at approximately 125 ^{0}C indicating un-reacted monomer, cross-linker or template-monomer complex and a second one at around 160 ^{0}C implying smaller polymer chains present. For polymer II the decomposition starts at approximately 220 ^{0}C indicating that a smaller amount of shorter polymer chains are present than in polymer I and III.

(A)

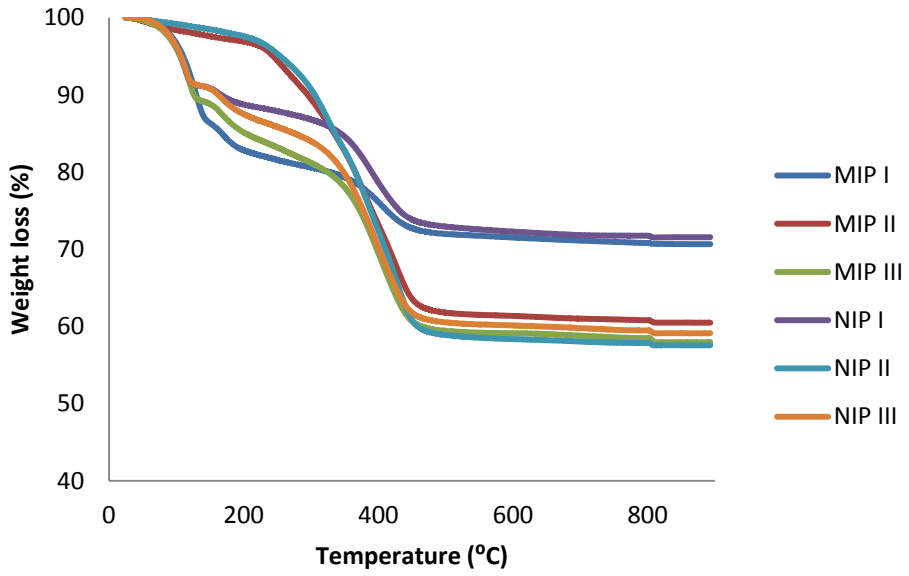

(B)

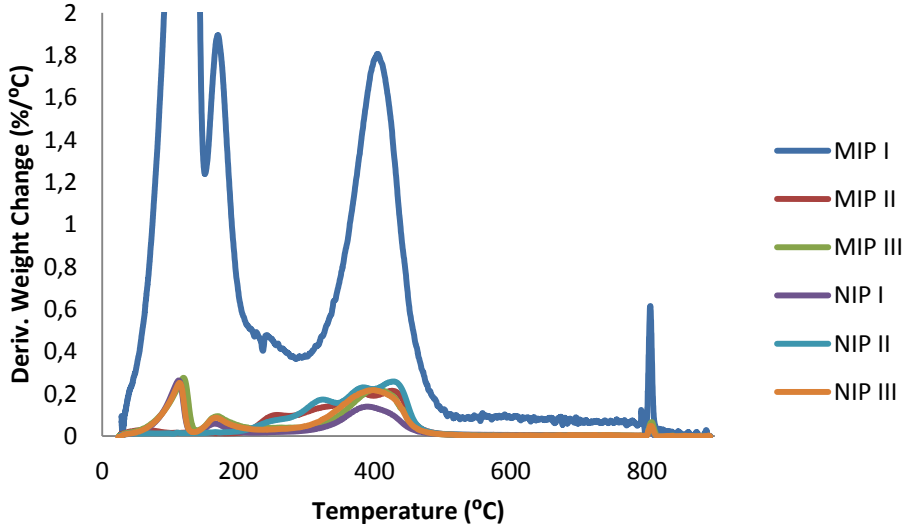

Figure 64 TGA curves of pore-filling polymers MIP and NIP I, II, III before etching. (A) The weight change in % as function of temperature (◦C), and (B) the derivative of the weight change as function of temperature (◦C).

The pore-filled polymers are analyzed with TGA once more after etching in order to control that no remaining silica is present. The resulting TGA curves (Figure 65) show that the weight loss is close to 100 %, indicating that the silica was removed successfully for the three synthesized polymers. The polymers, apart from MIP III, all essentially follow the same degradation pattern, with the onset temperature just above 200 ^{0}C and full degradation reached at approximately 400 ^{0}C. MIP III on the other hand has a more distinguished two-peak

degradation pattern rather than a broader tailing one-peak pattern observed for the other polymers in the derivate weight change diagram. MIP III displays one peak at approximately 160 ^{0}C and the second peak at approximately 380 ^{0}C. As discussed earlier in this section the peak at 160 ^{0}C implies that smaller polymer chains are present.

The result indicating smaller polymer chains in MIP III is contrary to the results observed before etching, where polymer II showed indication of smaller polymer chains rather than polymer III. This change might be explained by polymer chains being washed out during the etching procedure.

(A)

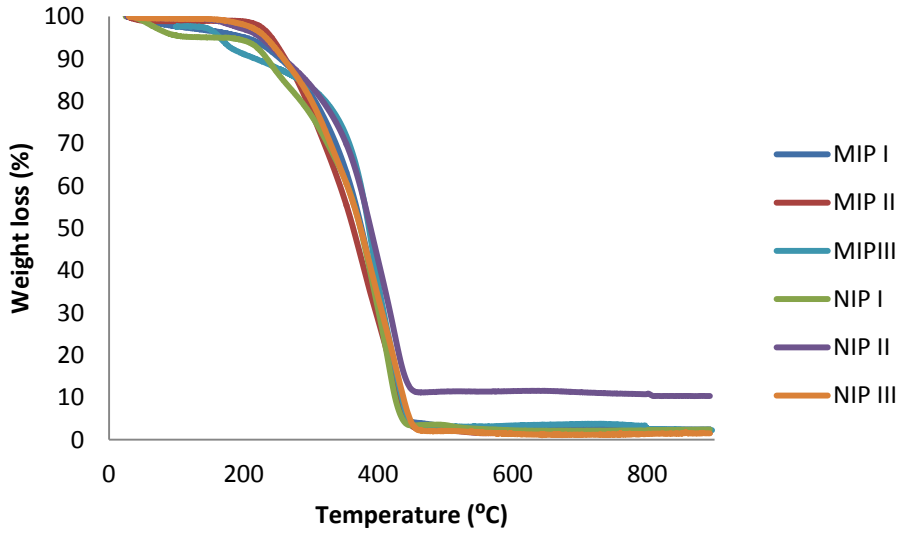

(B)

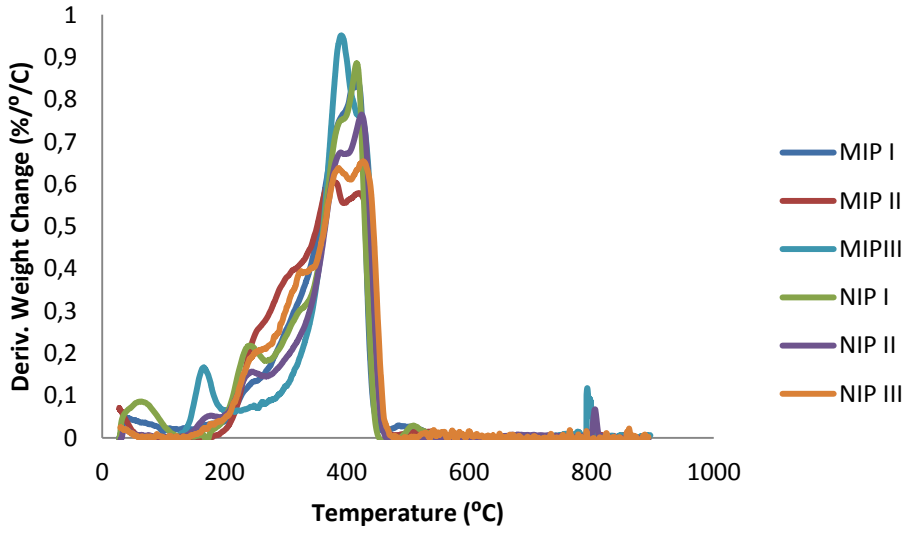

Figure 65 TGA curves of pore-filling polymers MIP and NIP I, II, III after etching. (A) The weight change in % as function of temperature (◦C), and (B) the derivative of the weight change as function of temperature (◦C).

3.2.3. DIFFERENTIAL SCANNING CALORIMETRY ANALYSIS

DSC was used to further study the synthesized MIP format. The thermograms obtained give an indication of the crystallization, melting and degradation temperatures for the MIPs.

Table 5 summarizes the results obtained for the different synthesized MIPs. It is observed that, apart from porefilling MIP and NIP II, the MIPs and corresponding NIPs have comparable temperatures, thus indicating that the template does not affect the polymerization process. Furthermore, the bulk and iso-octane polymers display two melting temperatures and the iso-octane polymers whereas the pore-filling polymers only display one. The melting temperatures for the iso-octane and pore-filling polymers are higher compared to the bulk polymers (around 250 – 300 ^{0}C and approximately 220 ^{0}C respectively). The value for the bulk polymers are corresponding to the on-set temperature for the degradation observed in the TGA analysis (Section 3.2.2), however the temperatures for the iso-octane and pore-filling polymers are slightly higher. In addition the iso-octane and pore-filling polymers display one characteristic peak not observed in the bulk polymers, namely crystallization. The crystallization temperature suggests that adjacent polymer chains are stacked to form crystalline structure in the iso-octane and pore-filling polymers, thus possibly leading to higher melting temperatures. One possible explanation why this is not observed in the bulk polymer is that the polymer chains are not free to stack, even though the three MIP formats should have the same degree of cross-linking. As discussed in Section 3.2.2 the degradation patterns for the iso-octane and the pore-filling polymers suggest that smaller polymer chains might be present.

Table 5 Summary of the DSC results. Where T_c is crystallization temperature, T_m the melting temperature and T_d the degradation temperature.

	T_{c1} (°C)	T_{c2} (°C)	T_{m1}(°C)	T_{m2}(°C)	T_d(°C)
Bulk PA3	n.f	-	149	218	349
Bulk PAN3	n.f	-	151	225	349
Iso-octane MIP 25:75	145	-	171	277	n.f
Iso-octane NIP 25:75	148	-	183	304	n.f
Iso-octane MIP 50:50	151	-	164	263	n.f
Iso-octane NIP 50:50	150	-	163	260	n.f
Iso-octane MIP 75:25	n.f	-	158	275	n.f
Iso-octane NIP 75:25	n.f	-	164	266	n.f
MIP I	153	-	252	-	n.f
NIP I	n.d	n.d	n.d	n.d	n.d
MIP II	159	223	254	-	n.f
NIP II	128	157	312	-	n.f
MIP III	144	-	269	-	n.f
NIP III	134	159	283	-	n.f

3.2.4. POROMETRY USING BET AND DSC ANALYSIS

Porometry analysis of the acetamide imprinted polymer was performed by BET as well as DSC, and the results are summarized in (Table 6). The data for the polymers, independent of the format, display some significant differences between the dry and swollen state. The BET adsorption-desorption curves obtained indicated type IV hysteresis loop and thus indicating the polymers are of mesoporous character. The super-porous iso-octane 25:75 and 50:50 polymers have the smallest pore diameter (around 4 nm), and the 75:25 polymer and the bulk polymers display double the pore diameter size (approximately 10 nm). The surface area of the iso-octane polymers on the other hand are roughly the same for all three polymers, approximately 100 m^2/g compared to almost 400 m^2/g for the bulk polymers. Because of shortage of material no BET analysis was performed for NIP I, MIP II and NIP II. However, the results for the rest of the pore-filling polymers display larger pore size (approximately 20 nm) compared to the 75:25 and bulk polymer. It should be noted that the super-porous iso-octane polymers and the pore-

filling polymers did display indications of the polymer possibly collapsing during analysis, because the desorption curve had higher values than adsorption.

Pore analysis with DSC in the swollen state was also performed, although all polymers were analyzed three of them did not display the characteristic peak so no pore parameters could be calculated. As observed in BET analysis, DSC analysis displays the smallest pore sizes for the super-porous iso-octane polymers. Contrary to the BET analysis the bulk polymers have the largest pore size, around 25 nm compared to 10 nm in the dry state. This increase in pore size may indicate that the bulk polymers swell to some extent in the acetonitrile. The super-porous iso-octane polymers do not display any significant change in pore size, thus indicating that they might swell less than the bulk polymers. The swelling tests performed in Section 3.2.6 show indications of the same trend, although not as distinct as in the DSC results. Interestingly the pore size for the pore-filling polymers is smaller in the swollen state compared to the pore size observed in the dry state.

The surface area for the bulk polymers by DSC analysis do not change significantly compared to in the dry state. The results for the super-porous iso-octane and pore-filling polymers on the other hand are significantly different in the swollen state than the results achieved in the dry state. The higher surface area (ranging from 440 m^2/g to 780 m^2/g) observed for the pore-filling polymers compared to the bulk polymers are expected when using porous silica as a mould for synthesis. The super-porous iso-octane polymers display extremely high surface areas of approximately 1700 m^2/g. Surface areas with these high values have been observed in precipitation polymerization microporous polymer microspheres.[223] The ultra-high surface areas observed for the super-porous iso-octane polymers probably arise from high micropore contents.

Table 6 Pore analysis parameters for the acetamide imprinted polymer formats measured by BET and thermoporometry. Where n.d is not determined.

	BET - dry state			DSC - swollen state		
	Pore diamater (nm)	Pore volume (cc/g)	Surface area (m^2/g)	Pore diamater (nm)	Pore volume (cc/g)	Surface area (m^2/g)
Bulk PA3	10.9	1.01	367	23.3	1.6	270
Bulk PAN3	10.6	1.03	391	29.3	1.8	257
Iso-octane MIP 25:75	4.3	0.11	105	4.2	1.9	1812
Iso-octane NIP 25:75	5.1	0.08	64	-	-	-
Iso-octane MIP 50:50	4.3	0.07	64	4.3	1.8	1688
Iso-octane NIP 50:50	2.4	0.03	51	4.5	1.9	1677
Iso-octane MIP 75:25	10.0	0.2	88	-	-	-
Iso-octane NIP 75:25	9.5	0.3	108	-	-	-
MIP I	18.3	0.6	126	10.1	1.5	608
NIP I	n.d	n.d	n.d	n.d	n.d	n.d
MIP II	n.d	n.d	n.d	10.1	1.7	696
NIP II	n.d	n.d	n.d	9.2	1.8	789
MIP III	15.0	0.7	174	11.0	1.5	540
NIP III	17.2	-	-	10.7	1.2	440

3.2.5 SEM CHARACTERIZATION

For further characterization of the three synthesized polymer formats the surface morphology was studied with SEM. In addition to the particle shapes information about the pore size can also be obtained. The SEM images of the bulk, iso-octane, and pore-filling polymers demonstrate a strong change in surface morphology as expected.

The bulk polymers display the characteristic irregular shape caused by the crushing and sieving procedure (Figure 66). Randomly distributed mesopores and macropores are observed on the surface.

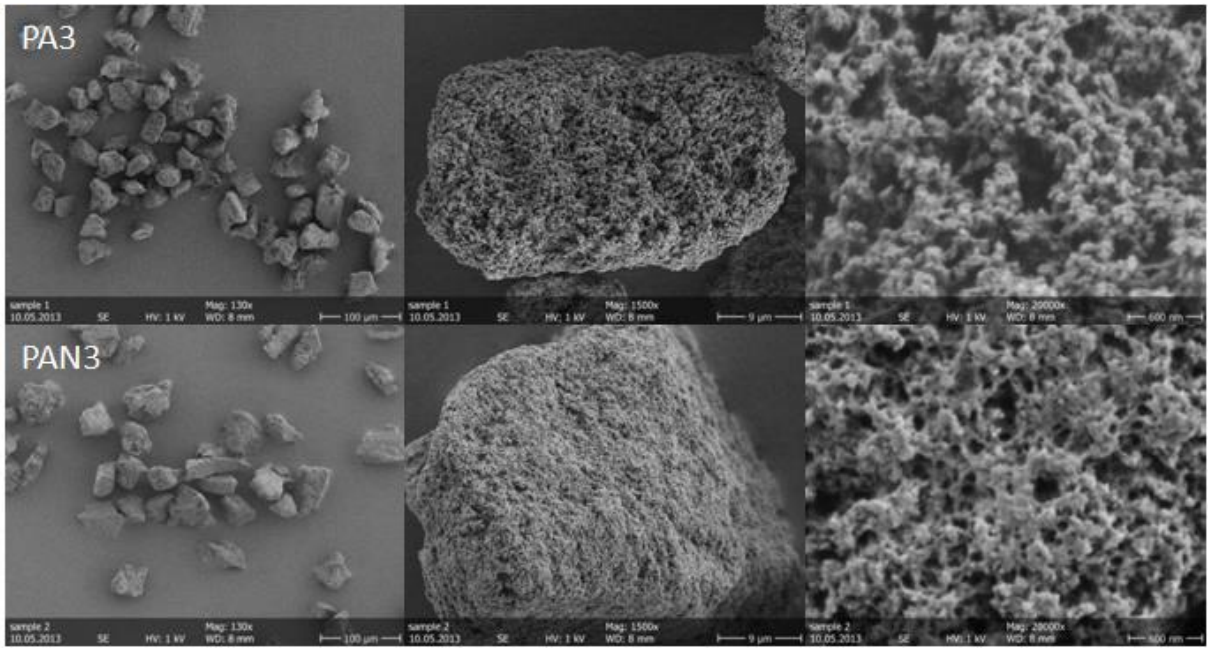

Figure 66 SEM pictures of MIP (PA3 top) and NIP (PAN3 bottom) acetamide imprinted bulk polymers. With increasing resolution from left to right (100 µm, 9 µm, 600 nm).

In the SEM images of the iso-octane acetamide imprinted polymers typical characteristics of super-porous MIPs are observed.[217] Like the bulk polymers the iso-octane polymers display irregular shaped particles (Figure 67). However, for the 25:75 and 50:50 iso-octane polymers at the lowest resolution (100 µm) it can be observed that the particles are composed by smaller particles. This may be explained by agglomeration of smaller particles that when crushed and sieved form larger particles. The third polymer, 75:25 iso-octane, displays irregular particles like the conventional bulk polymers, but with higher resolution the same agglomeration of small particles is observed. The polymer particles are significantly smaller for the 75:25 iso-octane polymer than for the 25:75 and 50:50 iso-octane polymers. Agglomeration of smaller particles is further supported when studying the highest resolution images.

Contrary to the bulk polymers, smaller pores are not observed in the iso-octane polymers. Instead µm-sized round components of macro-porous MIPs with so called super-pores connecting them are observed. The polymers with the largest amount of iso-octane, polymer 75:25, display significantly smaller round components. An explanation for the smaller formed polymer components are that when using an excess of the bad solvent iso-octane the polymer precipitates more rapidly than when using an excess of toluene. The smaller agglomerates observed in the 75:25 polymers also explain the fragility noticed during the crushing and sieving procedure.

The SEM images of the pore-filled MIPs display uniformly shaped circular particles complementary to the porous silica moulds, indicating that the pore-filling polymerization was successful (Figure 68). Pore-filling of porous silica moulds results in MIP particles with a size range and morphology reflecting the characteristics of the original silica mould. Spherical polymer particles are observed for all three polymer pairs, thus indicating that the amount of solvent used in the pre-polymerization mixture probably does not influence the pore-filling polymerization.

Further magnification show a more homogenous pore size distribution than for the conventional bulk polymers. The pores observed for the polymers, especially pairs I and II, appear to be larger than the conventional bulk polymers. The apparent more homogenous pore size distribution may be attributed to the pre-defined pores in the silica moulds. MIP III displays smaller pore size compared to the other pre-filled polymers, this could be due to the fact that some of the silica is not entirely removed during the etching procedure.

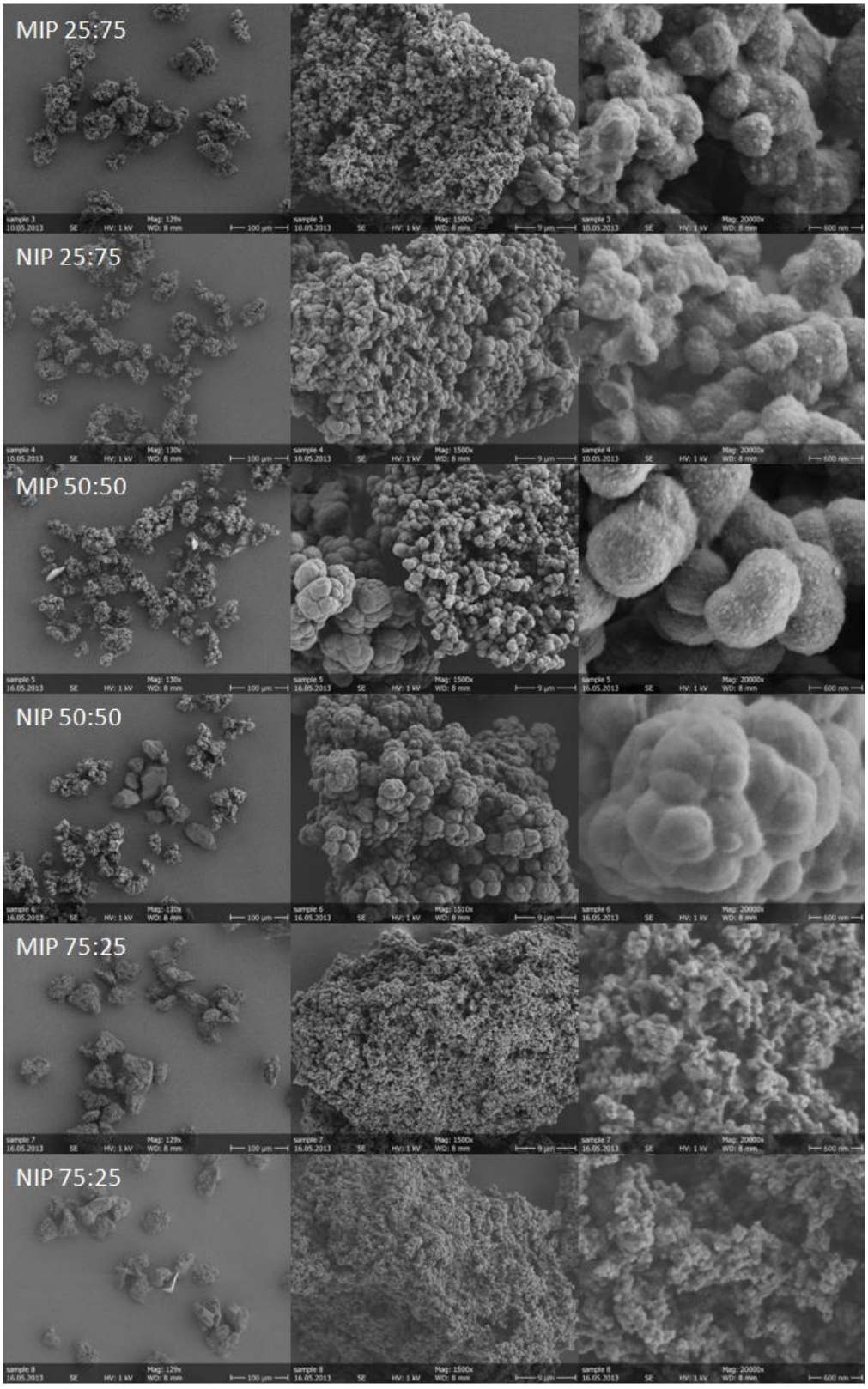

Figure 67 SEM pictures of iso-octane acetamide imprinted bulk polymers. With increasing resolution from left to right.

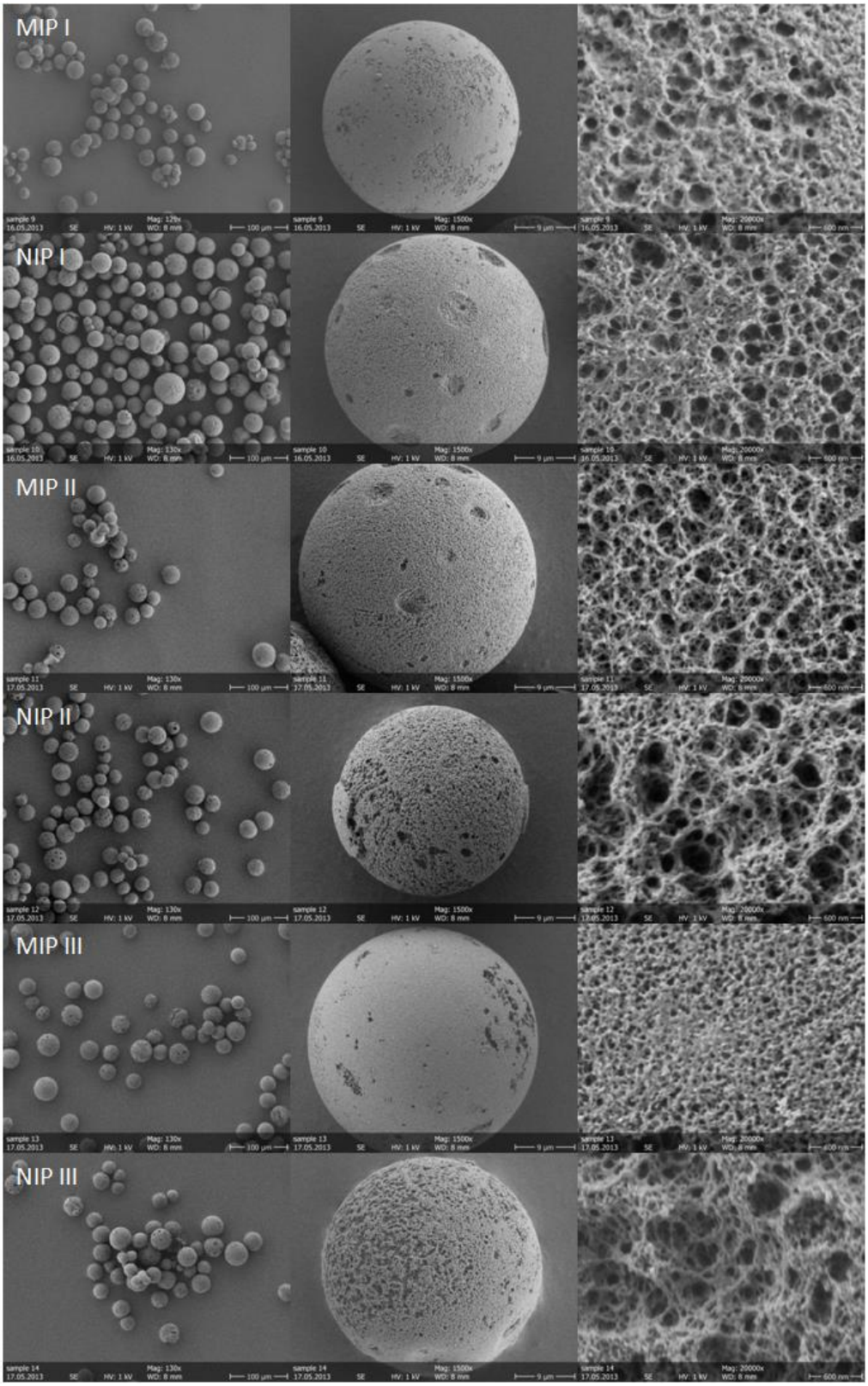

Figure 68 SEM images of the acetamide imprinted pore-filling polymers I, II, and III, and the corresponding NIPs after etching for removal of the silica. Increasing resolution from left to right.

3.2.6 SWELLING TESTS

The polymers swelling behavior was evaluated by swelling tests in both MeCN and ethyl acetate (Figure 69). No swelling tests were performed for the pore-filling polymers due to limited amount of polymer available. The MIPs synthesized in this thesis are all highly cross-linked polymers, therefore high swelling ratios are not expected. No significant difference in swelling ratios between the two different polymer formats is observed.

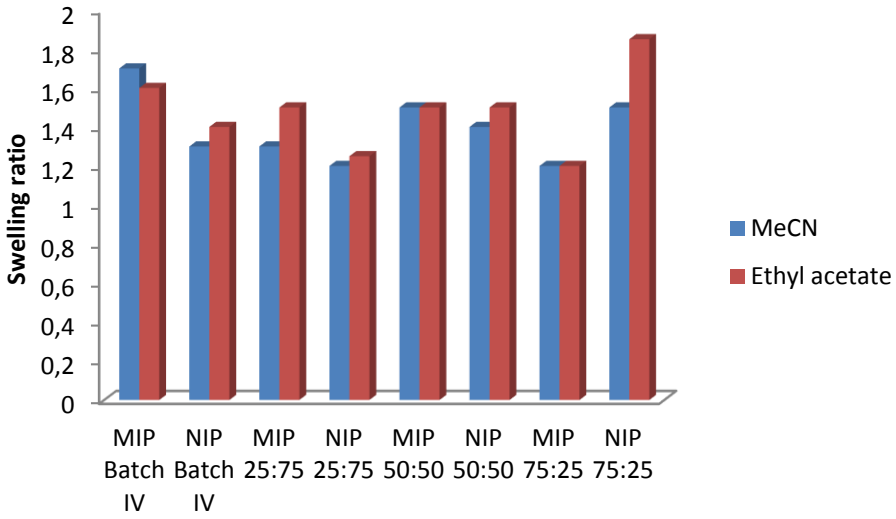

Figure 69 Swelling ratios for bulk and iso-octane polymers in MeCN and ethyl acetate.

3.2.7 CONCLUSION ACETAMIDE IMPRINTED POLYMERS

Novel molecularly imprinted polymers have been designed and synthesized, which can recognize the pharmaceutical impurities acetamide. Thorough testing and evaluation of these MIPs have demonstrated potentials to purify APIs as selective adsorbents because of their high affinity binding sites. Rebinding tests indicates that high affinity interactions are present between the binding sites of the MIP and the target impurity acetamide, which results in high efficiency purification. The new MIPs developed answer to the industrial call for systems that provide a high binding specificity between acetamide and MIPs.

For the aim of synthesizing polymers with a high capacity for pharmaceutical applications different formats were compared for optimization. The first generation bulk polymers were

synthesized for optimization of the monomer composition and proof of concept. The strategy was to use common commercially available monomers and cross-linkers for facilitating future scale-up processes. HPLC analysis, batch rebinding test and SPE experiments demonstrated strong imprinting and high specific binding of acetamide. However, for successful industrial application an improved loading capacity would be beneficial.

Two further formats were synthesized with the aim to improve the binding capacity and with the same or stronger specific binding. The two formats chosen were super-porous MIPs and pore-filling of porous silica particles, where the idea was that the inherent defined porous characteristics would improve the desired features. In general the binding capacity in ethyl acetate is slightly higher than in acetonitrile across all the formats tested. This is probably because of the difference in polarity of the two solvents, where the more polar acetonitrile disrupt the binding of acetamide. The super-porous polymers do not display an increase in binding capacity as expected, they do however demonstrate an increase in the specific binding compared to the bulk polymers. An explanation for this observation may be that with the additional iso-octane in the pre-polymerization mixture acting as a bad solvent the self-assembly of acetamide and MAA is promoted, and thus creating stronger binding sites. A successful increase in binding capacity was observed in pore-filling polymer II and III. Pore-filling polymer II being the better of the two with an increase of approximately 60 % compared to the bulk polymers. The increased binding capacity can be attributed to the more defined pores present in the pore-filling polymers after removal of the silica mold. In the bulk polymers the pore system is more heterogeneous and the higher binding capacity in the pore-filling polymers may be attributed to the more homogeneous pore system. This is supported by the SEM images displaying the pores in the polymers and by the porometry analysis performed where increased surface area is observed for the pore-filling polymers. In general the rebinding tests demonstrate stronger specific binding for the super-porous polymers and the pore-filling polymers compared to the bulk polymers.

The degradation patterns and swelling properties of the polymer formats are rather similar, as can be expected since they are all highly cross-linked polymers with the same monomer and cross-linker composition.

It can be concluded that the binding capacity for acetamide could successful be increased, without sacrificing the specific binding via pore-filling polymerization.

3.3 THIOACETAMIDE IMPRINTED POLYMERS

One aim of this work is to investigate the feasibility to use MIPs for purification of active pharmaceutical ingredients of different sizes. It is thus interesting to investigate the possible removal of other genotoxins. Following the positive results obtained from the acetamide imprinted polymers the same monomer recipe was used for imprinting of the structural similar thioacetamide as proof of concept.

3.3.1 REBINDING EVALUATION

The static rebinding tests were performed in both acetonitrile and ethyl acetate, the same solvents as the experiments performed for the acetamide imprinted polymers. In addition to facilitate a comparison of the performance with the acetamide imprinted polymers, the use of acetonitrile and ethyl acetate also represent possible real circumstances for thioacetamide removal.

The first rebinding test was carried out in acetonitrile and the results are shown in Figure 70. Binding capacities are similar to the ones observed for the acetamide imprinted polymers. However, no significant difference between the binding capacities of the MIP and NIP is observed, indicating poor thioacetamide imprinting. Rebinding in acetonitrile indicate that unspecific binding is present in the MIPs.

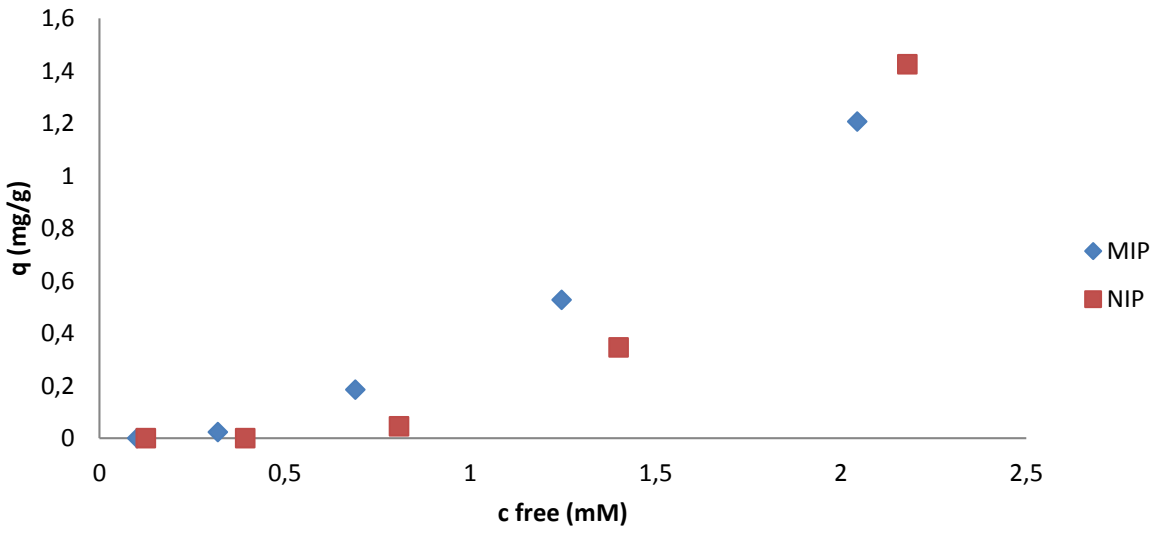

Figure 70 Rebinding isotherms of thioacetamide polymers in MeCN.

Following the rebinding in acetonitrile further rebinding test were performed in ethyl acetate (Figure 71). In contrast to the rebinding experiment in acetonitrile a significant difference in binding of thioacetamide between the MIP and NIP is observed. Furthermore, the binding capacity in ethyl acetate of the MIP is improved compared to in acetonitrile, with an increase from approximately 1.4 mg/g to 2.1 mg/g. The results indicate that specific binding of thioacetamide is taking place rather than unspecific binding.

The difference in the results for rebinding in acetonitrile and ethyl acetate observed might be explained by the different characteristics of the solvents. Acetonitrile is a more polar solvent with a polar term of 18 whereas ethyl acetate has a polar term of 5.3. This difference in polarity implies that acetonitrile might interfere with the specific binding of thioacetamide in the imprinted binding sites.

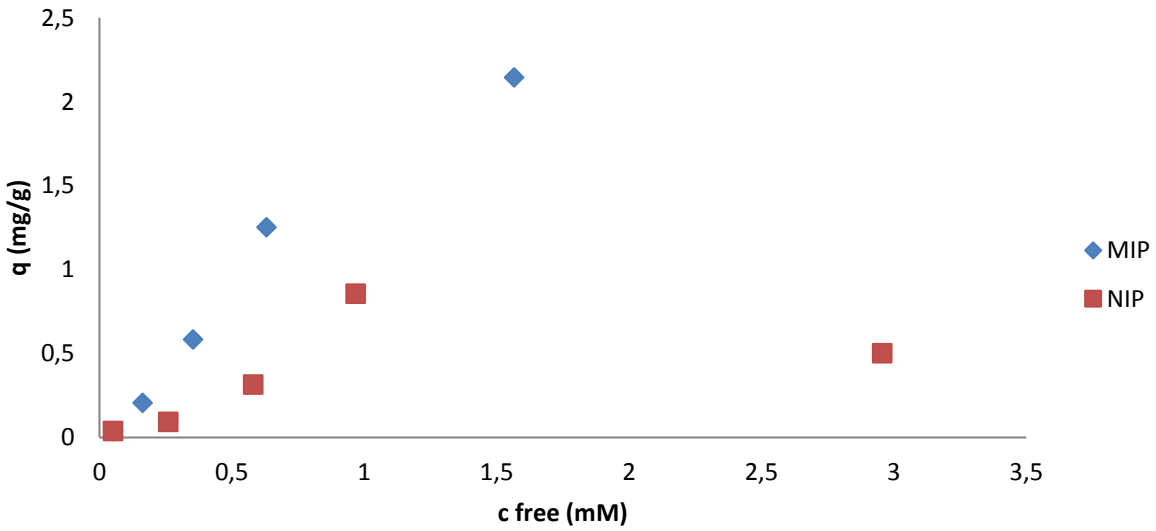

Figure 71 Thioacetamide imprinted polymer rebinding isotherms in ethyl acetate.

The thioacetamide imprinted polymers were further tested by SPE removal of thioacetamide in ethyl acetate (Figure 72). A solution with 25 ppm thioacetamide in ethyl acetate was added to a SPE column with 100 mg of polymer followed by addition of pure ethyl acetate washes, the elution fractions were collected and analyzed. The results display that the MIP bind roughly 20 % more than the NIP in the loading fractions, thus indicating specific binding of the thioacetamide. After wash 1 nearly all the loaded thioacetamide has been eluted from both the MIP and NIP and in the rest of the washes trace amounts are eluted.

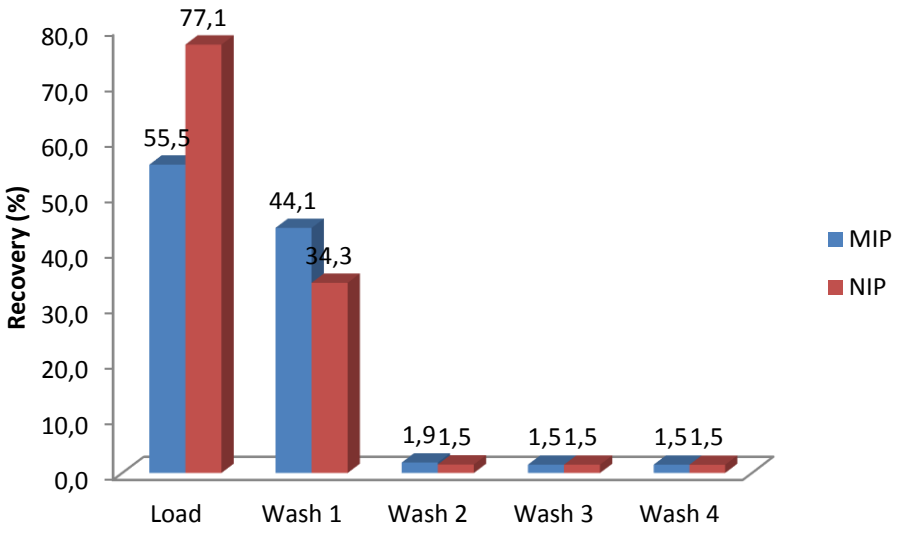

Figure 72 Recovery diagram of SPE removal of thioacetamide in ethyl acetate.

3.3.2 CHARACTERIZATION OF THIOACETAMIDE IMPRINTED POLYMERS

For an indication of the crystallization, melting and degradation temperatures of the thioacetamide polymers DSC analysis was performed. The heat flow behavior displayed is the same as for the acetamide imprinted bulk polymers in Section 3.2.3. DSC analysis of the MIP and NIP displays two melting peaks and a degradation peak (Figure 73). Like for the acetamide imprinted bulk polymers, no crystallization peak is observed, the first melting peak appears at 152 ^{0}C and the second at 227 ^{0}C, and a degradation peak is observed at 346 ^{0}C. The melting and degradation temperatures are in accordance to the temperatures observed for the acetamide imprinted polymers.

DSC analysis was also used for thermoporometry to determine the pore area, size and volume. However, the pore area, size and volume could not be determined with this characterization technique because no peak was detected (See Appendix).

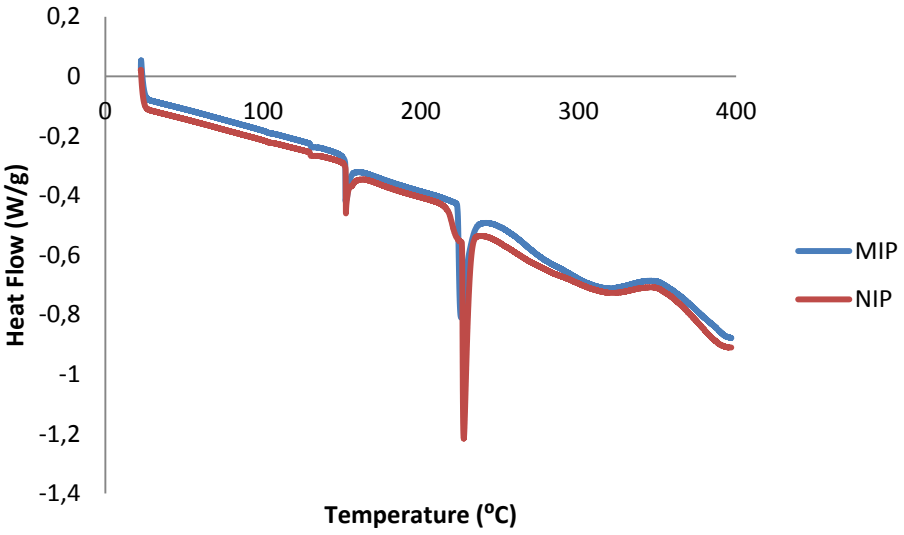

Figure 73 DSC thermogram of the thioacetamide imprinted polymers.

BET was used for pore analysis of the thioacetamide polymers and the results are summarized in Table 7. The pore analysis corresponds well to the data obtained for the acetamide imprinted polymers. The pore diameter and volumes are slightly smaller for the thioacetamide polymers than for the acetamide polymers, but they are still in the same range as may be expected since the same polymerization mixture and porogen were used.

Table 7 BET pore analysis parameters for the thioacetamide MIP and NIP polymers.

	BET - dry state		
	Pore diamater (nm)	Pore volume (cc/g)	Surface area (m^2/g)
MIP	8.1	0.74	368
NIP	7.5	0.76	406

Swelling tests in acetonitrile and ethyl acetate display swelling ratios of approximately 1.4 in both solvents for MIP and NIP (Figure 74). This corresponds to the values observed for the acetamide bulk polymers and are expected from highly cross-linked polymers.

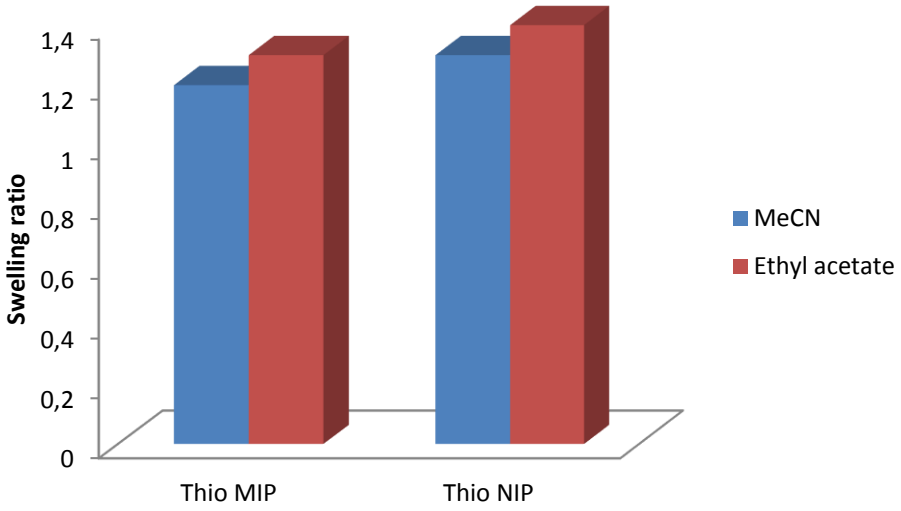

Figure 74 Swelling ratios for thioacetamide imprinted polymers in MeCN and ethyl acetate.

3.3.3 Conclusion Thioacetamide Imprinted Polymers

The aim of this experiment was to further investigate the feasibility to use MIPs for purification of active pharmaceutical ingredients. After the first positive results of acetamide imprinting and the subsequent removal thereof, it is of great interest to investigate the imprinting and specific removal of other possible genotoxins. Therefore, the same monomer composition was used to imprint thioacetamide.

Thioacetamide imprinted bulk polymers were successfully synthesized and evaluation of the MIP indicate the polymer contains specific binding sites for thioacetamide. Although, the static rebinding tests display that no specific binding takes place in the MIP when tested in acetonitrile, the results in ethyl acetate display a strong specific binding in the MIP. This observation may be explained by the difference in polarity of the two solvents, with acetonitrile being more polar than ethyl acetate. Furthermore, sulfur is slightly less electronegative than nitrogen thus probably less inclined to form strong hydrogen bonds with methacrylic acid. This may explain why the formation of thioacetamide specific binding sites is not as good as observed for the acetamide imprinted bulk polymers.

The thioacetamide bulk polymers display an increased binding capacity in ethyl acetate compared to the acetamide bulk polymers. The SPE experiment performed in ethyl acetate

further indicate that specific binding sites for thioacetamide are present in the MIP even if the difference between the MIP and the NIP is not so large. However, with further optimization of the polymer composition, such as another functional monomer or choice of porogen, more specific binding and higher binding capacities may be achieved. For the purpose of proof of concept in this thesis the results obtained are satisfactory.

3.4 2-AMINOPYRIMIDINE IMPRINTED POLYMERS

The feasibility of applying MIPs as scavengers for purification of APIs was further examined by synthesizing bulk imprinted 2-aminopyrimidine polymers (Figure 75). As described in section 1.4.3 aminopyridine derivatives can be used as starting materials and catalysts in API synthesis. These derivatives are considered to be compounds of concern, thus efficient removal of residue amounts is of interest. In this case study 2-aminopyrimidine was chosen because it and its derivatives are also considered compounds of concern due to the structural similarity to aminopyridine.

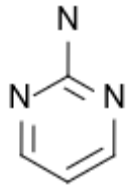

Figure 75 Structure of 2-aminopyrimidine.

A total of four polymers were synthesized and the composition of the polymers is summarized in Table 8. In addition to the polymer composition used for both the acetamide and thioacetamide imprinted polymers a second functional monomer and sovent was used, namely 4-vinylpyridine (4-VP) and dimethylformamide (DMF) respectively. 4-VP was selected as an alternative because of its capability to form non-covalent bonds and DMF was chosen because of future possible combination with synthesis of imprinted OSN membranes.

Table 8 Composition of the 2-aminopyrimidine imprinted bulk polymers.

	Monomers	Stoichiometry	Porogen
M I	T/MAA/EDGMA	1/4/20	Tol
N I	MAA/EDGMA		
M II	T/4-VP/EDGMA		
N II	4-VP/EDGMA		
M III	T/MAA/EDGMA	1/4/20	DMF
N III	MAA/EDGMA		
M IV	T/4-VP/EDGMA		
N IV	4-VP/EDGMA		

3.4.1 Rebinding Evaluation of 2-Aminopyrimidine Imprinted Polymers

Initial batch rebinding tests in acetonitrile were performed in order to evaluate the imprinting effect of the synthesized polymers. 50 mg of polymer was weight in HPLC-vials and two concentrations 0.3 and 0.6 mg/mL were added. After equilibration over night the samples were analyzed with HPLC.

The obtained results indicate that polymers with MAA as the functional monomer resulted in successful imprinting of 2-aminopyrimidine, whereas the polymers using 4-VP as the functional monomer were not successful. This can be observed when studying the imprinting factors for the four synthesized polymers (Table 9), where values above 1 indicate specific binding sites in the MIP.

Table 9 Imprinting factors for the 2-aminopyrimidine imprinted polymers.

	Imprinting factor
PI	1,5
PII	0,9
PIII	1,6
PIV	0,6

Imprinting factor (IF) was calculated from the maximum bound amount for MIP and NIP.

$$IF = m_{bound,MIP} / m_{bound,MIP}$$

It is observed that both M I and M III bind more than their respective NIPs, thus indicating that specific binding sites are present in both polymers and that successful imprinting is achieved in both toluene and DMF (Figure 76). However, the binding capacity for M I is slightly higher than for M III, this can probably be explained by the difference in polarity of toluene and DMF. DMF is more polar than toluene and can thus disturb the interactions between the template and functional monomer, where DMF has a polar term of 13.7 and toluene 1.4 (Section 1.4.7).

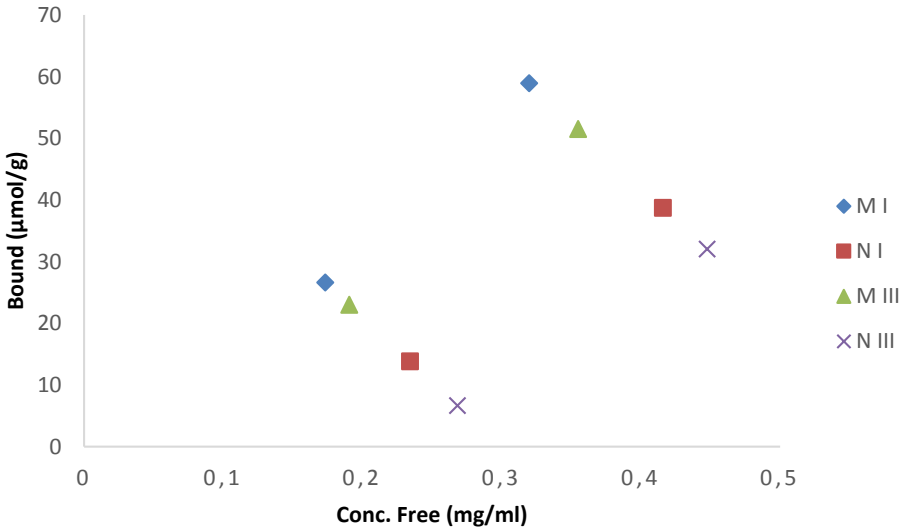

Figure 76 Rebinding test results for polymer I and III imprinted with MAA as the functional monomer in MeCN. M I and N I using toluene as the porogen , M III and N III using DMF as the porogen.

For the rebinding results for the polymers using 4-VP as the functional monomer no specific binding by the MIPs can be observed (Figure 77). In both cases the NIPs bind more than the MIPs. For polymer IV the difference between the MIP and NIP is more pronounced than in polymer II, indicating that the more polar porogen DMF promotes more unspecific binding sites in the polymers.

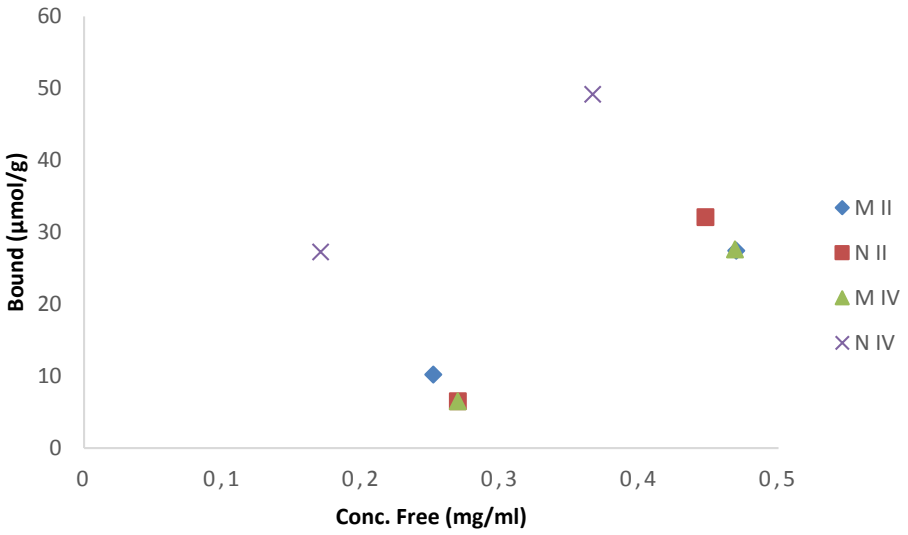

Figure 77 Rebinding test results for polymer II and IV imprinted with 4-VP as the functional monomer in MeCN. M II and N II using toluene as the porogen , M IV and N IV using DMF as the porogen.

3.4.2 Conclusion 2-Aminopyrimidine Imprinted Polymers

The aim of this experiment was to further investigate the feasibility to use MIPs for purification of active pharmaceutical ingredients. Specific binding of two small impurities using commercial available monomers has already been demonstrated in this thesis, and to investigate how versatile the monomer composition used for acetamide and thioacetamide is for pharmaceutical applications 2-aminopyrimidine was imprinted. A second commonly used monomer, 4-VP, was used in addition to MAA. For the purpose of potentially transfer the MIPs to synthesis of imprinted OSN membranes, imprinting in DMF besides in toluene was performed.

Four different 2-aminopyrimidine bulk polymers were successfully synthesized, however the evaluation of the polymers indicate that specific binding sites for the template is only present in the MAA-based polymers. In the polymers using 4-VP as the functional monomer unspecific binding seems to be more prominent. The preliminary rebinding tests display that polymers synthesized with MAA as the functional monomer in both toluene and DMF result in successfully imprinted polymers. When using the more polar solvent DMF it is observed that the binding capacity decreases slightly, indicating that the interaction between the template-monomer may be disrupted to some extent.

It can be concluded from the first preliminary binding tests that specific binding of 2-aminopyrimidine could be achieved using the same monomer composition as for acetamide and thioacetamide. The observation that specific bind sites are present also in the polymer synthesized in DMF indicates that the MIP composition may be used in the synthesis of imprinted OSN membranes. However, with further testing and optimization of the polymer composition more efficient MIPs may be achieved. For the purpose of proof of concept in this thesis the results obtained are satisfactory.

3.5 Hybrid Approach – a Case Study of Application for the Combination of MIP and OSN

As extremely low contamination levels are required for APIs, efficient impurity removal and high accuracy low level analysis is crucial. For this purpose OSN and MIPs are viable solutions, as they are two emerging separation techniques, indicating promising performance in lab-scale studies. OSN separates solutes primarily based on steric factors and as many genotoxins are small (commonly 50-150 Da) compared to drug substances (commonly 250-1000 Da) a large separation potential is often present.

MIPs can be designed to selectively bind to specific impurities hence enabling specific removal of a selected genotoxin. Both techniques are described in detail in the introduction part. Although both MIPs and OSN display a high potential for efficient purification applications in the pharmaceutical industry, they also have their own disadvantages. For MIPs the loading capacity, the sometimes tedious screening procedures needed and the use of (large amounts of) templates for the imprinting process are factors limiting the industrial implementation. The process of screening solvents is a reoccurring issue in OSN membrane field too. Furthermore, the lack of literature on performance and applicability in comparison to the traditional processes used, unsatisfactory separation performance leading to intolerable API loss or purity level, and high solvent consumption all have an influence on the slow pharmaceutical industrial implementation. In an attempt to address these issues, especially the separation performance and solvent use by the OSN membranes and the loading capacity of the MIPs, the two techniques were tested in a so called hybrid approach.

In collaboration with Elin Rundquist, the PhD student within the project based in GlaxoSmithKlein, the two techniques were tested and compared in a process mimicking real application processes. However, it should be noted that the system used was made up to fit the testing parameters and the drug candidate used has no acetamide impurities in the real purification processs. The test was designed to comply with the strict regulations pharmaceutical companies have. It employed a range of approaches including re-design of processes to avoid generation of genotoxins, alteration of process parameters to reduce impurities to acceptable levels, increased process understanding to prove that genotoxin cannot be formed or is effectively removed and toxicity studies to demonstrate that genotoxins are not harmful at the low levels envisaged.[224,225]

In our case study we assumed that the genotoxin, namely acteamide, was formed during the work-up despite the introduced controls and that the drug substance may still be viable for use after removal of the harmful material. The case study aims can be summarized as:

- Investigate the feasibility for removal of genotoxic impurity acetamide through individual use of OSN and MIP respectively
- Investigate the feasibility of using a combined approach of OSN and MIP, i.e. a hybrid approach, to improve potential acetamide removal from the individual techniques
- Provide a process comparison of OSN and MIP to evaluate strengths and weaknesses of the individual methods

3.5.1 PROCESS PARAMETERS

The process stream set up in this experiment was based on a, at the time, recently published project from UCB Pharma (Belgium)[226]. In this work aqueous washes are used to eliminate acetamide during the work-up steps and the final concentration of acetamide obtained was lower than the limit of quantification and in many cases even lower than 0.1 ppm (the limit of detection). Therefore the aim of the hybrid experiment was to reach the same concentration in order to be able to compare the different approaches.

As the API test molecule a GSK drug candidate that was under development was used. The selected GSK API has a molecular weight of approximately 480 g mol^{-1} and it was identified as a suitable test molecule, because one process step deals with the removal of thioactetamide.

However, it should be noted that no real problem to remove thioacetamide exists and the API was only chosen on the basis that thioacteamide is structurally similar to acetamide, so that the conditions are as close to reality as possible. As a result the acetamide imprinted MIPs and acetamide as the impurity are used in this case study, but as a test the cross-selectivity to thioacetamide will be examined. For the purpose of recreating the conditions in the UCB paper ethyl acetate was used as the solvent, in addition a second experiment with acetonitrile was performed based on the HPLC results (Section 3.1.1.2). Selected process stream conditions are summarized in Table 10.

Table 10 Summary of selected process stream for OSN and MIP collaboration

Process parameters	
API	GSK API under development
API molecular weight	480 g mol^{-1}
Impurity	Acetamide
Impurity molecular weight	59.07 g mol^{-1}
Solvent	Acetonitrile and ethyl acetate
API concentration	1 % wt
Impurity concentration	1000 ppm
Target impurity concentration	0.1 ppm

The choice of membranes was based on the matching of the molecular weights of the compounds with the reported cut-off curves for commercial OSN membranes. For processing in ethyl acetate Starmem™122 and Duramem™200 were selected as the most suitable membrane candidates and membranes were used for screening. For processing in acetonitrile Duramem™150 was selected as the most suitable membrane candidate and used for all processing. No membrane screening was carried out as all other commercially available membranes were deemed too loose for the suggested application.

3.5.2 METHODS FOR GENOTOXIC REMOVAL

Three different scenarios were selected for testing of genotoxin removal:

1. OSN operated in a continuous diafiltration mode
2. MIP packed columns
3. OSN and MIP operated in a combined approach with OSN used for removal of the majority of the genotoxic impurity and MIP used as a final polishing phase

For operation in ethyl acetate a membrane screening was carried out to investigate the separation potential of the GSK API and the selected genotoxin acetamide. Screening was carried out in a cross-flow system at 30 bar and ambient pressure. The feed solution was re-circulated for 4.0 h to reach close to maximum membrane compaction before the permeate was sampled for rejection testing. Screening was limited to study in ethyl acetate where two membranes are screened simultaneously.

Diafiltration was carried out in a MET dead-end cell to minimize the feed volume requirement. For operation in ethyl acetate a total of 200 mL feed solution was used for the diafiltration. To minimize the overall solvent requirement and processing time the feed solution was reduced to 100 mL for testing in acetonitrile. All processing was carried out at 30 bar and ambient temperature. MIP polymer (100 mg) was packed in a SPE column and sealed with a frit. Prior to operation the MIPs and NIPs columns were washed with methanol in order to remove any remaining acetamide and then equilibrated in ethyl acetate using a SPE vacuum manifold (Figure 78). NIPs were used as a control to verify that a potential separation is based on a successful imprinting step.

For removal test 1 MIPs were compared with OSN for removal of the complete selected concentration of 1000 ppm. During initial test 800 µL of the feed solution was loaded on the MIP and NIP columns, and pulled through using the SPE vacuum manifold. The loading elutant was collected in HPLC vials and analyzed as the initial sample. The columns were further washed with 3 x 800 µL ethyl acetate, followed by 2 x 800 µL methanol containing 0.1% formic acid. All washing fractions were collected separately and analyzed for API and acetamide content.

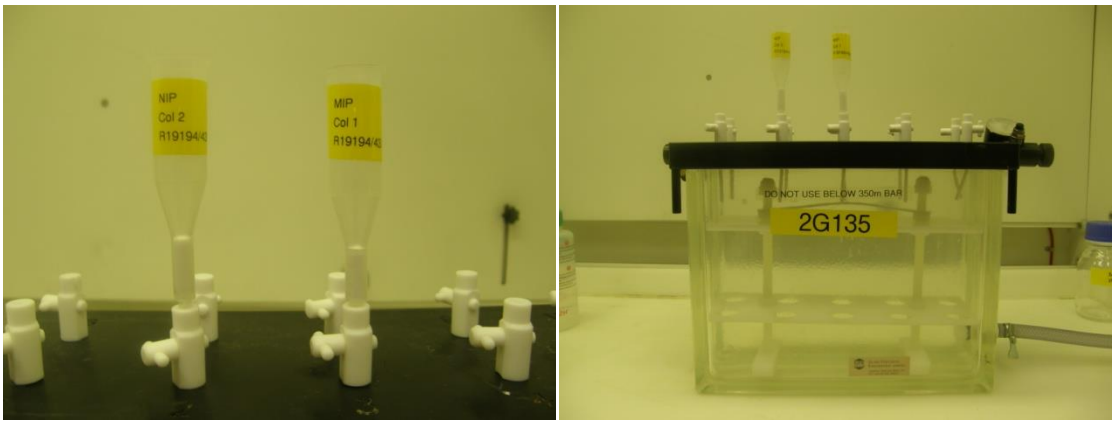

a b

Figure 78 Illustration of the columns used to pack the polymers (a) and the SPE vacuum manifold used to perform the removal tests (b).

For removal test 2 the MIPs were tested as a polishing phase after membrane filtration. Retentate from diafiltration in ethyl acetate after 3.0 and 3.6 diafiltration volumes (containing 40 and 25 ppm respectively) was used as the feed solution. Multiple samples were tested to investigate MIP performance at different concentration levels of acetamide. Removal test 2 was carried out according to the protocol detailed for removal test 1. However, the final two washes with methanol and formic acid were exchanged for pure ethyl acetate as methanol disturbs the acetamide analysis as it is eluting simultanously as the acetamide, thus making it more difficult to detect low concentrations of acetamide.

3.5.3 RESULTS HYBRID APPROACH

3.5.3.1 OSN ANALYSIS

A membrane screening was carried out to investigate the separation potential of the API and acetamide in ethyl acetate. Screening data is summarized in Table 11.

Table 11 Summary of screening data for API and acetamide in ethyl acetate.

Membrane	Batch	Equipment	API R (%)	Acetamide R (%)	Flux ($Lm^{-2}h^{-1}$)
Duramem™200	M128	Cross-flow	93.9	6.9	12.7
Starmem™122 (1)	255.1	Cross-flow	81.9	0.9	100.4
Starmem™122 (2)	255.1	Dead-end	85.2	1.0	111.5
Starmem™122 (3)	9104.1	Dead-end	96.8	1.5	83.7
Starmem™122 (4)	9104.1	Dead-end	97.9	1.4	86.1

Screening data indicates significantly varying API rejection data for Starmem™122. The differences could be a result of membrane damage, membrane not sealing properly or a result of minor batch variations. To ensure that the performance of the membrane disc is accurate a leak test was carried out for Starmem™122 (4).

An ideal membrane for the given separation has a high API rejection close to 100%, while maintaining a significantly lower acetamide rejection. The screening data indicates that the highest API rejection was observed for Starmem™122 at 97.9% compared to 93.9% for Duramem™200. Additionally the acetamide rejection was lower for Starmem™122 indicating a larger overall separating potential. Starmem™122 was hence selected as the most suitable membrane for processing in ethyl acetate.

For operation in acetonitrile Duramem™150 was identified as the only potential membrane for use. Therefore no membrane screening was carried out but a rejection test was performed after 2.0 h re-circulation to investigate the API rejection prior to diafiltration processing. Rejection data for Duramem™150 in acetonitrile is summarized in Table 12.

Table 12 Summary of rejection data for Duramem™150 in acetonitrile.

Membrane	Batch	Equipment	API R (%)	Acetamide R (%)	Flux ($Lm^{-2}h^{-1}$)
DuramemTM150	M087	Dead-end	99.8	5.2	14.9

Data in Table 12 indicate that in acetonitrile Duramem™150 has an API rejection of 99.8% while still maintaining a low acetamide rejection of 5.2%. This is close to the ideal membrane

performance and in combination with the intermediate flux of 14.9 $Lm^{-2}h^{-1}$ Duramem™150 is deemed a highly suitable membrane for acetamide removal.

Because of the data obtained in the membrane screening suggest a potential leak for Starmem™122, a leak test was performed. To ensure accurate measurement of membrane performance a leak test was carried out using a large API molecule (~600 g mol-1) which has previously measured > 99% rejection in ethyl acetate. Rejection and flux data for the marker molecule is summarized in the table below.

Table 13 Rejection and flux data for marker test.

Membrane	Batch	Equipment	Marker R (%)	Flux ($Lm^{-2}h^{-1}$)
Duramem™150	9104.1	Dead-end	99.4	126.7

The data displayed in Table 13 indicates that the rejection of the marker molecule is above 99 % which is consistent with previously observed data. The consistent and high rejection indicates that the membrane disc is sufficiently sealed and the recorded rejection in the membrane screening is an accurate measurement of the membrane performance.

Diafiltration was carried out in ethyl acetate and acetonitrile respectively. For each test the permeate was collected in 100 mL fractions and the feed concentration of the API and acetamide was calculated based on a mass-balance. Additionally retentate samples was taken after 1, 2 and 3 diafiltration volumes for the ethyl acetate test and after 3 and 6 diafiltration volumes passed for the acetonitrile test. In addition to the measured concentrations for the API and acetamide estimated levels based on a rejection mass-balance are included as a comparison. Diafiltration data for ethyl acetate and acetonitrile is summarized in Figure 79 and Figure 80 respectively.

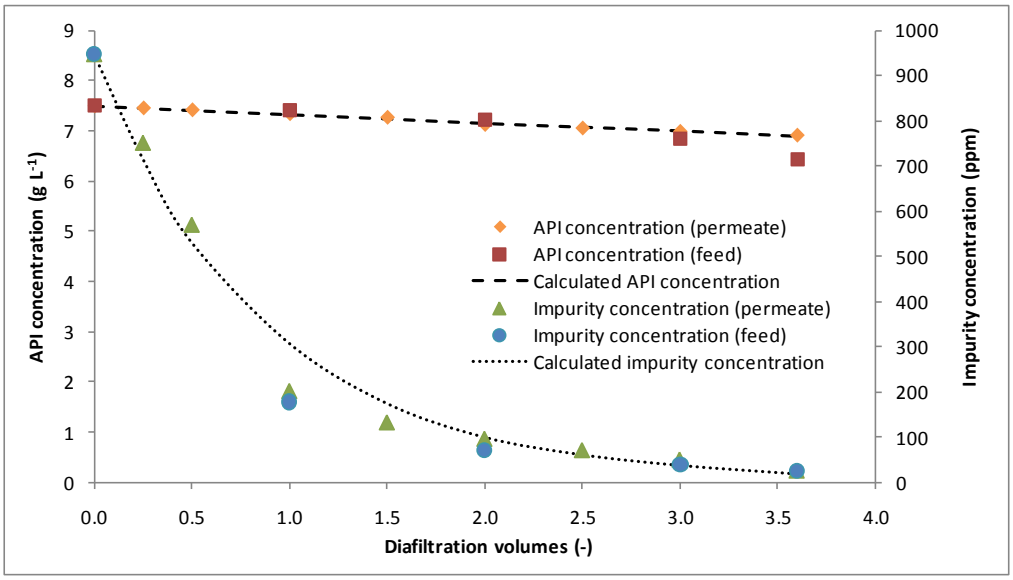

Figure 79 Estimated and measured concentration levels of API and acetamide in the feed vessel during diafiltration in ethyl acetate.

Data in Figure 79 indicate that there is a significant decrease in the acetamide concentration with increasing volumes of solvent passed. This is consistent with expected behavior as acetamide has a low rejection of 1.4% and is likely to wash out. The decrease in acetamide concentration is further consistent with the estimated mass-balance concentration based rejection values. Some deviations between the measured and estimated values can be observed around 1.0 and 1.5 diafiltration volumes of solvent passed. The deviation is believed to be a direct result of the permeate removed after 1.0 diafiltration volumes being slightly lower than 100 mL making the retentate volume larger and hence indicating a lower concentration than the accurate value. The volume was adjusted over the next diafiltration volume passed after which the measured and estimated concentrations again correlated well.

The rejection of the API was measured to 97.9 %, which is close to the ideal value of 100 %. However, the small deviation from full rejection will result in some API losses over time and the API concentration was observed to decrease throughout the test. Data in Figure 79 further indicate that the measured and estimated API concentrations are similar. Smaller deviations observed for the measured API concentration in the feed samples are likely to be a result of 2 mL retentate samples being removed from the filtration to be used as feed in MIP processing.

Diafiltration was continued until 3.6 diafiltration volumes of solvent had passed after which the acetamide concentration had been reduced to 25 ppm and the API concentration to 6.9 g L^{-1}

(based on permeate samples to avoid introducing error from retentate sampling). The decrease in API concentration is equivalent to an overall API loss of 7.6 % to reach an acetamide level of 25 ppm. To reach the target level of 0.1 ppm mass-balance estimations indicate that a total of 8.75 diafiltration volumes solvents must be passed, which would result in an overall API loss of 16.8 %. Losses are deemed too significant for processing and the test in ethyl acetate was aborted.

For testing in acetonitrile the feed volume was reduced to 100 mL to reduce the overall processing time and solvent requirement. Data for diafiltration in acetonitrile is summarized in Figure 80.

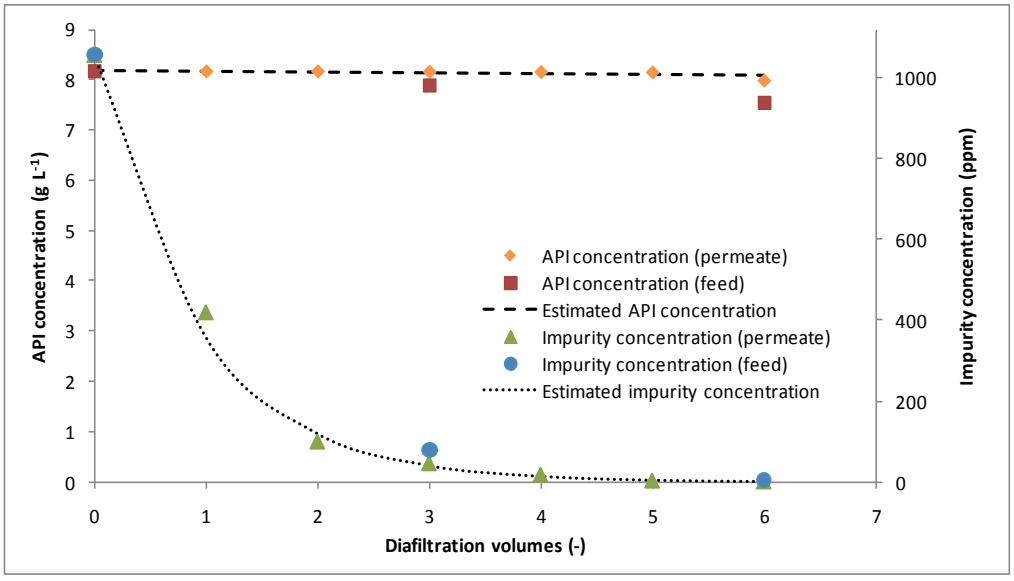

Figure 80 Estimated and measured concentration levels of API and acetamide in the feed vessel during diafiltration in acetonitrile.

Similar to Figure 79 the data in Figure 80 indicates a significant decrease in the acetamide concentration during the diafiltration. Based on the measured acetamide concentration in the permeate samples data in Figure 80 further indicate that the decrease in acetamide concentration is similar to the expected behavior based on mass-balance estimations. Important to note is that the retentate samples indicate that the acetamide concentration is slightly higher than the expected value based on both the permeate samples and the mass-balance estimation. This could be a result of the acetamide rejection being higher than the originally measured value. Mass-balance calculations indicate that to obtain the measured acetamide levels, after 3 and 6 diafiltration volumes respectively, the acetamide rejection would have to be 20 %, which is 4

times higher than the measured value of 5.2 %. For such a large difference in the measured rejection to be possible a significant error must have been made during the screening test. However as the API rejection, which is based on the same sample, appears consistent with the diafiltration data such a significant error is deemed unlikely and the small difference seen is more likely to be a result of small errors in the removed permeate volume.

The API rejection remains > 99% throughout the experiment and the losses of API can be considered rather small. The measured API concentration based on the permeate samples are consistent with the expected performance based on the calculated mass-balance. Smaller deviations can be observed between the measured API concentrations in the retentate samples and the permeate samples. This is likely to be a direct result of 2 mL retentate samples being removed from the filtration to be used as feed in a MIP phase.

The experimental data for the diafiltration in ethyl acetate and acetonitrile is summarized in Table 14. In addition mass-balance estimations of the overall API loss and solvent requirement to reach the desired acetamide concentration of 0.1 ppm are included for comparison. Finally an estimation of the solvent requirement for a potential acetamide rejection of 20 % is included to investigate the impact on the diafiltration for a higher retention of the impurity.

Table 14 Summary of experimental and calculated diafiltration data.

Sample	Acetamide (ppm)	API losses (%)	Solvent usage (DV)
Ethyl acetate, experimental data	24.9	7.6	3.6
Ethyl acetate, estimation	0.1	16.8	8.8
Acetonitrile, experimental data (feed)	1.7	1.3	6.0
Acetonitrile, experimental data (permeate)	5.4	1.3	6.0
Acetonitrile, estimation 5.2% rejection	0.1	1.7	8.7
Acetonitrile, estimation 20% rejection	0.1	2.1	10.5

Data in Table 5 indicate that the lack of 100 % API rejection for Starmem™122 operated in ethyl acetate will result in significant losses of API over time. Large API losses in combination with the reasonably high solvent requirement indicate that OSN is not suitable for removal of acetamide from the given ethyl acetate solutions. OSN might however still be useful as an initial

rough clean to reduce the acetamide concentration sufficiently for MIP purification to be viable. Additionally if the API was slightly larger hence resulting in a larger rejection OSN could be a viable option for the separation.

For acetonitrile the API rejection of Duramem™150 is close to the desired value of 100 % and only minor losses of API are seen throughout the test. The overall solvent requirements for the full diafiltration to reach 0.1 ppm acetamide are still very large however and suitability for OSN purification will have to be evaluated based on the process in question.

3.5.3.2 MIP ANALYSIS

Removal test 1 uses the complete concentration 1000 ppm sample for testing and aims to investigate the MIP separation capability compared to OSN. Acetamide and API concentrations are measured for each samples and concentration and mass-recovery is summarized in Table 15 and Figure 81 for acetamide and in Table 16 and Figure 82 for the API.

Table 15 Acetamide concentration and mass-recovery in MIP and NIP samples from removal test 1.

	Loading elutant	Wash 1	Wash 2	Wash 3	Wash 4	Wash 5	Total
				Concentration in ppm			
MIP	0.5	946.2	22.0	3.2	2.9	1.2	-
NIP	57.5	843.6	6.1	0.3	1.0	0.6	-
				Mass-recovery in µg			
MIP	0.4	757	17	4	2	1	781
NIP	46	675	5	0.2	0.8	0.5	727
				Mass-recovery in %			
MIP	0.05	94.6	2.2	0.3	0.3	0.1	97.6
NIP	5.7	84.4	0.6	0.03	0.1	0.6	90.9

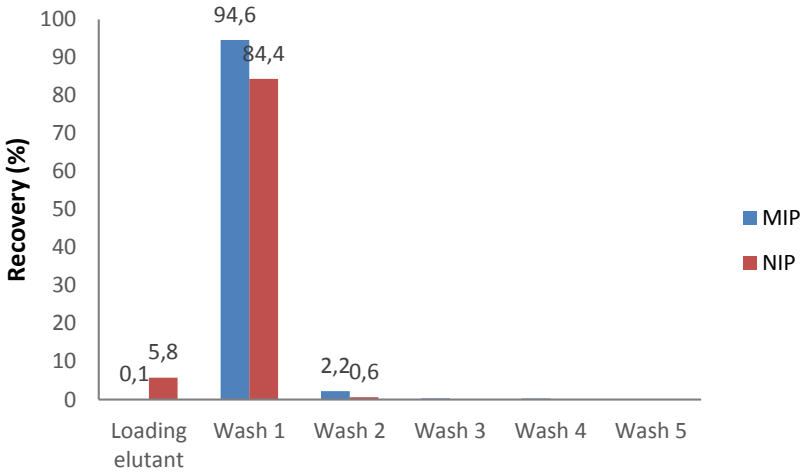

Figure 81 Percentage mass-recovery for acetamide in removal test 1.

Table 16 API concentration and mass-recovery in MIP and NIP samples from removal test 1.

	Loading elutant	Wash 1	Wash 2	Wash 3	Wash 4	Wash 5	Total
			Concentration in ppm				
MIP	7.1	2.8	0.04	0	0	0	-
NIP	6.1	2.7	0.02	0	0	0	-
			Mass-recovery in mg				
MIP	5.7	2.3	0.04	0	0	0	8.0
NIP	4.9	2.2	0.02	0	0	0	7.1
			Mass-recovery in %				
MIP	78.0	31.1	0.5	0	0	0	109.5
NIP	67.2	30.2	0.2	0	0	0	97.6

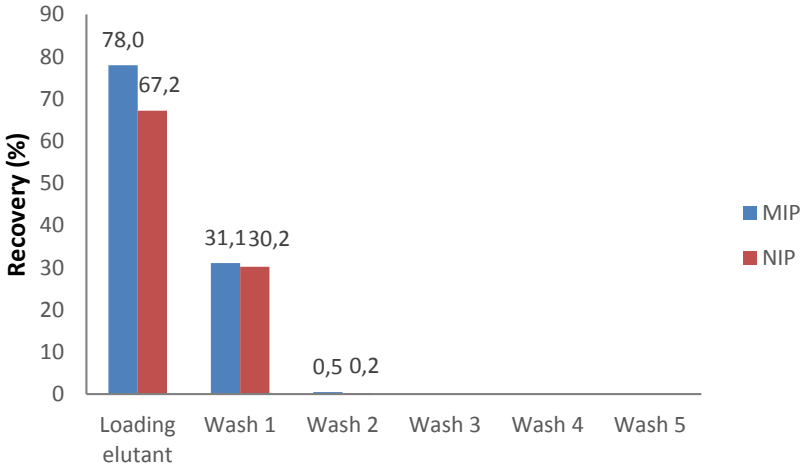

Figure 82 Percentage mass-recovery for API in removal test 1.

The data from removal test 1 indicates that the MIPs are retaining acetamide better than the NIPs. This is illustrated in Table 15 where only 0.05 % of the acetamide is eluted in the loading fraction on the MIP column compared to 5.7 % on the NIP column. Important to note is that the acetamide concentration used (1000 ppm) is very high and might be above the loading capacity of the MIPs. One indication that this might be the case is illustrated in the 1st washing fraction where the majority of the acetamide (94.6 %) is washed out. The early elution of acetamide indicates that only a limited amount of acetamide was bound to the MIP and the majority of the separation effect observed might be a result of the packed column rather than the imprinting. Some acetamide was however bound to the MIP as indicated by the difference between the MIP and NIP columns.

Data in Table 16 indicate that the API is not retained by the polymers and all of the loaded API appears to elute in the loading elute and wash fraction 1. However, data in Figure 81 indicates that the majority of the acetamide is eluting in wash fraction 1 hence making the 30 % of API eluting in this fraction unusable. The significant loss of API indicates that though some degree of separation is possible, MIPs operated in a single stage are not suitable as a means of separation at the concentration levels used for removal test 1.

Table 17 Acetamide concentration and mass-recovery in MIP and NIP samples from removal test 2.1 (sample 3.6 diafiltration volumes retentate).

	Loading elutant	Wash 1	Wash 2	Wash 3	Wash 4	Wash 5	Total
				Concentration in ppm			
MIP	0	< 0.2	7.9	11.0	14.2	1.1	-
NIP	< 0.2	18.6	4.8	0.05	3.7	0.7	-
				Mass-recovery in µg			
MIP	0	0	6	9	11	0.9	27
NIP	0	15	4	0.01	3	0.5	22
				Mass-recovery in %			
MIP	0	0	36.1	49.9	64.4	5.1	155.5
NIP	0	84.5	21.8	0.2	16.6	3.0	126.2

In removal test 2 the viability using MIPs in the hybrid approach as a polishing phase is evaluated. The samples removed during the membrane diafiltration are tested on the MIP columns. Removal test 2 was repeated for OSN retentate samples taken after 3.0 and 3.6 diafiltration volumes had passed and the acetamide concentration is 40 and 25 ppm in the respective samples. Data from removal test 2.1 using the lowest concentration acetamide

sample (3.6 diafiltration volumes retentate) is summarized in Table 17 and Figure 83 for acetamide and Table 18 and Figure 84 for the API.

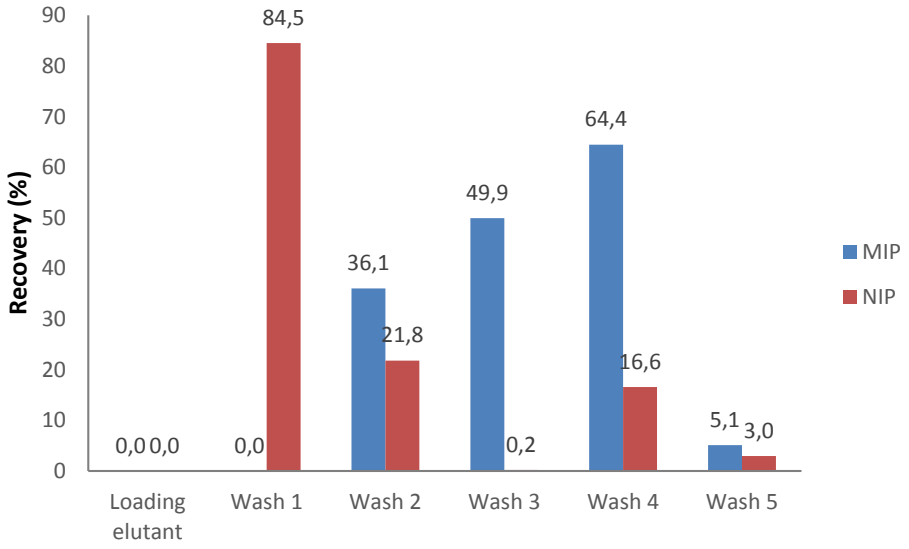

Figure 83 Percentage mass-recovery for acetamide in removal test 2.1 (sample 3.6 diafiltration volumes retentate)

Table 18 API concentration and mass-recovery in MIP and NIP samples from removal test 2.1 (sample 3.6 diafiltration volumes retentate).

	Loading elutant	Wash 1	Wash 2	Wash 3	Wash 4	Wash 5	Total
				Concentration in ppm			
MIP	5.3	2.6	0.05	0	0	0	-
NIP	5.2	2.6	0.04	0	0	0	-
				Mass-recovery in mg			
MIP	4.26	2.06	0.04	0	0	0	6.35
NIP	4.17	2.11	0.04	0	0	0	6.31
				Mass-recovery in %			
MIP	82.6	40.0	0.7	0	0	0	123.3
NIP	80.9	40.9	0.7	0	0	0	122.4

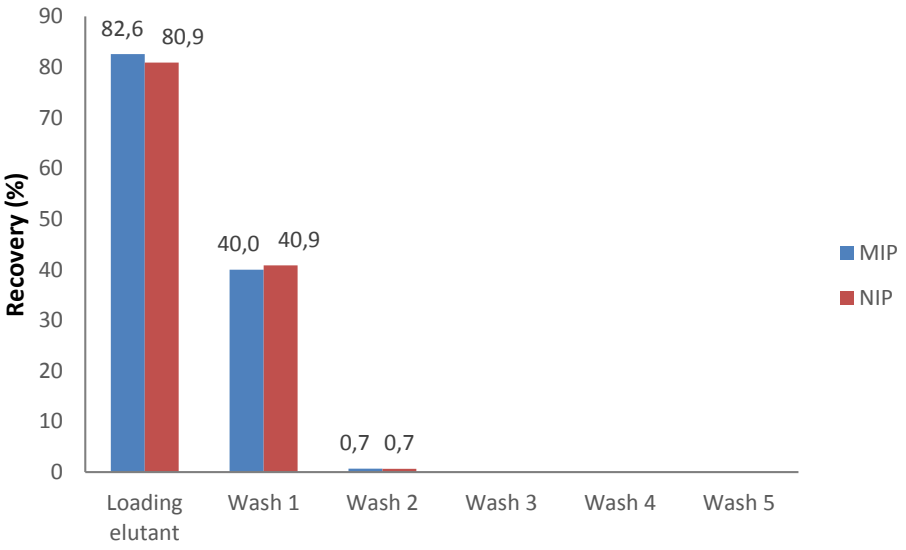

Figure 84 Percentage mass-recovery for API in removal test 2.1 (sample 3.6 diafiltration volumes retentate).

The data for acetamide in removal test 2.1 indicates that the lower concentration acetamide is clearly retained by the MIP, as the recovery is close to zero in the load elutant and wash fraction 1 compared to the NIP where 84.5 % of the acetamide is eluted in the 1st wash. Furthermore the API data display the same behavior as previously seen in removal test 1; that the majority of the API is eluted in the load elutant and the 1st wash fraction. The data obtained for both acetamide and API clearly indicate that for a low acetamide concentration of 25 ppm MIPs are an efficient polishing phase. Acetamide is successfully removed down to the specified levels while the overall API losses are estimated to be less than 1 %.

Table 19 Acetamide concentration and mass-recovery in MIP and NIP samples from removal test 2.2 (sample 3.0 diafiltration volumes retentate)

	Loading elutant	Wash 1	Wash 2	Wash 3	Wash 4	Wash 5	Total
				Concentration in ppm			
MIP	0	2.7	1.7	8.8	3.2	1.0	-
NIP	< 0.2	29.5	3.9	<0.2	<0.2	<0.2	-
				Mass-recovery in µg			
MIP	0	2	1	7	3	0.8	14
NIP	0	24	3	0	0	0	22
				Mass-recovery in %			
MIP	0	6.9	4.3	22.3	7.8	2.6	44
NIP	0	74.6	9.9	0	0	0	84

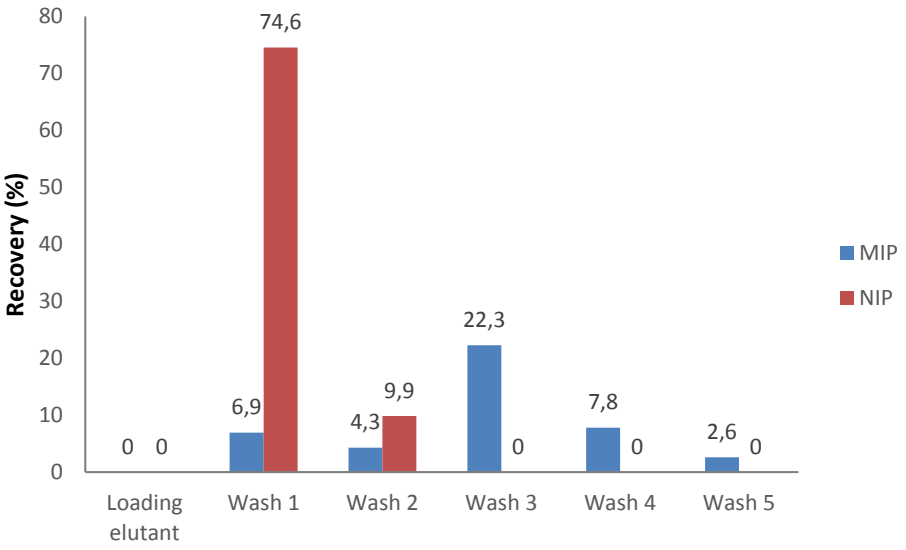

Figure 85 Percentage mass-recovery for acetamide in removal test 2.2 (sample 3.0 diafiltration volumes retentate).

Following removal test 2.1, a second test was performed for the investigation of the loading capacity limit. Removal test 2.2 has a higher concentration acetamide sample, 3.0 diafiltration volumes retentate containing 40 ppm acetamide. The data obtained will give an indication on the minimum diafiltration volumes needed for the amount of MIPs used in this test to function satisfactory as a polishing phase. Data from removal test 2.2 using the 3.0 diafiltration volumes retentate sample is summarized in Table 19 and Figure 85 for acetamide and Table 20 and Figure 86 for the API.

Table 20 API concentration and mass-recovery in MIP and NIP samples from removal test 2.2 (sample 3.0 diafiltration volumes retentate).

	Loading elutant	**Wash 1**	**Wash 2**	**Wash 3**	**Wash 4**	**Wash 5**	**Total**
				Concentration in ppm			
MIP	5.7	2.7	0.1	0	0	0	-
NIP	5.6	2.8	0.1	0	0	0	-
				Mass-recovery in mg			
MIP	4.6	2.2	<0.1	0	0	0	6.8
NIP	4.5	2.3	<0.1	0	0	0	6.8
				Mass-recovery in %			
MIP	84	40	0.9	0	0	0	124
NIP	83	41	0.8	0	0	0	124

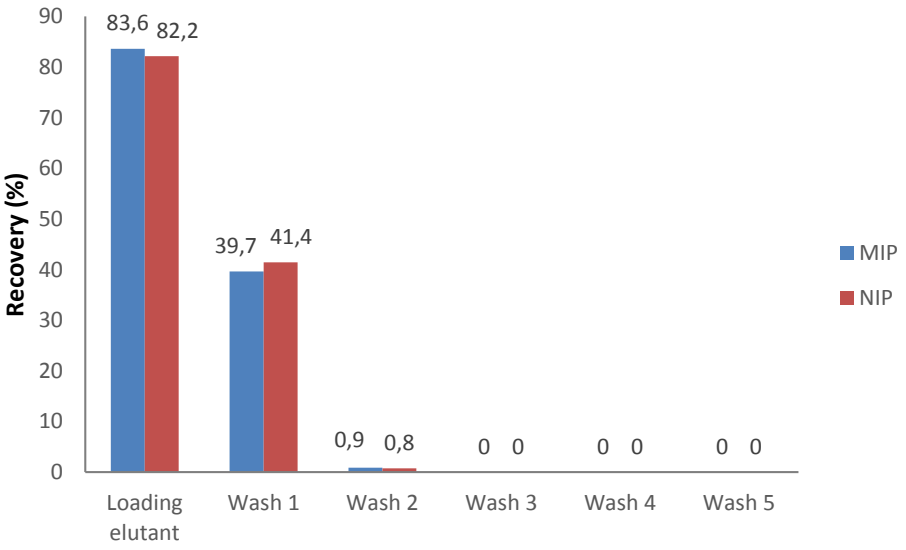

Figure 86 Percentage mass-recovery for API in removal test 2.2 (sample 3.0 diafiltration volumes retentate).

The acetamide data indicate that acetamide is retained better on the MIP compared to the NIP and after wash 1 6.9 % acetamide is eluted from the MIP compared to 74.6% eluted from the NIP. The mass recovery data is also a good indication that the separation of acetamide on the MIP can be attributed to imprinting and not just the column effect. The MIP mass-recovery from the loading and washes 1-5 only adds up to 43.9 % indicating that significant amounts of acetamide remain on the MIP column, whereas the same number for the NIP is 84.4 %. For a conventional MIP test the column would be washed with methanol and 0.1 % formic acid directly after 100 % of the desired solute has eluted. However for this test methanol is disturbing the acetamide LC-MS analysis with overlapping peaks and to ensure accurate analysis the process solvent is used for all washes. The washing of the column is hence less effective resulting in some acetamide remaining in the column.

The data obtained for the API shows that the entire amount of API is eluting in the loading fraction and in wash fraction 1. Because some acetamide is eluting already in the wash fraction 1 the API eluting in wash 1 is therefore lost. The early elution of acetamide in wash fraction 1 indicates that the loading capacity of the MIPs are somewhere between 40 and 25 ppm (retentate concentrations after 3.0 and 3.6 diafiltration volumes passed). To ensure API purification without significant losses of API the MIP loading capacity must not be exceeded.

3.5.4 CONCLUSION HYBRID APPROACH

This case study aims to investigate the combination of MIPs and OSN for application in the pharmaceutical industry. In order to demonstrate the viability of this hybrid approach the two techniques were tested separately and finally combined, so that a good comparison as well as eventual shortcomings of the techniques can be identified.

The OSN experiments demonstrate feasibility for acetamide removal in both ethyl acetate and acetonitrile. In the case of removal in ethyl acetate the screening tests indicated that Starmem^{TM}122 is the most suitable membrane for the specified experiment parameters, with a measured API rejection of 97.9 % and acetamide rejection of 1.4 %. Mass-balance calculations demonstrate that in order to reach the desired acetamide concentration of 0.1 ppm a total of 8.8 diafiltration volumes are required. This would result in an estimated overall API loss of 16.8 % for the full process. Diafiltration results show that the overall loss of API after the second and last sample taken for the MIP testing, 3.6 diafiltration volumes, is 7.6 %. These results clearly demonstrate the feasibility of separation of the API and acetamide using OSN, however the large API losses in combination with high solvent requirements application in similar processes is not recommended.

For the specified separation in acetonitrile, DuramemTM150 is deemed the most suitable membrane based on the obtained results. The measured rejection of API and acteamide was 99.8 % and 5.2 % respectively. Mass-balance calculations indicate that a total of 8.7 diafiltration volumes are required to reach the desired acetamide concentration of 0.1 ppm. this results in an overall API loss for the full process of 1.7 %. Once again the solvent requirement for the diafiltration process is large, but the high rejection in acetonitrile results in a low overall loss of API. For this application in acetonitrile OSN might be a suitable alternative for acetamide removal nonetheless solvent usage must be evaluated compared to alternative techniques.

The OSN experiments show that the acetamide rejections are generally low resulting in a rapid decrease in concentration over the initial diafiltration volume. After a limited volume of one diafiltration volume the API losses are still limited and OSN might be a suitable alternative for “rough” cleaning process. This is where the hybrid approach using OSN for initial “rough”

separation and MIPs as a polishing phase for removal of impurities to very low concentrations potentially could exhibit a benefit.

The removal tests for the MIPs were limited to testing in ethylacetate. For removal test 1 where the starting concentration was loaded on the MIP column an imprinting effect could be distinguished, although no effective removal of acetamide was observed in the overall process. The results obtained indicate a clear over-loading of the column, reflected in amount of acetamide retained on the column after the loading. The main part of acetamide is eluted in wash fraction 1 and hence has a concentration close to the feed. This elution in the first wash fraction is therefore not suited for further processing and the API eluted in this fraction is unusable. The overall API loss hence adds up to a significant value of approximately 30 % indicating that it is not feasible to use MIPs for high concentration removal of acetamide.

The full feed concentration removal test was followed by two removal tests using samples taken from the OSN retentate after different diafiltration volumes. For removal test 2.1 where the lowest concentration acetamide of 25 ppm was loaded on the MIP column, a clear separation of acetamide and the API can be observed. In comparison to the NIP the MIP effectively removes acetamide and thereby decreasing the concentration from 25 ppm to < 0.2 ppm. In addition more or less no API is retained on the column and after wash 1 everything is eluted, indicating that there is no cross-selectivity or binding site competition of the API on the MIP column. Hence the MIPs can effectively remove acetamide to the specified concentration with on overall API loss of less than 1 %. In removal test 2 a higher concentration of acetamide in the loading step was used. The small amount acetamide that is eluting in wash fraction 1 indicates that the loading capacity of the MIPs is reached and must hence be between 25 and 40 ppm for this experiment. So depending on the purity specifications of the API the amount of MIPs used can be adjusted accordingly.

3.6 High-Throughput Synthesis for MIPs via Grafting on Membranes

There is a rather large number of parameters that can be varied during the optimization process of MIPs, hence conventional polymerization, processing and evaluation techniques are not suitable for optimizations where time is of the essence. This limits industrial applications of MIPs where time is often constrained, therefore new robust time-efficient screening techniques is of great importance for the future of MIPs in industry. The screening techniques available in literature today are based on combinatorial design and high-throughput synthesis and analysis to synthesis so called miniMIPs, basically monolithic MIPs scaled down. Automation of the process can easily be achieved by using liquid handling robots and 96-well microtiter and filter plates. The miniMIPs are synthesized in the 96-well microtiter plate followed by transfer of the miniMIPs to a 96-well filterplate, where the template removal and the template rebinding step is performed. With this method it is possible to synthezise and evaluate a library of miniMIPs in a couple of weeks. [227,228,229,230,231]

However, the time needed for synthesis and analysis of a library is still rather substantial and the critical step contributing to a large part of the time is template removal. Because of the small amounts of solvents used for washing and the inherent slow diffusion kinetics of the template, as many as 20-30 washing steps can be required. In order to reduce the time needed for library synthesis and analysis, Hovarth *et. al.* introduced thin polymer layers/films on the surface of porous membrane 96-well filter plates.[232] The considerably decreased diffusion path length improves the template release and the washing can be performed in a flow-through mode. The grafting of thin MIP films on porous membrane surfaces has already been prepared for affinity purposes.[233,234,235,236] This combination of thin film grafted membranes and filtration microplates offers a new system for high-throughput synthesis and testing of MIPs. It offers some advantages over the conventional miniMIP approach, for example less time-consuming template removal, flow-through mode instead of a large number of consecutive steps of batch washing, evaluation of imprinting effect can be performed in situ and that the material can be analyzed directly under SPE conditions.[232]

The aim of this work is to develop this screening method further by combining the approach of Hovarth *et al.* [232] with the work published by Belfort *et al.* [237]. A new high throughput system was developed using 96-well membrane filter plates by grafting directly from the membrane

by UV-initiation. Belfort *et al.* has shown that a thin layer of monomers can be grafted on the surface of polyether sulfone (PES) membranes by immersion in a monomer mixture. The special feature of these membranes is that no initiator is needed because radicals are formed on the surface upon UV-radiation (Figure 87). During the development of the HTS using PES membranes two different types with pore sizes of 300 kDa and 0.45 µm were used. After the development of a working grafting procedure the template chosen for screening and imprinting was somatostatin. The reason for this is that in the following section the application of MIPs as catalysts, in this particular case the enhancement of cyclisation of the peptide somatostatin, will be investigated.

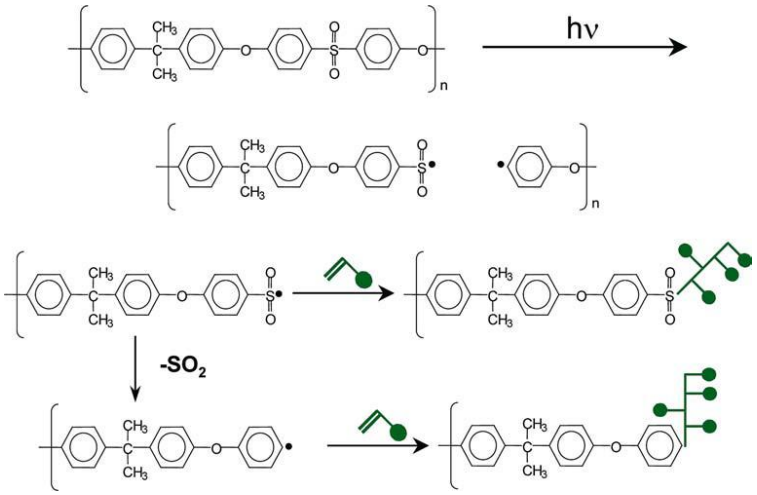

Figure 87 Cleavage of PES from illumination by UV.[237]

3.6.1 Preparation of Grafted Membranes

The grafting on PES membranes follows a very simple procedure, where the membrane is first washed with methanol and deionized water to remove surfactants before use. Then the membrane is soaked in the monomer solution and subsequently illuminated with UV for grafting from the surface. Since the permeability of the membranes is a key attribute for the improved screening system it is important to be examined. For this purpose a stock solution with the ratio 1:3 of monomer to solvent was prepared.[238,239] The mother solutions containing the template somatostatin, functional monomer acrylamide and MAA, cross-linker ethylene bisacrylmamide (EBA) were prepared from dilution of the stock solution. After soaking in the monomer solution the plate or loose membranes are placed in a special built glass box with

quartz lid, designed to create an oxygen free environment, in an incubator (Figure 88). After UV polymerization the template is removed by washing the membranes with warm 40 ^{0}C methanol containing 1% formic acid. Template removal of somatostatin can be followed by measuring the fluorescence after each wash. Residual acid is washed away with extensive methanol.

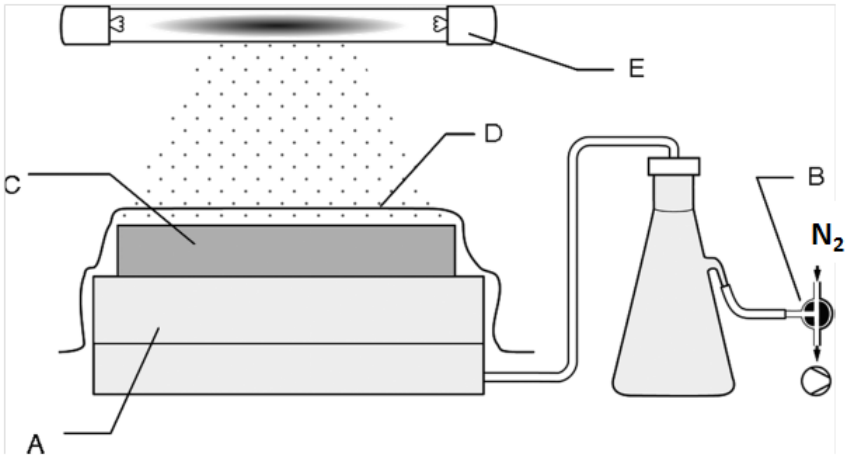

Figure 88 System setup for UV polymerization of the MIPs supported in microfiltration plates: (A) vacuum manifold, (B) nitrogen gas, (C) filterplate, (D) cling film, and (E) UVC lamp. Modified from reference 232.

3.6.2 Grafting Optimization and Method for Initial Testing

In the first step the different pore sizes of the membrane were examined in order to find the most suitable one to avoid blockage of the pores. The two 96-well plates with the pore sizes 300 kDa and 0.45µm were treated the same and polymerizations were carried out under the same conditions. For the first grafting test two different parameters were varied in order to find the optimal polymerization conditions, namely monomer dilution and polymerization time (Figure 89). An aqueous polymerization system was used, with acrylamide and MAA as the functional monomers, ethylene bisacrylamide (EBA) as the crosslinker, and somatostatin as the template. The cross-linking level was 50 %.

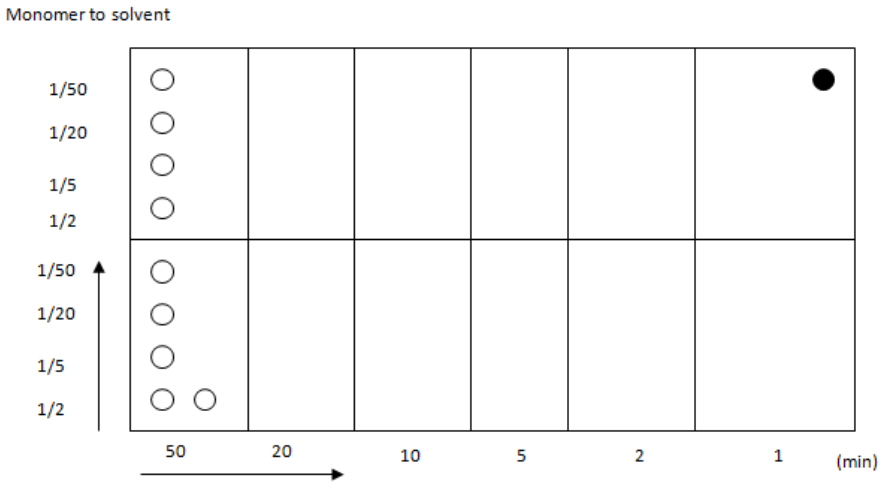

Figure 89 Schematic representation of the varying monomer dilution and polymerization time optimization.

Independent of the monomer dilution and polymerization time, the 300kDa pore size 96-well filter plate does not seem suited for polymer grafting experiments. During template removal it is observed that the 300 kDa filter plate is blocked and no washing solution passes through the membrane. The 45 µm pore size filter plate on the other hand is not blocked and the template is successfully removed. Hence, only the 45 µm pore size filter plate is used for further experiments. The template was removed with repeated washes of MeOH (40 ºC) containing 1 % formic acid and the procedure was followed by fluorescence measurements at 375 nm. Template removal followed the same trend independently of monomer dilution and polymerization time, and two representative removal diagrams are shown in Figure 90. The template removal diagrams indicate that the template somatostatin is successfully removed after 10 washes. The majority of somatostatin is washed out during the first five washes.

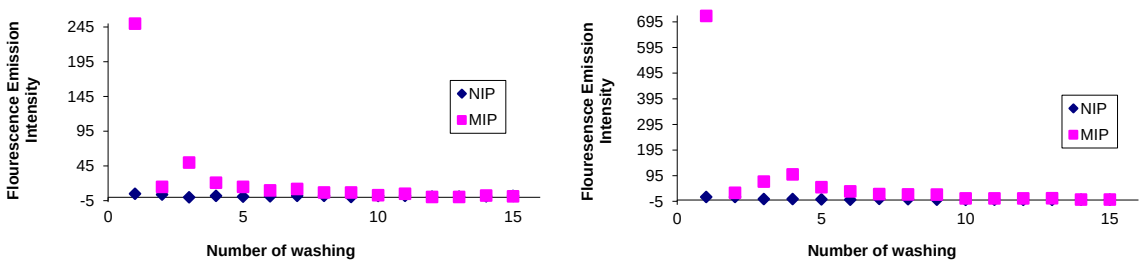

Figure 90 Example of template removal for 20 minutes (left) and 50 minutes (right) polymerization time with 1:20 monomer dilution.

Following template removal, a first preliminary rebinding test was performed. A solution of 0.025 mM somatostatin in HEPES buffer was added to each well and equilibrated for 5 hours. The amount of bound somatostatin in percentage was calculated from the fluorescence measurements and summarized in Figure 91. Although the amount of bound somatostatin observed is rather low (roughly 20%), the obtained results indicate a difference in binding between the MIPs and NIPs for the grafted membranes with monomer dilutions of 1:5 and 1:20. When studying the binding percentages for these monomer dilutions over time, indication of a larger difference in binding between the MIPs and NIPs is observed for longer polymerization times.

		50 min	20 min	10 min	5 min	2 min	1 min
Ratio 1:3	NIP	11	8	5	11	13	4
	MIP	26	22	15	17	19	23
Ratio 1:5	NIP	0	0	1	13	10	3
	MIP	21	21	19	23	26	24
Ratio 1:20	NIP	0	3	1	6	5	3
	MIP	24	19	23	21	35	12
Ratio 1:50	NIP	33	39	35	35	33	87
	MIP	4	10	13	13	21	10

Figure 91 Rebinding test result, comparison of bound somatostatin between MIP and NIP. The values shown are in percentage (%).

Following the first grafting optimization experiment further tests were performed to determine the optimal polymerization time. Since the first optimization test indicated that a longer polymerization time might be beneficial UV exposure times of up to 180 minutes were investigated (Table 21). In this test the polymerization mixture composition (monomer: solvent ratio 2:1) was kept constant in order to observe the exposure time influence in detail. Because of limited amounts of somatostatin the grafting optimization experiment was carried out with the cyclic peptide desmopressin as an analog.

Table 21 Summary of polymerization time optimization test. The monomer:solvent ratio is 2:1. A control non-imprinted grafted membrane was also prepared.

Composition of the polymerization mixture		
Compound		Ratio
Template	Desmopressin	0.2 mmol
Functional monomer	Acrylamide	3 mmol
Functional monomer	Methacrylic acid	1 mmol
Cross-linker	Ethylene bisacrylamide	4 mmol
Solvent	HEPES buffer	0.48 ml
Polymerization times		
min		
1, 5, 10, 30, 60, 90, 180		

After polymerization according to the specified times the membranes were cut out from the filter plate and analyzed with TGA. The thermal stability of the blank membrane was investigates by TGA for comparison of grafted membranes (Figure 92). The TGA curve of the blank PES membrane demonstrates one-step degradation with an onset temperature at approximately 500 ^{0}C. This is slightly higher than observed for bulk polymers.

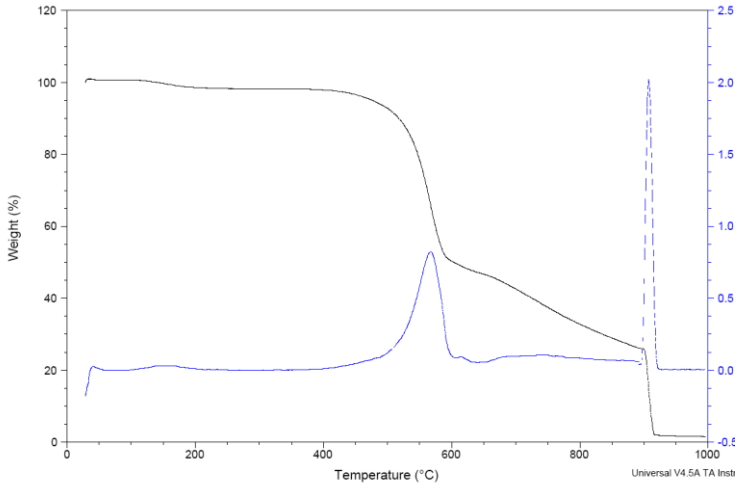

Figure 92 TGA curve of the blank membrane.

After polymerization and washing of the membranes TGA was performed in order to see if the grafting procedure may be monitored with this analysis. The curves for the NIP grafted membranes with polymerization times 5, 10, 30, 60, and 90 minutes are summarized in Figure 93. It is observed that with increasing polymerization time the plateau between 200 ^{0}C and 400 ^{0}C is higher, hence indicating a smaller weight loss. This may be explained by formation

of highly cross-linked polymer grafted to the membrane surface, indicating that a higher polymerization time is more beneficial. When comparing the TGA curves obtained for the polymerization times 90 and 180 minutes no difference in mass loss is observed, indicating that polymerization is completed (Figure 94). Thus, polymerization times longer than 90 minutes do not improve the grafting of the membranes.

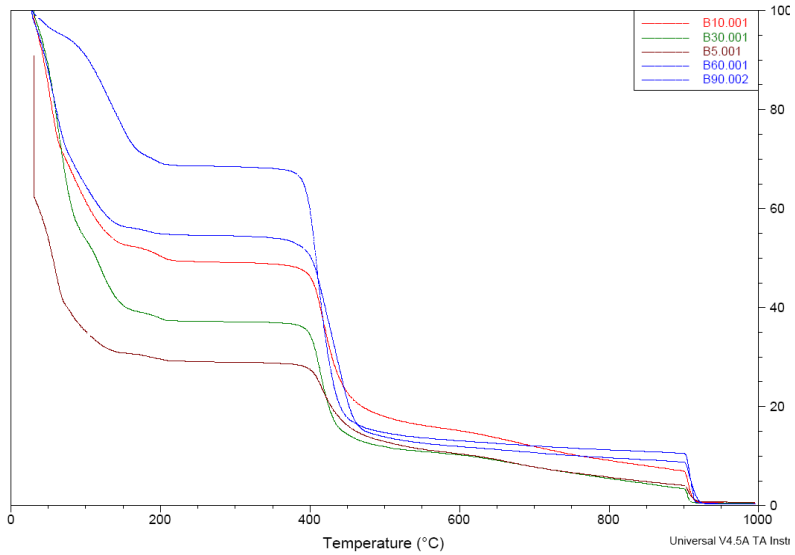

Figure 93 TGA curves of the grafted NIP membranes with different polymerization times; 5, 10, 30, 60, and 90 minutes.

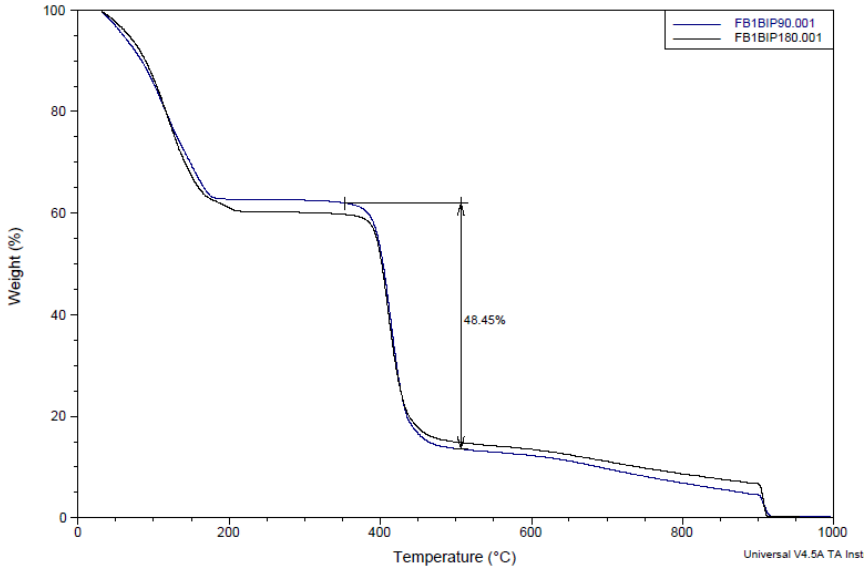

Figure 94 TGA curves of the grafted NIP membranes comparing the two different polymerization times 90 and 180 minutes.

The grafted NIP membrane with the polymerization time of 90 minutes was also analyzed with SEM to study the surface compared to a non-grafted blank PES membrane (Figure 95). A clear difference between the grafted and non-grafted surfaces can be observed. The surface of the non-grafted blank membrane is smooth and the pores are distinct, whereas the grafted membrane surface displays a rougher surface and blocked pores indicating that polymer is successfully grafted on the membrane surface. Both membrane surfaces were additionally analyzed with EDX to obtain information on the elemental composition (Table 22). The grafted NIP and MIP membranes display an increased amount of nitrogen compared to the non-grafted membrane, indicating that polymer is successfully grafted on the surface. As a result of nitrogen containing monomers being present on the surface. The slightly higher level of nitrogen present on the MIP membrane compared to the NIP membrane can be explained by the template desmopressin.

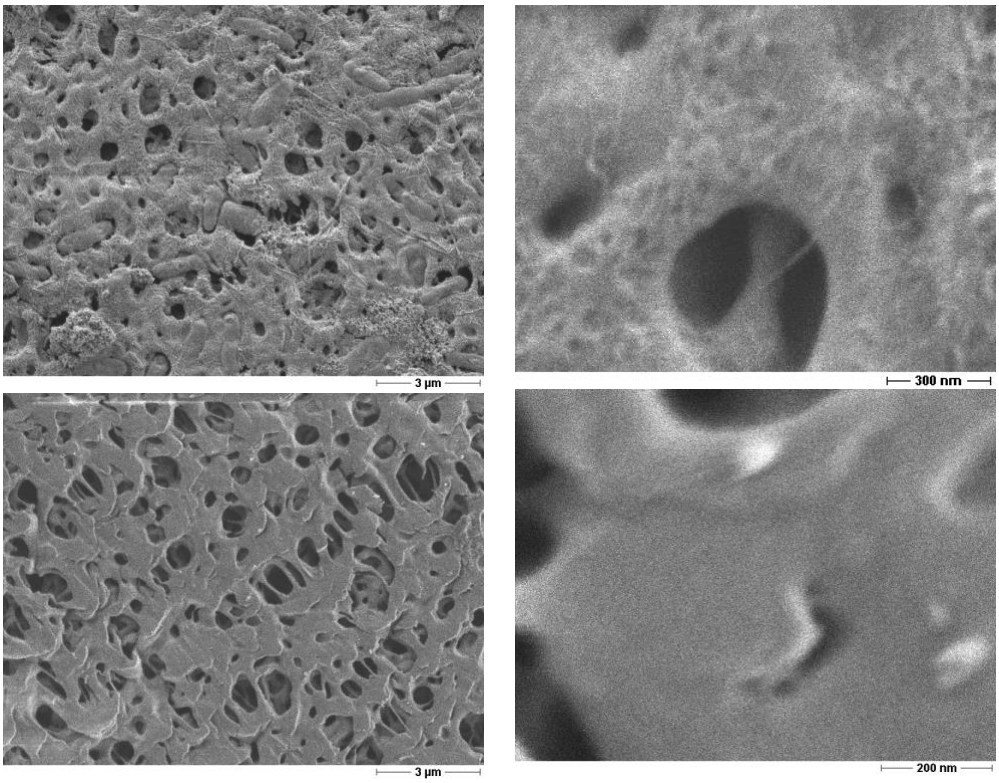

Figure 95 SEM images of grafted PES membrane, 90 minutes exposure time (top) and non-grafted blank PES membrane (down).

Table 22 Elemental composition of non-grafted blank membrane, NIP membrane, MIP membrane determined by EDX analysis.

	Elemental composition			
Sample name	C (%)	N (%)	O (%)	S (%)
Blank membrane	63.46	0.41*	30.11	5
NIP membrane	57.77	4.9*	32.01	4.66
MIP Membrane	54.29	7.23*	34.65	2.91

**>2 Sigma*

The SEM images displayed partially blocked pores by grafted polymer. Hence, following the polymerization time optimization the amount of grafted polymer on the surface is investigated. For proper function of the membranes it is crucial that the grafting of polymers do not block the pore and thus decrease the permeability to the extent where a solution can pass through the membrane anymore. For the grafting optimization loose membranes were soaked in the pre-polymerization mixture and subsequently polymerized under UV for 90 minutes. In order to calculate the grafting amount the membranes were weighed before and after polymerization. In this experiment two different cross-linking levels are used to investigate the influence of cross-linker amount of pore blockage (namely 20 % and 40 %), in addition one NIP pre-polymerization was prepared for each cross-linking level. The composition of the pre-polymerization mixtures is summarized in Table 23.

After polymerization, washing in methanol, and drying the membranes were weighed and the amount of grafted polymer was calculated for the MIP membranes. Furthermore, the permeability of the MIP and NIP membranes was compared to a blank membrane, in order to gain information about blockage of the pores. The results for the grafting and permeability are shown in Table 24. It is observed that the amount of grafted polymer increases slightly with 40 % cross-linking level compared to the membrane grafted with 20 % cross-linking level. This observation may be expected with the larger amount of cross-linker. However, with the increased amount of grafted polymer the permeability of the membrane subsequently decreases, thus indicating that the pores of the membrane are getting blocked.

Table 23 Composition of the polymerization mixtures used in the grafting optimization experiment. The NIP pre-polymerization mixtures were prepared according to the same compositions but without the template.

Composition of the polymerization mixtures		
MIP 20% CL		
Template	Somatostatin	4 μmol
Functional monomer	Methacrylamide	40 μmol
Functional monomer	Methacrylic acid	280 μmol
Cross-linker	Methylene bisacrylamide	80 μmol
Solvent	Phosphate buffer, 50 mM pH 7	500 μL
MIP 40%CL		
Template	Somatostatin	4 μmol
Functional monomer	Methacrylamide	40 μmol
Functional monomer	Methacrylic acid	200 μmol
Cross-linker	Methylene bisacrylamide	160 μmol
Solvent	Phosphate buffer, 50 mM pH 7	500 μL

The SEM images further support the blockage of the pores with increasing cross-linking level (Figure 96). It can be observed that with the 40 % cross-linking level a larger amount of polymer is formed at the surface and that the pores are more blocked. Although the permeability of the membrane grafted with 20 % cross-linking level also displays a decrease, it is not as large as for the 40 % cross-linking level and can thus be considered acceptable for the purpose of this thesis. Grafting of polymer on the surface will subsequently increase the polymer density on the surface and consequently block the pores, so a balance between the amount of polymer grafted and the permeability of the membrane needs to be found.

Table 24 Amount of grafted polymer and permeability of the MIP membranes with 20 % and 40 % cross-linking and blank membrane for comparison.

	Grafted polymer amount	**Permeability**
	mg	ml/min
MIP 20 % CL	5.2	218
MIP 40% CL	7.9	152
Blank membrane	-	333

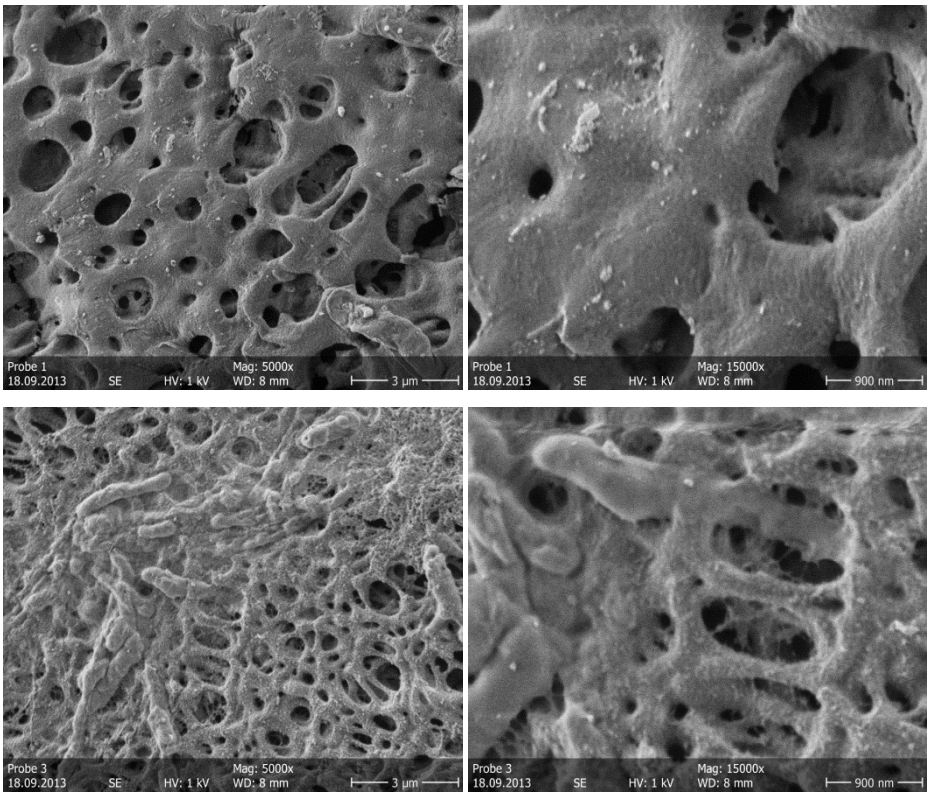

Figure 96 SEM images of the MIP grafted PES membranes with 20 % cross-linking (top) and 40 % cross-linking (bottom).

Following the grafting optimization where the 20 % cross-linking level grafted membrane was established as the most suitable membrane composition for HTS grafting of membrane filter plates, a rebinding test over time was performed to investigate the imprinting effect. The 20 % cross-linking level MIP membrane and the corresponding NIP membrane were soaked and equilibrated in 1 mg/ml somatostatin phosphate buffer. Sampling was done at different times and analyzed by HPLC to determine any difference between the MIP and NIP membranes. The resulting rebinding curves demonstrate a saturation of somatostatin binding over time for both the MIP and NIP membranes (Figure 97). After the full 24 h equilibration it is observed that saturation for the MIP and NIP has been reached and no difference in binding amount can be detected. Although the MIP membrane bind marginally more than the NIP membrane, the saturation effect is observed at 7 h equilibration as well. However, even though the binding results indicate that there is no difference in binding between the MIP and NIP membrane after saturation, a difference is displayed for the first three data points where the MIP membrane binds more somatostatin than the NIP membrane. This can probably be explained by imprinting sites being present in the MIP membrane and not only non-specific binding sites as for the NIP membrane. Overloading of the binding capacity is a possible explanation why the MIP and NIP

display the same saturation level after longer equilibration time. Since the purpose of the HTS imprinted membrane plates is to be tested by directly passing the template solution over the membrane without any significant equilibration time, the difference observed in the first data points thus indicate that the imprinted membranes may be a suitable screening technique.

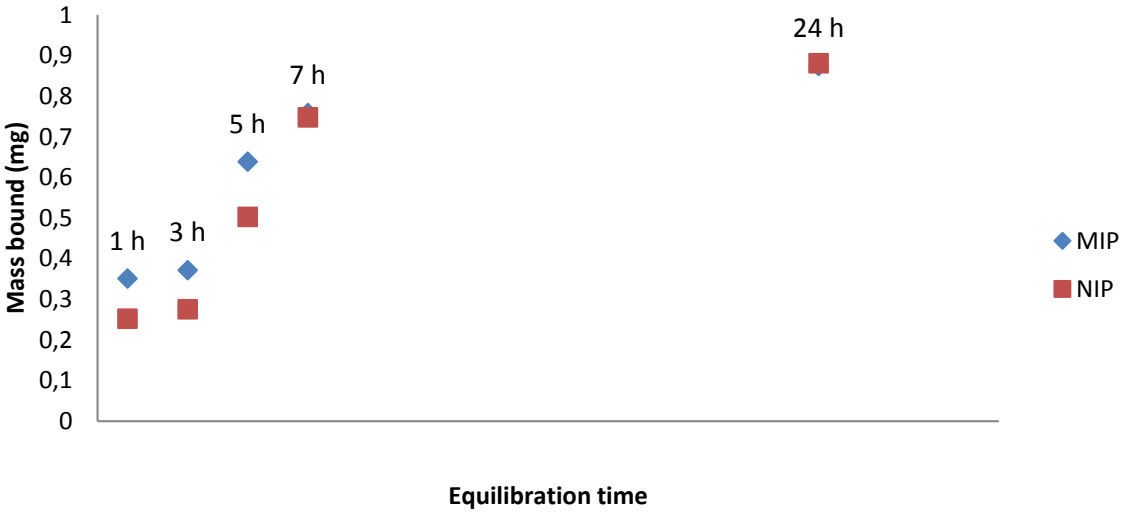

Figure 97 Rebinding test results over time for the MIP and NIP grafted membrane with 20 % cross-linking level. Sampling at; 1 h, 3 h, 5 h, 7 h, and 24 h.

3.6.3 Conclusion High-Throughput Synthesis for MIPs via Grafted Membranes

In this experiment a novel and more effective HTS screening method for MIP libraries was developed. General mini-libraries are time-consuming with several steps including moving the polymers from the polymerization tray to a filter plate for template extraction. With MIP grafted membrane surfaces the screening process is more straightforward. The grafting polymerization process, with radicals forming at the surface because of cleavage of PES by UV illumination (Figure 87), support polymer chain growth at the pore surfaces.

Successful grafting of both membrane filter plates and loose membrane discs is supported by calculations of the grafting amount and permeability. Furthermore TGA, SEM and EDX analysis also strongly indicate that polymer is successfully grafted on the membrane surface. The results display that there is a delicate line between the amount of polymer grafted and

blockage of the pores. Since permeability of the membranes after grafting of the MIP is an important characteristics for successful screening of MIPs. Thus it is imperative to find the optimal polymerization conditions for the grafting amount so that a difference in binding behavior can be observed without sacrificing permeability of the membrane.

The rebinding tests performed on both the grafted membranes filter plates and grafted loose membrane discs display that a difference in binding between the MIP and NIP can be observed. This is a good indication that grafted membrane filter plates can be used for efficient screening of MIP libraries.

3.7 SOMATOSTATIN IMPRINTED POLYMERS FOR CATALYTICALLY APPLICATIONS

One interesting application of MIPs is as catalysts. As mentioned in the introduction examples of MIPs used as catalysts have been published in literature. In this chapter the feasibility to use MIPs as catalysts for cyclic peptide synthesis in pharmaceutical industry is examined. Therapeutic peptides offer a great potential of new and powerful targets and applications for the pharmaceutical industry (for more details see section 1.7). However the inherent challenges handling and synthesizing peptides calls for new and innovative solutions.

A common method for the synthesis of peptides is the so called solid phase peptide synthesis (SPPS).[240] This technique is based on the growing peptide chain being immobilized on a solid porous support enabling a facile wash step in order to remove e.g. unreacted reagents or side-products. SPPS is performed by repeated cycles commencing with a coupling reaction of a protected amino acid to the support, followed by a wash and then deprotection and finishing with an additional wash step. When synthesizing a cyclic peptide connected via a sulfur bridge there is always a risk of dimerization and oligomerization, i.e. two or more peptide chains are bound together instead of an intra reacted sulfur bridge. Here MIPs could possibly offer a solution to this problem by functioning as catalysts, where the binding pockets imprinted with the cyclic peptide somatostatin could possibly promote the cyclization over dimerization and oligomerization (Figure 98).

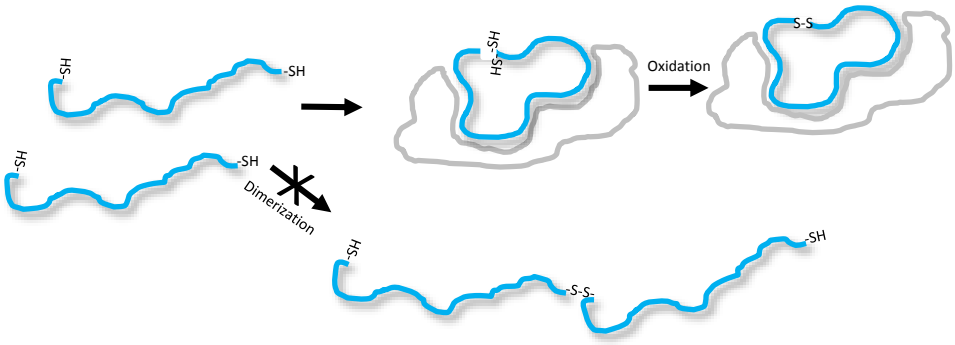

Figure 98 Schematic drawing of how somatostatin imprinted polymers in theory could promote cyclisation of the peptide and thus minimize dimerization.

3.7.1 SOMATOSTATIN IMPRINTED BULK POLYMERS

The first generation imprinted somatostatin polymers for applications as catalysts were synthesized in bulk format using organic solvents as porogens. Although peptides can be difficult to dissolve in organic solvents they are suitable for imprinting purposes because they are less polar than aqueous solutions, and thus do not compete with the template - monomer interactions. Solubility test showed that methanol and acetonitrile containing 1% trifluoretic acid (TFA) were the most suitable solvents to use for the imprinting of somatostatin. In order to investigate whether the somatostatin is degraded or structurally affected, the polymerization was initiated with both UV and 50 ^{0}C. Composition of the pre-polymerization mixture used for the synthesis is summarized in Table 25.

Table 25 Composition of the pre-polymerization mixture of the somatostatin imprinted polymers.

Name	Composition	Stoichiometry	Porogen	Polymerization
Som MIP 1	T/MAA/EDGMA	0.2/4/20	MeCN with 1% TFA	UV
Som NIP 1	MAA/EDGMA			
Som MIP 2	T/MAA/EDGMA	0.2/4/20	MeCN with 1% TFA	50 ^{o}C
Som NIP 2	MAA/EDGMA			
Som MIP3	T/MAA/EDGMA	0.2/4/20	MeOH	50 ^{o}C
Som NIP3	MAA/EDGMA			

After template removal by extraction, crushing and sieving the polymers were slurry packed in HPLC-columns for analysis. A 1 mM somatostatin in 10 % acetic acid solution was injected to

study whether a difference in the retention of somatostatin is present in the polymers. The only polymer that displayed retention of the injected somatostatin was Som MIP 1 and the resulting chromatograms of cross-reactivity testing between somatostatin and desmopressin are displayed in Figure 99. The results show that the somatostatin imprinted polymer retains somatostatin better than the corresponding NIP, retention time of 26 min and 11 min respectively. The broad and tailing somatostatin retention peak observed is typical of imprinted polymers, indicating that specific binding sites are present in the polymer. Desmopressin on the other hand has roughly the same retention time, approximately 5 minutes, on both the MIP and NIP, suggesting that specific binding sites are present in the somatostatin imprinted polymer.

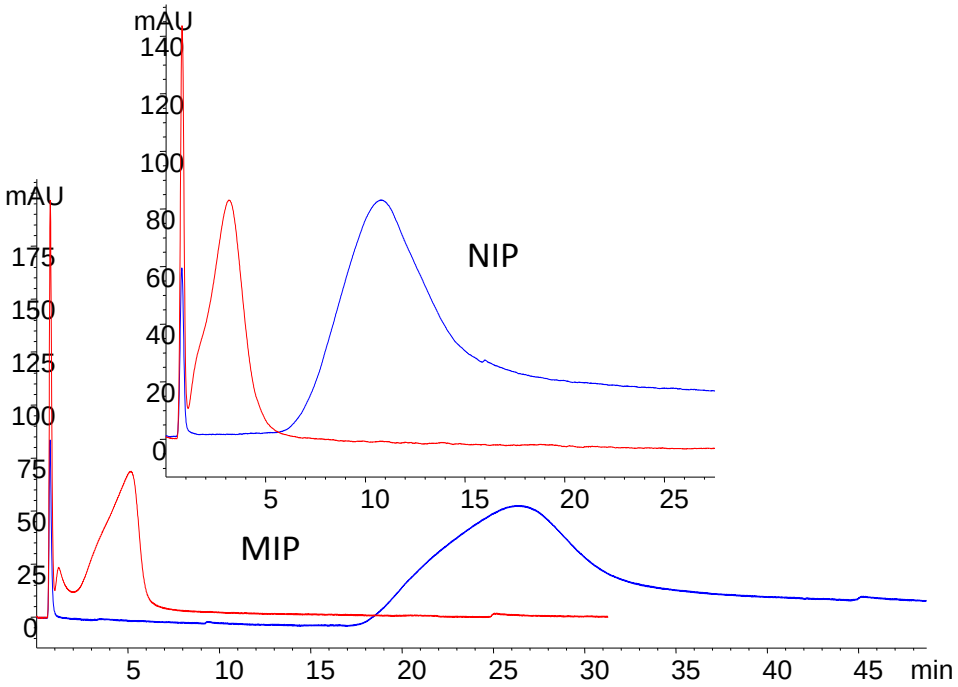

Figure 99 Retention of somatostatin (red) and desmopressin (blue) on Som MIP 1 and Som NIP 1 in HPLC analysis. 1 mM somatostatin in 10 % acetic acid (HAc) solution. Mobile phase 95% ACN 5% H_2O 0.1% HAc.

Since one of the objectives for the application of MIPs as catalysts is peptide synthesis, the synthesized MIPs need to demonstrate functionality in aqueous solutions. Thus further HPLC-analysis was performed to investigate the binding behavior in different mobile phases. With the 95 % MeCN 5 % H_20 0.1 % HAc mobile phase as a starting point a number of different MeCN mixtures were tested for the Som MIP 1 (Figure 100). The results display that for three of the mobile phases, no elution of somatostatin is detected, represented by columns with 120 minute elution time. This behavior is consistently observed for the mobile phases not containing any acid. Although elution is observed for the 50 % MeCN 50 % H_2O mobile phase, the retention times are very long at around 1 hour. The acid containing mobile phases on the other hand do

display elution of somatostatin. However, the results indicate that TFA is too strong an acid because the TFA containing mobile phases do not retain the peptide at all.

The results where somatostatin is completely retained on the column can possibly be explained by precipitation of somatostatin in MeCN and MeCN/ H_2O mobile phases. The precipitation seems to be hindered by addition of an acid in the mobile phase. However, addition of a strong acid indicates that the acid compete with the non-covalent interactions between the template and the functional groups in the binding site, thus somatostatin is not retained in the column. Using the less strong acetic acid seems to be a good choice for a balance between avoiding precipitation and still observing specific binding of somatostatin.

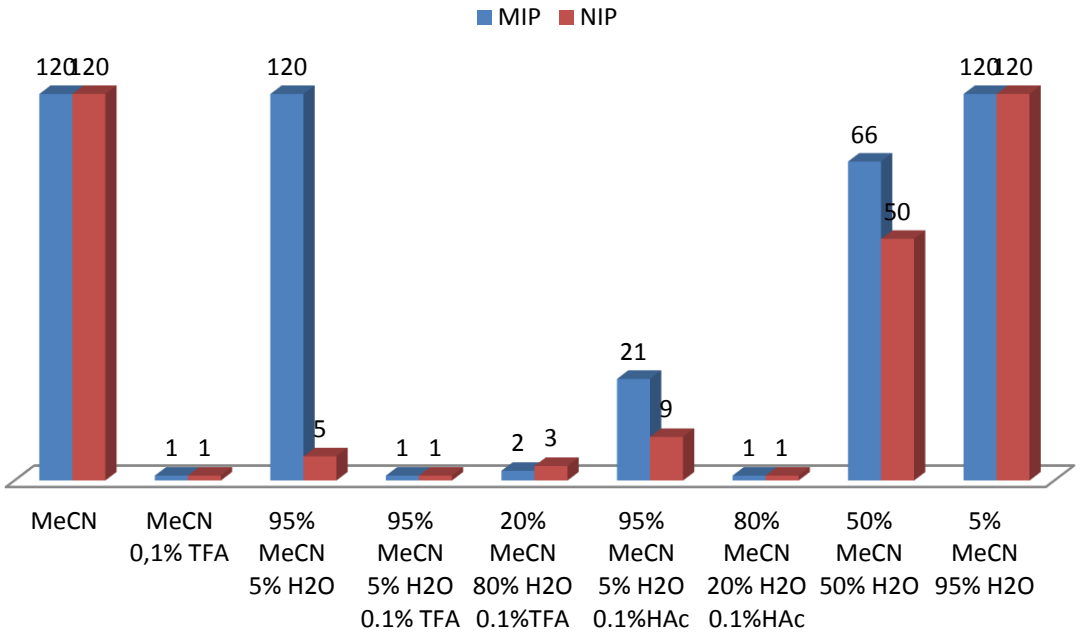

Figure 100 Evaluation of retention of somatostatin in different mobile phases.

The somatostatin imprinted bulk polymer showed that the template was successfully retained on the column during HPLC-analysis, thus indicating selective binding sites. However, with limited solubility and precipitation problems the somatostatin imprinted polymers do not demonstrate any binding in aqueous solutions. For application of MIPs as catalysts in peptide synthesis in aqueous solution, new somatostatin imprinted polymers using water compatible monomers and cross-linkers have to be synthesized.

3.7.2 SOMATOSTATIN IMPRINTED MINIMIP LIBRARY

The first generation imprinted somatostatin bulk polymers showed good imprinting effect in organic solvents but they failed to perform in aqueous solutions. In an attempt to find the optimal composition for somatostatin MIPs exhibiting imprinting in aqueous solutions a miniMIP library was prepared for screening. The parameters investigated were cross-linking level and functional monomer composition (Figure 101). Phosphate buffer was used as the porogen and two comonomers N-isopropylacrylamide (NIPAM) and methacrylamide (MAAm) were used. The molar ratio between the template somatostatin and total monomer was kept constant for the library (1:100). An automated robot system was used to prepare the library in a 96-well plate and polymerization was initiated thermally. A control NIP plate was prepared in the same way but without template. After polymerization was completed the miniMIPs were transferred to a filter plate for template removal by extensive washing. The template extraction was followed by fluorescent measurements. Rebinding tests were performed to find the most promising compositions.

		Comonomer NIPAM						Comonomer MAAm					
Funtional monomer		None	HEMA	DMAEMA	MAA	4-VP	MAA+4-VP	None	HEMA	DMAEMA	MAA	4-VP	MAA+4-VP
		1	2	3	4	5	6	7	8	9	10	11	12
A	10% CL		5%	5%	5%	5%	5%		5%	5%	5%	5%	5%
B	10% CL		10%	10%	10%	10%	10%		10%	10%	10%	10%	10%
C	20%CL		5%	5%	5%	5%	5%		5%	5%	5%	5%	5%
D	20%CL		10%	10%	10%	10%	10%		10%	10%	10%	10%	10%
E	30%CL		5%	5%	5%	5%	5%		5%	5%	5%	5%	5%
F	30%CL		10%	10%	10%	10%	10%		10%	10%	10%	10%	10%
G	40% CL		5%	5%	5%	5%	5%		5%	5%	5%	5%	5%
H	40% CL		10%	10%	10%	10%	10%		10%	10%	10%	10%	10%

Figure 101 Overview of the library prepared with different cross-linking levels and monomer compositions. Porogen 50 mM phosphate buffer pH=7. The molar ratio template to total monomer was 1:100. Where N,N'-Methylenebisacrylamide (MBA) is the cross-linker; methacrylic acid (MAA), 2-Hydroxyethyl methacrylate (HEMA), 4-vinylpyridine (4-VP), 2-(dimethylamino)ethyl methacrylate (DMAEMA) are functional monomers; methacrylamide (MAAm), N-isopropylacrylamide (NIPAM) are co-monomers.

Rebinding test was performed to screen the MIP and NIP filter plates. The amount of somatostatin bound was determined by bicinchoninic acid (BCA) assay and for facilitating the evaluation the results are color coded according to the amount bound (Figure 102). The rebinding results demonstrate some imprinted polymer compositions that selectively bind more somatostatin over the corresponding NIPs. Based on the binding capacity data and the imprinting factors of the library as shown in Figure 103 monomer compositions that tend to form successfully imprinted polymers can be distinguished and thus give an indication of composition to scale up.

		Concentration (µg bound/mg polymer)											
		1	2	3	4	5	6	7	8	9	10	11	12
A	MIP			3,1	1,7							3,2	
	NIP			1,6	1,6							1,9	
B	MIP			2,9	3,3		2,3			2,1			2,4
	NIP			2,9	3,3		2,1			0,6			0,1
C	MIP			2,4	2,6		3,9						
	NIP			1,9	2,4		1,9						
D	MIP								2,3		2,2		
	NIP								1,6		1,4		
E	MIP								0,4			2,4	2,8
	NIP								0,4			1,4	0,2
F	MIP				3,7		1,7			0,7		0,3	1,1
	NIP				2,0		0,8			0,0		0,0	0,1
G	MIP	1,9		1,9	2,1			0,0	3,2	1,6	3,0	1,8	1,9
	NIP	0,2		1,6	2,1			0,0	0,0	1,0	1,0	1,1	1,0
H	MIP			1,8			1,9					0,7	1,1
	NIP			1,7			1,2					0,4	0,5

0-1 µg/mg
1-2 µg/mg
2-3 µg/mg
3< µg/mg

Figure 102 Rebinding test results of the MIP library. 0.4 mg somatostatin in 500 µl phosphate buffer was added to each polymer and equilibrated for 24 h. For numbers marked red the MIP and NIP bind an equal amount of somatostatin.

		Imprinting factor mass bound MIP/mass bound NIP											
		1	2	3	4	5	6	7	8	9	10	11	12
A	MIP	<1	<1	1,9	1,1	<1	<1	<1	<1	<1	<1	1,6	<1
	NIP												
B	MIP	<1	<1	1,0	1,0	<1	1,1	<1	<1	3,5	<1	<1	25,7
	NIP												
C	MIP	<1	<1	1,3	1,1	<1	2,1	<1	<1	<1	<1	<1	<1
	NIP												
D	MIP	<1	<1	<1	<1	<1	<1	<1	1,4	<1	1,6	<1	<1
	NIP												
E	MIP	<1	<1	<1	<1	<1	<1	<1	1,0	<1	<1	1,7	12,8
	NIP												
F	MIP	<1	<1	<1	1,9	<1	2,1	<1	<1	0,7/0	<1	0,3/0	8,1
	NIP												
G	MIP	11,2	<1	1,2	1,0	<1	<1	3,2	3,2/0	1,5	3,1	1,6	1,9
	NIP												
H	MIP	<1	<1	1,1	<1	<1	1,7	<1	<1	<1	<1	1,9	2,2
	NIP												

1 IF
1 - 2 IF
2-5 IF
5> IF

Figure 103 Calculated imprinting factors for the MIP library. For the rebinding test 0.4 mg somatostatin in 500 µl phosphate buffer was added to each polymer and equilibrated for 24 h. For numbers marked red the imprinting factor is equal to 1.

When comparing the results depending on the co-monomer used with varying functional monomers it can be observed that the co-monomer MAAm display more imprinted polymer compositions than NIPAM, 18 and 13 respectively (Figure 104). Furthermore, the rebinding data also indicate that DMAEMA, MAA, 4-VP, and a combination of MAA and 4-VP are suitable functional monomers for successful imprinting of somatostatin. The results also indicate that the higher cross-linker content 30 % and 40 % might be beneficial for successful imprinting. This can probably be explained by that with the lower cross-linker levels the formed polymers are gel-like and can thus swell in solution. A certain amount of cross-linking is necessary to form rigid specific binding sites able to recognize the imprinted template, with too much swelling the binding site may no longer structurally correspond to the template.

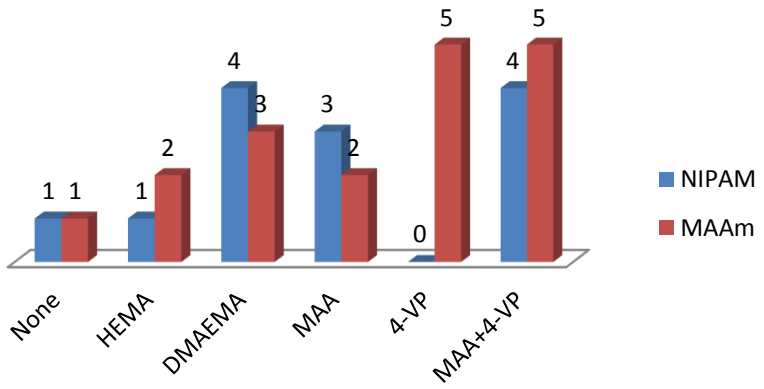

Figure 104 Number of polymers with imprinting for the two co-monomers with varying functional monomers.

The screening of the miniMIP library displayed some hit polymer compositions and with this in mind different polymer compositions were scaled up for further testing. Based on the rebinding results from the miniMIP library it was decided to use different combinations of MAA and 4-VP as functional monomers, MAAm as the co-monomer and MBA as the cross-linker, the exact composition is summarized in Table 26. Two different cross-linking levels were used, whereas the molar ratio of the functional monomer was kept constant in the experiment. An example of the prepared polymers is shown in Figure 105 displaying a slight discoloration of the MIP compared to the NIP after polymerization. This might be explained by possible degradation of somatostatin during the polymerization process.

Table 26 Composition of the scaled up somatostatin imprinted polymers from the miniMIP library.

	Somatostatin	MAA	4-VPy	MAAm	MBA	Mol ratio
P_M1	4.0	20	20	280	80	4:40:280:80
P_M2	4.0	40	-	280	80	4:40:280:80
P_M3	4.0	-	40	280	80	4:40:280:80
P_M4	4.0	20	20	200	160	4:40:200:160
P_M5	4.0	40	-	200	160	4:40:200:160
P_M6	4.0	-	40	200	160	4:40:200:160
P_N1	-	20	20	280	80	40:280:80
P_N2	-	40	-	280	80	40:280:80
P_N3	-	-	40	280	80	40:280:80
P_N4	-	20	20	200	160	40:200:160
P_N5	-	40	-	200	160	40:200:160
P_N6	-	-	40	200	160	40:200:160

Figure 105 Prepared PN1 (left) and PM1 (right) after polymerization.

After polymerization the template somatostatin was removed with repeated washes of H_2O: MeOH: FA (60:20:20) and the fractions were analyzed with HPLC. The chromatograms from the HPLC analysis are summarized in Figure 106 where the first and last washes are displayed. It can be observed that somatostatin is successfully removed from the polymers, this is further supported by the calculated recovery of the template (Figure 107). The low recovery percentage for PM2 can be explained by loss of the first washing fraction.

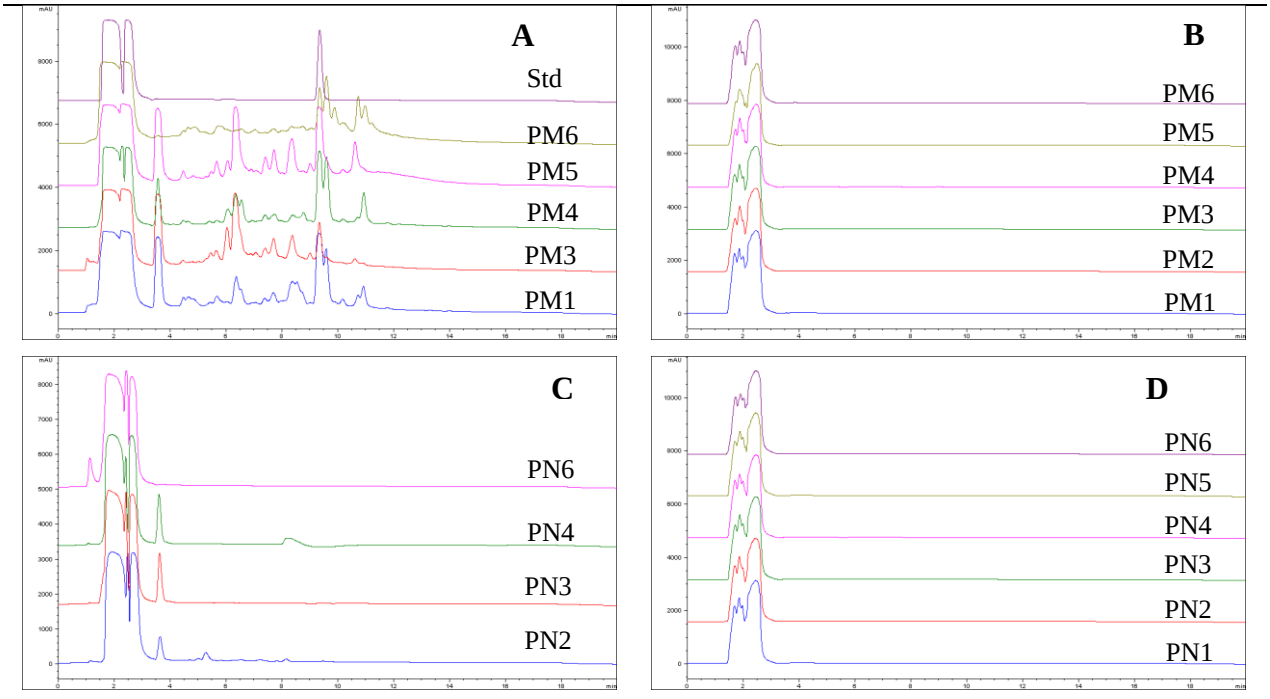

Figure 106 HPLC chromatogram of: A) The first washing fraction of MIP, B) last washing fraction of MIP, C) The first washing fraction of NIP, D) The last washing fraction of NIP.

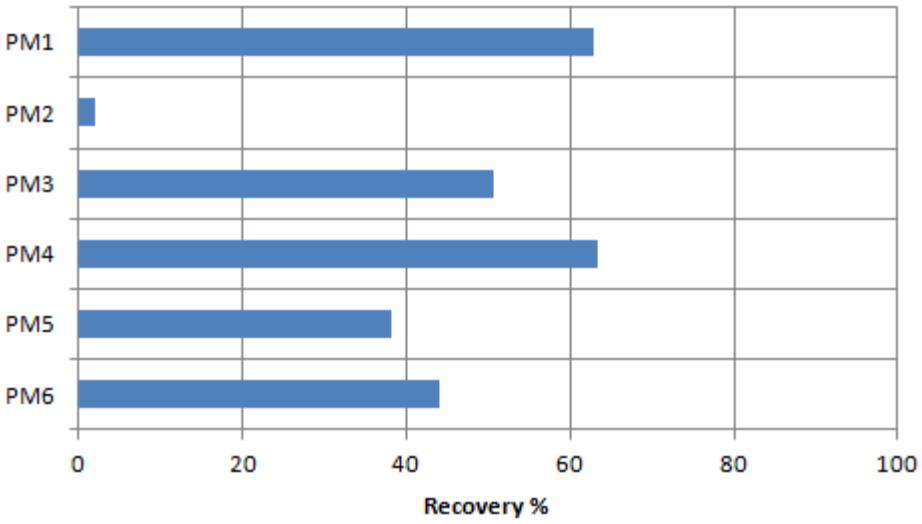

Figure 107 Calculated recovery of template from template extraction. The first washing fraction of PM2 was lost hence the low recovery percentage.

In order to determine the polymer amount needed for the rebinding test, a sample of PM2 was first dried by filtration and subsequently analyzed with TGA. Based on the results observed in Figure 108 it is predicted that 15% of the weight is polymer. Hence 100 mg of wet polymer was used for the rebinding tests with a theoretical dry weight of 15 mg.

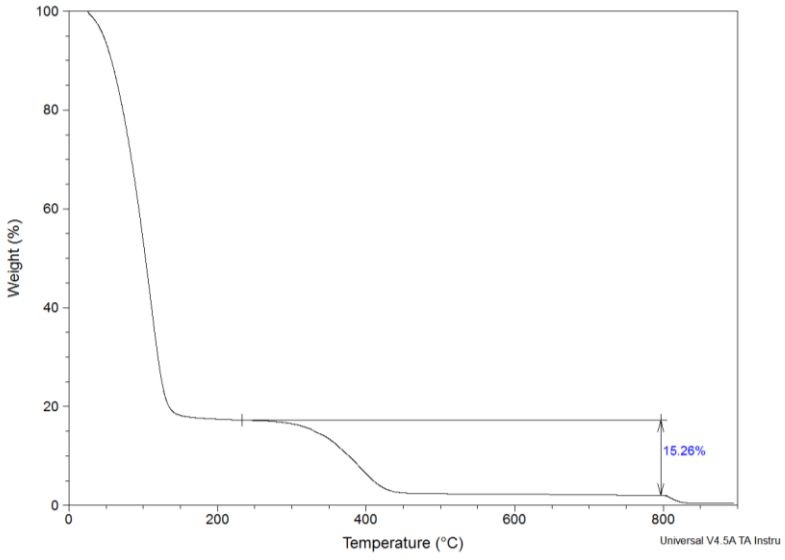

Figure 108 Determination of dry weight of PM2 by TGA.

For the rebinding tests 100 mg of wet polymers was incubated with two different somatostatin concentrations (10 µM and 100 µM) for 24 hours and analyzed with HPLC. For the resulting rebinding test results for the somatostatin imprinted polymers it is observed that PM2 and PM5

bind more somatostatin than their corresponding NIPs (Figure 109), indicating that the polymer composition with only MAA a the functional monomer form specific binding sites for both cross-linking levels used. The binding capacity displayed for PM2 is slightly higher than for PM5, this can probably be explained by the lower cross-linking level allowing the polymer to swell more and thus making the binding sites accessible for binding of somatostatin. Evaluation of the imprinting factors for the polymers shows that the highest imprinting factor is obtained for PM2 at the lower rebinding concentration, however for the higher concentration the imprinting factor is significantly decreased from 21 to 1.5 (Figure 110). This observation might be explained by overloading of the polymer and thus non-specific binding behavior becomes more significant.

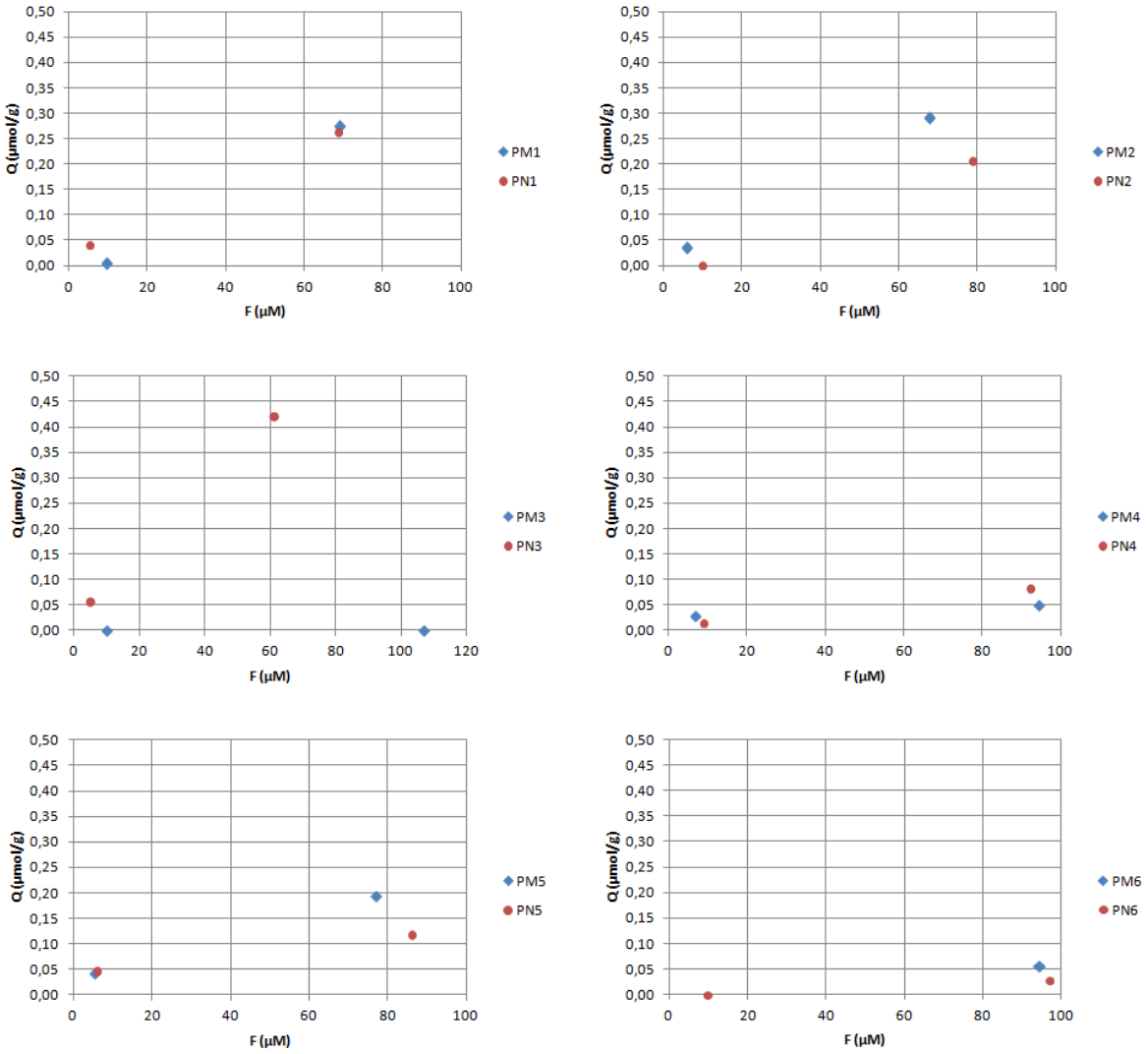

Figure 109 Rebinding test for polymer P1-P6: Somatostatin (10 µM and 100 µM), phosphate buffer pH 7, 24 h.

The up-scaling experiments showed that somatostatin imprinted polymers for rebinding in aqueous solutions were successfully synthesized. In addition the results obtained from the screening of the miniMIP library gave a good indication of suitable polymer compositions for larger scale imprinted polymers.

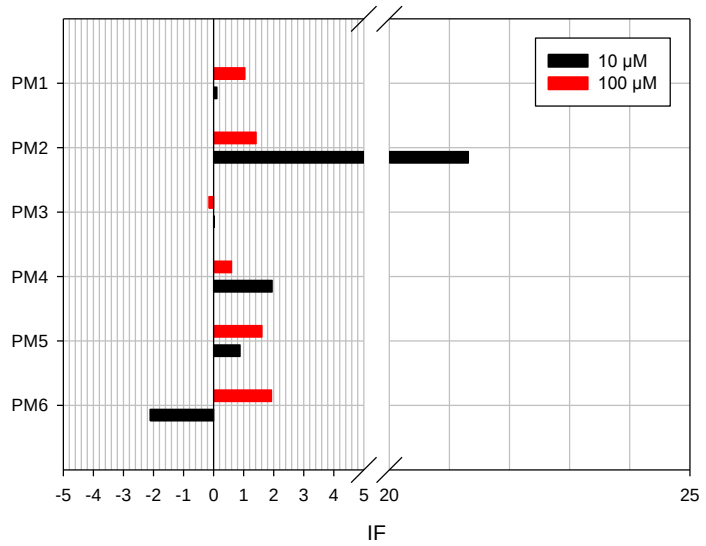

Figure 110 Imprinting factors for PM1 to PM6.

3.7.3 Catalytic Testing of Somatostatin Imprinted Polymers

With the successful development of somatostatin imprinted polymers in section 3.6.2 demonstrating specific binding of somatostatin in aqueous solutions, the possibility to use these MIPs as catalysts for cyclisation of linear somatostatin is investigated. A first preliminary concept experiment is performed with the somatostatin imorinted polymer PM2 that demonstrated a good selective binding of somatostatin in section 3.6.2.

As a result of only the cyclic somatostatin product being available, the first step of the experiment is to open the cyclic somatostatin to form linear peptides. A reduction protocol that opens the thiol ring was adapted from one used by colleagues in the group. Dithiothreitol (DTT) (50 mM) was prepared in phosphate buffer and added to the peptide solution. Following shaking over night, the samples were analyzed with LC-MS and compared with a sample containing the non-reduced cyclic somatostatin. LC-MS analysis showed that with the reduction protocol the linear form of somatostatin could be detected.

Following the reduction test an oxidation protocol was tested for ring closing. The oxidation protocol promotes intramolecular disulfide formation by potassium ferricyanide. Efficient rates of oxidation have been reported, and has proved to be especially efficeient for the somatostatin family, when using the relatively mild inorganic oxidizing reagent potassium ferricyanide ($K_3Fe(CN)_6$) .[241]

After reduction of the somatostatin samples 0.01 M $K_3Fe(CN)_6$ solution in phosphate buffer was added in 20 % excess of the theoretical peptide amount and after oxidation over 4.5 hours the samples were analyzed with LC-MS. In this first experiment the concentration of the linear and cyclic amount of somatostatin could not be determined, thus the ratio between linear and cyclic somatostatin was compared in oxidized somatostatin sample without polymer, and oxidized somatostatin in the presence of PM2 and PN2 (Table 27). In addition an experiment with desmopressin was performed in the same manner to investigate the selectivity of any possible catalytic cyclisation of the somatostatin imprinted polymers.

Table 27 Ratio linear:cyclic peptide after oxidation with $K_3Fe(CN)_6$ solution.

	Ratio linear: cyclic peptide	
	Somatostatin	Desmopressin
Oxidation no polymer	105	475
Oxidation PN2	44	390
Oxidation PM2	35	363

Although the results obtained are not quantitative the differences in ratios between linear to cyclic can be observed. The results display that for every cyclic peptide detected there are 105 linear somatostatin peptides and 475 linear desmopressin tested in absence of polymer. When comparing the corresponding values for oxidation in the presence of PN2 and PM2 the ratios for somatostatin are smaller than in the free solution. It is also observed that the ratio for PM2 is smaller compared to the PN2 ratio, thus indicating that as possible promotion of cyclisation is occurring in the PM2 sample. The fact that the ratios for both PM2 and PN2 are smaller compared to free solution might be explained by peptide being retained on the polymer, as the solutions were measured directly from the samples and no washing of the polymers was performed before analysis. This can also be seen when studying the peak areas (Appendix). Furthermore, the results observed for oxidation of desmopressin, indicate that desmopressin is not retained to the same extent as somatostatin on the polymers since the ratios of free solution

and polymer differentiate less compared to somatostatin. The desmopressin results might be an indication of the somatostatin imprinted polymers selectively promoting cyclisation of linear somatostatin.

3.7.4 Conclusion Somatostatin Imprinted Polymers for Catalytically Applications

Therapeutic peptides offer a great potential of new and powerful targets and applications for the pharmaceutical industry (Section 1.7). However the inherent challenges handling and synthesizing peptides calls for new and innovative solutions. The objective for this chapter was to investigate the application of MIPs as catalysts for cyclic peptide synthesis in pharmaceutical industry. In this work the cyclic peptide somatostatin is used for feasibility testing and a second cyclic peptide, desmopressin, is used as a control for selectivity of the imprinted polymers.

The first approach was to use bulk polymerization in organic for imprinting of somatostatin. The successfully synthesized polymer showed that the template was successfully retained on the column during HPLC-analysis, thus indicating selective binding sites. Furthermore, the cross-reactivity test of injecting desmopressin, a peptide very similar in shape and size, did not display retention like for somatostatin, thus supporting the observation of somatistatin selective binding sites. As a result of problems with precipitation and limited solubility no retention of somatostatin was observed in aqueous solutions. For application of MIPs as catalysts in peptide synthesis in aqueous solution, new somatostatin imprinted polymers using water compatible monomers and cross-linkers are evaluated.

For the second approach a miniMIP library was used for screening of monomer compositions forming good imprinted binding sites for somatostatin. Two 96-well plates, one MIP and one NIP, with varying functional monomers, co-monomers and cross-linking levels, were successfully prepared and analyzed. The results obtained from the rebinding test display that the co-monomer MAAm exhibit more successfully imprinted polymer compositions than NIPAM. Furthermore, the rebinding data also indicate that DMAEMA, MAA, 4-VP, and a combination of MAA and 4-VP are suitable functional monomers for successful imprinting of somatostatin. The results also indicate that the higher cross-linker content 30 % and 40 % might

be beneficial for successful imprinting. This might be explained by that with the lower cross-linker levels the formed polymers do not exhibit rigid binding sites because of their gel-like appearance and inherent swelling behavior. Therefore the swelling might lead to decreased recognition of the imprinted template.

Based on the screening of the miniMIP libraries a total of six polymer compositions were scaled up with three different functional monomers composition and two cross-linking levels. The up-scaling experiments showed that somatostatin imprinted polymers for rebinding in aqueous solutions were successfully synthesized. In addition the results obtained from the screening of the miniMIP library gave a good indication of suitable polymer compositions for larger scale imprinted polymers.

With the objective of the chapter in mind, application of MIPs as catalysts, the polymer with the most promising selectivity for somatostatin was used to test the catalytically properties. The first preliminary tests showed that by using reduction and oxidation protocols for peptides, somatostatin and desmopressin could be opened and re-closed and followed by LC-MS analysis. By studying the linear to cyclic peptides ratios obtained by LC-MS, it can be observed that the ratio of linear to cyclic peptide decreases, meaning that the cyclic form increases and thus indicating that the presence of polymer promotes the cyclisation of somatostatin. Furthermore, the preliminary results suggest that the imprinted polymer promotes the cyclisation better than the corresponding NIP and the promotion also exhibits selectivity for the imprinted somatostatin as the desmopressin does not display any significant change in ratio compared to the free solution control sample.

4 CONCLUSION AND OUTLOOK

In this work new molecularly imprinted polymer based scavangers for purification of small and large APIs are developed, analyzed and evaluated for application in pharmaceutical industry. The work can be broken down into three projects focusing on removal of small genotoxic impurities, new efficent screening method for MIPs, and MIPs as catalysts in peptide synthesis.

Novel molecularly imprinted polymers have been designed and synthesized which can recognize pharmaceutical impurities such as acetamide, thioacteamide and aminopyrimidine. Thorough testing and evaluation have demonstrated the feasibilty to use MIPs as selective sorbents for purification of APIs. Rebinding tests indicate that high affinity interactions are present between the binding sites of the MIP and the target impurities, resulting in a high efficient purification. The new MIPs developed present a new and inventive purification technique for the pharmaceutical industry, and offer an efficeint and selective sorbent.

With industrial applications in mind, where scalability, costs and efficiency are important factors to consider, different MIP formats were compared for optimization of a high capacity sorbent for pharmaceutical applications. The imputity chosen for imprinting was acetamide, as it was decided within the consortium that it is a good represenattion of small impurities in the pharmaceutical industry. The first generation bulk polymers were synthesized for optimization of the monomer composition and proof of concept. The strategy was to use common commercially available monomers and cross-linkers for facilitating future scale-up processes. HPLC analysis, batch rebinding test and SPE experiments demonstrated strong imprinting and high specific binding of acetamide. Thus highly specific MIPs could be synthesiszed using common commercial chemicals. However, for successful industrial application an improved loading capacity would be beneficial.

Two further formats were synthesized with the aim to improve the binding capacity and with the same or better binding properties. The two formats chosen were super-porous MIPs and pore-filling of porous silica particles, where the idea was that the inherent defined porous characteristics would improve the desired features. For the synthesis the same monomer composition as for the bulk polymers was used, and with only the porogen amount and composition was altered for optimization. Both super-porous and pore-filled MIPs were

succesfully synthesized, they did however display some different characteristics. For the two different polymer formats the binding capacity in ethyl acetate is in general slightly higher than in acetonitrile. This observation might be explained by the difference in polarity of the two solvents, where the more polar acetonitrile disrupt the binding of acetamide. The super-porous polymers do not display an increase in binding capacity as expected, they do however exhibit an increased specific binding compared to the bulk polymers. An explanation for this observation may be that with the additional iso-octane in the pre-polymerization mixture acting as a bad solvent the self-assembly of acetamide and MAA is promoted, and thus creating stronger binding sites. Pore-filling polymer II and III on the other hand exhibit an increased binding capacity, with pore-filling polymer II being the better of the two with an increase of approximately 60 % compared to the bulk polymers. The increased binding capacity might be attributed to the more defined pores present in the pore-filling polymers after removal of the silica mold. In the bulk polymers the pore system is more heterogeneous and the higher binding capacity in the pore-filling polymers may be attributed to the more homogeneous pore system. This is supported by the SEM images displaying the pores in the polymers and by the porometry analysis performed where increased surface area is observed for the pore-filling polymers.

In conclusion the rebinding tests in general demonstrate stronger specific binding for the super-porous polymers and the pore-filling polymers compared to the bulk polymers. Furthermore the binding capacity for acetamide could successful be increased without sacrificing the specific binding via the pore-filling approach.

With the imprinting of acetamide demonstrating that highly specific MIP based sorbents could be synthesiszed using commerical monomers, it is of great interest to investigate the imprinting and specific removal of other possible genotoxins. For MIP sorbents to become implemented as an alternative purification technique in industry the facile production and braod range of target compounds need to be demonstrated. In order to further investigate the feasibility to use MIPs for purification of small active pharmaceutical ingredients the same monomer composition was used to imprint thioacetamide.

Thioacetamide imprinted bulk polymers were successfully synthesized and evaluation of the MIP indicate the polymer contains specific binding sites for thioacetamide. Although the static rebinding tests display that no specific binding takes place in the MIP when tested in acetonitrile, the results in ethyl acetate display a strong specific binding in the MIP. This

observation may be explained by the difference in polarity of the two solvents, with acetonitrile being more polar than ethyl acetate. Furthermore, sulfur is slightly less electronegative than nitrogen thus probably less inclined to form strong hydrogen bonds with the functional monomer methacrylic acid. This may explain why the formation of thioacetamide specific binding sites is not as good as observed for the acetamide imprinted bulk polymers. The thioacetamide bulk polymers display an increased binding capacity in ethyl acetate compared to the acetamide bulk polymers. The SPE experiment performed in ethyl acetate further indicate that specific binding sites for thioacetamide are present in the MIP even if the difference between the MIP and the NIP is not so large. However, with further optimization of the polymer composition, such as another functional monomer or choice of porogen, more specific binding and higher binding capacities may be achieved. For the purpose of proof of concept in this thesis the results obtained are satisfactory.

A third small impuruty was imprinted in order to further investigate the application of MIP based sorbents in pharmaceutical purification. Since specific binding of two small impurities using commercial available monomers has already been demonstrated in this work, this experiment study how versatile the monomer composition used for acetamide and thioacetamide is for pharmaceutical applications. The impurity imprinted in this experiment was 2-aminopyrimidine. In addition to MAA, a second commonly used monomer, 4-VP, was used. For the purpose of potentially transfer the MIPs to synthesis of imprinted OSN membranes, imprinting in DMF besides in toluene was performed.

In total four 2-aminopyrimidine imprinted bulk polymers were successfully synthesized, however the evaluation of the polymers demonstrate that specific binding of the template is only present in the MIPs synthesized using MAA as the functional monomer. The polymers with 4-VP as the functional monomer unspecific binding seems to be more prominent. The preliminary rebinding tests display that polymers synthesized with MAA as the functional monomer in both toluene and DMF result in successfully imprinted polymers. When using the more polar solvent DMF it is observed that the binding capacity decreases slightly, indicating that the interaction between the template-monomer may be disrupted to some extent.

It can be concluded from the first preliminary binding tests that specific binding of 2-aminopyrimidine could be achieved using the same monomer composition as for acetamide and thioacetamide. Hence suggesting that MAA can be used over a broad range of impurities to

achive specific MIP sorbents. With the results in DMF displayingt specific binding of 2-aminopyrimidine suggests that the MIP composition can be used in the synthesis of imprinted OSN membranes. However, with further testing and optimization of the polymer composition more efficient MIPs may be achieved. For the purpose of proof of concept in this thesis the results obtained are satisfactory.

Within the framework of the NEMOPUR project two purification techniques were investigated, namely MIPs and OSN. Apart from studying MIPs and OSN separately it is also of interest to study the impact of combining the two. This case study aims to investigate the combination of MIPs and OSN for application in the pharmaceutical industry. In order to demonstrate the viability of this hybrid approach the two techniques were tested separately and finally combined, so that a good comparison as well as eventual shortcomings of the techniques can be identified. The benchmark for the study is a paper describing acetamide removal where a final concentration of 0.1 ppm acetamide is reached.[226]

A membrane screening in acetaonitrile and ethyl acetate was performed for the OSN experiments in order to demonstrate feasibility for acetamide removal in both ethyl acetate and acetonitrile. These results clearly demonstrate the feasibility of separation of the API and acetamide using OSN, however the overall large API losses in combination with high solvent requirements means that the application for API purification might be limited.

The OSN experiments show that the acetamide rejections are generally low resulting in a rapid decrease in concentration over the initial diafiltration volume. After a limited volume of one diafiltration volume the API losses are still limited and OSN might be a suitable alternative for “rough” cleaning process. This is where the hybrid approach using OSN for initial “rough” separation and MIPs as a polishing phase for removal of impurities to very low concentrations potentially could exhibit a benefit.

The removal tests for the MIPs were limited to testing in ethylacetate. For removal test 1 where the starting concentration was loaded on the MIP column an imprinting effect could be distinguished, although no effective removal of acetamide was observed in the overall process. The results obtained indicate a clear over-loading of the column, reflected in the amount of acetamide retained on the column after the loading. The main part of acetamide is eluted in wash fraction 1 and hence has a concentration similar to the feed. This elution in the first wash

fraction is therefore not suited for further processing and the API eluted in this fraction is unusable. The overall API loss hence adds up to a significant value of approximately 30 % indicating that it is not feasible to use MIPs for high concentration removal of acetamide.

The full feed concentration removal test was followed by two removal tests using samples taken from the OSN retentate after different diafiltration volumes. For the first removal test with a concentration of 25 ppm acetamide was loaded on the MIP column, a clear separation of acetamide from the API can be observed. In comparison to the NIP the MIP effectively removes acetamide and thereby decreasing the concentration from 25 ppm to < 0.2 ppm. In addition more or less no API is retained on the column and after wash 1 everything is eluted, suggesting that the API does not bind to the MIP. Hence the MIPs can effectively remove acetamide to the specified concentration with on overall API loss of less than 1 %. In the second removal test a higher concentration of acetamide in the loading step was used in order to examine the loading capacity of the MIP. However the results suggest that the loading capacity of the MIPs is reached because acetamide is eluting in already in the first washing step. Thus the loading capacity for the MIP is most likely between 25 and 40, hence depending on the purity specifications of the API the amount of MIPs used can be adjusted accordingly.

The case study of the hybrid approach suggests that depending on the specified purification requirements, a combination of MIPs and OSN can be beneficial. The OSN membranes work as a first rough spearation with their high rejection values, and the MIPs function as a polishing phase with their high specific binding properties. However, before the hybrid approach can be imlemented on a large scale application in the pharmaceutical industry a number of process parameters need to be evaluated. Currently OSN and MIP are operated on different volume scales therefore scale-up should preferably be addressed as a future objective. For a better comparison of the two technologies with one and other, and with other conventional purification techniques further studies needs to be conducted. Where suggested parameters for process comparison include but are not limited to; obtainable impurity levels, API yield losses, solvent requirements, scale-up opportunities, maintenance and operational cost, equipment investment cost, and energy requirements.

One of the drawbacks with MIPs is the time-consuming screening process for monomer compositions forming efficent imprinted polymers. For en implementation of MIP based sorbents in the pharmaceutical industry, functioning MIPs need to be developed in a timely

manner. The screening processes are precently based on miniMIPs, although this screening process is fairly fast, a couple of weeks is still quite some time. Therefore a novel and more effective HTS screening method based on grafting of membranes for MIP libraries was developed in this work. General mini-libraries are time-consuming with several steps including moving the polymers from the polymerization tray to a filter plate for template extraction. With MIP grafted membrane surfaces the screening process is more straightforward.

It was shown that successful grafting of both membrane filter plates and loose membrane discs is supported by calculations of the grafting amount and permeability. Furthermore TGA, SEM and EDX analysis also strongly indicate that polymer is successfully grafted on the membrane surface. The results display that there is a delicate line between the amount of polymer grafted and blockage of the pores. Since permeability of the membranes after grafting of the MIP is an important characteristics for successful screening of MIPs. Thus it is imperative to find the optimal polymerization conditions for the grafting amount so that a difference in binding behavior can be observed without sacrificing permeability of the membrane.

The rebinding tests performed on both the grafted membranes filter plates and grafted loose membrane discs display that a difference in binding between the MIP and NIP can be observed. This is a good indication that grafted membrane filter plates can be used for efficient screening of MIP libraries. It is suggested that future work should include screning of different templates in order to show that the screening process works over a broad range of compounds – from small to large. Furthermore, the screnning outcome should be directly compared to a conventional miniMIP library in order to evaluate if the screening can be transferred smoothly without any impact on the imprinting results.

One interesting and growing part in pharmaceutical industry is peptide therapeutics. Therapeutic peptides offer a great potential of new and powerful targets and applications for the pharmaceutical industry. However, the inherent challenges handling and synthesizing peptides calls for new and innovative solutions, hence opening up an opportunity to implement MIPs. The objective for this chapter was to investigate the application of MIPs as catalysts for cyclic peptide synthesis in pharmaceutical industry. In this work the cyclic peptide somatostatin is used for feasibility testing and a second cyclic peptide, desmopressin, is used as a control for selectivity of the imprinted polymers.

The first approach was to use bulk polymerization in organic for imprinting of somatostatin. The successfully synthesized polymer showed that the template was successfully retained on the column during HPLC-analysis, thus indicating selective binding sites. Furthermore, the cross-reactivity test of injecting desmopressin, a peptide very similar in shape and size, did not display retention like for somatostatin, thus supporting the observation of somatistatin selective binding sites. As a result of problems with precipitation and limited solubility no retention of somatostatin was observed in aqueous solutions. For application of MIPs as catalysts in peptide synthesis in aqueous solution, new somatostatin imprinted polymers using water compatible monomers and cross-linkers are evaluated.

For the second approach a miniMIP library was used for screening of monomer compositions forming good imprinted binding sites for somatostatin. Two 96-well plates, one MIP and one NIP, with varying compositions, were successfully prepared and analyzed. The results obtained from the rebinding test display that the co-monomer MAAm exhibit more successfully imprinted polymer compositions than NIPAM. Furthermore, the rebinding data also indicate that DMAEMA, MAA, 4-VP, and a combination of MAA and 4-VP are suitable functional monomers for successful imprinting of somatostatin. The results also indicate that the higher cross-linker content 30 % and 40 % might be beneficial for successful imprinting. This might be explained by that with the lower cross-linker levels the formed polymers do not exhibit rigid binding sites because of their gel-like appearance and inherent swelling behavior. Therefore the swelling might lead to decreased recognition of the imprinted template.

Based on the screening of the miniMIP libraries a total of six polymer compositions were scaled up with three different functional monomers composition and two cross-linking levels. The up-scaling experiments showed that somatostatin imprinted polymers for rebinding in aqueous solutions were successfully synthesized. In addition the results obtained from the screening of the miniMIP library gave a good indication of suitable polymer compositions for larger scale imprinted polymers.

In order to evaluate a possible application of MIPs catalysts, the up-scaled polymer with the most promising selectivity for somatostatin was used to test the catalytically properties. The first preliminary tests showed that by using reduction and oxidation protocols for peptides, somatostatin and desmopressin could be opened and re-closed and followed by LC-MS analysis. By studying the linear to cyclic peptides ratios obtained by LC-MS, it can be observed

that the ratio of linear to cyclic peptide decreases, meaning that the cyclic form increases and thus indicating that the presence of polymer promotes the cyclisation of somatostatin. Furthermore, the preliminary results suggest that the imprinted polymer promotes the cyclisation better than the corresponding NIP and the promotion also exhibits selectivity for the imprinted somatostatin as the desmopressin does not display any significant change in ratio compared to the free solution control sample.

Although the results suggest that MIPs can function as catalysts and promote cyclisation of somatostatin, the results obtained are only preliminary. For future work a method where quantitative and not only qualitative determination of linear and cyclic somatostatin needs to be developed. One possibility is to use the so called Ellman analysis to determine the thiol group concentration in a sample. Furthermore, optimization of the sampling method should be performed, e.g. SPE format with washing of the MIPs to ensure that no peptide is bound to the polymer when analysing the samples.

In conclusion the work described in this thesis suggests that MIPs may be an attractive new alternative purification method. It is also suggested that before succesful implementation of MIPs on a large scale, further work concerning scale-up, reproducibilty, good manufaturing practice, and process optimization should be performed.

5 EXPERIMENTAL

5.1 MATERIALS

Acetamide (AA) was obtained from Fluka (Buchs, Switzerland); Methacrylic acid (MAA), methacrylamide (MAAM), Ethylene glycol dimethacrylate (EGDMA) from Sigma Aldrich (Germany), Toluene, Acetonitrile (MeCN) and Trifluoroacetic acid (TFA) from Acros (Geel, Belgium) and Methanol (MeOH) from AppliChem GmbH (Germany); 2,2'-Azobis(2,4-dimethylvaleronitrile) (ABDV) from Wako Pure Chemical Ind. Ltd. (Japan). Formic acid from AppliChem GmbH (Darmstadt, Germany. The amides used for the selectivity tests were the following; acrylamide from Sigma Aldrich (Germany), formamide from AppliChem GmbH (Darmstadt, Germany), benzamide from Fluka (Buchs, Switzerland), MAAM from Sigma Aldrich (Germany) and N-tert butylacrylamide from Sigma Aldrich (Germany). For the AA removal tests Etodolac was used and kindly provided by Lonza (Switzerland). Silicaparticles for the porefilling polymers (Si500, 0.16 cm^3/g, 5 µm, 35 m^2/g) were received from Silicycle.

Before use EGDMA was purified according to the following procedure: EGDMA was washed with 10% aqueous NaOH, water, brine and water once more in this order. The EGDMA was subsequently dried over MgSO4 and then distilled under vacuum. The other chemicals were used as received. Anhydrous solvents, toluene and acetonitrile, were stored over molecular sieves. All other chemicals were of reagent grade or higher. For analysis HPLC grade acetonitrile and LC-MS grade acetonitrile was used.

For synthesis of the thioacetamide imprinted polymers, thioacetamide was purchased from Sigma Aldrich (Germany). The monomers and solvents used for synthesis and analysis were the same as for the acetamide imprinted polymers.

2-aminopyrimidine was obtained from Sigma Aldrich (Germany) for the synthesis of the 2-aminopyrimidine imprinted polymers. MAA and EGDMA are the same as for the other synthesized polymers and the monomer 4-vinyl pyridine (4-VP) was obtain from Sigma Aldrich (Germany). Anhydrous solvents, toluene and dimethylformamide (DMF) from Acros (Geel, Belgium), were stored over molecular sieves. For rebinding tests and analysis HPLC-grade acetonitrile was used.

For the hybrid approach acetamide and thioacetamide were obtained from Sigma Aldrich (Germany). MS-grade MeCN and ethyl acetate were used for rebinding tests and analysis.

For the high-throughput synthesis for MIPs via grafting on membranes, 96-well filterplates (Seahorse Labware, Chicopee, MA, USA) with PES membrane (pore sizes 0.45 µm and 300 kDa) mounted and sealed by the manufacturer (Seahorse Bioscience, North Billerica, MA, USA) were used. Loose membrane discs (pore sizes 0.45 µm) were obtained from Satorius Stedim Biotech (France). Acrylamide, methacrylamide, methacrylic acid, ethylene-bis-acrylamide (EBA), N,N-methylenebisacrylamide (MBA), phosphate buffer (Na_2HPO_4 and NaH_2PO_4) and 4-(2-Hydroxyethyl)piperazine-1-ethanesulfonic acid (HEPES) were purchased from Sigma-Aldrich. The templates desmopressin and somatostatin were kindly provided by Lonza (Switzerland).

The somatostatin imprinted miniMIP library and the scaled up bulk polymers were synthesized using a variety of different monomers, co-monomers and crosslinkers including; MAA, MBA, N-isopropylacrylamide (NIPAM), hydroxyethyl methacrylate (2- HEMA), 4-VP, 2-(Dimethylamino)ethyl methacrylate (DMAEMA) and MAAM. The inititators ammonium persulfate (APS) and Tetramethylethylenediamine (TMEDA) were purchased from Sigma-Aldrich. For the cyclisation tests dithithreitol (DTT) and potassium ferricyanide ($K_3Fe(CN)_6$) in phosphate buffer were used for reduction and oxidation of somatostatin and desmopressin respectively.

5.2 APPARATUS AND METHODS

ELEMENTAL ANALYSIS

Elemental Analysis was performed at the Department of Organic Chemistry, Johannes Guttenberg Universität Mainz using a Heraeus CHN-rapid analyzer (Hanau, Germany). Before analysis the polymers were dried under vaccum and 50°C over night and afterwards the Eppendorf tubes were sealed before shipment.

HPLC

HPLC measurements were carried out on Hewlett-Packard HP 1050 or 1100 instruments (Agilent Technology, Waldbronn, Germany) equipped with a diode array UV detector and a workstation. Depending on the analyte analyzed the method was adjusted accordingly.

MASS SPECTROMETRY

LC-MS analysis was performed on a Thermo Scietific LTQ Orbitrap mass spectrometer with a resolution of 60000 at *m/z* 400. Depending on the method mass range of 50 to 1800 u was analyzed.

MICROSCOPY

Optical microscopy was performed using a LEICA DMR fluorescence microscope HC (Leica, Bensheim, Germany). The polymer particles were placed on a glass slide and covered with a glass slide before analysis.

THERMAL GRAVIMETRIC ANALYSIS

Thermal gravimetric analysis (TGA) was carried out using a TGAQ50 (TA instruments, Eschborn, Germany). The sample (~ 10-15 mg) was placed in a platinum pan, which is suspended in a sensitive balance together with the reference pan. The sample was then heated, in a furnace, with at a rate of 10 or 20°C/min, under N_2 atmosphere.

DIFFERENTIAL SCANNING CALORIMETRY ANALYSIS

DSC analysis was performed on a DSC Q200 TA instrument (TA instruments, Eschborn, Germany). Approximately 5 mg of polymer sample was placed into an aluminum pan. The pan was then sealed and crimped with an aluminum lid. The pan was placed into the calorimeter and a reference pan was placed beside it. The atmosphere was then made inert by purging with nitrogen gas. A nitrogen flow rate of 50 mL/min was sustained in order to avoid interference by oxygen during isothermal scanning mode. The DSC scans were started at 30 °C and increased to 120 °C at a rate of 10 °C/min.

For thermoporometry analysis a sample of approximately 1-2 mg is immersed in 2-5 µL solvent in a hermetic aluminum pans. The samples are quenched at -60 °C at a scanning rate of 5 °C/min and the melting behavior of the solvent is analyzed. For the analysis in this work MeCN was used with a melting point of -46 ±0.3 °C.

POROMETRY ANALYSIS

BET nitrogen adsorption analysis was carried out on a Quantachrome Nova 4000e (Quantachrome Corporation, USA) automatic adsorption instrument. Before analysis sample

was prepared by placing approximately 50 mg of polymer in a glass cell and degassing under vaccum over night at 50 °C.

SCANNING ELECTRON MICROSCOPY

SEM images were taken on a Hitachi H-S4500 FEG in secondary mode with an acceleration voltage of 1 kV. Before analysis the sample was placed on special SEM holders with carbon foil. Different resolutions were recorded depending on the sample.

SWELLING TESTS

For the swelling tests NMR tubes were filled with dry polymer until 1 cm was reached and then 1 mLof the intended solvent was added. After equilibration of the particles in the solvent for 24 h the volume of the swollen particles was measured. To calculate the volume swelling ratio can be calculated by dividing the wet bed volume with the dry bed volume.

5.3 ACETAMIDE IMPRINTED POLYMERS

5.3.1 POLYMER PREPARATIONS

For the bulk polymers a total of four different imprinted polymers (PA1 - 4) were prepared for the acetamide with two different functional monomers and the same cross-linker polymerized in two different porogens. The imprinted polymers were prepared in the following manner. The acetamide template (1 mmol), functional monomer (4 mmol) and the cross-linker EGDMA (20 mmol) were dissolved in toluene or acetonitrile (13.8 ml). The initiator ABDV (1% w/w of total monomers) was added to the solution. The solution was transferred to a glass ampoule, cooled to 0 °C and purged with a flow of dry nitrogen for 10 min. The tubes were then flame-sealed while still under cooling and the polymerization initiated by placing the tubes in an incubator pre-set at 15 °C and illuminated with UV-light. After 24 h the tubes were broken and the polymers lightly crushed. They were thereafter extracted in a Soxhlet-apparatus with a solution of 80 % MeOH, 15 % formic acid and 5 % water for 48 h. The remaining acid in the polymers was then washed away with methanol using a Soxhlet-apparatus with methanol for 24 h. This was followed with further crushing and sieving. The desired particle size fractions (25-50 μm) were repeatedly sedimented (80:20 = methanol:water) to remove fine particles and then slurry-

packed into HPLC columns (125 mm x 4.0 mm i.d.) using the same solvent mixture as pushing solvent. Non-imprinted polymers (PAN1 - 4) were prepared in the same way as imprinted polymers, but with no template molecule in the pre-polymerization solution.

For the preparation of the super-porous iso-polymers a total of three different polymers were prepared with varying total amounts of iso-octane as the porogen (25 %, 50 % and 75 % iso-octane of the total porogen volume). The acetamide template (1 mmol), functional monomer (4 mmol) and the cross-linker EGDMA (20 mmol) were dissolved in toluene and iso-octane mixture (total volume of 13.8 ml). The initiator ABDV (1% w/w of total monomers) was added to the solution. The solution was transferred to a glass ampoule, cooled to 0 °C and purged with a flow of dry nitrogen for 10 min. Samples were polymerized under UV at 15 °C for 24h and then incubated in the fridge (8 °C) over night. The formed polymers were crushed in particle size fractions (25-50 μm) after Soxhlet removal of the template. Non-imprinted control polymers were prepared in the same manner without the template.

A total of three different porefilling imprinted polymers were prepared with the same ratio as for the bulk polymers but with varying amounts of porogen. The acetamide template (1 mmol), functional monomer (4 mmol) and the cross-linker EGDMA (20 mmol) were dissolved in toluene (6.9 mL and 1.4 mL) and for polymer III no porogen was used. The initiator ABDV (1% w/w of total monomers) was added to the solution. The pre-polymerization mixture was purged with nitrogen before added in smaller portions to the silica (300 μL per 500 mg silica) and carefully stirred. Polymerization was perfermoed at 50 °C for 24 hours. Following polymerization the particles were suspended in 15 mL aqueous solution of NH_4HF_2 (3 M) in polyethylene flasks to etch the silica. The resulting polymers were washed with destilled water to ensure the removal of SiF_4 and $[NH_4]F$. Complete removal of silica from the matrix of the polymers was followed with TGA.

The success of the bulk polymer synthesis was evaluated with elemental analysis:
Anal. calc. for PA1 in percent: C=60.21, H=7.11. Found: C=59.02, H=7.20, N=0.15
Anal. calc. for PAN1 in percent: C=60.21, H=7.11. Found: C=58.64, H=7.23, N=0.13
Anal. calc. for PA2 in percent: C=60.26, H=7.21, N=1.30. Found: C=59.31, H=7.64, N=1.18
Anal. calc. for PAN2 in percent: C=60.26, H=7.21, N=1.30. Found: C=59.29, H=7.67, N=1.33
Anal. calc. for PA3 in percent: C=60.21, H=7.11. Found: C=59.53, H=7.47, N=0.13
Anal. calc. for PAN3 in percent: C=60.21, H=7.11. Found: C=59.56, H=7.43, N=0.13

Anal. calc. for PA4 in percent: C=60.26, H=7.21, N=1.30. Found: C=59.48, H=7.52, N=1.24
Anal. calc. for PAN4 in percent: C=60.26, H=7.21, N=1.30. Found: C=59.38, H=7.58, N=1.30

5.3.2 HPLC TESTING OF ACETAMIDE MIP PERFORMANCE

The evaluation of the extraction procedures was carried out by HPLC using an Agilent HP1050 or HP 1100 system (Agilent Technologies, Wilmington, DE) equipped with a diode array-UV detector and a workstation. HPLC columns (125 x 4.0 mm i.d.) slurry packed with the MIPs were evaluated. The instrument was operated in an isocratic mode using a mobile phase consisting of MeCN at 0.5 mL/min flow rate. Chromatograms were obtained by injecting a fixed volume (10 μL) of spiked solutions of the compounds and subsequently monitoring the absorbance at 230, 220 and 205 nm depending on the analyte. The retention factor (k) was calculated as $k=(t-t_0/t_0)$, where t is the retention time of the analyte and t_0 is the retention time of the void marker (acetone).

5.3.3 TEST MODEL FOR ACETAMIDE REMOVAL

Scavenging experiments were performed using cartridges from Isolute SPE Accessories, Biotage (Sweden), that were packed with 25 mg of the PA3 polymer or the corresponding non imprinted polymer PAN3. The cartridges were washed extensively with methanol and then equilibrated with acetonitrile. 0.5 mL of a solution of Etodolac (5 g/L) and acetamide (250 ppm) in acetonitrile was loaded on the cartridges. A SPE-cartridge manifold was used to pull the sample through the packed polymers to be collected in a 1 vial. The SPE cartridges were then washed with 1 mL of acetonitrile and the washing elutants were collected in separate vials. The loading eluent and washing eluents were analyzed by HPLC, using a Hewlett-Packard HP 1050 or 1100 instruments (Agilent Technology, Waldbronn, Germany) equipped with a C-18 column (250 x 4.60 mm, 5 micron, 48790-52) using a gradient. The gradient used was 100% H_2O the first five min followed by a mixture of MeCN and H_2O, 95% and 5% respectively (6-16 min), and then the mobile phase was switched back to 100% H_2O (17-20min). Acetamide was monitored at 220 nm and Etodolac at 300 nm.

5.3.4 Equilibrium Rebinding Tests

Rebinding tests were performed for the three different formats of acetamide imprinted polymers in order to compare the rebinding properties of the polymers. The tests were done in HPLC vials or Eppendorf tubes depending on the amount of polymer used. Solutions with a range of specified template concentrations are added to a known amount of polymer (50 mg for bulk and isopolymer and 10 mg for porefilling polymer) and let to equilibrate under constant mixing. After equilibrium is reached (24 hours) the polymers are sedimented and a sample is withdrawn from the vial or tube for LC-MS analysis for determination of the free concentration. For LC-MS analysis a gradient was applied to Gemini-NX C18 column (length 150x2 mm, particle size 3 µm, Phenomenex Inc) with solvent A (H_2O 0.1 % FA) and solvent B (MeOH 0.1 % FA) (0-1 min 100 % A, 10-11 min 0 % A, 11,5 min 100 %, 15 min 100 % A). UV was monitored at 250 nm over a mass range of 50 to 550 *m/z*.

5.4 Thioacetamice Imprinted Polymers

5.4.1 Polymer Preparation

The thioacetamide imprinted bulk polymers were prepared according to the recipe for PA3 polymer (Section 5.3.1) but with thioacetamide as the template instead of acetamide. The imprinted polymers were prepared in the following manner. The thioacetamide template (1 mmol), functional monomer (4 mmol) and the cross-linker EGDMA (20 mmol) were dissolved in toluene (13.8 ml). The initiator ABDV (1 % w/w of total monomers) was added to the solution. Non-imprinted control polymers were also synthesized. Polymerization and sample preparation was otherwise conducted as described in section 5.3.1.

5.4.2 Equilibrium Rebinding Tests

Evaluation rebinding tests of the thioacetamide imprinted polymers was conducted in the same manners as for the acetamide MIPs (Section 5.3.4).

5.5 2-AMINOPYRIMIDINE IMPRINTED POLYMERS

5.5.1 POLYMER PREPARATION

A total of four different 2-aminopyrimidine imprinted polymers were synthesized, with two different functional monomers in two different solvents. The first two MIPs were based on the successful acetamide recipe for PA3 with MAA as the functional momomer. The second functional monomer used was 4-VP. The template 2-aminopyrimidine (1 mmol), functional monomer (4 mmol) and the cross-linker EGDMA (20 mmol) were dissolved in toluene or DMF (13.8 ml). The initiator ABDV (1% w/w of total monomers) was added to the solution. Non-imprinted control polymers were also synthesized. Polymerization and sample preparation was otherwise conducted as described in section 5.3.1.

5.5.2 EQUILIBRIUM REBINDING TESTS

Evaluation rebinding tests of the 2-aminopyrimidine imprinted polymers was conducted in the same manners as for the acetamide MIPs (Section 5.3.4). The rebinding tests were analyzed by HPLC, using a Hewlett-Packard HP 1100 instruments (Agilent Technology, Waldbronn, Germany) equipped with a C-18 column (250 x 4.60 mm, 5 micron, 48790-52) using isocratic mode. Mobile phase 40 mM ammonium acetate, pH 4.4/MeCN (1:1) with a flow rate of 1 mL/min and UV detection at 220 nm.

5.6 HYBRID APPROACH – MIPS AND OSN

5.6.1 MATERIALS

Acetamide and thioacetamide was purchased from SigmaAldrich. The inhouse API was kindly provided by GlaxoSmithKline. The MIPs used was 1st generation bulk polymers synthesized at TU Dortmund. For processing in ethyl acetate Starmem™122 (batch 255.1 and 9104.1) and

Duramem™200 (M128) were used (MET Evonik). For processing in MeCN Duramem™150 (M087) (MET Evonik) was used. All solvents were of LC-MS grade.

5.6.2 Analysis

Acetamide was analyzed using LC/MS with single ion detection set at MH^+ = 60. Level of quantification was determined to 0.2 ppm and level of detection is slightly lower ranging between 0.1-0.2 ppm. API was detected and quantified using a project specific HPLC method.

5.7 High-Throughput Synthesis for MIPs via Grafting on Membranes

5.7.1 Materials

The 96-well filter plates with pore sizes 300 kDa and 0.45 µm were purchased from Seahorse Bioscience, US. Ninety-six well 2 mL Seahorse Bioscience membrane filter plate, polyether sulfone (PES) membrane. Functional monomer acrylamide, crosslinking monomer ethylene bisacrylamide (EBA), 10mM HEPES buffer pH=7 as porogen. Template was somatostatin (provided by Lonza, Switzerland).

5.7.2 Preparation of Grafted Membranes

The grafting on PES membranes follows a very simple procedure where the membrane is first washed with methanol and deionized water to remove surfactants before use. Then the membrane is soaked in the monomer solution and subsequently illuminated with UV for grafting from the surface. For this purpose a stock solution with the ratio 1:3 of monomer to solvent was prepared. The mother solutions containing the template somatostatin, functional monomer acrylamide and MAA, cross-linker EBA were prepared from dilution of the stock solution. Solutions for the non-imprinted control membranes were also prepared in the same way but without the template. The solutions were purged with nitrogen gas for approximately

10 minutes before 50 µL was pipetted to each well and for the loose membranes incubation in the solution for 10 minutes. After soaking in the monomer solution the plate or loose membranes are placed in a special built glass box with quartz lid, designed to create an oxygen free environment, in an incubator. Before addition of the membrane the glass box is purged with nitrogen for 20 minutes. For the membrane to stay wet and not dry out circa 1 cm of Millipore water is filled at the bottom of the box. After addition of the membranes the oxygen free environment is re-equilibrated for 10 minutes before the UV-lamp is turned on and during the polymerization the temperature in the incubator chamber is kept constant at 15 ^{0}C. For template removal warm 40 ^{0}C methanol containing 1 % formic acid is used for washing the membranes. Template removal of somatostatin can be followed by measuring the fluorescence after each wash. Residual acid is washed away with extensive methanol.

5.7.3 GRAFTING OPTIMIZATION AND METHOD FOR INITIAL TESTING

Both types of the membrane filter plates were used (300 kDa and 0.45 µm pore size). The crosslinking level used was 50 %. Polymer composition in molar ratio was Som/MAA/Acrylamide/EBA 0.2/1/3/4 with 10mM HEPES buffer pH=7 as porogen. Solutions for the nonimprinted wells were also prepared in the same way but without the template. The solutions were purged with nitrogen gas for approximately 10 minutes before 50 µl was pipetted to each well. The plate was place in a special built glass box with quartz lid, designed to create an oxygen free environment, in the incubator. In order to try not to dry the membranes out a collecting plate was placed at the bottom of the box, with every second well filled with millipore water. The plate was purged with nitrogen for 20 minutes before the UV-light was turned on. The temperature in the incubator chamber was kept constant at 15 ˚C. The plate was exposed to the UV light for varying times. The template was then removed by adding varm (40 ˚C) MeOH containing 1 % formic acid fifteen times. The fluorescence was measured after each wash to record the extraction of somatostatin. The acid was then removed with extensive washing with MeOH. For the first rebinding test 400 µL of 0.025 mM Somatostatin in 10mM HEPES pH= 7 was added to the each well and equilibrated for 5 hours. Fluorescense was measured between 300 and 500 nm for the samples.

5.8 Somatostatin Imprinted Polymers for Catalytical Applications

5.8.1 Preparation Somatostatin Imprinted Bulk Polymers

A total of three different somatostatin imprinted polymers were synthesized. The template somatostatin (0.2 mmol), functional monomer (4 mmol) and the cross-linker EGDMA (20 mmol) were dissolved in 1 % TFA in MeCN and MeOH. (4/3 of total volume). The initiator ABDV (1% w/w of total monomers) was added to the solution. Non-imprinted control polymers were also synthesized. Polymers prepared in 1 % TFA in MeCN were polymerized using both UV and thermal initiation. Polymers prepared in 1 % TFA in MeCN and MeOH were initiated by UV at 15 °C for 24 h and cured at 60 °C for 48 h. The thermally initiated polymer prepared in 1 % TFA in MeCN was initiated at 50 °C for 24 h and cured at 60 °C for 48 H. Polymerization and sample preparation was otherwise conducted as described in section 5.3.1.

HPLC analysis was carried out on slurry packed columns (50 x 4.6 mm) using an isocratic mode (mobile phase 0.1 % HAc in MeCN/ H_2O 95/5). UV was recorded at 220 nm.

5.8.2 Somatostatin Imprinted miniMIP library

MiniMIP library was synthesized using 96-well PTFE microtiter plate and PTFE coated closures (Radleys) and for pipetting of the polymer solutions a LISSY sample handler with four ports was used (Zinsser Analytic). Two plates were prepared one with and one without template in phosphate buffer (50 mM, pH= 7). Stock solutions of the functional monomers (0.2 M and 1 M) were prepared in the same porogen except for 4-VP that was prepared in a 9:1 mixture of phosphate buffer and DMF. Stock solutions of the initiators APS and TEMEDA was prepared (90 mg/mL and 46 mg/mL respectively). For the MIP plate somatostatin was added in a 1:100 molar ration template to total monomer to one initiator solution. Prior to pipetting the monomer stock solutions were purged with nitrogen. The solutions were then pipetted into the 96-well PTFE microtiter plate (Figure 111). Before polymerization the plate was sealed with a PTFE-coated silicone lid and then polymerization took place at 50 °C for 24 h.

			Comonomer NIPAM						Comonomer MAAm					
		(µL)	None	HEMA	DMAEMA	MAA	4-VP	MAA+4-VP	None	HEMA	DMAEMA	MAA	4-VP	MAA+4-VP
	X-linker	Co-monomer	1	2	3	4	5	6	7	8	9	10	11	12
A	470	25		2.5	2.5	2.5	2.5	2.5		2.5	2.5	2.5	2.5	2.5
B	425	25		12.5	12.5	12.5	12.5	12.5		12.5	12.5	12.5	12.5	12.5
C	445	50		2.5	2.5	2.5	2.5	2.5		2.5	2.5	2.5	2.5	2.5
D	400	50		12.5	12.5	12.5	12.5	12.5		12.5	12.5	12.5	12.5	12.5
E	395	100		2.5	2.5	2.5	2.5	2.5		2.5	2.5	2.5	2.5	2.5
F	350	100		12.5	12.5	12.5	12.5	12.5		12.5	12.5	12.5	12.5	12.5
G	345	150		2.5	2.5	2.5	2.5	2.5		2.5	2.5	2.5	2.5	2.5
H	300	150		12.5	12.5	12.5	12.5	12.5		12.5	12.5	12.5	12.5	12.5

Figure 111 Amount of stock solution added to each well. To each well APS (10 µL) and TEMEDA (10 µL) was added. Two plates were prepared, with and without somatostatin template (template was added to one initiator solution). Cross-linker was MBA.

After polymerization the polymers were transferred to a 96-well filter plate. The template was extracted by repeating washing steps with 1 % FA in MeOH (500 µL) until no absorbance of somatostatin was detected using a plate reader SAFIRE (Tecan Deutschland GmbH). Before rebinding experiments, the plates were washed with the same solvent as in the rebinding test for reconditioning. Rebinding tests were performed by addition of 500 µL somatostatin solution in phosphate buffer (50 mM, pH= 7) and the filter plates were sealed and equilibrated under shakingfor 24 hours. The rebinding tests were analyzed with HPLC Luna 5u C18 column, Phenomenex and the elution was performed at a flow rate of 1 mL/min and 5 µL injections for a duration of 10 minutes in isocratic mode 0.1 % FA in H2O/MeCN (95/5 % w/w). Absorbance at 220 nm was monitored. The rebinding tests were also analyzed using BCA protein assay reagent kit (Sigma Aldrich) according to accompanying protocol.

For the upscaling of the miniMIP library hit polymers a total of six different polymers were synthesized based on the hit polymers from the miniMIP library. A detailed overview of the polymer composition is summarized in Table 26. Three polymers were prepared as followed, template somatostatin (4 µmol), functional monomer (40 µmol), co-monomer MAAm (280 µmol) and cross-linker MBA (80 mmol) were dissolved in phosphate buffer (50 mM, pH= 7, 500 µL). The other three polymers were prepared as followed, template somatostatin (4 µmol), functional monomer (40 µmol), co-monomer MAAm (200 µmol) and cross-linker MBA (160 mmol) were dissolved in phosphate buffer (50 mM, pH= 7, 500 µL). The initiators APS and TEMEDA (2% w/w of total monomers) was added to the solution. Non-imprinted control polymers were also synthesized. Polymerization took place at 50 °C for 24 hours. For template

removal the polymer (2 g, wet) was washed with 3 x 10 mL of H2O: MeOH: FA (60:20:20). The fraction was collected and measured by HPLC for calculations of the recovery. For calculations of the somatostatin recovery a standard solution in 50 mM phosphate buffer was prepared based on the amount used in the pre-polymerization mixture (13 mg/ml).

Gradient for HPLC method used for analysis; 0 min 21 % mobile phase B, 15 min 40 % mobile phase B, 17 min 21 % B, 20 min 21 % B. Where mobile phase A is prepared by diluting 11 ml of phosphoric acid with water, adjusting to pH 2.3 with triethylamine and diluting to 1000 ml with water. Mobile phase B is acetonitrile 100 %. Flow rate 1.0 mL/min and UV detection at 215 nm. Injection volume of 100 µL. Column used is Luna C18 (155 mm× 4.6 mm I.D., 5µm) HPLC column protected by an RP18 guard column (4.0 mm×3.0 mm I.D., 5 µm), both from Phenomenex (Torrance, CA, USA).

For the rebinding tests 100 mg of wet polymers was incubated with 100 µL of 10 µM and 100 µM of standard Somatostatin in 50 mM phosphate buffer, pH 7, for 24 hours.

5.8.3 CATALYTIC TESTING OF SOMATOSTATIN IMPRINTED POLYMERS

10 mg of PM2 and PN2 was weighed in Eppendorf tubes. 1 mM Somatostatin and Desmopressin phosphate solutions were prepared (16.38 mg in 10 mL). For reduction of the peptides 50 mM dithiothreitol (DTT) was prepared in phosphate buffer pH 4 (77.4 mg in 10 mL). 5 mL of DTT solution was added to 5 mL peptide solution. The solutions were shaken over night for the reduction of the peptides to take place. 500 µl of reduced peptide solution was added to the eppendorfs with the polymer and two control eppendorf without polymer. For oxidation a 20 % excess of $K_3Fe(CN)_6$ solution prepared in phosphate buffer was added to the eppendorfs. The samples were shaken and oxidized for 4.5 hours and then 100 µl of solution was taken for LC-MS analysis after the polymer was sedimented.

6 REFERENCES

1 Raphals, P. Science 1990, 249, 619.

2 Impurities in new drug substances, Q3A(R2), Step 4 version (25.10.06): http://www.fda.gov/RegulatoryInformation/Guidances/ucm127942.htm#i

3 G. A. Frampton, D. R. Hannah, N. Henderson, R. B. Katz, I. H. Smith, N. Tremayne, R. J. Watson, I. Woollam, Org. Process Res. Dev. 2004, 8, 415.

4 Q. Yang, B. P. Haney, A. Vaux, D. A. Riley, L. Heidrich, P. He, P. Mason, A. Tehim, L. E. Fisher, H. Maag, N. G. Anderson, Org. Process Res. Dev. 2009, 13, 786.

5 Europen Medicines Agency Doc. Ref. EMA/CHMP/492059/2007.

6 A. N. Mayeno, F. Lin, C. S. Foote, D. A. Loegering, M. M. Ames, C. W. Hedberg, G. J. Gleich, Science 1990, 250, 1707.

7 D. Swinbanks, C. Anderson, Nature 1992, 358, 96.

8 C.W. Abell, R.S. Shen, W. Gessner, A. Brossi, Science 1984, 224, 405.

9 G. Székely, J. Bandarra, W. Heggie, B. Sellergren, F. C. Ferreira, J. Membr. Sci., 2011, 381, 21–33.

10 R. Kecili, D. Nivhede, J. Billing, M. Leeman, B. Sellergren, E. Yilmaz, Org. Process Res. Dev. 2010, 14, 993-998.

11 G. Székely, E. Fritz, J. Bandarra, W. Heggie, B. Sellergren, J. Chrom. A, 2012, 1240, 52.

12 Brittain, H. G.; Boganowich, S. J.; Bugay, D. E.; DeVincentis, J.; Lewen, G.; Newman, A. W. Pharm. Res. 1991, 8, 963.

13 Remenar, J. F.; MacPhee, J. M.; Larson, B. K.; Tyagi, V. A.; Ho, J. H.; McIlroy, D. A.; Hickey, M. B.; Shaw, P. B.; Almarsson, O. Org. Process Res. Dev. 2003, 7, 990.

14 Practical Process Research and Development (Second Edition), Chapter 13 Final Product Form and Impurities, 2012.

15 A.M. Thayer, Chem. Eng. News 2010, 88(22), 13.

16 U.S. Food and Drug Administration. Guidance for Industry, Q3A Impurities in New Drug Substances. February 2003.

17 N. L. Kruhlak, J. F. Contrera, R.D. Benz, E. J. Matthews, Adv. Drug Delivery Rev. 2007, 59, 43.

18 G. Székely, PhD Thesis *Degenotoxification of pharmaceuticals by molecular imprinting and organic solvent nanofiltration.* August 2012

19 D. P. Elder, A. Teasdale, A. M. Lipczynski, J. Pharm. Biomed. Anal. 2008, 46, 1.

20 K. Mosbach, Anal. Chim. Acta., 2001, 435, 3.

21 D. J. Snodin, Regul. Toxicol. Pharmacol. 2006, 45, 79.

22 C. C. M. Garcia, J. P. F. Angeli, F. P. Freitas, O. F. Gomes, T. F. de Oliveira, A. P. M. Loureiro, P. Di Mascio, M. H. G. Medeiros, J. Am. Chem. Soc. 2011, 133, 9140.

23 Q. Dai, D. Xu, K. Lim, R. G. Harvey, J. Org. Chem. 2007, 72, 4856.

24 M. R. O'Donovan, C. D. Mee, S. Fenner, A. Teasdale, D. H. Phillips,. Mutat. Res. 2011, 724(1–2), 1.

25 Guidelines for genotoxicity testing and data interpretation have been described in ICH Guidance S2: http://www.ema.europa.eu/docs/en_GB/document_library/Scientific_guideline/2011/12/WC500119604.pdf

26 Guideline on the limits of genotoxic impurities. CPMP/SWP/5199/02European Medicines Evaluation Agency, Committee for Medicinal Products for Human Use (CHMP), June 28, 2006, London http://www.ema.europa.eu/docs/en_GB/document_library/Scientific_guideline/2009/09/WC500002903.pdf

27 D. I. Robinson, Org. Process Res. Dev. 2010, 14, 946.

28 *Kirk-Othmer Encyclopedia of Chemical Technology.*1999-2014. John Wiley & Sons, Inc.

29 International Agency for Research on Cancer (IARC) *Monographs on the Evaluation of Carcinogenic Risks to Humans: Re-evaluation of some Organic Chemicals, Hydrazine and Hydrogen Peroxide*, Vol. 71, IARC, Lyon, France, 1999, pp.1–225.

30 L.G. Hernández, H. van Steeg, M. Luijten, J. van Benthem, Mutat. Res. 2009, 682,94.

31 IARC Monogr. Eval. Carcinog. Risks Hum.: Acetamide, 1999, 71, 1211.

32 A. Schülé, C. Ates, M. Palacio, J. Stofferis, J. Delatinne, B. Martin, S. Lloyd, Org. Proc. Res. & Dev. 2010, 14, 1008.

33 L. K. Dow, M. M. Hansen, B. W. Pack, T. J. Page, S. W. Baertschi, J. OF Pharmaceu. Sci., 2013, 102, 1404.

34 G. Erhart, DE Patent 1111642, 1958.

35 IARC Acetamide, vol. 71, International Agency for the Research on Cancer, Lyon, France, 1987.

36 H. Yamasaki, J. Ashby, M. Bignami, W. Jongen, K. Linnainmaa, R.F. Newbold, G. Nguyen-Ba, S. Parodi, E. Rivedal, D. Schiffmann, J.W. Simons, P. Vasseur, Mutat. Res. 1996, 353, 47.

37 J.W. Lee, K.D. Shin, M Lee, E.J. Kim, S.S. Han, M.Y. Han, H Ha, T.C. Jeong, W.S. Koh, Toxicol. Letters 2003, 136, 163.

38 O.G. Fitzhugh, A.A. Nelson, Science 1948, 108, 626.

39 T.Y. Low, C.K. Leow, M Salto-Tellez, M.C. Chung, Proteomics 2004, 4, 3960.

40 S.K. Natarajan, S Thomas, P Ramamoorthy, J Basivireddy, A.B. Pulimood, A Ramachandran, K.A. Balasubramanian, J. of Gastroenterology and Hepatology 2006, 21, 947.

41 H. Hajovsky, G. Hu, Y. Koen, D. Sarma, W. Cui, D.S. Moore, J.L. Staudinger, R.P. Hanzlik, Chem. Res. Toxicol. 2012, 25, 1955.

42 A. Zaragoza, D. Andres, D. Sarrion, M. Cascales. Chemico-Biological Interactions 2000, 124, 87.

43 N. Sanz, C. Diez-Fernandez, D. Andres, M. Cascales. Biochimica et Biophysica Acta 2002, 1587, 12.

44 V. Moronvalle-Halley, B. Sacre-Salem, V. Sallez, G. Labbe, J.C. Gautier. Toxicol. 2005, 207, 203.

45 Brookes, P.S., Yoon, Y., Robotham, J.L., Anders, M.W., Sheu, S.S., 2004. Cell Phys. 287, C817.

46 Bernardi, P., Petronilli, V., Di Lisa, F., Forte, M., 2001. Trends in Biochem. Sci. 26, 112.

47 R.W. Draper, A.T. McPhail, M. S. Puar, E. J. Vater, L. Weber, Tetrahedron, 1999, 55, 3355.

48 L.Huang, D. Yub, P. Hoa, K. Leeb, C. Chen, Lett. Drug Des. Discov. 2007, 4, 471.

49 B.Venkateswara Rao, K. Ramanjaneyulu, T. Bhaskara Rao, J. Chem. Pharm. Res. 2011, 3, 589.

50 U. Zutter, H. Iding, P. Spurr, B. Wirz, J.Org.Chem.2008, 73, 4895.

51 Y.Y. Yeung, S. Hong,E. J. Corey, J.Am. Chem. Soc. 2006, 128, 6310.

52 L. Gentric, I. Hanna, L. Ricard, Org. Lett. 2003, 5, 1139.

53 L. Müller, R.J. Mauthe, C.M. Riley, M.M. Andino, D. Antonis, C. Beels, J. DeGeorge, A.G.M. Knaep, D. Ellison, J.A. Fagerland, R. Frank, B. Fritschel, S. Galloway, E. Harpur, C.D.N. Humfrey, A.S. Jacks, N. Jagota, Regul. Toxicol. Pharm. 2006, 44, 198.

54 F. Renauld, S. Moreau, A. Lablache- Combier, B. Tiffon, Tetrahedon, 1985, 41, 955.

55 T. Traoré, A. Cavagnino, N. Saettel, F. Radvanyi, S. Piguel, I. Bernard-Pierrot, V. Stoven, M. Legraverend, European J. of Med. Chem., 2013, 70, 789.

56 A. F. Stepan, D. P. Walker, J. Bauman, D. A. Price, T. A. Baillie, A. S. Kalgutkar, M. D. Aleo, Chem. Res. Toxicol. 2011, 24, 1345.

57 A. Mally, J. K. Chipman, Toxicology 2002,180, 233.

58 C. Cowles, A. Mally, J.K. Chipman, Toxicology 238 (2007) 49.

59 C. Martinat, C. Amar, P. M. Dansette, J. Leclaire, P. Lopez-Garcia, T. Do Cao, H. N. N'Guyen, D. Mansuy, European J. of Pharmacology 1992, 228, 63-71.

60 B. Sellergren, eds., Molecularly imprinted polymers. Man made mimics of antibodies and their applications in analytical chemistry.; Elsevier Science B.V.: Amsterdam, 2001; Vol. 23.

61 Philp, D.; Stoddart, J. F. Angew. Chem., Int. Ed. 1996, 35, 1154.

62 Alexander, C.; Andersson, H. S.; Andersson, L. I.; Ansell, R. J.; Kirsch, N.; Nicholls, I. A.; O'Mahony, J.; Whitcombe, M. J. J. Mol. Recognit. 2006, 19, 106.

63 B. Sellergren, and A. J. Hall, 2012. Molecularly Imprinted Polymers. Supramolecular Chemistry: From Molecules to Nanomaterials

64 Wulff, G., Biffis, A., Molecular imprinting with covalent or stoichiometric non-covalent interactions, In *Molecularly imprinted polymers. Man made mimics of antibodies and their applications in analytical chemistry*; Sellergren, B., Elsevier Science B.V., Amsterdam, 2001; p 102

65 Nicholls, I.A., Andersson, H. S., Thermodynamic principles underlying molecularly imprinted polymer formulation and ligand recognition. In *Molecularly imprinted polymers. Man made mimics of antibodies and their applications in analytical chemistry*; Sellergren, B., Elsevier ScienceB.V., Amsterdam, 2001; p 59

66 G. Wulff, Chem. Rev., 2002, 102, 1-28.

67 K. Haupt and K. Mosbach, Chem. Rev., 2000, 100, 2495.

68 G. Wulff, Angew. Chem. Int. Ed. Engl., 1995, 34, 1812.

69 Molecularly Imprinted Polymers; Haupt, K.; Linares, A.; Bompart, M.; Bui, B., Eds.; Springer Berlin Heidelberg, 2011; Vol. 325.

70 Owens, P.K.,Karlsson, L., Lutz, E.S.M., Andersson, L.I., TrAC Trends Anal. Chem. 1999, 18, 146.

71 Piletsky, S., Alcock, S., Turner, A., Trends Biotechnol. 2001, 19, 3.

72 http://www.biotage.co.jp/pages/446/Japan_NovDec_ExploraSepSeminar.pdf

73 E. Yilmaz, R. Kecili,, Fast identification of selective resins for genotoxic impurity removal via screening of molecularly imprinted resins libraries, HPLC2012, 16-21/06/2012, Anaheim, CA, USA.

74 G. Székely, J. Bandarra, W. Heggie, F.C. Ferreira, B. Sellergren, Sep. Purif. Technol. 2012, 86, 190.

75 M. J. Whitcombe, M. E. Rodriguez, P. Villar, and E. N. Vulfson, J. Am. Chem. Soc., 1995, 117, 7105.

76 P. K. Dahl and F. H. Arnold, J. Am. Chem. Soc., 1991, 113, 7417.

77 T. P. Rao, R. Kala, and S. Daniel, Anal. Chim. Acta, 2006, 578, 105.

78 K. Mosbach, Trends Biochem. Sci., 1994, 19, 9.

79 B. Sellergren, M. Lepistoe, and K. Mosbach, J. Am. Chem. Soc., 1988, 110, 5853.

80 D. C. Sherrington, Chem. Commun., 1998, 2275.

81 A. G. Mayes, Chapter 12: Polymerisation techniques for the formation of imprinted beads, in Molecularly Imprinted Polymers: Man Made Mimics of Antibodies and their Applications in Analytical Chemistry, ed. B. Sellergren, Elsevier Science B. V., Amsterdam, 2001, vol. 23, p. 305.

82 B. Sellergren, Chapter 13: Imprinted monoliths, in Monolithic Materials: Preparation, Properties and Applications, ed. F. Svec, Elsevier Science, Amsterdam, 2003.

83 K. Flavin, M. Resmini, Adv. Nanomater., 2010, 2, 651.

84 Moad, G.; Solomon, D. H. The Chemistry of Free Radical Polymerization; Elsevier Science Ltd, 1995.

85 Odian, G. Principle of polymerization; John wiley and Sons,Inc., Hoboken, New Jersey, 2004; Vol. Fourth Edition.

86 G. Wulff and A. Sarhan, Angew. Chem. Int. Ed. Engl., 1972, 11, 341.

87 M. Komiyama, T. Takeuchi, T. Mukawa, H Asamuma, (ed) *Molecular Imprinting. From Fundamentals to applications*, Wiley-VCH, 2003.

88 K. Takeda, A. Kuwahara, K. Ohmori, and T. Takeuchi, J. Am. Chem. Soc., 2009, 131, 8833–8838.

89 O. Ramström, L. I. Andersson, and K. Mosbach, J. Org. Chem., 1993, 58, 7562.

90 C. Widstrand, S. Kronauer, H. Bjoerk, et al., Am. Lab.Shelton, CT, U. S.), 2008, 40, 6.

91 A. Bhaskarapillai, N. V. Sevilimedu, and B. Sellergren, Ind. Eng. Chem. Res., 2009, 48, 3730.

92 K. J. Shea, T.K. Dougherty, J. Am. Chem. Soc. 1986, 108, 1091.

93 a. G. Mayes, M. J. Whitcombe, Adv. Drug Deliv. Rev. 2005, 57, 1742.

94 R. Arshady, K. Mosbach, Macromol. Chem. 1981, 182, 687.

95 L. Andersson, B. Sellergren, K. Mosbach, Tetrahedron Letters, 1984, 25, (45), 5211.

96 K.J. Shea, D. A. Spivak and B. Sellergen, J. Am. Chem. Soc., 1993, 115, 3368.

97 B. Sellergren, K.J. Shea, J. Chromatogr. A 1993, 635, 31.

98 B. Sellergren, J. Chromatogr., A 2001, 906, 227.

99 B. Sellergren, K.J. Shea, J. Chromatogr., A 1995, 690, 29.

100 A. Zander, P. Findlay, R. Thomas; B. Sellergren, Anal. Chem. 1998, 70, 3304.

101 Y. Chen, M. Kele, P. Sajonz, B. Sellergren, G. Guiochon, Anal. Chem. 1999, 71, 928.

102 P. Sajonz, M. Kele, G. Zhong, B. Sellergren, G. Guiochon, J. Chrom. A 1998, 810, 1.

103 B. Sellergren, L. Andresson J. Org. Chem. 1990, 55, 3381.

104 M. J. Whitcombe, M. E. Rodriguez, P. Villar, E. N. Vulfson, J. Am. Chem. Soc. 1995, 117, 7105.

105 K. Nemoto, T. Kubo, M. Nomachi *et al.*, J. Am. Chem. Soc. 2007, 129, 13626.

106 A. Rachkov and N. Minoura, Biochim. Biophys. Acta, 2001, 1544, 255.

107 M. Quaglia, K. Chenon, A. J. Hall, E. De Lorenzi, and B. Sellergren, J. Am. Chem. Soc., 2001, 123, 2146.

108 H. Nishino, C.-S. Huang, and K. J. Shea, Angew. Chem. Int. Ed., 2006, 45, 2392.

109 M. M. Titirici, A. J. Hall, and B. Sellergren, Chem. Mater., 2003, 15, 822.

110 K. Karim, F. Breton, R. Rouillon, E. V. Piletska, A. Guerreiro, I. Chianella, S. A. Piletsky, Adv. Drug Deliv. Rev., 2005, 57, 1795

111 B. C. G. Karlsson, J. O'Mahony, J. G. Karlsson, H. Bengtsson, L. A. Eriksson, I. A. Nicholls, J. Am. Chem. Soc., 2009, 131, 13297.

112 M. J. Whitcombe, L. Martin, and E. N. Vulfson, Chromatographia, 1998, 47, 457.

113 K. Tanabe, T. Takeuchi, J. Matsui, K. Ikebukuro, K. Yano and I. Karube, J. Chem. Soc. Chem. Commun., 1995, 22, 2303.

114 A. G. Strikovsky, D. Kasper, M. Gruen, et al., J. Am. Chem. Soc., 2000, 122, 6295.

115 O. Norrlöw, M. Glad, and K. Mosbach, J. Chromatogr. A, 1984, 299, 29.

116 B. Sellergren, B. Ruckert, and A. J. Hall, Adv. Mater., 2002, 14, 1204.

117 E. Yilmaz, K. Haupt, and K. Mosbach, Angew. Chem. Int Ed., 2000, 39, 2115.

118 Z. Zeng, Y. Hoshino, A. Rodriguez, H. Yoo, and K. J. Shea., ACS Nano., 2010, 4, 199.

119 L. Ye, P. A. G. Cormack, and K. Mosbach, Anal. Commun., 1999, 36, 35.

120 J. Wang, P. A. G. Cormack, D. C. Sherrington, and E. Khoshdel, Angew. Chem. Int. Ed., 2003, 42, 5336.

121 A. Cutivet, C. Schembri, J. Kovensky, and K. Haupt, J. Am. Chem. Soc., 2009, 131, 14699.

122 Y. Hoshino, T. Kodama, Y. Okahata, and K. J. Shea, J. Am. Chem. Soc., 2008, 130, 15242.

123 M. Ulbricht, J. Chromatogr. B, 2004, 804, 113.

124 B. Sellergren and A.-M. Esteban, Chapter 23: The use of molecularly imprinted polymers for sampling and sample preparation, in Handbook of Sample Preparation, eds. J. Pawliszyn, and H. L. Lord) John Wiley & Sons, Hoboken, New Jersey, 2010, vol. 1, p. 445.

125 Y. Xia, J. E. McGuffey, S. Bhattacharyya, B. Sellergren, E. Yilmaz, L. Wang, and J. T. Bernert, Anal. Chem. 2005, 77, 7639.

126 S. Ambrosini, S. Shinde, E. De Lorenzi and B. Sellergren Analyst, 2012, 137, 249

127 N. Harun, R. A. Anderson and P. A. G. Cormack, Anal. Bioanal. Chem., 2010, 396, 2449.

128 S. Shinde, A. Bunschoten, J. A. W. Kruijtzer, R. M. J. Liskamp, and B. Sellergren, Angew. Chem. Int. Ed. 2012, 51, 8326.

129 M. Le Noir, A.-S. Lepeuple, B. Guieysse, and B. Mattiasson, Water Res., 2007, 41, 2825.

130 http://www.niehs.nih.gov/health/topics/agents/endocrine/index.cfm. Lasr reviewed June 5, 2013.

131 P. Manesiotis, C. Borrelli, C. Aureliano, et al., J. Mater. Chem., 2009, 19, 6185.

132 C. Borrelli, S.Barsanti, D. Silvestri, P. Manesiotis, G. Ciardelli and B. Sellergren. J. of Food Processing and Preservation 2011, 35, 112-128.

133 M.C. Blanco-Lopez, M.J. Lobo-Castanon, A.J. Miranda-Ordieres, P. Tunón-Blanco, Trends in Analytical Chemistry 2004, 23, 36.

134 D. Kriz and K. Mosbach, Analytica Chimica Acta 1995, 300, 71.

135 K. Haupt, K. Noworyta, W. Kutner, Analytical Communications 1999, 36, 391.

136 R. Levi, S. McNiven, S.A. Pilesky, S.H. Cheong, K. Yano, I. Karube, Anal. Chem. 1997, 69, 2017.

137 O.Y.F. Henry, D.C. Cullen, S.A. Pilesky, Anal. Bioanal. Chem. 2005, 382, 947.

138 F. L. Dickert, P. Lieberzeit, and M. Tortschanoff, Sens. Actuators, B, 2000, B65, 186.

139 J. Matsui, H. Kubo, and T. Takeuchi, Anal. Chem., 2000, 72, 3286.

140 N. T. K. Thanh, D. L. Rathbone, D. C. Billington, and N. A. Hartell, Anal. Lett., 2002, 35, 2499.

141 R. Wagner, W. Wan, M. Biyikal, E. Benito-Pena, M. Cruz Moreno-Bondi, I. Lazraq, K. Rurack and B. Sellergren, J. Org. Chem. 2013, 78, 1377.

142 G. Vlatakis, L. I. Andersson, R. Mueller, and K. Mosbach, Nature, 1993, 361, 645.

143 J. L. Urraca Javier, C. Moreno-Bondi Maria, G. Orellana, et al., Anal. Chem., 2007, 79, 4915.

144 K. Kotova, M. Hussain, G. Mustafa, P. A. Lieberzeit, Sensors and Actuators B 2013, 189, 199.

145 M. E. Byrne, K. Park, and N. A. Peppas, Adv. Drug. Deliv. Rev., 2002, 54, 149.

146 R. Suedee, T. Srichana, and G. P. Martin, J. Control. Release, 2000, 66, 135.

147 J. Damen and D. C. Neckers, J. Am. Chem. Soc., 1980, 102, 3265.

148 K. J. Shea, E. A. Thompson, S. D. Pandey, and P. S. Beauchamp, J. Am. Chem. Soc., 1980, 102, 3149.
149 G. Wulff, J. Vietmeier, Makromol. Chem., 1989, 190, 1727.
150 Y. Yu, L. Ye, K. Haupt, and K. Mosbach, Angew. Chem. Int. Ed., 2002, 41, 4459.
151 K. Polborn and K. Severin, Chem. Eur. J., 2000, 6, 4604.
152 A. N. Cammidge, N. J. Baines, and R. K. Bellingham, Chem. Commun., 2001, 2588.
153 B. Sellergren and K. J. Shea, Tetrahedron Asymmet., 1994, 5, 1403.
154 J.-Q. Liu and G. Wulff, J. Am. Chem. Soc., 2004, 126, 7452.
155 J.-Q. Liu and G. Wulff, Angew. Chemie. Int. Ed., 2004, 43, 1287.
156 F. Lanza, B. Sellergren, Anal. Chem. 1999, 71, 2092.
157 T. Takeuchi, D. Fukuma, J. Matsui, Anal. Chem. 1999, 71, 285.
158 B. Dirion, Z. Cobb, E. Schillinger, et al., J. Am. Chem. Soc., 2003, 125, 15101.
159 G. Ceolin, F. Navarro-Villoslada,M. C. Moreno-Bondi, G. Horvai, V. Horvath, J. Comb. Chem. 2009, 11, 645.
160 C. Widstrand, E. Yilmaz, B. Boyd, et al., Am. Lab. (Shelton,CT, U. S.), 2006, 38, 12.
161 C. Jiménez-González, D. J. C. Constable and C. S. Ponder, Chem. Soc. Rev., 2012, 41, 1485.
162 C. Jiménez-González, P. Poechlauer, Q. B. Broxterman, B.-S. Yang, D. am Ende, J. Baird, C. Bertsch, R. E. Hannah, P. Dell'Orco, H. Noorman, S. Yee, R. Reintjens, A. Wells, V. Massonneau and J. Manley, Org. Process Res. Dev., 2011, 15, 900.
163 Limit_of_genotoxic_impurities, EMEA, 2006.
164 M. Degerman, N. Jakobsson, B. Nilsson, Chem. Eng. Technol., 2008, 31, 875.
165 T. Winkelnkemper, G. Schembecker, Sep. Purif. Technol.,2010, 72, 34.
166 J. F. Kim, G. Székely, I. B. Valtcheva, A. G. Livingston, Green Chem., 2014, 16, 133.
167 B. Van der Bruggen, M. Mänttäri, M. Nyström, Sep. Purif. Technol., 2008, 63, 251.
168 Y. H. See Toh, F. W. Lim, A. G. Livingston, J. Membr. Sci., 2007, 301, 3.
169 Y. H. See-Toh, M. Silva, A. Livingston, J. Membr. Sci., 2008, 324, 220.
170 P. Vandezande, L. E. M. Gevers, I. F. J. Vankelecom, Chem. Soc. Rev., 2008, 37, 365.
171 C. Pink, H. Wong, F. C. Ferreira, A. G. Livingston, Org. Process Res. Dev., 2008, 12, 589.
172 S. So, L. G. Peeva, E. W. Tate, R. J. Leatherbarrowb, A. G. Livingston, Chem. Commun., 2010, 46, 2808.
173 E. M. Rundquist, C. J. Pink, A. G. Livingston, Green Chem., 2012, 14, 2197.

174 J. Geens, K. Boussu, C. Vandecasteele, B. Van der Bruggen, J. Membr. Sci., 2006, 281, 139.

175 B. Van der Bruggen, J. Schaep, D. Wilms, C. Vandecasteele, J. Membr. Sci., 1999, 156, 29.

176 P. Marchetti, A. Butté, A. G. Livingston, J. Membr. Sci., 2012, 444, 415.

177 S. Zeidler, U. Kätzel and P. Kreis, J. Membr. Sci., 2013, 429, 295.

178 W. J. Koros, Y. H. Ma, T. Shimidzu, J. Membr. Sci., 1996, 120, 149.

179 R. J. Petersen, J. Membr. Sci., 1993, 83, 81.

180 A. A. Kaspar and J. M. Reichert. Drug Discovery Today, 2013, 18, 807.

181 P.M. McNeely, A. N. Naranjo, A. S. Robinson, Biotechnol. J. 2012, 7, 1451.

182 T.K Sawyer, Chem Biol Drug Des 2009, 73, 3.

183 G. Weckbecker, F. Raulf, B. Stolz, C. Bruns, Pharmac. Ther. 1993, 60, 245.

184 J. E. F. Rivier, J. A.C.S. 1974, 96(9), 2986.

185 http://www.uptodate.com/contents/physiology-of-somatostatin-and-its-analogues. Accessed March 3, 2014

186 http://www.drugs.com/drug-class/somatostatin-and-somatostatin-analogs.html. Accessed March 3, 2014

187 Y. C. Patel, K. K. Murthy, E. E. Escher, D. Banville, J. Spiess, C. B. Srikant, Metabolism, 1990, 39, 63.

188 S. Lamberts, A.J Van der Lely, W. de Herder, L. Hofland, New Eng. J. of Med., 1996, 334 (4), 246.

189 F.L. Dickert, O. Hayden, In Molecularly imprinted polymers. Man made mimics of antibodies and their applications in analytical chemistry; B.Sellergren, Elsevier Science B.V.: Amsterdam, 2001; Vol. 23, p. 521.

190 Introduction booklet on Electron Microscopy. FEI ElectronOptics 2004 ISBN nummer 90-9007755-3

191 L.C. Sawyer and D.T. Grubb. *Polymer Microscopy* ; Chapman & Hall Second Edition 1996.

192 G.W. Ehrenstein, G. Riedel, P. Trawiel. Praxis der Thermischen Analyse von Kunststoffen. Hanser 1998.

193 Wulff, M. Thermochimica Acta 2004, 419, 291.

194 Landry, M. R. Thermochimica Acta 2005, 433, 27.

195 Wheeler, A., Catalysis. Vol. 2. 1955, New York Reinhold Pub. Corp.,

196 Unger, K. K. *Porous silica, its properties and use as support in column liquid chromatography.*; Elsevier Scientific Publishing Co.: New York, 1979.

197 Sing, K. S. W.; Everett, D. H.; Haul, R. A. W.; Moscou, L.; Pierotti, R. A.; Rouquerol, J.; Siemieniewska, T. Pure and Applied Chemistry 1985, 57, 603.

198 M. Khalfaoui, S. Knani, M.A. Hachicha, and A. Ben Lamine J. of Colloid and Interface Science 2003, 263, 350.

199 Brunauer, S.; Emmett, P. H.; Teller, E. J. Am. Chem. Soc. 1938, 60, 309.

200 Gregg, S. J.; Sing, K. S. W. Adsorption Surface Area and Porosity; Academic Press: London, 1982.

201 Gurvich, L. J. Phy. Chem. Soc. Rus. 1915, 47, 805.

202 Barrett, E. P.; Joyner, L. G.; Halenda, P. P. J. Am. Chem. Soc.1951, 73, 373.

203 G. Wulff, W. Vesper, R. Grobe-Einsler, A. Sarhan, Makromol. Chem. 1977, 178, 2799.

204 Chemical & Engineering News, May 30, 2011, 89, 22, 21.

205 G. Ciardelli, B. Cioni, C. Cristallini, N. Barbani, D. Silvestri, P. Giusti, Biosens. Bioelectron., 2004, 20, 1083.

206 W. Cai, R. B. Gupta, Sep. Purif. Technol. 2004, 35, 215.

207 H. Dong, A. J. Tong, L. D. Li, Spectrochim. Acta A, 2003, 59, 279.

208 F. G. Tamayo, J. L. Casillas, A. Martin-Esteban, Anal. Chim. Acta, 2003, 482, 165.

209 M. J. Syu, J. H. Deng, Y. M. Nian, Anal. Chem. Acta, 2004, 504, 167.

210 H. Y. Wang, S. L. Xia, H. Sun, Y. K. Liu, S. K. Cao, T. Kobayashi, J. Chromatogr. B, 2004, 804, 127.

211 F. Chapuis, V. Pichon, F. Lanza, B. Sellergren, M. C. Hennion, J. Chromatogr. B, 2004, 804, 93.

212 J. Jodlbauer, N. M. Maier, W. Lindner, J. Chromatogr. A, 2002, 945, 45.

213 P. T. Vallano, V. T. Remcho, J. Chromatogr. A, 2000, 888, 23.

214 Y. Tunc, N. Hasirci, A. Yesilada, K. Ulubayram, Polymer 2006, 47, 6931.

215 G. Lancelot, C. Helene, Nucleic Acids Res. 1979, 6, 1063.

216 B. Sellergren, K.J. Shea, J. Chromatogr. A 1995, 690, 29.

217 L. Schweitz, L. I. Andersson, S. Nilsson J. Chrom. A 1998, 817, 5.

218 L. Schweitz, L. I. Andersson, S. Nilsson, Analyst, 2002, 127, 22.

219 Molecular imprinting, Topics in Current Chemistry, Vol. 325, Ed. K.Haupt, 2012.

220 S. Azodi-Deilami, M. Abdouss, S. R. Seyedib Cent. Eur. J. Chem. 2010, 8(3), 687.

221 M. Khajeh, Y. Yamini, E. Ghasemi, J. Fasihia, M. Shamsipur, Anal. Chim. Acta 2007, 581, 208.

222 N. Arabzadeh, M. Abdouss, Colloid J. 2010,72, 446.

223 P.A.G. Cormack, A. Davies, N. Fontanals, Reactive & Functional Polymers, 2012, 72, 939.

224 D. I. Robinson, Org. Proc. Res. & Dev., 2010 14, 946.

225 N.V.V.S.S. Raman, A.V.S.S. Prasad, K. Ratnakar Reddy, J. of Pharma. and Biomed. Analysis, 2011, 55 662.

226 A. Schülé, C. Ates, M. Palacio, J. Stofferis, J.-P. Delatinne, B. Martin, S. Lloyd, Org. Proc. Res. & Dev. 2010, 14, 1008.

227 F. Lanza, B. Sellergren, Anal. Chem. 1999, 71, 2092.

228 T. Takeuchi, D. Fukuma, J. Matsui, Anal. Chem. 1999, 71, 285.

229 F. Lanza, A. J. Hall, B. Sellergren, A. Bereczki, G. Horvai, S. Bayoudh, P.A.G. Cormack, D.C. Sherrington, Anal. Chim. Acta 2001, 435, 91.

230 T. Takeuchi, A. Seko, J. Matsui,T. Mukawa, Instrum. Sci. Technol. 2001, 29, 1.

231 B. Dirion, Z. Cobb, E. Schillinger, L.I. Andersson, B. Sellergren, J. Am. Chem. Soc. 2003, 125, 15101.

232 G. Ceolin, F. Navarro-Villoslada, M. C. Moreno-Bondi, G. Horvai, V. Horvath, J. Comb. Chem. 2009, 11, 645.

233 H. Y. Wang, T. Kobayashi, N. Fujii, J. Chem. Technol. Biotechnol. 1997, 70, 355–362.

234 S. A. Piletsky, H. Matuschewski, U. Schedler, A. Wilpert, E.V. Piletska, T.A. Thiele, M. Ulbricht, Macromolecules 2000, 33, 3092.

235 T.A. Sergeyeva, H. Matuschewski, S.A. Piletsky, J. Bendig, U. Schedler, M. Ulbricht, J. Chrom. A 2001, 907, 89.

236 X.L. Zhu, Q.D. Su, J.B. Cai, J. Yang, Y. Gao, J. Appl. Polym. Sci. 2006, 101, 4468–4473.

237 J. E. Kilduff, S. Mattaraj, M. Zhou, G. Belfort, J. Nanoparticle Research 2005, 7, 525.

238 M. Zhou, H. Liu, A. Venkiteshwaran, J. Kilduff, D. G. Anderson, R. Langerc, G. Belfort, J. Mater. Chem., 2011, 21, 693.

239 M. Taniguchi, G. Belfort, J. Mem. Sci., 2004, 231, 147.

240 R.B. Merrifield, J. Am. Chem. Soc., 1963, 85 (14), 2149.

241 L. Chen, I. Annis, G. Barany, Current Protocols in Protein Science (2001) 18.6.1-18.6.19 18.6 Disulfide Bond Formation in Peptides

7 APPENDIX

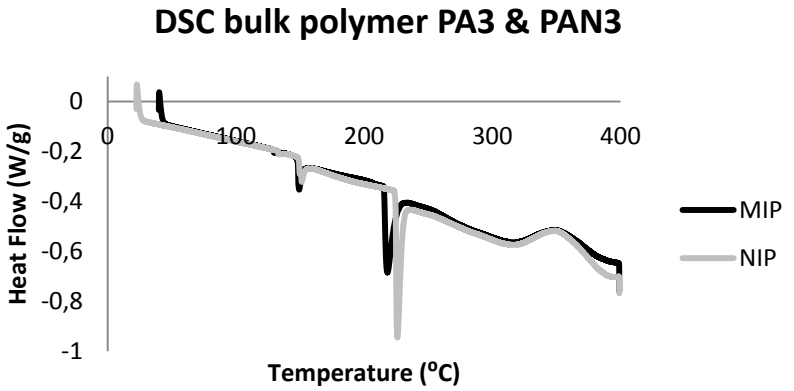

Figure 6. 1 DSC thermogram for the bulk polymers.

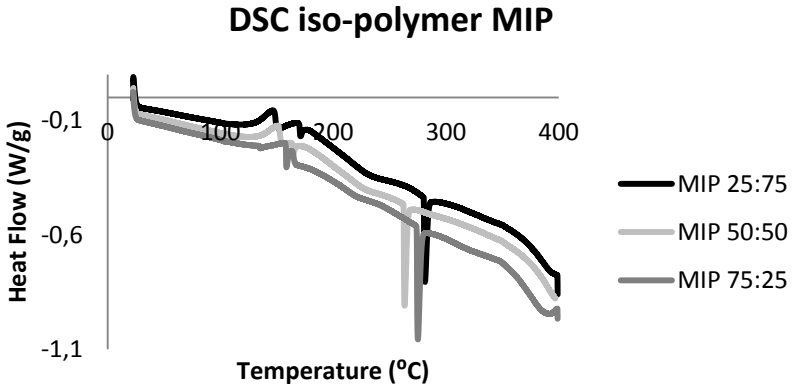

Figure 6. 2 DSC thermograms of the MIP iso-polymers.

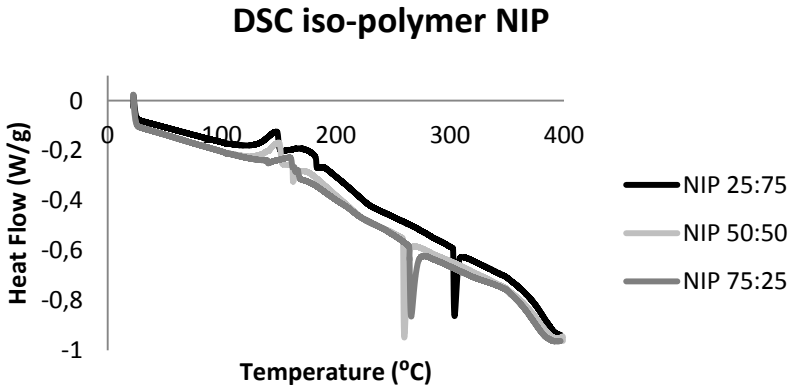

Figure 6. 3 DSC thermograms of the NIP iso-polymer.

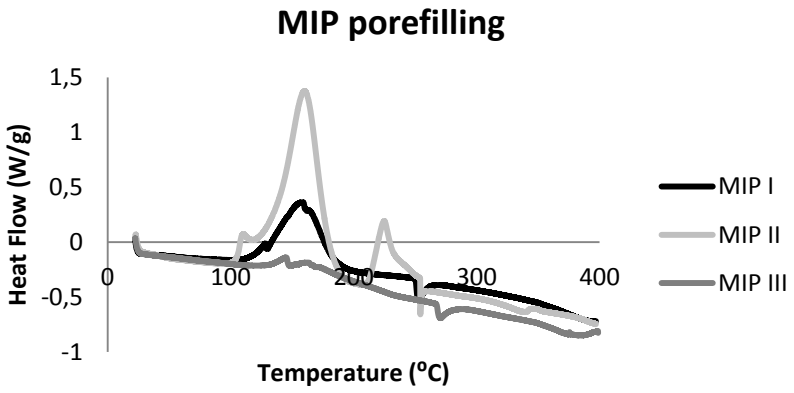

Figure 6. 4 DSC thermograms of the porefilling MIPs.

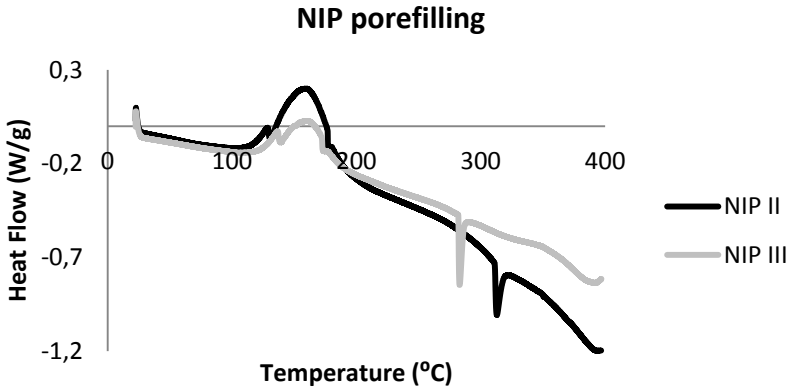

Figure 6. 5 DSC thermograms of the porefilling NIP.

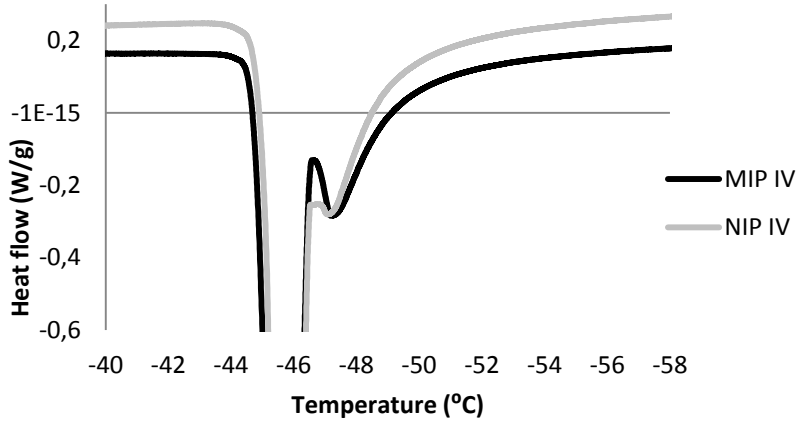

Figure 6. 6 DSC thermograms for porometry calculations for the bulk polymers.

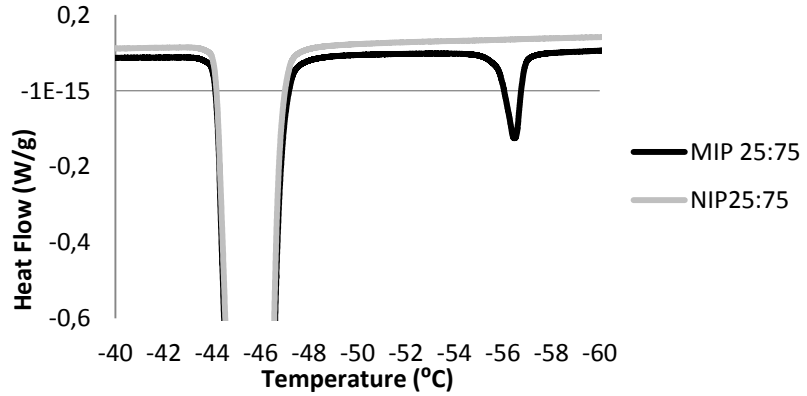

Figure 6. 7 DSC thermograms for porometry calculations for the 25:75 iso-octane polymers.

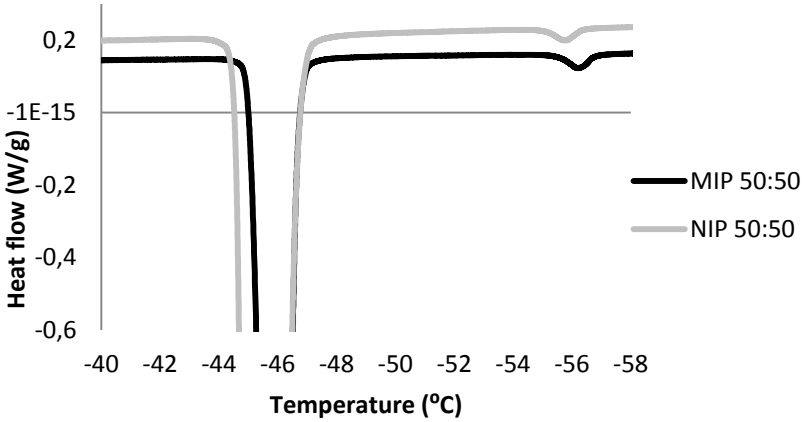

Figure 6. 8 DSC thermograms for porometry calculations for the 50:50 iso-octane polymers.

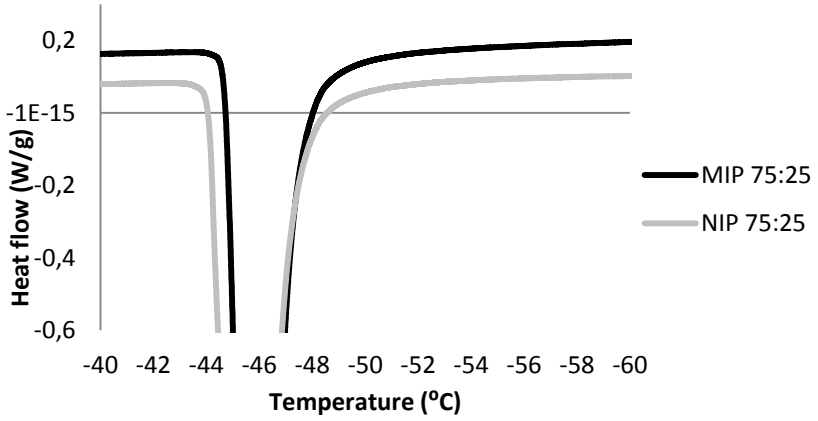

Figure 6. 9 DSC thermograms for porometry calculations for the 75:25 iso-octane polymers.

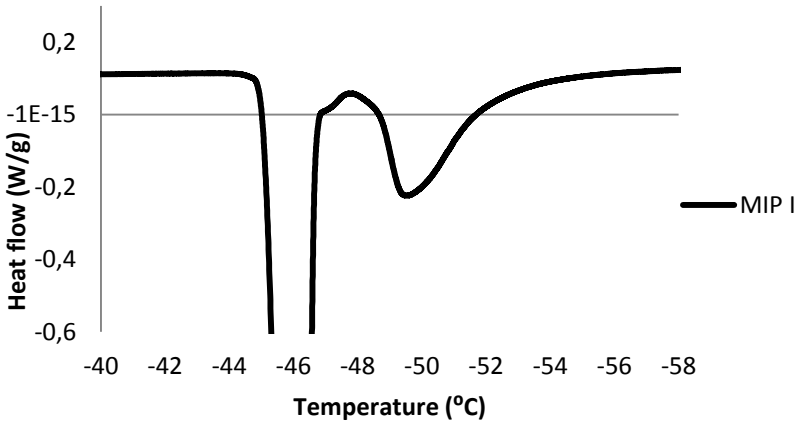

Figure 6. 10 DSC thermograms for porometry calculations for MIP I pore-filling polymer.

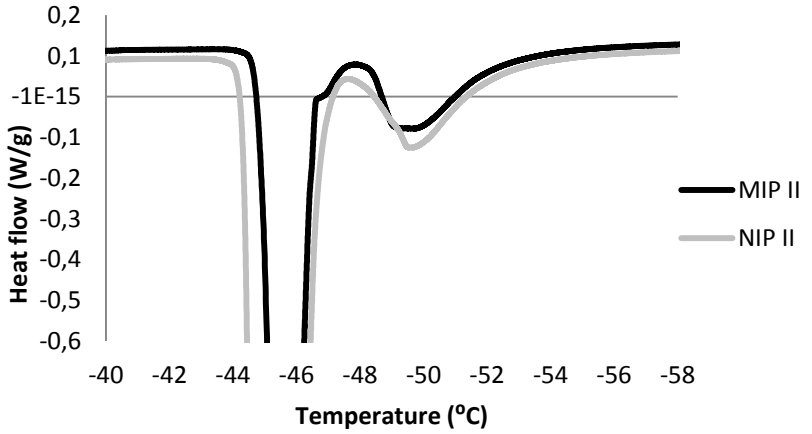

Figure 6. 11 DSC thermograms for porometry calculations for pore-filling polymer II.

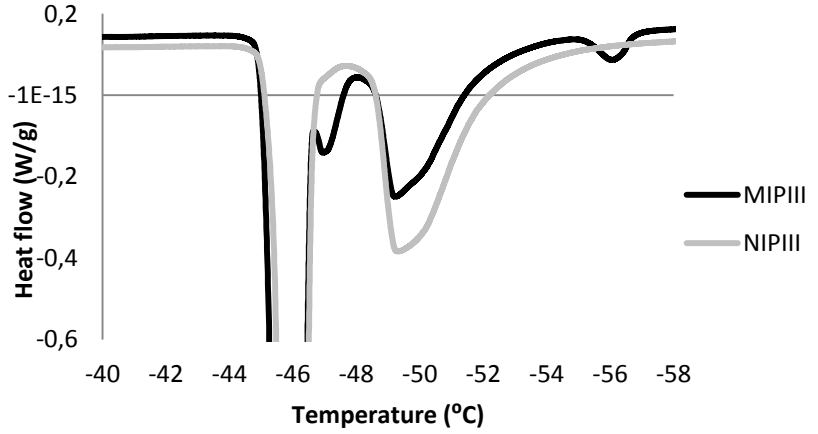

Figure 6. 12 DSC thermograms for porometry calculations for pore-filling polymer III.

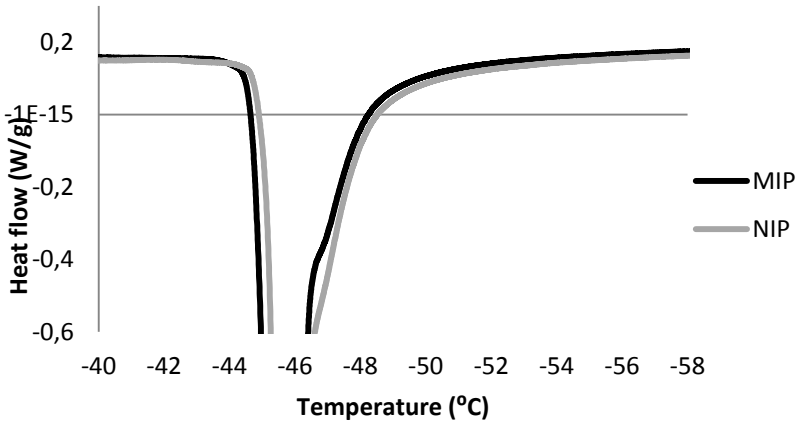

Figure 6. 13 DSC thermograms for porometry calculations for thioacetamide bulk polymers.

LIST OF CONTRIBUTIONS

The contributions based on the work performed in this thesis are listed below.

Publications

György Székely, Emelie Fritz, Joao Bandarra, William Heggie, Börje Sellergren, Removal of potentially genotoxic acetamide and arylsulfonate impurities from crude drugs by molecular imprinting Journal of Chromatography A Vol. 1240, 2012, Pages 52–58.

Patent

Patent Internationale Patentanmeldung PCT/EP2012/061498– GENOPURMIP György Székely, Emelie Fritz and Börje Sellergren

Oral Presentations

OSN Workshop 23 – 25 April Cetraro, Italy. Feasibility study of a membrane-MIP hybrid approach to remove genotoxic impurities from pharmaceuticals

MIP Graduate Symposium Imperial College London Sep 2011.Removal of the genotoxic impurities acetamide and thioacetamide from pharmaceutical formulations

Lecture in Supramolecular chemistry TU Dortmund. On the topic: Polymers in Purification of Pharmaceuticals

Poster Presentations

7th International conference on Molecularly Imprinted Polymers 27th – 29th August 2012 Paris, France. MIPs for solid phase extraction of endotoxins

243rd ACS National meeting San Diego March 25th – 29th 2012.Removal of the genotoxic impurities acetamide and thioacetamide from pharmaceutical formulations using a hybrid approach

3rd EuCheMS Chemistry Congress, Nürnberg, Germany, 29 August to 2 September 2010. Molecularly imprinted polymers for purification of crude pharmaceutical products

Marie Curie Conference Torino 1-2 July 2010. The benefits of collaborations with the private sector as an academic researcher

3rd "Tag der Chemie" (Chemistry Day), TU Dortmund, Germany, 05 February 2010. Molecularly imprinted polymers (MIPs) as a purification and polishing phase in the pharmaceutical industry

CURRICULUM VITAE

Emelie Fritz
Date of birth: 27.12.1984
Nationality: Swedish

ACADEMIC AND PROFFESIONAL QUALIFICATIONS

Sep 2013 – Present 3M Deutschland GmbH, Germany

Senior product development engineer industrial tapes.

April 2012 – Aug 2013 Project manager PEPMIP, Marie Curie ITN project, Malmö Högskola, Sweden

Project manager assisting the coordinator in the management of the project.

April 2009 – Aug 2013 TU Dortmund, Germany

PhD student in polymer chemistry at the Institute of Environmental Research (INFU) of the Faculty of Chemistry

2008 Academic work (Borealis), Stenungsund, Sweden

Working as a consultant at Borealis for four months in their innovation centre laboratory.

2007 - 2008 University of Nottingham, Nottingham, UK

Master of Science (MSc) in Chemistry& Entrepreneurship (interdisciplinary MSc program combining courses in chemistry and business courses). Graduating Class of 2008 with Merit

2003-2007 University of Gothenburg, Gothenburg, Sweden

Bachelor of Science (BSc) in chemistry. Graduated with Distinction

PROFESSIONAL COURSES

March 4th 2013 Business Development Seminar, MIP Technologies Biotage, Lund, Sweden

April – June 2010-2012 Organisation of inorganic laboratory course, TU Dortmund, Germany

2011 Supervision of summer exchange student from Canada in the RISE DAAD Program, TU Dortmund, Germany

2011 Design of Experiment Course, Lonza, Visp, Switzerland

2009 Introduction to Active Pharmaceutical Ingredient Manufacture, GlaxoSmithKline, Stevenage, UK

2009 Business Development Course, WeDoTech, Porto, Portugal

PUBLICATIONS/PATENTS/PRESENTATIONS

Publications

György Székely, Emelie Fritz, Joao Bandarra, William Heggie, Börje Sellergren Removal of potentially genotoxic acetamide and arylsulfonate impurities from crude drugs by molecular imprinting Journal of Chromatography A Vol. 1240, 2012, Pages 52–58.

Annemarie B. Wöhri, Gergely Katona, Linda C. Johansson, Emelie Fritz, Erik Malmerberg, Magnus Andersson, Jonathan Vincent, Mattias Eklund, Marco Cammarata, Michael Wulff, Jan Davidsson, Gerrit Groenhof, Richard Neutze. Laue diffraction snapshots reveal light induced structural changes in a photosynthetic reaction center. Science, 328, 630 (2010)

Patent

Patent Internationale Patentanmeldung PCT/EP2012/061498– GENOPURMIP György Székely, Emelie Fritz and Börje Sellergren

Oral Presentations

OSN Workshop 23 – 25 April Cetraro, Italy. Feasibility study of a membrane-MIP hybrid approach to remove genotoxic impurities from pharmaceuticals

MIP Graduate Symposium Imperial College London Sep 2011.Removal of the genotoxic impurities acetamide and thioacetamide from pharmaceutical formulations

Lecture in Supramolecular chemistry TU Dortmund. On the topic: Polymers in Purification of Pharmaceuticals

Poster Presentations

7th International conference on Molecularly Imprinted Polymers 27th – 29th August 2012 Paris, France. MIPs for solid phase extraction of endotoxins

243rd ACS National meeting San Diego March 25th – 29th 2012.Removal of the genotoxic impurities acetamide and thioacetamide from pharmaceutical formulations using a hybrid approach

3rd EuCheMS Chemistry Congress, Nürnberg, Germany, 29 August to 2 September 2010. Molecularly imprinted polymers for purification of crude pharmaceutical products

Marie Curie Conference Torino 1-2 July 2010. The benefits of collaborations with the private sector as an academic researcher

3rd "Tag der Chemie" (Chemistry Day), TU Dortmund, Germany, 05 February 2010. Molecularly imprinted polymers (MIPs) as a purification and polishing phase in the pharmaceutical industry

AWARDS/ FUNDING

PhD Scholarship (2009 – 2012)- Early Stage Researcher in 7th Framework Program of the European Commission Marie Curie Initiative (NEMOPUR, Grant number: ITN 214226)

Mentee in the Mentoring^3 program, ScienceCareer Net Ruhr, Germany